Integrating Microbial Fuel Cells (MFCs) into the Treatment of Sulphate-Rich Wastewater

In fulfilment of the requirements for the degree of

Masters in Engineering

Jennifer Couperthwaite

Supervisor/s:

Prof Susan T.L Harrison; Dr Robert Pott

Department of Chemical Engineering
Faculty of Engineering and the Built Environment
University of Cape Town

24 May 2016

PLAGIARISM DECLARATION

I know the meaning of plagiarism and declare that all the work in the document (Integrating of Microbial Fuel Cells (MFCs) into the Treatment of Sulphate-Rich Wastewater), save for that which is properly acknowledged, is my own. I have not allowed, and will not allow, anyone to copy this work with the intention of passing it off as his or her own work.

Signed: Signed by candidate **Date**: 24/05/2016

ACKNOWLEDGEMENTS

I would like to acknowledge and thank a group of very special people who have helped me so much throughout my research. In no particular order:

- Matthew Burke, thank you for looking after my ongoing experiments so many times when I could not, and being a friend to me in the lab.
- Prof Harrison, thank you for your supervision, support and editing.
- Rob Huddy, thank you for all your help with the SRB cultures.
- Durga Madras Rajaraman Iyer, thank you for your help on so many different things. I would have had a much tougher time of it if you had not done the groundwork for doing research on bioelectrical systems in our labs. Thank you for sharing what you have learned with me.
- Tynan Marias, thank you for being so patient and sharing your knowledge of SRBs and LFCRs with me and being a friend to me in the lab.
- Rob Pott, thank you for your co-supervision and help in the lab
- Mariette Smart, thank you for all your hard work on biological analysis of my samples.
- Adam van Niekerk, thank you so much for your help with the data logger. Your help saved me a lot of time.
- A very big thank you to HySA and CatSA for their help with the preparation of the electrodes and the use of your equipment for cyclic voltammetry.

ABSTRACT

The use of laboratory scale Microbial Fuel Cells (MFCs) for the combined generation of electricity and the treatment of wastewater has been well documented in literature. In addition to this the integration of MFCs into wastewater treatment reactors has also been shown to have several benefits. These include the improved treatment of wastewater, reduced solid waste and the potential to offset the energy costs of the process through the generation of electricity (Du *et al*., 2007).

The treatment of sulphate-rich wastewater, and in particular Acid Rock Drainage (ARD), has become of increasing importance in water sparse countries like South Africa where mining is currently and has taken place. A semi-passive method of continuous ARD waste treatment is currently being investigated within the Centre for Bioprocess Engineering Research (CeBER) (van Hille *et al*., 2015). This research involves the use of a Linear Flow Channel Reactor (LFCR) designed for combined biological sulphide reduction and sulphide oxidation to yield a sulphur product. Sulphate Reducing Bacteria (SRB) mediate the biological sulphide reduction. Chemical and biological sulphide oxidation takes place in a Floating Sulphur Biofilm (FSB) on the surface of the reactor and is mediated by Sulphide Oxidising Bacteria (SOB). Sulphate-rich wastewater can therefore be remediated through total sulphur species removal.

In recent years much research has been conducted into the treatment of wastewater polluted with sulphur species using MFCs and mixed microbial communities of SRB and SOB (Rabaey *et al*., 2006; Zhao *et al*., 2008; Zhao *et al*., 2009; Sun *et al*., 2010; Lee *et al*., 2012; Chou *et al*., 2013; Chou *et al*., 2014; Lee *et al*., 2014; Weng & Lee, 2015). The opportunity was therefore presented for the integration of a MFC into the LFCR. The overall aim of this study was to incorporate the elements of a MFC into a LFCR. The integration aimed to create a LFCR-MFC that functioned as a wastewater treatment reactor yielding a sulphur product and electricity through the MFC.

A constructed single-chambered MFC was used to test the ability of the microbial community, selected for use in the linear flow channel reactor (LFCR), to produce electricity. The performance of the mixed community from the LFCR in the single-chambered MFC provided a basis on which the integrated system could be compared and could be used to determine whether an integrated system was likely to produce electricity.

The design of the single-chambered MFC was originally proposed by Liu and Logan (2004) and was chosen as a result of the significant amount of research that has been conducted on the fuel cell (Liu & Logan, 2004; Liu *et al*., 2005a; Liu *et al*., 2005b; Cheng *et al*., 2006a; Cheng *et al*., 2006b; Cheng & Logan, 2007). Verification of the adequate construction of the single-chambered MFC was tested using a pure culture of *Shewanella oneidensis* MR-1 utilising lactate. The experimental procedures given by Wu *et al*., (2013b) were followed.

The results of the replication of the experiments conducted by Wu *et al*. (2013b) revealed that the constructed MFC produced only 18.6% of the power density reported in the journal. This was believed to be as a result of many shortcomings associated with the constructed cell mainly surrounding the cathode electrode. It was, however, concluded that the constructed MFC was suitable for the testing of other microbial communities.

The SRB and SOB community was tested in the single-chambered MFC with both a carbon felt anode and a carbon microfibre brush anode similar to that used in the LFCR-MFC. The MFC with the carbon felt anode produced 2.86 ± 0.009 mW/m^2 whereas the carbon microfibre brush anode produced

0.966 ± 0.002 mW/m^2. The gradient of the curves of potential difference as a function of time for the MFCs revealed that the internal resistance was 21600 ± 571 Ω and 7720 ± 253 Ω respectively.

With verification of the ability of the community to produce current, a LFCR-MFC was constructed. The LFCR-MFC had a working volume of 935 mℓ with two cathode electrodes and was operated at a 4 day residence time. A hydrodynamic study revealed that the stratification of liquid layers occurs within the bulk liquid of the reactor. This was also observed in biological experiments. A power density of 2.56 ± 0.005 mW/m^2 of cathode area (9.10 ± 0.017 mW/m^3) was produced with 10 mM lactate and sulphate feed. The internal resistance of the LFCR-MFC was approximately 980 ± 118 Ω which was considerably lower than that achieved in the single-chambered MFCs. This is considered a result of continuous flow through the reactor aiding mass transfer of charged particles, and anode design.

It was concluded that the successful integration of a MFC into a LFCR for the combined treatment of sulphate-rich wastewater and electricity production is possible. Improvements to the cathode electrode and electrical connections could significantly improve the power density produced by the LFCR-MFC. Although the concept of an integrated system was successfully proven, it is recommended that further research be done into understanding the relationship between sulphate reduction and sulphide oxidation mechanisms and the production of electricity as well as the factors affecting them in the system. It will then be possible to determine to what extent both can be achieved and the limits that exist around the operation of the LFCR-MFC.

CONTENTS

LIST OF FIGURES

LIST OF TABLES

LIST OF ABBREVIATIONS

BSR	Biological Sulphate Reduction
CE	Coulombic Efficiency
CeBER	Centre for Bioprocess Engineering Research
COD	Chemical Oxygen Demand
CV	Cyclic Voltammetry
DO	Dissolved Oxygen
EEM	Exoelectrogenic Microorganisms
EIS	Electrochemical Impedance Spectroscopy
EPS	Extracellular Polymeric Substance
FB	Fermentative Bacteria
GAC	Granular Activated Carbon
HPLC	High Performance Liquid Chromatography
HRT	Hydraulic Residence Time
IC	Ion Chromatography
LFCR	Linear Flow Channel Reactor
MB	Methanogenic Bacteria
MBR	Membrane Reactor
MFC	Microbial Fuel Cell
OCV	Open Circuit Voltage
PEM	Proton Exchange Membrane
SBR	Sequencing Batch Reactor
SEM	Scanning Electron Microscopy
SOB	Sulphide Oxidising Bacteria
SRB	Sulphate Reducing Bacteria

1 INTRODUCTION

1.1 BACKGROUND

The accelerated use of fossil fuels in recent years has resulted in growing concern of the impending global energy crisis and global warming. Much effort has been put into finding alternative energies and methods of electricity generation which use renewable resources and have no net carbon emissions. One such method which has gained growing interest among academic researchers is the Microbial Fuel Cell (MFC). This technology exploits the mechanism of microorganisms to both generate electricity while biodegrading organic matter or wastes (Du, et al., 2007).

In addition to the ability of the MFC to produce electricity, extensive research has been done into the use of MFCs as a method of wastewater treatment (Liu & Logan, 2004; Jang *et al*., 2004; Rabaey *et al*., 2005; You *et al*., 2007; Clauwaert *et al*., 2007; Ghangrekar & Shinde, 2007; Jiang & Li, 2009; Sukkasem *et al*., 2011; Zhu *et al*., 2011; Wang *et al*., 2012). Using MFCs, of higher removal of chemical oxygen demand (COD) have been reported than with other anaerobic treatments with the same retention time (Sukkasem *et al*., 2011). Anaerobic treatments, including MFCs, also require less operating energy than aerobic treatments due to the aeration requirements (Sevda *et al*., 2013). MFCs therefore present themselves as a promising economical and sustainable wastewater treatment.

Among the many different types of wastewater generated from human activities, is wastewater rich in sulphate. Sulphate-rich wastewaters are generated by many industrial processes which include mining, food processing, pulp and paper processing, animal husbandry and processing pharmaceuticals (Janssen *et al*., 1997; Lens *et al*., 1998; Pokorna & Zabranska, 2015). The passive generation of sulphate-rich wastewater as a result of mining activity, known as Acid Rock Drainage (ARD) is of particular concern in South Africa.

ARD and its contamination of surface and ground water presents itself as a significant problem in areas where mining activities are or have taken place, of which South Africa has many. The mining and processing of ores containing sulphidic minerals, results in the exposure of waste rock, tailings and unworked pits. ARD is a result of the oxidation of the sulphide minerals exposed to environmental oxygen and water. ARD contamination of water results in its acidification, increased salinity and poisoning by heavy metals, and poses a threat to the environment, agriculture and human health especially in water sparse countries like South Africa (Gazea *et al*., 1996; van Hille *et al*., 2015).

The biological treatment of sulphate containing wastewaters with Sulphate Reducing Bacteria (SRB) is an attractive option as a result of its low energy input, efficiency and sustainability (Lens, et al., 1998). SRB have the ability to use sulphate ions as electron acceptors during anaerobic respiration which provides the cell with energy for growth and maintenance. (Postgate, 1984; Widdel, 1988; Shen & Buick, 2004). A general equation for the reduction of sulphate is given by Equation 1 (Oyekola *et al*., 2009):

$$Electron\ donor + SO_4^{2-} = 2HCO_3^- + H_2S \qquad \text{Equation 1}$$

The sulphate is reduced to sulphide resulting mainly in the generation of bicarbonate which provides the alkalinity necessary to neutralise the acidity of the wastewater. Organic matter in the wastewater is also removed in this way.

A semi-passive method of continuous ARD waste treatment is currently being investigated within the Centre for Bioprocess Engineering Research (CeBER). This research involves the use of a Linear

Flow Channel Reactor (LFCR) (van Hille *et al*., 2015). The LFCR uses a combination of biological sulphate reduction in the bulk liquid mediated by SRB, and both chemical and biological sulphide oxidation which takes place in a Floating Sulphur Biofilm (FSB) on the surface of the reactor and is mediated by Sulphide Oxidising Bacteria (SOB). This reactor is of particular interest because of its ability to remove sulphate, sulphide and organics in single processing step with the recovery of an elemental sulphur product.

In recent years, research has been conducted into the treatment of wastewater polluted with sulphur species using microbial fuel cells and mixed microbial communities of SRB and SOB (Rabaey *et al*., 2006; Zhao *et al*., 2008; Zhao *et al*., 2009; Sun *et al*., 2010; Lee *et al*., 2012; Chou *et al*., 2013; Chou *et al*., 2014; Lee *et al*., 2014; Weng & Lee, 2015). It has been shown that sulphate-rich wastewater can be remediated through the removal of dissolved sulphur species using MFCs and the action of SRB and SOB. The mechanisms suggested for this are as follows (Sangcharoen *et al*., 2015): the first is the reduction of sulphate by SRB, either as planktonic cells or within the anodic biofilm or both. This removes organic compounds and produces sulphide. Sulphide is then either oxidised abiotically or by SOB to sulphur or polysulphide at the anode. SOB may also oxidise sulphur and polysulphides back to sulphate hence careful control of oxygen availability is required. Organic compounds may also be removed by exoelectrogenic microorganisms (EEM) at the anode

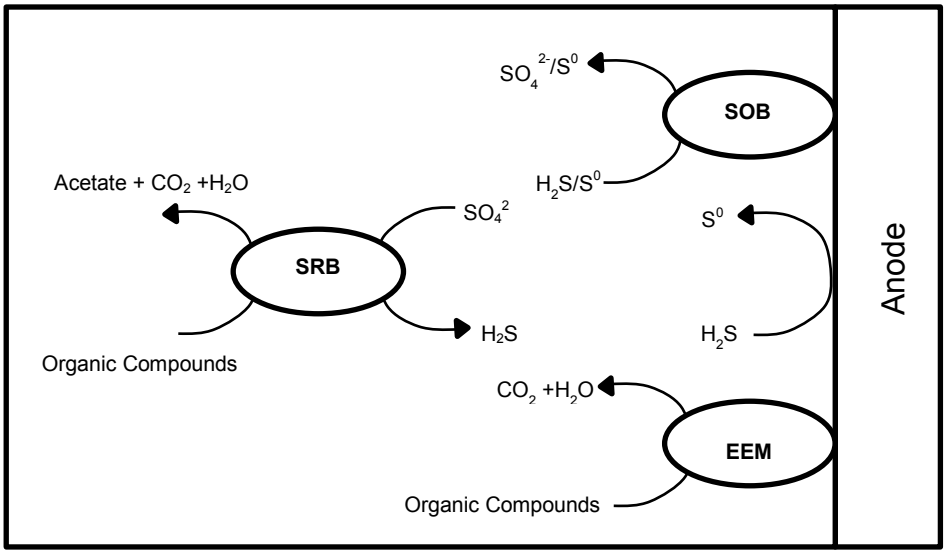

Figure 1-1: Possible mechanisms in a MFC treating sulphate laden wastewater (Sangcharoen *et al*., 2015)

Hence, the opportunity presents itself to make use of the reactions which are taking place within the LFCR to both treat wastewater and produce electricity. Previous research has revealed that integration of MFCs into wastewater treatment reactors is possible and often results in improved wastewater treatment (Cha *et al*., 2010; Liu *et al*., 2011; Wang *et al*., 2012; Wang *et al*., 2014).

This research aims to modify the existing LFCR developed by van Hille *et al*. (2015) to include the elements of a MFC in order for it to function as both a wastewater treatment reactor and a MFC. In order to have a basis on which to compare the performance of the integrated system, a single-chambered MFC was constructed. This was first tested by replicating a study from literature using the same MFC. Here a *Shewanella oneidensis* MR-1 system was used. Thereafter the microbial community and substrate being used within the LFCR was tested prior to integration into the LFCR.

1.2 DISSERTATION STRUCTURE

An extensive review of literature on microbial fuel cells is given in Section 2.1 to section 2.7. The definition of a microbial fuel cell and typical types of microbial fuel cells are given by Section 2.1 and 2.2. The current research being conducted on potential applications of MFCs is given in Section 2.3 and potential application of MFC is given in Section 2.4**Error! Reference source not found.**. In Section 2.5, various aspects of the design and operation of MFCs are discussed which affect their performance. Section 2.6 presents the benefits of integration of MFC into wastewater treatment processes and the potential use of MFCs in biological sulphate reduction reactors. Particular attention is given to the LFCR being developed within CeBER and its potential for modification to incorporate a MFC into its design. Specifics of the LFCR are given.

Research conducted in single-chambered MFC originally proposed by Liu and Logan (2004) is presented in Section 2.7. This includes the modification of the MFC and their effects on the electricity production as well as the different microbial cultures tested in the cell. Section 2.8 provides background on the two microbial systems selected for this study, namely *Shewanella oneidensis* MR-1 and the mixed community of sulphate reducing and sulphide oxidising bacteria. Research conducted on the use of SRB and SOB communities in the MFC is also specified. Section 2.9 concludes the literature review by providing the research motivation and the research objectives and key questions for this study.

Chapter 3 gives details of the procedures, experimental apparatus and experimental procedures employed in this research. Section 3.1 provides details on the cultivation of the microorganisms used in this study i.e. *Shewanella oneidensis* MR-1 and a mixed community of SRB and SOB. Sections 3.2 and 3.3 provide insight into the operation of the single-chambered MFC and the LFCR-MFC used in these experiments. The electrical, chemical and biological analysis techniques used in this study is provided in Section 3.4, 3.5 and 3.6 respectively.

Chapter 4 is introduced by Section 4.1 which exposes the need to evaluate the electrical performance of the microbial community as it is being used in the LFCR before alterations can be done to the reactor. It goes on to explain the choice of the single-chambered MFC originally proposed by Liu and Logan (2004) for the testing of the LFCR microbial community. It explains the need to test the chosen single-chambered MFC after construction, by operating it under the same conditions as used in literature. The choice to use a pure culture of the bacteria *Shewanella oneidensis* MR-1 to test the MFC which replicates the study performed by Wu et al. (2013b) is clarified. In Section 4.2 the experimental approach is discussed. The processed results of the experiments performed are given by Section 4.3 and discussed in detail in Section 4.4. Section 4.5 concluded that the MFC was suitable for testing of other microbial communities.

Chapter 5 concerns the operation of the single-chambered MFCs with a mixed community of SRB and SOB. Section 5.1 introduces the chapter and provides insight into the need to test the electricity producing ability of the community in the well-researched single-chambered MFC. In Section 5.2 the experimental approach is discussed which includes the testing of different substrate concentrations, different anodic materials, biological analysis through SEM and DNA sampling and electrical analysis by cyclic voltammetry. The calculations performed on the collected data are also given. The processed results of the experiments performed are given by Section 5.3 and discussed in detail in Section 5.4. Section 5.5 concludes that the community present in the LFCR is capable of electricity generation and an integrated LFCR-MFC is likely to produce electricity.

Chapter 6 concerns the integration of the elements of a MFC into the LFCR. The chapter is introduced by Section 6.1 in which the original LFCR and designed integrated system are discussed. The experimental approach is given by Section 6.2 which involves a hydrodynamic study on the constructed reactor, the testing of the electrical performance to prove the concept of the LFCR-MFC

and the calculations performed in the data handling of the results from the experiment. The processed results of the experiments performed are given by Section 6.3 and discussed in detail in Section 6.4. Section 6.5 concludes that an integrated LFCR-MFC is possible.

The conclusions from Chapter 4 to 6 are combined and recommendations for future research in this field are given in Chapter 7. Recommendations included improved cathode preparation and connected and further research into understanding the relationship between sulphate reduction and sulphide oxidation mechanisms and the production of electricity as well as the factors affecting them in the system.

2 LITERATURE REVIEW

2.1 DEFINITION

A microbial fuel cell (MFC) is an electrochemical device which makes use of the catalytic action of microorganisms to convert chemical energy to electrical energy (Kim *et al*., 2002; Jang *et al*., 2004; Liu & Logan, 2004; Du *et al*., 2007; Jiang & Li, 2009). The microorganisms oxidise organic biodegradable substrate and recover the electrons to the anode of the MFC instead of a soluble electron acceptor. The electrons then travel through an external circuit and are consumed in a reduction reaction at the cathode electrode. Therefore, in the closing of the circuit, electricity is produced (Wang *et al*., 2012; Jiang & Li, 2009; Sevda *et al*., 2013).

Previously MFCs have typically had two chambers: the anode which houses the bacteria and the cathode, generally aqueous, into which air is bubbled so that oxygen can be reduced. The two compartments are separated by a proton exchange membrane (PEM) (Liu & Logan, 2004; Jang *et al*., 2004; Du *et al*., 2007; Sukkasem *et al*., 2011). The PEM allows the protons to diffuse through the PEM to be used in the oxidation reaction at the cathode which completes the electrical circuit. It also helps to physically block the transfer of the oxygen into anode chamber (Liu *et al*., 2005b). The set-up of a typical two-chamber fuel cell is shown in Figure 2-1 below.

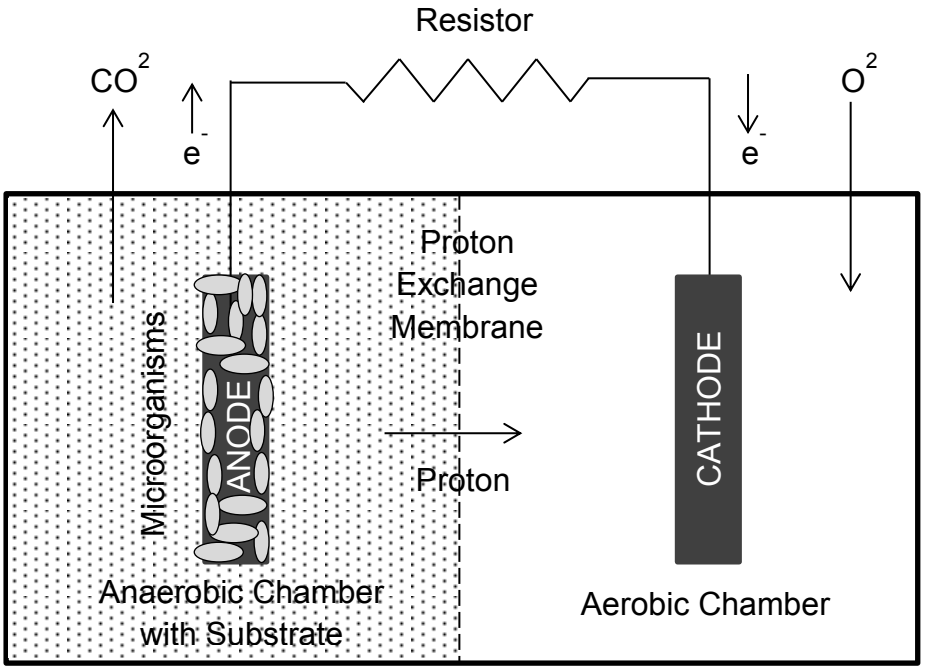

Figure 2-1: Schematic diagram of a typical two-chamber MFC (Adapted from Du *et al*., 2007)

The anodic chamber of the MFC must be kept anaerobic in order to separate the microorganisms from oxygen and any other terminal electron acceptors, other than the anode. The non-productive aerobic oxidation of substrate and the utilisation of electrons in solution in reduction reactions before being donated to the anode are therefore avoided, thereby maximising the electrical current generation achieved. Carbon dioxide is produced as a by-product of complete oxidation (Du *et al*., 2007).

2.2 TYPES OF MICROBIAL FUEL CELLS

2.2.1 Two-Compartment MFCs

Typically, two-compartment (or dual-chambered) MFCs have an anodic and cathodic compartment connected by a PEM as stated above. However, the compartments may take various practical shapes. This type of system design has thus far only been used on a laboratory scale and is typically run in batch mode (Du *et al*., 2007) although some research has incorporated through-flow or recirculation into the fuel cell design.

A very common and simple MFC design is the H-type cell. This consists of an anodic and cathodic chamber joined by a tube which houses a separator to prevent the mixing of the anolyte and catholyte solutions. This is usually in the form of a PEM (Logan *et al*., 2006). Due to the nature of the cell, the cathodes are aqueous and the cathode chamber must be aerated (Bond & Lovley, 2003; Chaundhuri & Lovley, 2003; Lanthier *et al*., 2008; Hassan *et al*., 2012) or contain a catholyte solution which provides the electron acceptor for the cathodic reduction reaction (Lanthier *et al*., 2008; Hassan *et al*., 2012). The anode compartment is also often agitated for improved mass transfer (Bond & Lovley, 2003; Chaundhuri & Lovley, 2003) or continuously purged with nitrogen to maintain anaerobic conditions (Chaundhuri & Lovley, 2003; Lanthier *et al*., 2008).

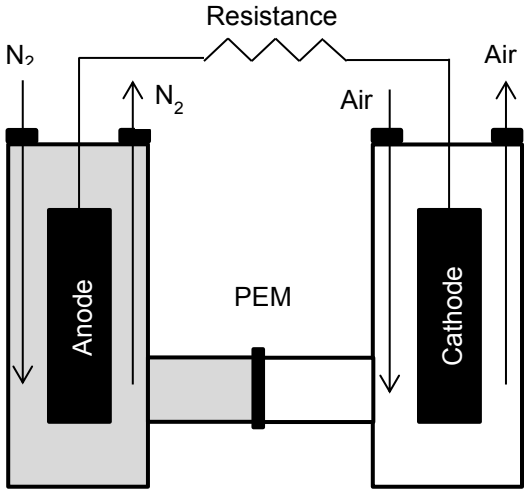

Figure 2-2: Schematic of an H-type MFC with set-up for oxygen and nitrogen sparging (Adapted from Du *et al*., 2007)

Despite the inexpensive design, the combination of the aeration, purging and stirring results in an energy intensive process which is likely to use more electricity than it produces. This cell design produces consistently lower power densities than other cell types as a result of the limit imposed by the high internal resistances of the design (Logan *et al*., 2006).

Dual-chambered MFCs operating continuously with good power density have been achieved. Ringeisen *et al*., (2006) developed a mini-MFC which was only 2 cm in diameter, resulting in a high power density per unit volume. A MFC operated in up-flow mode is continuous and more easily scaled. Min and Logan (2004) developed a cylindrical MFC with two chambers making use of up-flow in the anodic compartment. The cathodic compartment is situated on top of the anodic compartment and separated by a PEM (Figure 2-3C) Wastewater influent enters at the bottom of the anodic chamber, exits the top and is recycled back to the bottom. The cathodic compartment is filled with water and requires aeration.

He *et al*. (2005) and Rabaey *et al*. (2005) both developed tubular MFCs containing a packed bed anode. He *et al*. (2005) developed a U-shaped cathodic compartment which is situated within the anode compartment and surrounded by the granular anode packing (Figure 2-3A). Rabaey *et al*. (2005) developed a cathode compartment which circumvents the anode (Figure 2-3B). Both MFCs had PEMs separating the two compartments and used a hexacyanoferrate catholyte. These designs allowed a large surface area and close contact between the anode and cathode which reduced internal resistance.

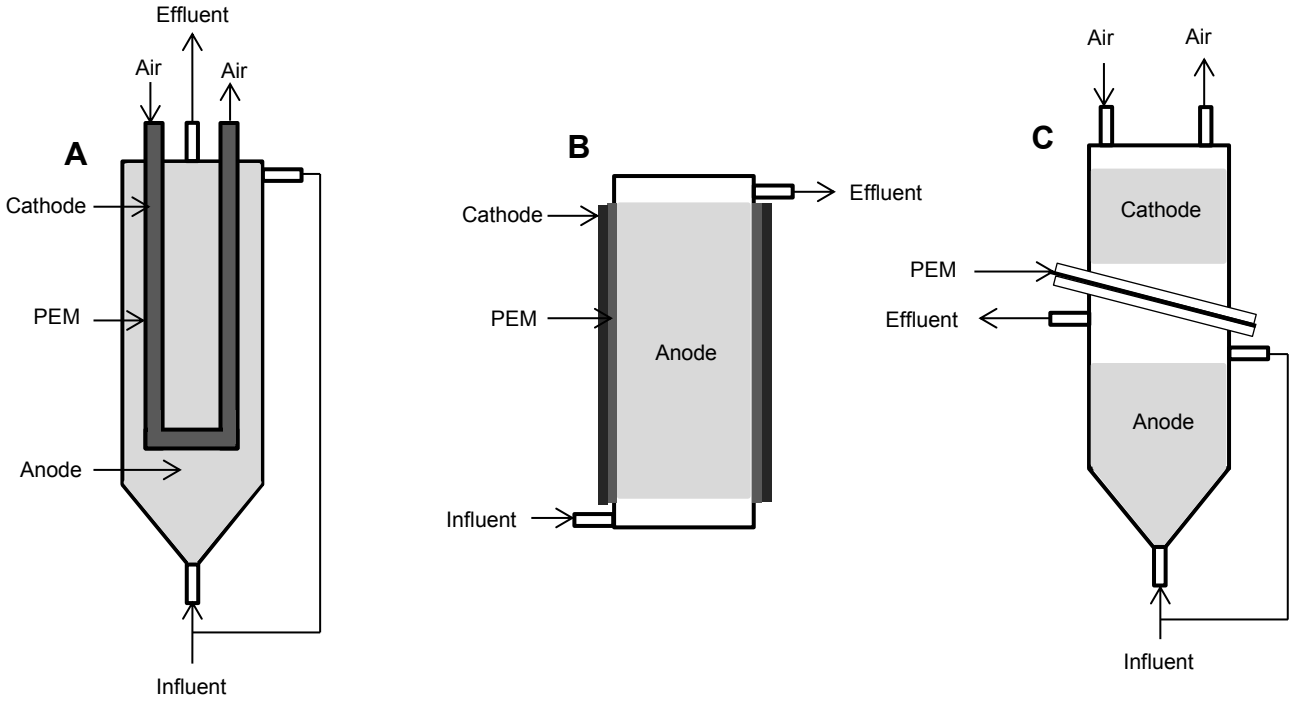

Figure 2-3: Schematic of continuous dual-chambered MFCs A: Tubular MFC with granular anode packing and U-shaped cathode compartment (He *et al*., 2005); B: Tubular MFC with granular anode packing and surrounding cathodic compartment (Rabaey *et al*., 2005); C: Continuous dual-chambered MFC (Min & Logan, 2004)

2.2.2 Single-Compartment MFCs

One of the biggest advantages of a single-chambered MFC is the ability to use a cathode exposed directly to air (air-cathode) (Park & Zeikus, 2002; Liu & Logan, 2004), saving on the operating cost of sparging. There is also improved mass transfer from the anode to the cathode, and the overall volume of the reactor is decreased. This typically makes single-chamber MFCs simpler and cheaper than two-compartment cells (Liu *et al*., 2005b; Du *et al*., 2007).

Liu and Logan (2004) conducted a study on a single-chambered MFC with an air-cathode, to which the PEM was directly bonded, and a covered anode (Figure 2-4B). Jiang and Li (2009) also investigated a single-chambered MFC with a Granular Activated Carbon (GAC) anode and air-cathode in a vertical arrangement (Figure 2-4A). Although both MFCs were operated in batch mode, both could be modified to incorporate a continuous feed without major adjustments.

Single-chambered MFCs are generally more appropriate for continuous operations as a result of a single chamber allowing for designs which better accommodate the flow of liquid through the system, such as cylindrical MFCs. This also makes them favourable for scale-up (Du *et al*., 2007). Several different types of tubular MFCs have been investigated.

Clauwaert *et al*. (2007) and You *et al*. (2007) both investigated tubular MFCs with a graphite granule anode packing throughout the length of the reactor. A carbon felt/cloth air-cathode was wrapped around the anode in the same manner as for the design by Rabaey *et al*. (2005) (Figure 2-5D). Clauwaert *et al*. (2007) used a PEM to separate the anode and cathode however the MFC remains a single chambered MFC as no catholyte is used. The designs used by Clauwaert *et al*. (2007) and You *et al*. (2007) are simpler and more sustainable than the design by Rabaey *et al*. (2005) as a result of not using an air-cathode instead of a catholyte.

Jang *et al*. (2004), Ghangrekar and Shinde (2007) and Zhu *et al*. (2011) conducted studies on a different design of tubular MFCs with the anode and cathode placed at the top and bottom of the vertical cylinder respectively (Figure 2-5A, Figure 2-5B and Figure 2-5C). Jang *et al*. (2004) and Ghangrekar and Shinde (2007) both had aerated cathodes and used a glass wool and glass bead packing to separate the anode and cathode compartments. This allowed for diffusion of protons from the anode to the cathode compartment but limited the diffusion of air to the anode, allowing it to remain anaerobic. The system investigated by Zhu *et al*. (2011) did not use any packing but attempted to change the direction of flow through the system to limit oxygen at the anode. The influent was allowed to flow from the cathode to the anode so dissolved oxygen (DO) in the feed could be used at the cathode and the DO concentration at the anode would be reduced.

A comparison of the various types of single-chambered MFCs discussed as well as the dual-chambered MFC investigated by Rabaey *et al*. (2005) can be found in Table 2-1. The basis on which power density is given differs across authors. Either electrode surface area, electrode compartment volume (sometimes given as the net volume) or total MFC volume are used as a basis, the latter particularly in the case of single compartment cells. In cases where the basis of the power density is not given in Table 2-1, it has not been specifically stated in the paper.

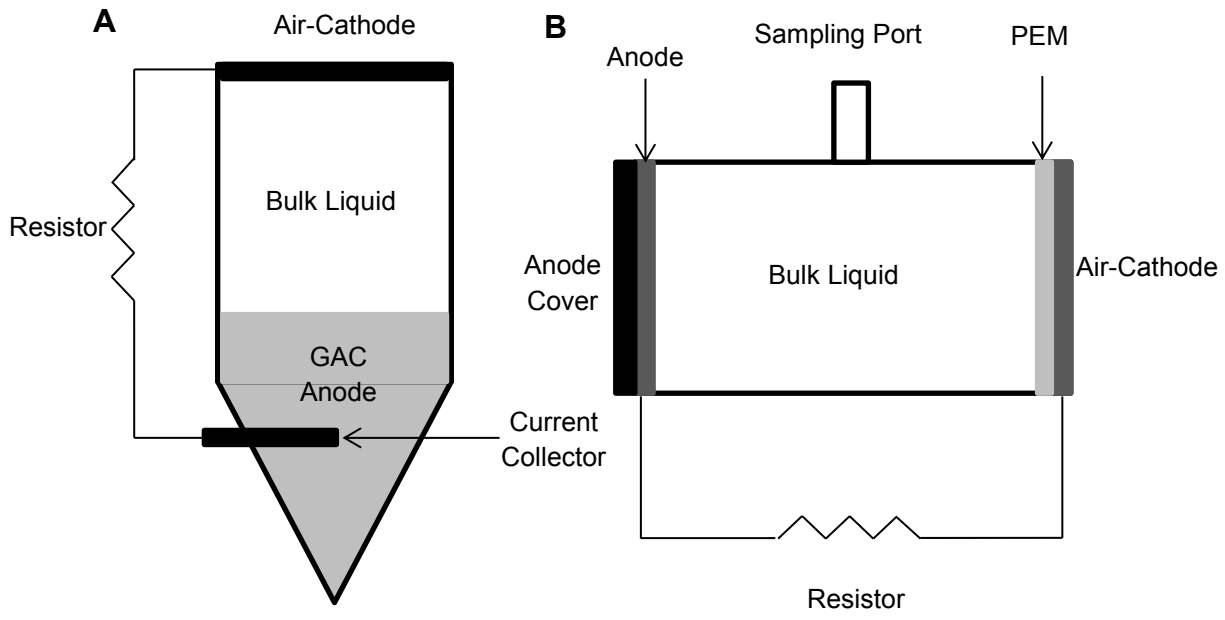

Figure 2-4: Schematic of batch single-chambered MFCs A: Cylindrical MFC with an air-cathode and GAC anode (Jiang & Li, 2009); B: Cylindrical MFC with carbon felt electrodes and air breathing cathode (Liu & Logan, 2004)

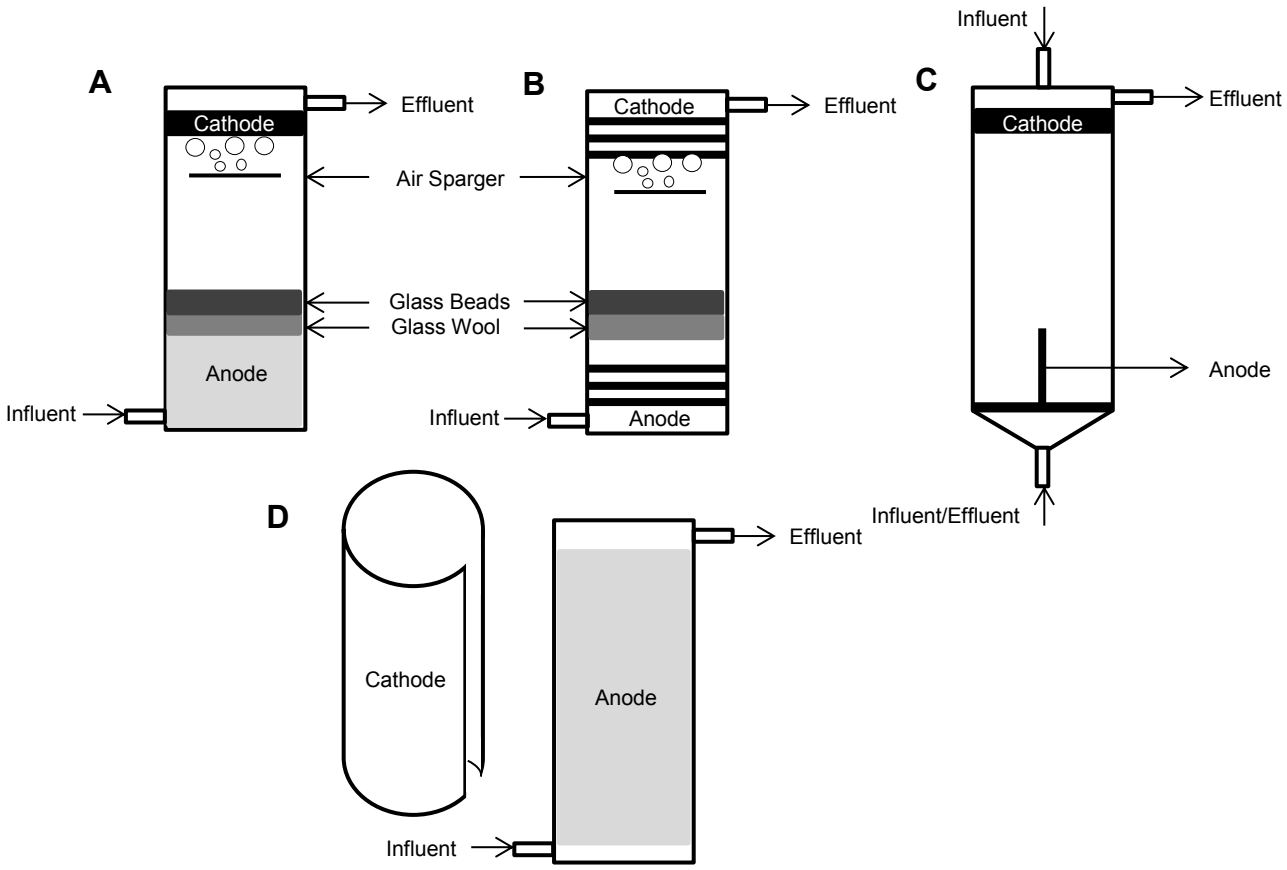

Figure 2-5: Schematic of continuous tubular single-chambered MFCs A: Tubular MFC with GAC anode and glass wool and bead packing (Jang *et al*., 2004); B: Tubular MFC with graphite rod electrodes and glass wool and bead packing (Ghangrekar & Shinde, 2007); C: Tubular MFC with air-cathode for both up-flow and down flow (Zhu *et al*., 2011). D: Basic set-up of tubular MFC with GAC anode and carbon felt/cloth cathode (Rabaey *et al*., 2005; Clauwaert *et al*., 2007; You *et al*., 2007)

Table 2-1: Performance and characteristics of various single-chambered MFCs

MFC Type	System Specifics	Electrodes	Maximum Power Density	Journal
Continuous Flow System in Tubular MFCs with GAC cathode	$K_3Fe(CN)_6$ catholyte (two–chambered with PEM)	GAC anode Graphite woven mat	90 W/m^3 (NAC)[c] 48 W/m^3 (TAC)[b]	Rabaey *et al*. (2005)
	Air-cathode (PEM)	GAC anode Carbon felt cathode	65 W/m^3 (MFC)[a] 83.2 W/m^3 (TAC)[b]	Clauwaert *et al*. (2007)
	Air-cathode	GAC anode Carbon cloth cathode	50.2 W/m^3 (NAC)[c] 29.1 W/m^3 (TAC)[b]	You *et al*. (2007)
Continuous Flow Systems in Tubular MFC with opposite end electrodes	Glass bead and glass wool packing, aerated cathode	Graphite felt anode and cathode	1.3 mW/m^2 (SAA)[d]	Jang *et al*. (2004)
	Glass bead and glass wool packing, aerated cathode	Graphite rod anode and cathode	10.9 mW/m^2 (SAA)[d]	Ghangrekar and Shinde (2007)
	No packing, deoxygenated feed, aerated cathode, up-flow	Carbon plate anode and cathode	33.2 mW/m^2 (SAC)[e]	Zhu *et al*. (2011)
	No packing, aerated cathode, down-flow		30 mW/m^2 (SAC)[e]	Zhu *et al*. (2011)
Batch Operated MFC	Single chamber, air-cathode, with PEM	Carbon paper anode Carbon cloth cathode	28 mW/m^2 (SAA)[d]	Liu and Logan (2004)
	Single chamber, air-cathode, without PEM		146 mW/m^2 (SAA)[d]	Liu and Logan (2004)
	Single chamber, air-cathode, no PEM	GAC anode Carbon cloth	7.2 W/m^3	Jiang and Li (2009)

[a] Total volume of MFC
[b] Total volume of anodic compartment
[c] Net volume of anodic compartment
[d] Surface area of anode

[e] Surface area of cathode

2.2.3 Stacked MFCs

The voltage and current output of the MFC can be enhanced by connecting several MFCs in a single electrical circuit in a parallel or series arrangement (Du *et al*., 2007). Aelterman *et al*. (2006) developed a stacked MFC in which six MFC units were separated by rubber gaskets (Figure 2-6). The granular packed anode and graphite rod cathode utilising a hexacyanoferrate catholyte were separated by a PEM. The MFC units were individually continuous. This arrangement is fairly complicated and makes use of two-chambered MFCs. It is expected to be difficult to scale-up and run on a continuous basis.

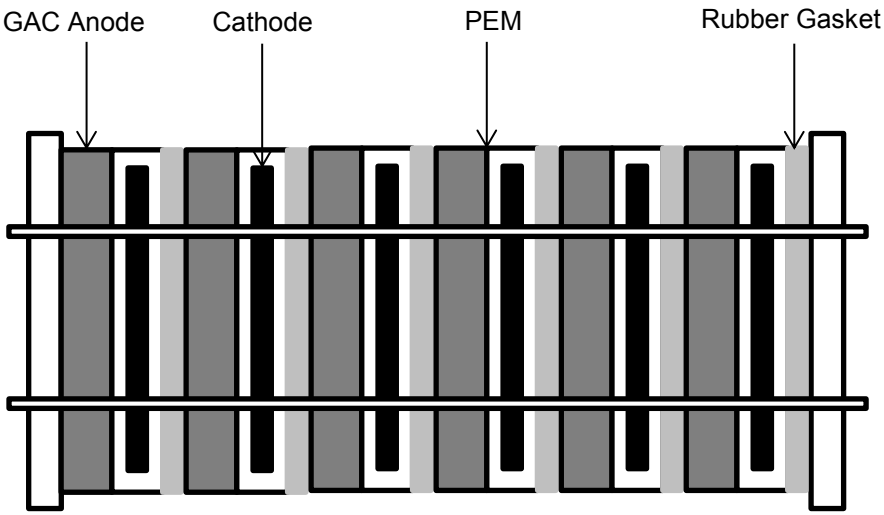

Figure 2-6: Schematic of a stacked microbial fuel cell as described by Aelterman *et al*. (2006)

2.3 CURRENT DEVELOPMENT IN MFCS

The transfer of electrons between the bacteria and the anode electrode is often inefficient. This results in low current generation and Coulombic yields produced by MFCs. The Coulombic yield is defined as the portion of electrons which can be abstracted from an electron-rich substrate via the electrodes (Du *et al*., 2007; Wang *et al*., 2012). This inefficiency is partly due to the non-conductive nature of the cell surface structures. Electrochemical mediators have been used to aid the transfer of electrons (Kim *et al*., 2002; Du *et al*., 2007). Mediators take the form of a chemical added to the anolyte of a MFC which shuttles electrons, accelerating their transfer to the anode. This is achieved by mediators crossing the cell membrane in an oxidised state and being reduced by capturing electrons within the membrane. They then diffuse back into the bulk liquid and release the electrons to become oxidised again. This process improves the transfer of electrons and therefore increases the electricity production (Ieropoulos *et al*., 2005). Mediators are often toxic phenolic compounds and expensive (Liu & Logan, 2004; Jang *et al*., 2004; Ghangrekar & Shinde, 2007; Cha *et al*., 2010) and therefore their use on a large scale is impractical.

The study by Kim *et al.* (2002) showed that mediator-less MFC could be operated using electrochemically active microbes capable of using the anode as an electron acceptor (anodophiles), negating the need for mediators. This has been confirmed in subsequent studies (Liu & Logan, 2004; Du *et al*., 2007).

Significant expenses are also associated with PEMs and the improvement of the reduction reaction at the cathode by means of catalysts (Jang *et al*., 2004; Liu & Logan, 2004; Sukkasem *et al*., 2011; Zhu *et al*., 2011; Kokabian & Gude, 2015). These factors have contributed to the limited application of the MFCs commercially (Sukkasem *et al*., 2011). Much research has therefore been done on the operation of mediator-less and membrane-less MFCs configurations for increased power generation and reduced construction and operating costs.

Kokabian and Gude (2015) estimated the current capital cost contributions of single cell design bio-electrochemical systems, capable of producing a current density of 1000 A/m^3 of reactor volume. The relative costs contributions are seen in Figure 2-7 below.

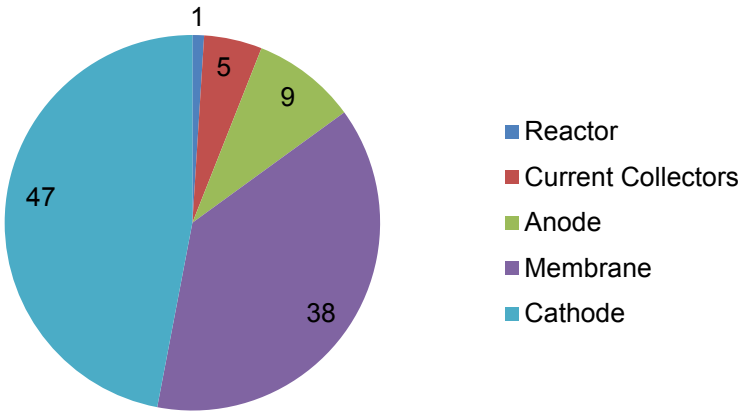

Figure 2-7: Estimated relative contribution to capital costs for bio-electrochemical systems (Kokabian & Gude, 2015)

2.4 POTENTIAL APPLICATION OF MFCS

Most studies on MFCs thus far have been conducted at a laboratory scale in small volume cells, using expensive and fragile material. Designs need to be developed further for scalability, higher power output and low cost for real-world application (Jiang & Li, 2009). Despite these limitations, several potential real-world applications of MFCs have already been identified.

MFCs are capable of generating enough electricity for use as small scale batteries and local area electricity generation (Kim *et al*., 2002; Rabaey *et al*., 2005; Du *et al*., 2007). A prospective way to better utilise the low electricity generated by the cells is to store the electricity in rechargeable devices to be used elsewhere at a later stage once enough charge has been stored (Du *et al*., 2007).

Extensive research has been done into the use of MFCs for wastewater treatment (Liu & Logan, 2004; Jang *et al*., 2004; Rabaey *et al*., 2005; You *et al*., 2007; Clauwaert *et al*., 2007; Ghangrekar & Shinde, 2007; Jiang & Li, 2009; Sukkasem *et al*., 2011; Zhu *et al*., 2011; Wang *et al*., 2012). MFCs are capable of higher removal of chemical oxygen demand (COD) than anaerobic treatments with the same retention time (Sukkasem *et al*., 2011). This has been suggested to be as a result of the anode of a MFC being a potential site for biochemical reactions other than the desired direct anodic oxidation reaction (DAO). Indirect anodic reactions (IAO) or secondary physio-chemical reactions are induced by the *in situ* generated potential. This results in an increase in the efficiency of the system (Krishna *et al*., 2014).

Anaerobic treatments also require less energy than aerobic treatments due to aeration requirements (Sevda *et al*., 2013). The potential incorporation of MFCs into existing wastewater treatment processes, for example after anaerobic treatment, has also been noted (Cha *et al*., 2010; Cheng *et*

al., 2010; Liu *et al*., 2011; Wang *et al*., 2012; Sevda *et al*., 2013; Wang *et al*., 2014) and is discussed in Section 2.6. MFCs have also been reported to be able to treat offshore marine sediments as well as sludge (Rabaey *et al*., 2005; Su *et al*., 2013).

Use of MFCs as biosensors has been noted (Kim *et al*., 2002; Jang *et al*., 2004; Du *et al*., 2007) wherein the biological oxygen demand (BOD) of the wastewater can be measured by relating the amount of current and the coulombic efficiency produced by the cell to the energy content of the wastewater. The sensors are reportedly accurate, stable and capable of good reducibility (Du *et al*., 2007).

The use of MFCs for the production of bio-hydrogen has been shown in Microbial Electrolysis Cells (MEC). An external potential must be applied in order to increase the cathode potential necessary to combine electrons and protons from the anodic reaction to form hydrogen. However, it is much lower than the potential required for direct electrolysis of water and is a potentially greener method of hydrogen production (Du *et al*., 2007).

The potential for MFCs to treat waste while simultaneously generating electricity which could potentially offset the energy demands of the treatment is an attractive prospect. Wastewater rich in organics is generated by numerous human activities on a daily basis and treatment is challenging as a result of its complexity and the energy and monetary costs associated with it. MFCs have the potential to produce enough electricity to halve the electricity demands of a conventional process and produce between 50-90% less solid waste (Du *et al*., 2007).

2.5 ELEMENTS OF MICROBIAL FUEL CELLS

2.5.1 Microorganisms

Many different microorganisms have been used in MFCs both with and without the addition of mediators. Early research conducted on MFCs used bacteria which required external mediators to take up electrons from the microbes and discharge them to the anode (Logan, 2009). For example *Actinobacillus succinogenes* (Park & Zeikus, 2000), *Desulfovibrio desulfuricans* (Ieropoulos *et al*., 2005), *Escherichia coli* (Choi *et al*., 2003; Ieropoulos *et al*., 2005), *Proteus mirabilis, Proteus vulgaris* (Choi *et al*., 2003) and *Pseudomonas fluorescens* (Ieropoulos *et al*., 2005) have been used in MFCSs with addition of electron shuttles.

Microorganisms with the ability to transfer electrons derived from their metabolism of organic substrates to the anode of a MFC (exocellular electron transfer) are known as exoelectrogens. They have also been termed electrochemically active bacteria, anodophiles or anode respiring bacteria and electricigens (Logan, 2009). These are most often dissimilatory metal reducing microorganisms (Du *et al*., 2007).

Metal reducing bacteria, primarily belonging to the families of *Shewanella, Rhodoferax* and *Geobacter,* produce useful energy in the form of ATP during the dissimilatory reduction of metal oxides under anaerobic conditions. This reaction is similar to the anodic reaction in mediator-less MFCs (Du *et al*., 2007). Research on dissimilatory metal reducing bacteria has demonstrated that these exoelectrogens transfer electrons either by direct contact of their outer membrane with the metal oxide or anode, by excreting their own electron shuttles or by nanowires which are conductive extensions of the cell membrane (Logan, 2009).

Electrogenic microorganisms are prevalent in marine sediments, soil, wastewater, fresh water sediment and activated sludge. These are often used as inocula in MFCs which results in a mixed community. Mixed consortia MFCs generally perform better than pure cultures (Du *et al*., 2007; Nevin *et al*., 2008; Logan, 2009). This is due to improved substrate utilisation and the likely presence of

electrophiles (which produce electrons in their metabolic pathway) and anodophiles as well as microorganisms which use natural mediators in mixed communities. Together they are able to work synergistically for improved electricity generation (Du *et al*., 2007).

In mixed community fuel cells, the communities of microorganisms which colonise the anodes of MFCs are typically complex and it is often very difficult to explain the generation of current in these systems (Nevin *et al*., 2008). During the enrichment period of a cell, the microbial community shifts towards bacterial strains which are more electrochemically active. This is due to the larger difference in redox potential between the reduced substrate and the anode than the reduced substrate and protons and carbon dioxide which the bacteria can use to form reduced metabolites such a methane and hydrogen gas. The bacteria which use the anode as an acceptor therefore gain more energy than those that use protons or carbon dioxide and in this way the system selects bacteria which use the anode (Rabaey *et al*., 2004).

2.5.2 Internal Resistance

2.5.2.1 Minimising Internal Resistance

When a power source is connected in a circuit and delivers current, the voltage recorded over the power source is lower than that of the open circuit voltage (OCV) or the voltage recorded when the power source is not delivering current. The voltage difference arises due to internal resistance.

The internal resistance of a cell has several components as a result of the several inefficiencies occurring within the cell. Activation losses arise from the activation energy required for the oxidation and reduction reactions. Mass transfer losses arise as result of the flux of reactants and products to and from the electrodes. Energy is also lost in the transfer of electrons from the cell to the anode surface (Logan, 2008).

Overcoming Ohmic losses is considered most important for optimum MFC design. Ohmic losses can also be considered as bulk phase mass transfer losses as they arise from the resistance of ion conduction as a result of the solution, the PEM and the flow of electrons through the electrode to the contact point with the external circuit wire (Logan, 2008).

Ohmic losses can be reduced by decreasing the spacing between electrodes, ensuring good contact between the electrodes and the external circuit and increasing solution conductivity and buffering capacity (Logan, 2008). Several studies have revealed the effects of internal resistance on power generation and these are discussed in Section 2.5.2.2- 2.5.2.6.

2.5.2.2 Distance Between Electrodes

Jang *et al*. (2004) found that lower current and power densities were obtained for the larger electrode distances tested. A decrease in distance between electrodes results in a shorter distance to be travelled by protons and therefore improves the power density produced. It was therefore suggested to keep the electrodes as close as possible to each other to aid proton transfer but maintain a large enough internal resistance to avoid an electrical short.

Jiang and Li (2009) and Zhu *et al*. (2011) both conducted studies on cylindrical single-chambered MFCs with air-cathodes in which the anode and the cathode were situated at the bottom and top of the cylinder respectively. The internal resistance was found to decrease as the distance between the electrodes decreased. Both studies also found that a maximum power density was reached. On attaining this, a further decrease in distance no longer improved power density. This maximum was believed to be due to the diffusion of oxygen from the cathode to the anode with concomitant inhibition of the anaerobic respiration of the bacteria, therefore outweighing the benefits of the continued decrease in resistance.

Ghangrekar and Shinde (2007) conducted an experiment in a cylindrical MFC in which three graphite rod anodes and cathodes were present at the bottom and top of the cylinder respectively. The distance between each anode and cathode differed. The highest power density was produced by the anode and cathodes which were closest together at all tested external resistances. This is in agreement with the finding of the other studies.

2.5.2.3 Current Collectors

In the experiments conducted by Jiang and Li (2009), the single-chamber MFC was also run with multiple graphite rod electron collectors situated within the granular activated carbon anode. This was done with the assumption that ohmic losses arise from the electrons having to travel from all GAC anode particles, on which the oxidation reaction occurs, to the graphite rod which is varying distances away from each particle. The use of more rods could therefore potentially decrease the internal resistance in the cell and result in more efficient electron transfer to the anode. It was noted that the internal resistance of the cell decreased in the multiple rod systems where electron transfer was better facilitated.

The multiple rod systems were also used to identify whether the anode or cathode was the limiting factor for power generation. It was found that the combined current produced in a multiple rod system was the same as that produced using only one rod i.e. in a 4 rod system, each rod collected approximately one quarter of the current produced in a single rod system. Although internal resistance decreased, the total current remained the same which indicates that the reduction at the cathode was limiting in terms of power production. The reduction reaction has often been found to be the limiting step in electricity generation (Jang *et al*., 2004; Du *et al*., 2007; Jiang & Li, 2009; Wang *et al*., 2014).

2.5.2.4 Solution Conductivity

As stated previously, ohmic losses occur in the electrolyte as a result of the movement of ions through solution and in the electrode as a result of the movement of electrons through the electrode and wires. Ohmic losses in the solution are often much more significant in MFCs as a result of the very low conductivity of domestic wastewater (Jiang & Li, 2009).

Jiang and Li (2009) and Wang *et al*. (2014) noted the internal resistance of the cell decreased with an increase in COD. Both studies thought this to be as a result of the increase in ionic strength at high substrate concentration which reduces ohmic losses.

Jang *et al*. (2004) and Liu *et al*. (2005a) both noted that the addition of sodium chloride (NaCl) to the bulk liquid resulted in the improved generation of current. This was attributed to the improvement of the transfer of charged particles. Liu *et al*. (2005a) also noted an increase in the coulombic efficiency of the system.

2.5.2.5 Electrode Surface Area

In the study conducted by Jiang and Li (2009), the distance between electrodes in the single-chambered MFC was kept the same but the amount of GAC particles was changed (400 g, 700 g and 1000 g). It was noted that the internal resistance of cell changed very little with a change in GAC particles although the power density improved from 4.2 W/m^3 to 7.2 W/m^3 when the amount of GAC particles was changed from 400 g to 700 g. No further increase in power density was seen when the amount of GAC was changed to 1000 g. This increase was attributed to an increase in anodic surface area which results in more bacteria adhering to the anode surface which leads to more electrons been generated and therefore higher power production. Further increasing of anode area resulted in the rate electron generation at the anode exceeding the rate of electron acceptance at the cathode.

2.5.2.6 Electrode Material

Different electrode materials perform differently as a result of having different activation polarisation losses (Du *et al*., 2007). Significant research has been dedicated to improvements in the cathodic reaction (discussed in section 2.5.8 below) however, improvements to the anode have also been attempted.

Jiang and Li (2009) further investigated the effect of use of different anodic material. Two dual-chambered MFCs were operated, containing a 6 cm^2 carbon cloth anode and graphite rod inserted into 150 g of GAC particle respectively. Similar power densities were produced for both cells although slightly higher values were achieved for the GAC anode.

Liu *et al*. (2005a) noted that the power density of a single-chambered MFC was improved by 68% when the carbon paper cathode was replaced with a carbon cloth anode with the same platinum catalyst loading.

Cheng and Logan (2007) treated carbon cloth anodes with ammonia gas which increased the surface charge of the electrode which resulted in improved electricity generation. It has also been shown that the addition of Mn^{4+}, Fe_3O_4 or Fe_3O_4 and Ni^{2+} to graphite anodes improves the power production by increased kinetic activity of microbial reduction at the anode (Lowy *et al*., 2006). The presence of positively charged compounds also improves the adhesion of negatively-charged bacteria as a result of the attraction of the cells to the anode (Cheng & Logan, 2007).

2.5.3 Proton Exchange Membrane

As was mentioned previously in Chapter 2, a proton exchange membrane is necessary in dual-chambered MFC to separate the two compartments and prevent the mixing of the anolyte and catholyte. They have also been used in single-chambered MFCs however, due to the significant cost associated with their use (Jang *et al*., 2004; Liu & Logan, 2004; Sukkasem *et al*., 2011; Zhu *et al*., 2011; Kokabian & Gude, 2015); the operation of single-chambered MFCs with and without a PEM has been investigated.

Liu and Logan (2004) conducted a study on a single chamber MFC operated with and without a PEM. In the cells with the PEM, the membrane was bonded directly to the platinum coated carbon cloth cathode electrode, which was exposed directly to the air.

It was found that the MFCs with the PEM reached stable power generation much faster than the cells without, however a higher power density was reached for the cell without the PEM. The Coulombic efficiency however was higher for cells with PEMs, which Liu and Logan (2004) attribute to loss of substrate due to aerobic oxidation by bacteria at the anode. However, it is mentioned that oxygen diffusion could potentially be reduced by means of improved coating on the side of the cathode exposed to the chamber. Increased biofilm development on the cathode electrode could also decrease the diffusion of oxygen. The absence of a PEM in a single-chambered MFC will result in the formation of a biofilm on the cathode which has several benefits to power generation. This is discussed further in section 2.5.8.

In the study mentioned above conducted by Jiang and Li (2009), it was discovered that power density produced in the single-chamber MFC (with no PEM and GAC anode) was seven times that of the power density produced by the two-chamber MFC with a PEM and the same GAC anode. Although the cathode in the dual-chambered cell was aqueous and an air-cathode was used in the single chambered MFC, the higher power density was attributed mainly to the absence of the PEM, which decreased the internal resistance of the cell.

The successful operation of single-chambered MFCs in the absence of a PEM is therefore possible and could result in improved power densities and more economical designs.

2.5.4 Continuous Flow Systems

In considering the use of MFCs as a wastewater treatment method, it is noted that wastewater is constantly being produced in many industrial applications. If an industrial scale MFC was to be used to treat wastewater, it would be most sensible to use a continuous flow system (Rabaey *et al*., 2005; Wang *et al*., 2012) as allowance would need to be made for storage if batch systems were used. Batch operation is also typically applied in two-compartment cells, which as mentioned previously utilises a PEM which is expensive and scale up is difficult (Du *et al*., 2007).

Much research has been done into continuous flow MFC systems. Jang *et al*. (2004), Zhu *et al*. (2011), Ghangrekar and Shinde (2007), Rabaey *et al.* (2005), Clauwaert *et al*. (2007) and You *et al*. (2007) all conducted studies on continuous flow systems. In all cases the MFC was tubular in shape and the direction of flow was upwards (up-flow).

In the case of Jang *et al*. (2004) Zhu *et al*. (2011) and Ghangrekar and Shinde (2007), the anode was positioned at the bottom of the tubular MFC and the cathode was positioned at the top.

Zhu *et al*. (2011) investigated the effect of downward flow from the cathode to the anode (down-flow) on the performance of the cell. It was noted that the cell with the down-flow of wastewater produced a higher power output (approximately double) than the cell with up-flow. This was believed to have been due to non-productive oxidation of substrate and reduction of oxygen at the anode due to the DO in the influent at the anode in an up-flow system.

In the case of the fuel cells used in the investigations by Jang *et al*. (2004) and Ghangrekar and Shinde (2007), a packing material of glass beads and glass wool was used to separate the anode and cathode thereby essentially making a MFC with two chambers. In the study conducted by Zhu *et al*. (2011) no packing material was used and the fuel cell consisted of a single chamber. In a MFC with no packing the organic compounds in the incoming influent are able to diffuse through the fuel cell to be oxidised at the anode regardless of the direction of flow. In the case of a cell with packing, it is illogical to allow the influent to flow into the cathode chamber to create a down-flow system, as the diffusion of the organic compounds would be hindered by the packing material resulting in a limiting step in current generation.

The MFC systems used by Rabaey *et al*. (2005), Clauwaert *et al*. (2007) and You *et al.* (2007) differ from those of Jang *et al.* (2004) Zhu *et al*. (2011) and Ghangrekar and Shinde (2007) in that the tubular cells are packed with a granular activated carbon (GAC) anode and surrounded by the cathode in the form of carbon cloth or felt.

Clauwaert *et al*. (2007) and You *et al*. (2007) make use of carbon felt air-cathodes coated with magnesium oxide and C/Pt powders respectively, whereas Rabaey *et al*. (2005) used a ferricyanide catholyte solution. The advantage of having a cathode which surrounds the tubular fuel cell is that that a low internal resistance can be achieved by having a small distance between the anode and the cathode (Rabaey *et al*., 2005; You *et al*., 2007).

2.5.5 Chemical Oxygen Demand Loading

Several studies have tested a range of COD loading values for the MFC influent and its effect on the performance of the cell (Rabaey *et al*., 2005; Clauwaert *et al*., 2007; Jiang & Li, 2009; Sukkasem *et al*., 2011; Zhu *et al*., 2011; Wang *et al*., 2014). It was found in several cases that the power density produced by the cell increases with an increase in COD of the tested substrate for the tested range (Clauwaert *et al*., 2007; Jiang & Li, 2009; Zhu *et al*., 2011). In some cases a maximum power density

was achieved before an increase in COD loading resulted in a decrease in power density produced (Rabaey *et al*., 2005; Wang *et al*., 2014).

Rabaey *et al*. (2005), Jiang and Li (2009) and Wang *et al*. (2014) found that coulombic efficiency decreased with an increase in COD. This was thought to be due to the consumption of substrates for fermentation or bacterial growth instead of electricity generation (Jiang & Li, 2009; Wang *et al*., 2014), as much of the suspended bacteria in wastewater have been found to be non-electricity generating (Jiang & Li, 2009). It could also be as a result of the use of alternative electron acceptors instead of the anode (Rabaey *et al*., 2005).

Jiang and Li (2009) found that the efficiency of COD removal increases with increased COD loading. Wang *et al*. (2014) and Sukkasem *et al*. (2011) both investigated MFCs integrated into wastewater treatment systems and found there to be a maximum COD removal efficiency before decreasing with increasing COD loading was noted. In the case of the system investigated by Wang *et al*. (2014), the wastewater influent was fed into the MFC compartment, the effluent of which was fed into to the sequencing batch reactor (SBR). It was noted that in the coupled system, the COD shunted to the SRB was dependant on the COD loading as well as the COD removal capacity of the MFC. The amount of COD removed by the MFC increased in a linear trend with an increase in COD loading, however the contribution of the MFC to the removal of COD decreased with increased loading.

In the system investigated by Sukkasem *et al*. (2011), the wastewater flowed into the anode chamber, the effluent of which flowed into the cathode chamber. The percent of COD removed by the anode remained constant for all COD loading rates investigated however the COD removal of the cathode showed a maximum. This was explained to be as a result of the cathode requiring an optimum COD input and the biodegradation of the anode being limiting.

As was noted above, an increase in COD loading has also been shown to decrease the internal resistance of a MFC due to an increase in ionic strength at high substrate concentration which reduces ohmic losses (Jiang & Li, 2009; Wang *et al*., 2014). This is discussed in section 2.5.2.3 above.

2.5.6 Recirculation and Accumulation

Rabaey *et al*. (2005) noted that in a MFC operating under continuous flow with recirculation, a significant lag phase in power generation was observed. This was explained by the need for the accumulation of biomass within the reactor. Initially oxygen diffuses through the air-cathode in large enough quantities to lower the anodic potential while at the same time removing COD from the wastewater. Once a biofilm has grown the influx of oxygen can be substantially reduced. It was noted that during the lag phase only about 20% of the removed COD by the cell was related to current which implies that the majority of the COD was removed through alternative electron acceptors or the accumulation of biomass in the reactor. Clauwaert *et al*. (2007) also noticed the lag phase associated with biofilm development.

It is reasonable to assume that if during the start-up of the MFC, it is not operated in batch mode to allow for the growth of the biofilm, recirculation is necessary in order to prevent washout of the inoculum and allow time for the biofilm to grow.

Rabaey *et al.* (2005) also noted that in the tubular reactor investigated which was packed with GAC, approximately 50% of the reactor volume was taken up by the electrode and at higher loading rates in the case of sludge, there is less available space for biomass and the same power density outputs cannot be reached. It is therefore necessary to both remove insoluble organics from the reactor and to increase the specific area of the electrodes without volume losses. The recirculation of substrate in MFCs may cause the accumulation of insoluble organics in the fuel cell and will be a challenge in its continuous operation.

You *et al*. (2007) investigated the effects of recirculation rate on the performance of a tubular flow through MFC. It was noted that at a high COD loading, altering the recycle ratio had almost no effect on the power density produced and the internal resistance of the cell remained almost constant. However, at lower COD loading the power density and internal resistance increased and decreased significantly respectively with an increase in recycle ratio. The power density produced was however higher for all recycle ratios tested in the case of the higher COD loading.

It was suggested that in low COD loading the fuel cell behaved like a mixed system with all areas being of similar substrate concentration at a higher a recycle ratio and as a plug flow reactor at low recycle ratios with the substrate being depleted along the length of the reactor. The recommendation is given to operate the cell at higher COD loading in order to stabilise the power density produced and reduce the amount of recirculation necessary as the substrate is not depleted along the length of the reactor.

As a result of the slow mass transfer rates of reactants and products, loss of potential due to unequal substrate distribution in the bulk liquid often occurs. The concentration gradient should be reduced by means of mixing, bubbling or increased flow rate as in recirculation mentioned above. It must be noted however that currently the energy required for pumping fluid through the MFC is considerably larger than the power output of the cell. At present the primary advantage of these fuel cells is therefore wastewater treatment (Du *et al*., 2007).

2.5.7 Aeration and Air-cathodes

Zhu *et al*. (2011) attempted to avoid the non-productive oxidation of substrate due to oxygen reduction at the anode. This occurs when DO is present at the anode which should operate anaerobically. The wastewater feed for the up-flow reactor was purged with nitrogen in an attempt to deoxygenate it. This reduced the amount of DO present at the anode where the feed enters, and was found to improve the power output. Aeration at the cathode was then done for both the deoxygenated and non-deoxygenated up-flow feeds and found to improve the power output of both by approximately double. This demonstrates the need for anaerobic anode and aerobic cathode conditions.

In MFCs with packing to separate chambers such as those used by Jang *et al*. (2004) and Ghangrekar and Shinde (2007), although there is no separate anolyte and catholyte, the barrier does provide a DO gradient for proper operation of the cell (Du *et al*., 2007).

Jang *et al*. (2004) conducted experiments on a MFC with an aqueous aerated cathode chamber. The aeration rate was altered and current produced was monitored. It was noted that initially there was an increase in the current produced with an increase in aeration rate before becoming almost constant with very little change in current observed with an increase in aeration rate.

It was however noted that with an increase in aeration rate, the COD of the effluent from the cathode compartment decreased significantly whereas the effluent COD of the anode remained reasonably constant. This implied that the organic compounds were oxidised through aerobic bacterial respiration in the cathode compartment. It was hypothesised that with the critical oxygen concentration of the cathode being significantly higher than that of the aerobic bacteria, the cathode reaction is restricted as a result of oxygen being used by the aerobic bacteria present when the DO concentration is lower than the critical DO concentration of the cathode. It was therefore suggested to operate the MFC with a DO concentration higher than that of the critical oxygen concentration of the cathode which would improve the electricity production and simultaneously remove contaminants in the cathode through aerobic microbes. This therefore also improves the efficiency of the MFCs as a wastewater treatment method.

Coulombic yield was very low throughout the experiment which was attributed to the poor cathode reaction. It was noted that if the critical oxygen concentration of the electrode was more comparable

to that of the aerobic bacteria, the Coulombic yield might increase. This implies the need for improvement of cathode reaction in order to reduce the critical concentration of the electrode.

Despite improved power generation with aeration, the energy production by the MFC is unlikely at this point in time to exceed the energy utilisation of aeration. The ability of an air-cathode to use oxygen freely from air makes it a good option in terms of sustainability and operating costs (You *et al*., 2007). It is prudent to consider the reasons for use of the MFC when deciding whether to aerate it or not and whether electricity generation or wastewater treatment is the main focus. Some division of the anode and cathode will also be necessary to avoid transfer of oxygen to the anode in aerated systems. Whether this is done by a PEM or by packing it should be considered in the cost and scalability of the system.

Liu and Logan (2004) state that the main disadvantage of a two-chambered fuel cell is the need to aerate the cathode chamber which is energy intensive. In the study conducted on a cell using an air-cathode with and without a PEM, Liu and Logan (2004) state that the power density achieved by the MFC without the PEM is larger than sediment fuel cells without PEMs and with aqueous cathodes and attribute this to the inefficiency of the aqueous cathode which result from DO limitations.

There are however limitation to air-cathodes. You *et al*. (2007) noted that air-cathodes used in tubular reactors where the anode and cathode are placed on opposite ends may be difficult to scale up as a result of the need for the electrodes to remain close to achieve the same electricity production and maintain low internal resistance. Platinum catalyst use on air-cathodes should also to be avoided where possible due to the sensitivity of the catalyst to poisoning as well as the high costs involved.

The performance of a catholyte MFC cannot be matched with an air-cathode however, catholyte cathodes are not good for scale-up. There is therefore a clear need for improvement of the cathodic reaction if aeration and catholyte use is to be avoided. This is discussed further in section 2.5.8 below.

2.5.8 Improvements of the Cathode Reaction

Different electrode materials perform differently as a result of having different activation polarisation losses (Du *et al*., 2007). The reduction reaction at the cathode has often been found to be the limiting step in electricity generation (Jang *et al*., 2004; Du *et al*., 2007; Jiang & Li, 2009; Wang *et al*., 2014), and as a result of the slow rates of reaction it is often necessary to use catalysts or artificial electron mediators in the form of catholytes (He & Angenent, 2006) to reduce activation losses. Platinum is the most commonly used catalyst as a result of its excellent catalytic abilities, but is very expensive and susceptible to poisoning (Rabaey *et al*., 2005; You *et al*., 2007; He & Angenent, 2006).

Transition metals are often used as electron mediators between the cathode and oxygen as a result of the high rates of change between their possible redox states (He & Angenent, 2006) and can be in solid form on the cathode or liquid for as a catholyte. Catholytes such as potassium ferricyanide and potassium permanganate act as liquid-state electron acceptors and are often used. However due to the toxicity and need for regeneration of these chemicals, their use is impractical and unsustainable, especially in scale up of the MFC (Rabaey *et al*., 2005; You *et al*., 2007).

When bacteria are allowed to colonise both the cathode electrode and the anode electrode, the cathode is referred to as a bio-cathode. Bio-cathodes are good ionic conductors as a result of being more than 90% water (Cristiani *et al*., 2013) and are capable of functioning as a catalyst to assist in oxygen transfer and can potentially render metal catalysts or artificial electron mediators superfluous.

Some aerobic microbes are capable of adopting the cathode as an electron donor and as a result catalyse the oxygen reduction reaction (Clauwaert *et al*., 2007; Cha *et al*., 2010; Wang *et al*., 2014). Bio-cathodes can be beneficial over abiotic cathodes in terms of the cost of construction operation

and sustainability. They are cheap and do not need to be replaced. In some cases microorganisms such as algae are cable of producing oxygen via photosynthesis and therefore eliminate the need for external oxygen supply (He & Angenent, 2006).

Bio-cathodes can be used in aerobic and anaerobic systems. In aerobic systems oxygen is used as the terminal electron acceptor whereas in anaerobic systems bio-cathodes reduce compounds such as nitrates, sulphates, iron and manganese as terminal electron acceptors (He & Angenent, 2006). In the case of aerobic systems, the anode reaction should remain anaerobic to avoid loss of electrons to aerobic oxidation of substrate. A cathodic biofilm can contribute to preserving this by consuming oxygen entering through the porous cathode (Cristiani *et al*., 2013) in single chambered cells and eliminating the diffusion of oxygen to the anode through the PEM in two chambered cells (He & Angenent, 2006).

Oxygen has a high redox potential making it favourable for reduction. Nitrate manganese and iron have a comparable activity whereas sulphate has a negative potential is far more difficult to reduce. Advantage of using an anaerobic bio-cathode over an aerobic one is the elimination of oxygen transfer from the cathode to the anode across the PEM (He & Angenent, 2006).

Zhang *et al.* (2012) conducted a study in which the performance of three different cathode types were compared over a period of 400 days, namely a $K_3Fe(CN)_6$ catholyte, an air-cathode and an aerated bio-cathode. The catholyte and bio-cathode cells were dual-chambered cells separated by a PEM whereas the air-cathode cell was a single chamber.

It was noted that from the beginning of the experiment the bio-cathode MFC produced the highest voltage and power density followed by the catholyte and then the air-cathode cells. The voltage and power density produced by the fuel cells with the catholyte and air-cathode decreased over the duration of the experiment whereas both initially increased dramatically for the cell with the bio-cathode before dropping slightly. The coulombic efficiency for the cell with the bio-cathode was also considerably higher than the others and increased for the first 200 days whereas it decreased from the beginning of the experiment for the other two MFCs. The bio-cathode cell was therefore found to generate the most electricity for the longest amount of time with the highest efficiency.

The decrease in power generation with time was attributed to the internal resistances of the cells which increased with time for the catholyte and air-cathode cells but decreased for the bio-cathode cell. It was hypothesised that in the case of the catholyte fuel cell, the PEM and cathode were fouled with iron precipitation. In the case of the single-chambered air-cathode, a biofilm also formed on the cathode which grew over time. In both cases the diffusivity of protons from anode to cathode would be reduced and therefore increase internal resistance. For the bio-cathode cell, the formation of the biofilm had the opposite effect by reducing resistance to charge transfer.

Coulombic efficiency in the air-cathode MFC was very low and this is expected to be as a result of the aerobic respiration of the biofilm growing on the cathode. It was not made clear how the increase of biofilm thickness did not hinder proton transfer in the bio-cathode MFC. It is noted that the bio-cathode fuel cell was aerated and different inocula and media were used for the anodic and cathodic chamber. The bacteria on the bio-cathode were therefore different to those present on the air-cathode and oxygen transfer was improved for the bio-cathode fuel cell. This is likely to contribute to the catalytic effect of one cathodic biofilm over the other.

2.5.9 Temperature

It is often of interest to operate MFC at slightly elevated temperatures because of the effect on microbial kinetics, catalysed rates of oxygen reduction on a platinum coated cathode and improved mass transfer of protons through the liquid (Liu *et al*., 2005a; Du *et al*., 2007).

Most MFC studied are performed at temperature between 30-37°C (Liu *et al*., 2005a) and is done so in several ways: Liu and Logan (2004) maintained a constant fuel cell temperature by conducting the experiment in a constant temperature room (30°C). Jiang and Li (2009) conducted experiments in an incubator (30°C) and Zhu *et al.* (2011) made use of a water bath to maintain a constant fuel cell temperature (30°C).

Du *et al*. (2007) proposed that the biotransformation of substrate to electrons even at the maximum growth rate of microorganisms is slow as a result of the metabolism of the microorganisms and suggested accelerating the reaction by operating at higher temperatures or by using thermophilic microbial species.

When operating a MFC on an industrial scale, the system is most likely to be outdoors and the ambient temperature is likely to fluctuate considerably. It is possible to use insulation or a heating jacket to maintain a reasonably constant temperature however, this is often expensive and lower operational temperatures are attractive. Liu *et al*. (2005a) noted that a decrease in temperature from 32 to 20°C only reduced the power density by 9% which is likely to be a small enough change that operating at a lower temperature would be acceptable, especially in a wastewater treatment application.

2.6 INTEGREATION OF MICROBIAL FUEL CELLS INTO WASTEWATER TREATMENT SYSTEMS

2.6.1 Systems in Literature

The activated sludge process is the most widely used biological wastewater treatment technology today (Liu *et al*., 2011; Wang *et al*., 2014). An alternative to this process is the use of membrane bioreactors (MBRs) which are a highly efficient wastewater treatment method (Wang *et al*., 2012; Su *et al*., 2013).

As previously discussed, MFCs have presented themselves as a potentially effective method of wastewater treatment. There are however difficulties in directly treating wastewater with MFCs. For example wastewater produced in real-world applications contains various types of organic matter and bacteria including methanogens which as a result can disadvantage the electrochemically active bacteria in a MFC due to the complex metabolic process required and methanogenic competition. Wastewater also often has low buffer strength which hinders the transfer of charged particles and therefore electricity generation (Cha *et al.,* 2010). MFCs are regarded as biofilm reactors and therefore have difficulty removing particulate matter. It has been suggested to use post-treatment processing such as a solids contacting stage or a MBR (Logan, 2008), however the MFC removes a large amount of the organics which makes the operation of a bioreactor further downstream difficult.

In addition to this aeration is the largest fraction of energy consumption of the plant and can be anywhere between 45-75% of the energy costs. However, due to mass transfer limitations, much of the air cannot be consumed in the activated sludge process and is released to the atmosphere (Liu *et al*., 2011). It is therefore of interest to improve oxygen utilisation and lower energy consumption.

The opportunity to combine conventional processes with MFCs is therefore presented. The submerging of an air-cathode MFC into an aeration tank in the wastewater treatment process can be done easily with very little modification to the process and presents itself as a way to remove stages from the process, better utilise aerated oxygen, reduce electricity demand through electricity generation and potentially aid wastewater treatment.

A submerged air-cathode MFC system ultimately results in biofilm formation on the cathode to form bio-cathode. This is of interest due to its improved sustainability and catalytic properties compared to abiotic cathodes (He & Angenent, 2006; Cristiani *et al*., 2013)

Cha *et al.* (2010) conducted experiments in which two MFCs were submerged into the aeration tank in an activated sludge process. The anode chamber was rectangular with two carbon anodes inside it on opposite sides of the compartment. Cathodes separated from the anode by a PEM were placed on the outside of the chamber. In this way the aeration tank was used as the cathode chamber of the MFC.

The cell was initially run with activated sludge in the anode compartments and distilled water in the cathode compartment. It was found that the aeration of the cathodic chamber improved the mass transfer of oxygen to the cathode. If the aeration was stopped, despite having a high DO concentration in the bulk liquid which remained constant, the voltage over the MFC would drop. Even when nitrogen was replaced with air and the DO concentration was low the cell voltage remained high, implying that transfer of oxygen to the cathode was limiting and not the DO concentration.

It was found that when activated sludge replaced water as a catholyte the voltage across the cells dropped by almost half. This was attributed to aerobic bacteria using organic substances as electron donors instead of the cathode as expected in the case of a biofilm.

A study by Wang *et al*. (2012) investigated an integrated MFC-MBR system. The aeration chamber was used as a cathode and contained both a nylon membrane module and a non-woven fabric MFC chamber filled with a carbon fibre anode and surrounded by activated carbon fibre as a cathode. Wastewater was allowed to flow through the MFC with the effluent flowing into the aeration tank of the MBR. Initially the MFC was inoculated with anaerobic and activated sludge and submerged in an activated sludge reactor in order to enrich it with electroactive bacteria. Once the system became stable it was transferred to the aeration tank of the MBR.

The COD concentration of the effluent of the combined system was found to be considerably lower than for the MFC alone. Cyclic voltammetry was conducted on the biofilm on the cathode in order to determine its ability to catalyse oxygen reduction. The reduction peak potential was found to be similar to that of other biocatalysts for oxygen reduction. The peak was found to decrease when the system was sparged with nitrogen and rebound once oxygen was allowed to enter the system again indicating that oxygen reduction was occurring and being catalysed by the microorganisms.

Su *et al.* (2013) investigated a different type of integrated MFC-MBR system. It was noted that the MBR are subject to membrane fouling which is believed to be due to extracellular polymeric substances (EPS). It was hypothesised that these EPSs could be removed in the form of dissolved organic carbon after treatment with a MFC and therefore significantly reduce fouling.

The system consisted of two MBRs operating in parallel and fed with wastewater. The effluent from the system was fed to into a settling pool before being fed into a stack of single chamber MFCs with an anode and air-cathode on opposite sides. The effluent of the MFCs was fed back to the MBR.

It was found that the effective removal of sludge was improved with the addition of the MFC compared to a MBR system alone. Mitigation of membrane fouling was achieved by significantly reducing EPS content with the MFC.

Liu *et al*. (2011) investigated a system which used a membrane-less MFC submerged in a sequencing batch reactor (SBR). Wang *et al*. (2014) later gathered further information on the same integrated MFC-SBR. The MFC consisted of a tubular non-woven cloth, acting as a separator, filled with a granular graphite anode and graphite felt wrapped around the non-woven cloth as a cathode.

The influent to the system was allowed to flow through the MFC and then into the SBR which was aerated. This arrangement resulted in the formation of a thick biofilm on the cathode which was said to catalyse the reaction. Wang *et al*. (2014) discovered however that an excess amount of organic material in the aerobic SBR resulted in the growth of heterotrophs which consume large amount of the DO which hinders the reduction of oxygen.

Both studies found that increasing the hydraulic residence time (HRT) of the MFC resulted in more COD removed in this portion of the system. This has the benefits of improved electricity generation due to the increased degradation of organics by anodic bacteria and less organics in the SBR favoured the competition of cathode-respiring bacteria over heterotrophs and the sludge yield of the SBR was reduced. The overall effluent quality of the system was also improved in this way (Wang *et al*., 2014).

Cheng *et al*. (2010) investigated the use of membrane-less up-flow MFCs as a pre-treatment step in treating palm oil mill effluent. The system investigated used two MFCs to replace the conventional up-flow anaerobic sludge blanket (UASB) reactors. When compared to the conventional system, the MFC stage of the integrated system was found to have almost identical removal of COD to the UASB stage (above 90%). The MFC stage was however found to remove 76% of ammonia which UASB was unable to remove. This resulted in the integrated system performing more efficiently than the conventional anaerobic system.

What is apparent from the studies into integrated wastewater treatment systems is that many different configurations are possible which ultimately all result in varying degrees of improved water treatment and simultaneous electricity production. A summary of the performance and characteristic of the integrated systems is reported in Table 2-2. It may therefore be possible to integrate MFCs with various different types of existing systems, both as a step in the process or within an existing step. It may however be necessary to compromise on either electricity production or water treatment in order to better the other by altering several system variables.

Table 2-2: Performance and characteristics of systems combining MFCs with the activated sludge process

System Specifics	Electrodes	Power Density (W/m^3)	Reference
MFC in Activated Sludge Aeration Tank (PEM)	Graphite felt anode Graphite felt cathode	16.7 (MFC)[a]	Cha *et al*. (2010)
MFC - SBR	Graphite granule anode Carbon felt cathode	2.34 (TAC)[b]	Liu *et al*. (2011)
MFC-MBR	Activated carbon fibre anode Carbon felt Cathode	6 (MFC)[a]	Wang *et al*. (2012)
MFC-SBR	Graphite granule anode Carbon felt cathode	4.5 (TAC)[b]	Wang *et al*. (2014)

[a] Total volume of MFC
[b] Total volume of anodic compartment

2.6.2 Potential for Integration into Biological Sulphate Reduction Reactors

2.6.2.1 Background

The generation of sulphate-rich wastewater from Acid Rock Drainage (ARD) is of particular interest in South Africa. ARD and its contamination of surface and ground water presents itself as a significant problem in areas where mining activities have taken place, of which South Africa has many. It poses a threat to the environment, agriculture and human health especially in water sparse countries like South Africa (van Hille *et al*., 2015).

The mining and processing of ores containing sulphidic minerals, results in the exposure of waste rock, tailings and unworked pits. ARD is a result of the oxidation of the sulphide minerals, mainly pyrite (FeS_2), exposed to environmental oxygen and water. ARD contamination of water results in its acidification and poisoning by heavy metals (Gazea *et al*., 1996).

The diffusion of ARD into water sources may persist for several decades and may become expensive to treat, especially at decommissioned mining works where money is no longer being generated (Gazea *et al*., 1996). It is therefore of interest to find and economical method of treatment.

A suitable treatment method for ARD should result in its neutralisation and decreased concentration of sulphates, iron and other metals to environmentally acceptable concentration levels. It should also be low cost, easy to install and maintain and produce minimal unwanted by-products (Gazea *et al*., 1996).

Many technologies have been developed for the treatment of ARD and can be divided into two categories, namely active and passive treatment methods. Active treatments generally involve the use of chemicals such as lime ($CaCO_3$) or sodium hydroxide (NaOH) which is expensive and results in the formation of gypsum or metal hydroxides (Johnson & Hallberg, 2005).

Existing passive treatment methods involve the use of natural or constructed wetlands and anoxic limestone drains. Biological treatment systems which make use of the activity of sulphate reducing bacteria (SRB) can be used as both actively and passively (Gazea *et al*., 1996; Lens *et al*., 1998; Johnson & Hallberg, 2005).

2.6.2.2 Biological Sulphate Reduction Reactors

Many different types of reactors utilising BSR have been employed to treat sulphate-rich wastewater, and have been investigated and implemented on both a laboratory and full scale.

Continuously stirred tank reactors (CSTR) have frequently been utilised on a laboratory scale to elucidate the kinetics and microbial community structure associated with BSR (Moosa & Harrison, 2006; Oyekola *et al*., 2009; van Hille *et al*., 2015). Larger scale reactors include fluidised-bed reactors (FBR) (Kaksonen *et al*., 2003), up-flow anaerobic sludge blanked reactors (UASB) (Kaksonen, et al., 2003; Boshoff *et al*., 2004), up-flow packed bed reactors (Baskaran & Nemati, 2006), sequencing batch reactor (SBR) (Herrera *et al*., 1997), gas lift reactors (van Houten *et al*., 1995) and trench reactors (TR) (Boshoff *et al*., 2004)

As mentioned previously, there is often a significant amount of metals present in ARD wastewater. It is possible to use the hydrogen sulphide formed in the BSR bioreactor to precipitate metal sulphides from the incoming wastewater stream in a separate reactor (Hammack *et al*., 1994) or simultaneously in the BSR bioreactor (Kaksonen *et al*., 2003).

ARD is mainly derived from pyrite (FeS_2) and therefore the subsequent sulphate loading is typically higher than the metal loading. Even if a metal sulphide precipitation step was incorporated in the treatment process, it would be necessary to further treat the sulphide waste (van Hille *et al*., 2011)

A reactor of particular interest is a Linear Flow Channel Reactor (LFCR) currently being investigated by van Hille *et al*. (2015) to semi-passively treat ARD waste on a continuous basis. The reactors listed above are mainly active treatments methods which require large energy inputs in the form of pumping and sparging and/or will not fully remove the sulphide waste product which is formed in the BSR remediation of ARD waste. The LFCR presents itself as a low energy input treatment method which removes both sulphate and sulphide in a single processing step.

The LFCR attempts to make use of a combination of biological sulphate reduction in the bulk liquid and biological sulphide oxidation which takes place in a floating sulphur biofilm (FSB) which occurs on the surface. The FSB forms on the surface of the reactor as a result of the surface tension of the bulk liquid. The air-liquid interface is ideal for aerobic sulphide oxidising bacteria (SOB), as there is sufficient nutrients and oxygen which is required by the bacteria (Mooruth, 2011).

The FSB has been shown to be a true biofilm in its structure and functional features and can be anywhere from 50-500 µm thick. It has also been demonstrated to have aerobic, anoxic an anaerobic zones which are well differentiated. The redox conditions in the biofilm are poised over a narrow range around -150 mV which enables the formation of polysulphide and orthorhombic S_0 (Molwantwa & Rose, 2013).

Aqueous sulphide is generally in its dissociated state (HS^-). Both microbial and biotic sulphide oxidation can simultaneously occur within the biofilm as a result of the complex redox conditions within the reactor and biofilm (Mooruth, 2011).

Sulphide should be present in a ratio with oxygen of at least 2:1 in order to produce elemental sulphur. Therefore under oxygen limited conditions sulphur is the major product of bacterial sulphide oxidation (Equation 15), whereas sulphate is formed in a surplus of oxygen under high redox conditions (Janssen *et al*., 1997; Janssen *et al*., 1998).

The development of the biofilm is therefore very important as a fully developed biofilm ensures the correct sulphide to oxygen ratio by limiting the mass transfer of oxygen into the bulk liquid at the surface of the reactor. In a system with a poorly development biofilm, sulphide is likely to be fully oxidised back to sulphate as SOB gain more energy via this reaction than via partial oxidation to sulphur. In addition to this, if the sulphide loading in the reactor is low and no reduced sulphur compounds are available, the SOB will oxidise the elemental sulphur (Mooruth, 2011).

In conditions where the FSB is allowed to thicken, it will ultimately become too heavy and fall from the surface to the bottom of the reactor vessel where it will remain largely unreacted until removed. (Molwantwa & Rose, 2013). The reactor used by van Hille *et al*. (2015) therefore uses a mesh catchment device which sits just below the surface of the reactor and collect the biofilm as it falls. It is assumed not to affect the mass transfer of oxygen or sulphide significantly.

In a continuous system, the relatively slow growth rate of the SRB and their inability to attach well to solid substrates is a concern, as washout of the biomass can occur at low hydraulic residence times (HRT) (van Hille *et al*., 2015). In an attempt to achieve a high cell concentration and therefore improve the efficiency of sulphate reduction, van Hille *et al*. (2015) made use of carbon microfibers submerged in the bulk liquid of the reactor to provide a large surface area for bacterial adhesion, without significantly reducing the volume or altering the hydrodynamic properties of the reactor.

SRB and SOB have been shown to have the ability to use carbon electrodes as external electron acceptors and therefore produce electricity in MFCs which is discussed in detail in Section 2.8.2.5. The potential for an integrated MFC waste treatment system is therefore presented in which the carbon fibres could function as the anode electrode and the LFCR could be altered to include a cathode and therefore function as both a wastewater treatment reactor and a MFC.

van Hille *et al*. (2011) performed hydrodynamic studies on the LFCR by filling the reactor with sodium hydroxide. Acid was then pumped into the reactor at various concentrations and flow rates. The mixing profile in the reactor was revealed by a phenolphthalein tracer which turns bright pink at pH 8.2-12 and is colourless below pH 8.2. Therefore a colour change was observed as acid entered the reactor.

The hydrodynamic study revealed that no turbulent mixing took place and that partitioning of the solution into stagnant and motile zones occurred. A slight difference in the density of the two liquids resulted in the sinking of the acid to the base of the reactor. A similar difference in density was said to be expected between sulphide and incoming sulphate waste. It was noted that when an outlet port at the bottom of the opposite end of the reactor was used, influent would short circuit through the reactor by flowing along the bottom and out the outlet, and therefore significantly lower the residence time of each fluid element. This was avoided by using the outlet port on the same level as the inlet and resulted in the vertical displacement of fluid when the incoming solution reached the end of the reactor. In this way complete mixing could ultimately be achieved.

2.7 SINGLE-CHAMBERED CONTROL MFC

A significant amount of research has been conducted on the single chambered MFC originally proposed by Liu and Logan (2004). The fuel cell consists of a cylindrical chamber 3 cm in diameter and 4 cm long. The anode end is closed and the cathode end is open, allowing the diffusion of oxygen in the air through the carbon electrode as can be seen in Figure 2-8 below.

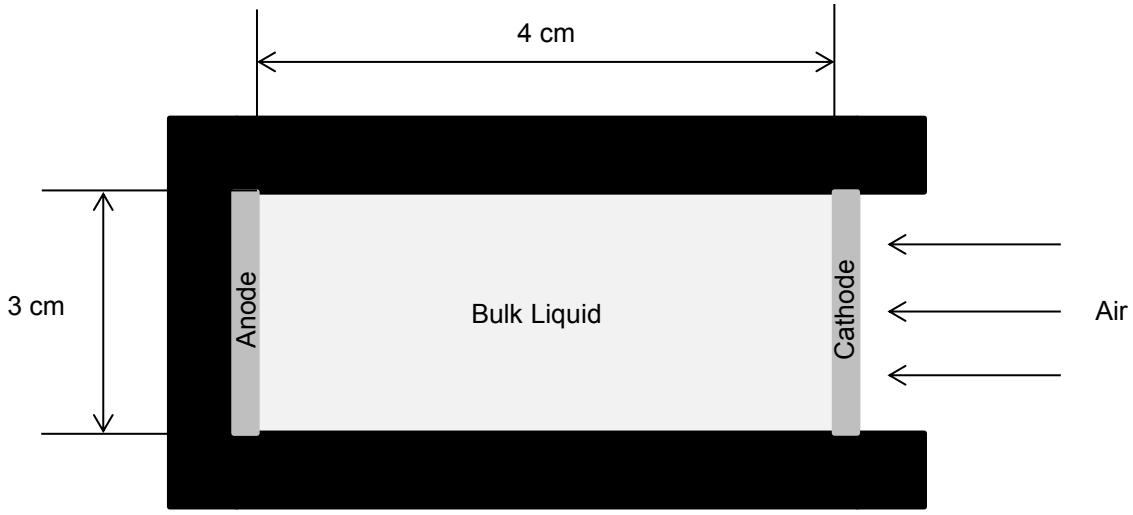

Figure 2-8: Schematic cross section of single-chambered MFC

The effect of several elements of this design on power generation have been investigated, the summary of which can be found in Table 2-3 below. Liu and Logan (2004) investigated the use of a PEM fixed to the cathode. Liu *et al*. (2005) investigated the effect of using different substrates (acetate and butyrate). Cheng *et al*. (2006) investigated the effects of adding several layers of polytetrafluoroethylene (PTFE) to the air facing side of the cathode electrode. Cheng and Logan

(2007) investigated the effects of treating the anode with ammonia and Logan *et al*. (2007) investigated the use of an ammonia treated carbon brush anode.

This design has also been investigated using several pure bacterial cultures. Xing *et al*. (2008) investigated both *Rhodopseudomonas palustris* strain DX-1, and a mixed consortium from a wastewater inoculum. Xing *et al*. (2009) investigated the electricity production of *R. palustris* DX-1 and *Rhodobacter. sphaeroides* DSM 9484 under different lighting conditions. *R. sphaeroides* was however found to perform poorly. Wu *et al*. (2013c) and Wu *et al*. (2013b) investigated *Shewanella sp.* HN-41 and *Shewanella oneidensis* MR-1 respectively. Both were found to perform reasonably well, producing 71.6 mW/m^2 and 73.9 mW/m^2 respectively when utilising lactate as a substrate. A summary of the investigation of these pure cultures can be found in Table 2-4 below.

Table 2-3: Summary of investigations done on single-chambered MFC

	Liu and Logan (2004)	**Liu *et al*. (2005)**	**Cheng *et al*. (2006)**	**Cheng and Logan (2007)**	**Logan *et al*. (2007)**
Cathode	Air-cathode, Carbon cloth (0.5mg/cm2 Pt catalyst)	Air-cathode, Carbon paper (0.35mg/cm2 Pt catalyst)	Air-cathode, Carbon cloth (0.5mg/cm2 Pt catalyst), Carbon powder with various diffusion layers of PTFE fixed in Nafion	Air-cathode, Carbon cloth (0.5mg/cm2 Pt catalyst), 4 diffusion layers of PTFE fixed in Nafion	Air-cathode, Carbon cloth (0.5mg/cm2 Pt catalyst), 4 diffusion layers of PTFE fixed in Nafion
Anode	Toray carbon paper (no wet proofing)	Toray carbon paper (no wet proofing)	Carbon paper (no wet proofing)	Carbon paper (no wet proofing), ammonia treated	Toray carbon paper (no wet proofing untreated), carbon brush ammonia treated
Bacteria	Bacteria in wastewater	Bacteria in wastewater	Bacteria in wastewater	Bacteria in wastewater	Bacteria in wastewater
Substrate	Domestic wastewater, glucose	Acetate, Butyrate	Glucose	Sodium Acetate with 200mM phosphate buffer	Acetate with 200mM phosphate buffer
Power Density (W/m^3) **(Total volume)**	6.6 W/m^3 (PEM glucose), 12.5 W/m^3 (no PEM glucose), 0.7 W/m^3 (PEM), 3.7 W/m^3 (no PEM)	12.7 W/m^3 (Acetate), 7.6 W/m^3 (Butyrate)	11.8 W/m^3 (carbon cloth), 13.5 W/m^3 (no DL), 19.4 W/m^3 (4 DLs)	95 W/m^3 (untreated), 115 W/m^3 (treated)	29 W/m^3 (Carbon cloth), 73 W/m^3 (brush)
Power Density (mW/m^2) **(Anode area)**	262 mW/m^2 (PEM glucose), 494 mW/m^2 (no PEM glucose), 28 mW/m^2 (PEM), 146 mW/m^2 (no PEM)	506 mW/m^2 (Acetate), 305 mW/m^2 (Butyrate)	473 mW/m^2 (carbon cloth), 538 mW/m^2 (carbon powder no DL), 776 mW/m^2 (Carbon powder 4 DLs)	1640 mW/m^2 (untreated), 1970 mW/m^2 (treated)	1070 mW/m^2 (Carbon cloth), 2400 mW/m^2 (brush)

Table 2-4: Summary of investigations done on single-chambered MFC using pure bacterial cultures

	Xing *et al*. (2008)	**Xing *et al*. (2009)**	**Wu *et al*. (2013c)**	**Wu *et al*. (2013b)**
Cathode	Air-cathode, Carbon cloth (0.5mg/cm2 Pt catalyst), 4 diffusion layers of PTFE fixed in Nafion (Membrane outside)	Air-cathode, Carbon cloth (0.5mg/cm2 Pt catalyst), 4 diffusion layers of PTFE fixed in Nafion	Air-cathode, Carbon cloth (0.5mg/cm2 Pt catalyst) fixed in Nafion	Air-cathode, Carbon cloth (0.5mg/cm2 Pt catalyst), 4 diffusion layers of PTFE fixed in Nafion
Anode	Carbon paper (no wet proofing), carbon brush, ammonia treated	Carbon paper (no wet proofing), carbon brush, ammonia treated	Carbon paper (no wet proofing)	Carbon paper (no wet proofing)
Bacteria	Bacteria in wastewater, *R. palustris* DX-1	*R. sphaeroides* DSM 9484, *R. palustris* DX-1	*Shewanella sp.* HN-41	*Shewanella oneidensis* MR-1
Substrate	Acetate with 200mM phosphate buffer	Acetate with 50mM phosphate buffer	Glucose, Lactate	Lactate with Fe(III) citrate
Power Density (W/m^3) **(Anode volume)**	34 W/m^3 (cloth) 86.6 W/m^3 (brush),	12.6 W/m^3 (*R. palustris*) 3.92 mW/m^3 (*R. sphaeroides*)	2 W/m^3 (lactate) 509 mW/m^3 (Glucose)	2.01 W/m^3 (No Fe(III)) 4.43 W/m^3 (6mM Fe(III))
Power Density (mW/m^2) **(Anode area)**	1170 mW/m^2 (cloth), 2720 mW/m^2 (brush)	450 mW/m^2 (*R. palustris*) 0.14 mW/m^2 (*R. sphaeroides*) 1000lx	71.6 mW/m^2 (Lactate) 18.2 mW/m^2 (Glucose)	73.9 mW/m^2 (No Fe(III)) 158.1 mW/m^2 (6mM Fe(III))

2.8 MICROBIAL SYSTEMS

2.8.1 Shewanella oneidensis MR-1

Shewanella oneidensis MR-1 has previously been called *Shewanella putrefaciens* MR-1 and *Alteromonas putrefaciens* MR-1 (Heidelberg *et al*., 2002; Tang *et al*., 2007b). *S. oneidensis* is a mesophilic facultative anaerobe (i.e. capable of both aerobic and anaerobic respiration) found primarily in sediment environments (Tang *et al*., 2007a; Pinchuk *et al*., 2011) and capable of utilising several different carbon sources including lactate, acetate, pyruvate and some amino acids (Tang *et al*., 2007b).

S. oneidensis is capable of reducing a variety of electron acceptors which include oxygen, oxidised metals (Fe(III), Mn(III) Mn(IV), Cr(VI) and U(VI)), sulphite, elemental sulphur, nitrate, fumarate, dimethyl sulphoxide, trimethylamine N-oxide and thiosulphate (Heidelberg *et al*., 2002; Tang *et al*., 2007b). As a result *S. oneidensis* has been used in several bioremediation applications involving toxic metals (Heidelberg *et al*., 2002; Tang *et al*., 2007b).

S. oneidensis is capable of the direct reduction of dissolved chromium and uranium in liquid states into insoluble oxides. It is also capable of producing large amounts of sulphide from thiosulphate or elemental sulphur which can form insoluble metal sulphides with toxic metals which in turn immobilises them. *S. oneidensis* has been proposed for use in removal of organic pollutants, as the redox potential of iron and manganese ions as terminal electron acceptors is high enough to drive oxidation of organics (Heidelberg *et al*., 2002).

More recently *S. oneidensis* has been used to produce electricity from different substrates under anaerobic conditions. Kim *et al*., (1991) demonstrated that *S. oneidensis* is capable of using lactate as an electron donor and a graphite electrode and an electron acceptor while producing electricity in a mediator-less system without any added metals. Subsequent studies have also used *S. oneidensis* in microbial fuel cells (Park & Zeikus, 2002; Kim *et al*., 2002; Lanthier *et al*., 2008; Wu *et al*., 2013b).

Ringø *et al.* (1984) found that a strain of *Altermonas putrefaciens* (now *Shewanella oneidensis*) did not grow anaerobically in the absence of an external electron acceptor, even when organic carbon in the form of glucose and ribose were present in solution. Fermentation is a form of heterotrophic growth in which organic carbon is used as a terminal electron acceptor in place of oxygen. As a result of the inability of *S. oneidensis* to use organic carbon as a terminal electron acceptor, it was said to have no fermentative energy metabolism. Bacteria without a fermentative metabolism are capable of completely oxidising substrate to CO_2 by means of tricarboxylic acid (TCA) cycle, in which anaerobic electron acceptors replace oxygen and therefore an aerobic type of metabolism is retained (Ringø *et al.,* 1984)

Ringø *et al.* (1984) also noted that when *S. oneidensis* was grown anaerobically with trimethylamine oxide (TMAO) as an electron acceptor, it preferred substrates more easily converted to pyruvate (such as serine, cysteine and lactate) or TCA cycle intermediates (i.e. glytamate and aspartate). It was noted that the use of lactate as a substrate resulted in the formation of 40 mol% of acetate per mol of lactate, whereas serine and cysteine were completely oxidised to CO_2. This was believed to be as a result of lactate conversion to acetyl-CoA being faster than further oxidation of acetyl-CoA via the TCA cycle. The pathway proposed by Ringø *et al.* (1984) for lactate degradation by *S. oneidensis* is given by Figure 2-9 below.

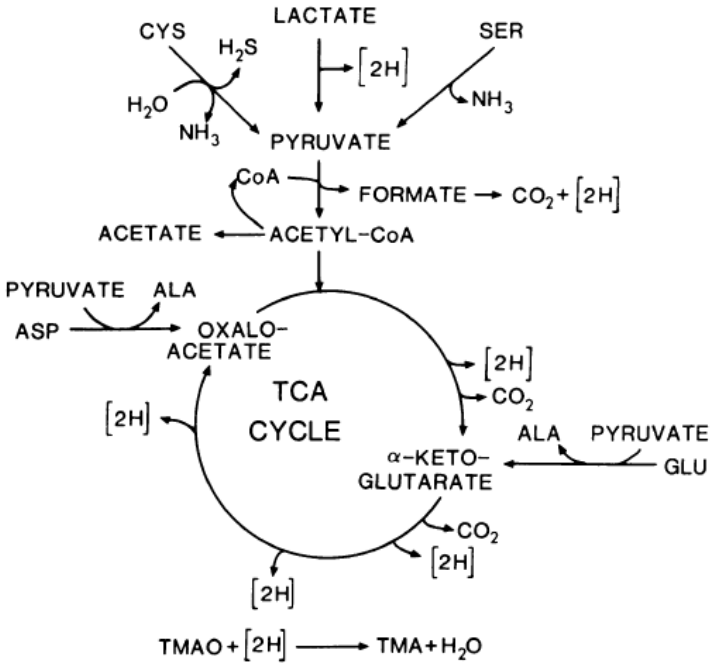

Figure 2-9: Pathways for degradation of lactate and preferred amino acids during TMAO-dependent anaerobic growth of *S. oneidensis* (Ringø *et al*., 1984)

Lovley *et al*. (1989) also noted that when *S. oneidensis* was grown anaerobically with Fe(III) as the terminal electron acceptor, when lactate and pyruvate were used as substrates, both were oxidised to acetate and not metabolised any further, resulting in the accumulation of acetate in the system.

When grown in oxygen limiting conditions, *S. oneidensis* can utilise both acetate and lactate as carbon sources simultaneously but has a strong preference for lactate (Tang *et al*., 2006). Tang et al. (2006) noted that from the growth curves observed for the aerobic digestion of lactate, that high acetate concentrations generally inhibit cell growth.

It is therefore unlikely to be a good microorganism for simultaneous wastewater treatment and electricity generation. Although it may effectively generate current, it will be unable to reduce the COD of wastewater significantly under the conditions of an MFC because acetate cannot be degraded further.

2.8.1.1 Shewanella oneidensis MR-1 in MFCs

Pure cultures of microorganisms have been used in MFCs in an attempt interpret the physiology of the processes involved in the electron transfer within the MFCs (Lanthier *et al*., 2008). *Shewanella* species were the first microorganisms shown to directly transfer electrons to an electrode and were proposed to do this means of electron–transfer proteins (Kim *et al*., 1999). This, in conjunction with the ease of growing these microorganisms, has resulted in common use in MFCs.

Kim *et al*. 2002 investigated a dual-chambered MFC with three strains of *S. oneidensis* (IR-1, MR-1 and SR-21) digesting lactate with all three showing good electrochemical activity when grown anaerobically without a mediator or external electron acceptor. Lanthier *et al*. (2007) investigated an H-type MFC using *S. oneidensis* MR-1 which produced 8.2 mW/m^2 using lactate as a substrate. Ringeisen *et al*. 2006 used a miniature MFC with a volume of 1.2 cm^3 to produce a power density of 500 W/m^3 (per anode compartment volume) with a graphite felt anode and lactate as a carbon source using *Shewanella oneidensis* DSP10. Parks and Zeikus (2002) used *S. oneidensis* in a single-

chambered MFC with a Mn^{4+} graphite anode to produce a power density of 10 mW/m^2 with lactate as a substrate.

Wu *et al*. (2013b) and Wu *et al*. (2013c) investigated *Shewanella sp.* HN-41 and *Shewanella oneidensis* MR-1 respectively. Both were found to perform reasonably well in single-chambered MFC with an air-cathode, producing 71.6 mW/m^2 and 73.9 mW/m^2 respectively when utilising lactate as a substrate.

2.8.1.2 Mechanism of Electron Transport

von Canstein *et al*. 2008 demonstrated that *Shewanella* species are able to produce flavins which act as soluble redox mediators which effectively shuttle electrons between the microbe and the metal to be reduced or the anode in the case of MFC. Flavin mononucleotide (FMN), flavin adenine dinucleotide (FAD) and riboflavin were all identified. FAD was found to be a predominantly intracellular flavin and not released by living cells. Electrochemical analysis has revealed that 70% of the electrons transferred from *Shewanella* species to the electrode, are done so by means of flavins (Wu *et al*., 2013a).

Wu *et al*. (2013a) investigated the effect that different electron acceptors present in solution had on the secretion of flavins by *S. oneidensis* MR-1. These included fumarate, ferrihydrite, Fe(III)-nitrilotriacetic acid (NTA), nitrate and trimethylamine oxide (TMAO). A large difference in flavin secretion was noted for the different electron acceptors. Nitrate and ferrihydrite was found suppress flavin secreting whereas Fe(III)-NTA, TMAO and fumarate caused an increase in flavin secretion and improved electricity generation. Wu *et al*. (2013b) demonstrated that the addition of Fe(III) citrate also resulted in improved flavin secretion and electricity generation.

Electron acceptors such as Fe(III) are largely insoluble in neutral pH environments. The production of flavins allows the microbe to reduce electron acceptors which are some distance away from the cell as a result of their solid form (von Canstein *et al*., 2008; Wu *et al*., 2013b).

The production of flavins results in both reduction of the electron acceptor and improved electron transfer from the microbe to the anode, resulting in improved electricity production (Wu *et al*., 2013a; Wu *et al*., 2013b).

It has also been shown that the bacterium is capable of producing conductive nanowires in oxygen limited environments containing electron acceptors (Myers & Myers, 1992; Logan & Regan, 2006; Pirbadian *et al*., 2014). Nanowires are a method of extracellular electron transport (EET) between the respiratory chain of the bacteria and external surfaces and touch both other cells and the surface of the electrode, or solid to be reduced (Logan & Regan, 2006; Pirbadian *et al*., 2014). They are essentially an extension of the outer cell membrane and periplasmic electron transport components (Pirbadian *et al*., 2014).

2.8.2 Sulphidogenic Microbial Systems

Sulphate-rich wastewaters are generated by many industrial processes which include mining, food processing, pulp and paper processing, animal husbandry and pharmaceuticals processing (Janssen *et al*., 1997; Lens *et al*., 1998; Pokorna & Zabranska, 2015).

The presence of sulphate in wastewater results in increased acidity and the production of sulphide by biological sulphate reduction (BSR) which is mediated by sulphate reducing bacteria (SRB). Sulphide takes the form of S^{2-}, H^{S-}, H^2S and insoluble metallic sulphides (Lens *et al*., 1998). Hydrogen sulphide gas is odorous and toxic to both humans and animals and dissolved sulphides are corrosive to metals and concrete, and increase the COD of wastewater. Sulphur species should therefore be removed from wastewater before it can be discharged to the environment (Zhao *et al*., 2008; Janssen *et al*., 1997).

As mentioned previously, the removal of sulphur compounds by means of chemical and physiochemical treatments (e.g. precipitation, aeration and gas stripping) is often complex and expensive, whereas microbial processes operate at moderate temperatures and atmospheric pressure and therefore have lower energy inputs and are simpler, sustainable and cost effective (Gazea *et al*., 1996; Johnson & Hallberg, 2005; van Hille *et al*., 2015). There are also likely to be several processing steps for the removal of both sulphate and sulphide.

Both SRB and SOB are naturally ubiquitous in both anaerobic and aerobic wastewater sludge as they play a vital role in the maintenance of the sulphur biogeochemical cycle within the earth's lithosphere (Shen & Buick, 2004). They also have the ability to work synergistically to remediate wastewater and remove both sulphate and sulphite simultaneously. In addition to this, their economical and sustainable implementation as a wastewater treatment method makes their combined use very attractive (Lens *et al*., 1998; van Hille *et al*., 2011).

2.8.2.1 Mechanism of Dissimilatory Sulphate Reduction

SRB have the ability to use sulphate ions as electron acceptors during anaerobic respiration which provides the cell with energy for growth and maintenance. (Postgate, 1984; Widdel, 1988; Shen & Buick, 2004). This pathway is referred to as dissimilatory sulphate reduction.

Dissimilatory sulphate reduction takes place within the cell. Exogenous sulphate is actively transported through the bacterial cell wall before undergoing several reduction steps to sulphite which is catalysed by soluble enzymes. Membrane-bound enzymes then further reduce sulphite to sulphide which is released back into solution. The biochemical pathway may differ between species (Shen & Buick, 2004).

SRB are either autotrophs, making use of H_2 and CO_2 as electron donors, or heterotrophs which oxidise organic substrate (Postgate, 1984). A general equation for the reduction of sulphate is given by Equation 2 below (Oyekola *et al*., 2009). In anaerobic conditions in the presence of sulphate, sulphite or thiosulphate, heterotrophic SRB carry out sulphate reduction by either complete or incomplete oxidation. Using the example of lactate as a carbon source, complete oxidisers oxidise substrate to either bicarbonate or CO_2 (Equation 3), whereas incomplete oxidiser oxidise substrate most often to acetate (Equation 4) (Widdel, 1988). It has been suggested that the metabolism of incomplete oxidisers does not include the TCA cycle (Widdel, 1988; Lens *et al*., 1998)

$$Electron\ donor + SO_4^{2-} = 2HCO_3^- + H_2S \qquad \text{Equation 2}$$

$$2\ lactate + 3SO_4^{2-} \rightarrow\ 6HCO_3^- + 3HS^- + H^+\ \ (\Delta G_\circ = -253.3\ kJ)$$ Equation 3

$$2\ lactate + SO_4^{2-} \rightarrow\ 2\ acetate + 2HCO_3^- + HS^- + H^+\ \ (\Delta G_\circ = -160.1\ kJ)$$ Equation 4

Although they degrade a wide variety of substrates, SRB do not degrade polymeric compounds such as polysaccharides, proteins or lipids SRB rely on fermentative bacteria for the degradation of these complex organics into substrate they are capable of degrading. As a result of the secondary pollutants which may be formed through the partial oxidation of complex organic compounds, it is of interest to use simple carbon sources in treatment of sulphidogenic wastewater if the addition of carbon sources is necessary (Ravenschlag *et al*., 2000).

Heterotrophic SRB have the ability to oxidise formate, acetate, pyruvate as well as other volatile fatty acids (propionate, butyrate, and lactate), alcohols such as methanol and ethanol, fumarate, succinate, malate and aromatic compounds (Lens *et al*., 1998).

Several studies have noted that the use of lactate as a substrate has several benefits. Brandt *et al*., (2001) conducted an experiment in a hypersaline environment in which H_2, lactate, acetate, propionate and butyrate were tested as substrates. It was found that the highest sulphate reduction rates were noted for systems with lactate and H_2 as a substrate. Purdy *et al*. (1997) tested the same VFAs (lactate, acetate, propionate and butyrate) as substrate in freshwater and marine sediments and reported higher sulphate reduction rates and substrate utilisation rates for lactate systems. Postgate (1984) reported higher doubling times for SRB utilising lactate as a substrate compared to acetate (3-6 hours and not less than 20 hours respectively).

In addition to this, Kuo and Shu (2004) reported that the use of lactate as substrate decreased the inhibition of microbial activity by sulphide. A system utilising lactate as a substrate was capable of operating steadily at concentrations of 200-400 mg/ℓ of dissolved sulphide and 100-150 mg/ℓ undissociated sulphide, whereas systems utilising acetate and butyrate were inhibited at concentrations of dissolved and undissociated hydrogen sulphide of 150-200 mg/ℓ and 60-75 mg/ℓ respectively.

Some strains of sulphate reducing bacteria are capable of fermentative metabolisms in the absence of sulphate, for example the fermentation of lactate for the production of acetate and propionate given by Equation 5 (Heimann *et al*., 2005).

$$3\ lactate \rightarrow\ acetate + 2\ propionate + CO_2 + H_2O\ \ (\Delta G_\circ = -169.7kJ)$$ Equation 5

2.8.2.2 Environmental Conditions Affecting Sulphate Reduction

Although SRB grow well over a wide range of temperatures and adapt well to temperature changes (Postgate, 1984), the majority of SRB are mesophilic and grow best in a temperature range of 25-40°C (Castro *et al*., 2000).

SRB require a redox potential below -200 mV for growth, and therefore exist only in a reducing environment. The low redox potential is achieved with high sulphide content from sulphate reduction and extremely low oxygen concentrations (Postgate, 1984).

SRB are inhibited at acidic and strongly alkaline pH ranges (below 6 and above 9 respectively). They buffer their environment through the consuming of H+ ions (Equation 6) (Widdel, 1988) and the production bicarbonate ions in sulphate reduction which (Equation 3 and Equation 4).

$$4H_2 + SO_4^{2-} + H^+ \rightarrow 4H_2O + HS^-$$ Equation 6

Sulphide has been shown to be toxic to many anaerobic microorganisms including SRB and MB, and as a result inhibits the metabolism of the cells (O'Flaherty *et al*., 1998; Lens *et al*., 1998; Moosa &

Harrison, 2006). Sulphide in its undissociated (H_2S) is cell permeable and interferes with intracellular pH. This form of the sulphide species is therefore considered to be toxic. The concentration of the different sulphide species is highly dependent on pH (O'Flaherty *et al*., 1998).

Hydrogen sulphide may dissociate according to the following reactions (Dean, 1999):

$$H_2S \leftrightarrow HS^- + H^+ \ (pK_{a1} = 6.97 \ at \ 25℃) \quad \text{Equation 7}$$

$$HS^- \leftrightarrow S^{2-} + H^+ \ (pK_{a2} = 12.9 \ at \ 25℃) \quad \text{Equation 8}$$

In a pH range of 6 to 8, hydrogen sulphide exists as both H_2S and HS^- . Further dissociation of HS^- to S^{2-} takes place around pH 12. Above pH 7, dissolved sulphide is predominantly in its ionic form, whereas low pH favors the undissociated species.

2.8.2.3 Interactions with Other Microbial Communities

Wastewater treatment environments contain many different microbial species and become complex ecosystems. Sulphate containing wastewater is degraded anaerobically through the collaborative mechanism of five main groups of organisms, namely: hydrolytic, fermentative, acetogenic, methanogenic and sulphate reducing (Menert *et al*., 2004).

As mentioned above, SRB are unable to degrade polymeric compounds and rely syntrophically on fermentative microorganisms to degrade complex substrates. Therefore methanogenisis and sulphate reduction are the terminal processes of the degradation reactions (Patidar & Tare, 2005).

SRB consequently compete with methanogenic bacteria (MB) for common available substrate. These are primarily hydrogen and acetate. (Lens *et al*., 1998; Menert *et al*., 2004; Patidar & Tare, 2005). The ability of SRB to outcompete MB therefore depends on their ability to utilize methanogenic substrates. Acetate utilising SRB have been shown to have higher growth rates than acetate utilising MB. The SRB also gain more energy from the consumption of acetate than MB, both of which give them an advantage over the MB (Oude Elferink *et al*., 1994; Lens *et al*., 1998). Hydrogen utilising SRB proliferate over MB by maintaining substrate at a partial pressure which is too low to be utilised by MB (Lovley & Phillips, 1987; Omil *et al*., 1996).

At sufficiently high sulphate concentrations, SRB are able to outcompete MB. By the same logic the growth of SRB is sulphate limited at low sulphate concentrations. Theoretically 0.67 g of O_2 per g SO_4^{2-} is needed for complete oxidation of substrate and reduction of sulphate. The ratio of COD to sulphate necessary for SRB to become dominant is below 1.7, whereas MB will predominate at ratios above 2.7. COD/sulphate. Ratios of 1.7-2.7 will result in the competition of SRB and MB (Lens *et al*., 1998; Pokorna & Zabranska, 2015).

It has been shown that sulphate limitations may occur as a result of mass transfer limitations into a biofilm. Nielsen *et al*. (1987) showed that in what was considered a thin biofilm (<300 µm), sulphate reduction was limited by diffusion of sulphate into the biofilm at concentrations lower than 50mM when organic concentration is not limited. It is therefore possible that MB will proliferate in areas of the biofilm where sulphate is limited.

It has also been suggested that MB have a better capacity for attachment than SRB (Omil *et al*., 1996) which is likely to affect the outcome of the competition between the two species in a case when MB become the dominant attached species in a continuous reactor with a short HRT.

The pH of a system has been shown to have a significant effect on the competition of SRB and MB. Acetogenic SRB and MB have optimal pH ranges of 7.3-7.6 and 6.5-7.8 respectively (Widdel, 1988; Lens *et al*., 1998). Although these values lie in the same range, SRB are better able to tolerate higher

pH values (above 7.7) than AMB, whereas the reverse is true for lower pH values (below 6.9) (Visser *et al*., 1996).

Mesophilic MB grow optimally in similar temperatures ranges to mesophilic SRB, and both respond similarly to changes in temperature between 10-50°C although SRB are more resilient to high temperature shocks (Lens *et al*., 1998)

The outcome of the competition between SRB and MB will determine to what extent sulphide and methane are produced (Lens *et al*., 1998). The intent of treating wastewater is both to lower the COD and remove toxic substances. Therefore when treating wastewater rich in sulphur species, MB may remove organics and produces methane as a useful by-product, however in order to remove sulphur species the conditions of the process should favour SRB and the production of sulphide.

2.8.2.4 Biological Sulphide Oxidation

Both abiotic and biological sulphide oxidation are capable of occurring simultaneously. The two most important oxidation reactions which sulphide may undergo are given as Equation 9 and 10 below (Janssen *et al*., 1997; Lens *et al*., 1998):

$$2HS^- + O_2 \rightarrow 2S^\circ + 2OH^- \qquad \text{Equation 9}$$

$$2HS^- + O_2 \rightarrow 2SO_4^{2-} + 2H^+ \qquad \text{Equation 10}$$

The partial oxidation of sulphide to elemental sulphur (Equation 9) occurs when dissolved oxygen concentrations are below 0.1 mg/ℓ and therefore considered oxygen limiting conditions. Complete sulphide oxidation to sulphate (Equation 10) occurs under sulphide limiting conditions at higher concentrations of dissolved oxygen (Janssen *et al*., 1997; Lens *et al*., 1998).

The partial biological oxidation of sulphide presents an economically viable method of wastewater treatment which can take place in varying availability of oxygen. The produced sulphur (S°) is nonsoluble and can be removed from wastewater as a precipitate, resulting in the total reduction of sulphur content of the wastewater. Sulphur is also a commodity raw material for several processes (Janssen *et al*., 1997; Janssen *et al*., 1998).

The biological oxidation of sulphides is based on the action of photoautotrophic or chemolithotrophic SOB. Photoautotrophic SOB obtain the energy required to oxidise sulphide from light energy, whereas chemolithotrophic SOB obtain it directly from the oxidising reaction. In this case oxygen is reduced in aerobic conditions whereas nitrates and nitrites serve as electron acceptors in anoxic systems (Lens *et al*., 1998; Pokorna & Zabranska, 2015).

Among the most frequent photoautotrophic SOB are green sulphur-oxidising bacteria and purple sulphur-oxidising bacteria. Photoautotrophic SOB have a slow growth rate and require a sufficiently strong light source for oxidation of sulphide to take place, which complicates their use in bioreactors (Pokorna & Zabranska, 2015).

Chemolithotrophic SOB are also known as colourless sulphur-oxidising bacteria. They are able to maintain a high rate of sulphide oxidation as a result of their high affinity for sulphide and oxygen (Pokorna & Zabranska, 2015), which allows them to effectively oxidise sulphide in environments with low oxygen concentrations and compete with chemical oxidation (Janssen *et al*., 1998). In addition to this, their low nutritional requirement makes them an appropriate choice for biological sulphide removal.

The conditions maintained for the sulphidogenic systems within the laboratory favour chemolithotrophic SOB. The light source is either limited or removed completely in most cases and they are most likely the dominant SOB in the systems used.

2.8.2.5 Sulphidogenic Bacteria in Microbial Fuel Cells

In recent years much research has been done into the treatment of wastewaters polluted with sulphur species using microbial fuel cells (Rabaey *et al*., 2006; Zhao *et al*., 2008; Zhao *et al*., 2009; Sun *et al*., 2010; Lee *et al*., 2012; Chou *et al*., 2014; Chou *et al*., 2013; Lee *et al*., 2014; Weng & Lee, 2015). Microbial fuel cells present a passive method of treatment which is both economical and environmentally compatible (Dutta *et al*., 2008).

Rabaey *et al*. (2006) investigated MFCs inoculated with a mixed culture of sulphide oxidising bacteria for the treatment of sulphide laden wastewater. One MFC was placed in parallel with a 50Ω resistor and the other remained in open circuit mode. No substantial removal of sulphide was observed in the open circuit cell. It was noted that the anodic potential remained around -0.310 V vs Standard Hydrogen Electrode (SHE). Sulphide oxidation is unlikely to occur, as potentials of higher than 0.274 V vs SHE are required. When the anode potential of the connected MFC was altered between -0.3 V to 0 V vs SHE (in intervals of 0.1 V), it was noted that the sulphide was oxidised rapidly at -0.2 V and further increases in potential resulted in considerably lower generation of current.

Chou et al. 2014 also demonstrated that a negative poised potential accelerated start-up time and improved electricity generation in a dual-chambered MFC degrading sulphate wastewater. The negative poised potential also promoted the growth of electrochemically active bacteria on the anode.

Although two sulphide oxidising bacteria were identified from samples taken from the MFCs (namely *Alcaligenes* sp. and *Paracoccus* sp.), the effects of abiotic oxidation of sulphide was not decoupled from biotic oxidation and although the presence of a biofilm in the system did not hinder the oxidation of sulphide, there is no proof that biological oxidation was significant.

Dutta *et al*. (2008) investigated the spontaneous electrochemical oxidation of aqueous sulphide in an abiotic fuel cell at ambient temperature, pressure and neutral pH. The fuel cell used was dual-chambered making use of a ferricyanide catholyte. It was found that sulphide oxidised spontaneously resulting in simultaneous power generation and sulphur product formation. A power density of up to 166 W/m^3 (net area of the anodic compartment) was achieved and was found to increase with an increase in sulphide concentration. It was also found that over time the sulphur product, which deposited on the anode, reduced the further oxidation of sulphides.

Zhao *et al*. (2008) also demonstrated that the addition of sulphide to an abiotic MFC in which the anode potential was poised at 0.2 V vs Ag/AgCl, resulted in substantial current generation. The capability of the cell to oxidise sulphur was observed to decrease with time and was hypothesised to be a result of the deposition of sulphur on the anode. Further research was conducted on a single-chambered MFC with and air-breathing cathode. A pure culture of *Desulfovibrio desufuricans* was used to treat synthetic sulphate laden wastewater. A pathway of sulphate removal was suggested whereby sulphate is reduced by *D. desulfuricans* to sulphide. Sulphide is then adsorbed onto the anode and chemically oxidised to elemental sulphur or soluble polysulphides. Depending on the potential of the anode, sulphur may be oxidised back to sulphate.

Lee *et al*. 2012 investigated the use of a mixed community of SRB for simultaneous wastewater treatment and electricity generation. Three identical dual-chambered MFCs were started up with a mixed SRB inoculum. Once the MFCs were running with similar performance, the lactate and sulphate was removed from the feed to two cells respectively. This resulted in a notable decrease in potential for both cells. The remaining cell was then fed with only sulphide. This too resulted in a

notable decrease in potential. When sulphide was added to the lactate only cell, the potential increased once more.

It was concluded that the enriched biofilm was unable to utilise lactate alone and required the presence of sulphate to produce sulphide. Sulphide was said to be the principal electron donor which was oxidised by the biofilm to from elemental sulphur.

Lee *et al*. 2014 further investigated the use of a mixed community of SRB and SOB in an anodic biofilm for the simultaneous removal of sulphate and organic carbon from wastewater. Electrochemical Impedance Spectroscopy (EIS) was used to measure the ohmic internal resistance of the MFC. It was noted that when an abiotic anode electrode was used with fresh media (consisting of sulphate and lactate), the resistance was of the order of 300 kΩ which would imply negligible electricity production. When spent media was applied (which contained sulphide), the resistance decreased to around 450 Ω although the power density produced remained very low at 1.05 mW/m^2. It was suggested that even though chemical oxidation of sulphide was feasible, it did not occur as a result of the diffusional resistance from the bulk solution to the anode surface.

Conversely when a biotic anode was used with both fresh and spent medium, the resistance was decreased to 120 Ω and 17.1Ω respectively with high power densities being achieved. It was assumed that electrical resistance between the SOB cell and anode was negligible. It was therefore concluded that the electricity production was primarily via biological activities rather than pure chemical reactions and oxidation of sulphide was not efficiently oxidised in the absence of a biofilm. The distance between an SRB an SOB cell was assumed to be about 4 µm. Sulphate reduction by SRB resulted in the formation of sulphide which was rapidly converted by the SOB to S^0.

Sun *et al*. (2010) conducted research on the microbial communities involved in the electricity generation by sulphide oxidation. Two single-chambered MFC with air cathodes were investigated. One remained abiotic. It was demonstrated that although instantaneous electrochemical oxidation of sulphide is possible, the involvement of SOB resulted in higher and more consistent power generation. The anode of the biotic MFC was replaced to investigate the power generation by planktonic cells. The colonised anode was placed into a new cell with fresh media. Both reactors were spiked with sulphide and both produced similar maximum current densities although the power produced in the reactor with the colonised anode decreased faster than the reactor with the planktonic cells. Both reactors also produced higher current than that of the abiotic control.

It was concluded that both the planktonic cell and cells within the biofilm are responsible for power generation and can work independently of each other although a synergistic relationship was proposed between the two, as higher electricity generation was seen when both were present. Classification of the microbial communities showed a significant difference between the planktonic cell and those in the biofilm. The communities present were consistent with the characteristics of electricity producing and sulphide oxidising bacteria. Exoelectrogenic bacteria were found on both the anode and in solution, although it was noted that the SOB present in the cell grew mainly on the electrode whereas the majority of SRB present were planktonic.

Sangcharoen *et al*. 2015 also conducted research on a single-chambered air-breathing MFC treating sulphate laden wastewater, and found that an analysis of the microbial community revealed that sulphur oxidising bacteria were the dominant species present on the anode and SRB were dominant in solution. It was also noted that over time the potential of the cell decreased. This was attributed to the build-up of elemental sulphur deposited on the anode. Replacement of the anode resulted in an increase of potential. This is in keeping with previous findings (Dutta *et al*., 2008; Zhao *et al*., 2008).

Sangcharoen *et al*. 2015 suggested possible mechanisms for the treatment of water containing sulphate and organics (Figure 2-10). The first is the reduction of sulphate by SRB either as planktonic

cell and/or within the anodic biofilm which remove organic compounds and produces sulphide. Sulphide is then either oxidised abiotically or by SOB to sulphur or polysulphide at the anode. SOB may also oxidise sulphur and polysulphides back to sulphate. Organic compounds may also be removed by exoelectrogenic microorganisms (EEM) at the anode.

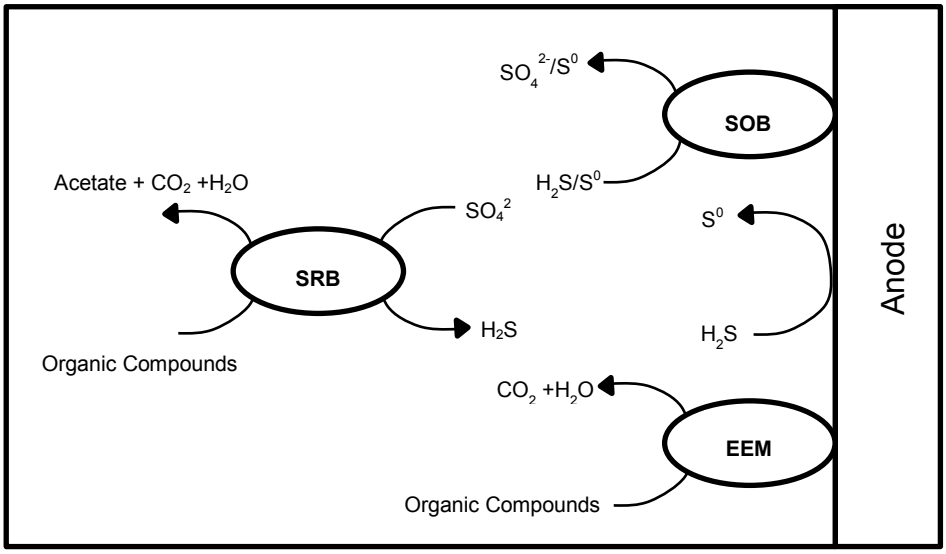

Figure 2-10: Possible mechanisms in a MFC treating sulphate laden wastewater (Sangcharoen, et al., 2015)

SRB such as *Geobacter sulfurreducens* (Bond & Lovley, 2003; Nevin *et al*., 2008) and *Desulfovibrio desulfuricans* (Ieropoulos *et al*., 2005; Zhao *et al*., 2009) have previously been used successfully in MFCs. *Geobacter* sp., *Desulfovibrio* sp. and *Desulfobacteraceae* have also been found to be dominant in mixed culture MFCs treating sulphate-rich wastewater (Chou *et al*., 2014; Sangcharoen, *et al*., 2015).

Geobacter sulfurreducens has been shown to produce nanowires (Logan & Regan, 2006) for electron transfer and *Desulfovibrio desulfuricans* do not transfer electrons directly to the anode but are capable of using the sulphate/sulphide redox couple as a mediator (Ieropoulos *et al*., 2005). These species and others are likely to be present in mixed cultures of SRB and active in a MFC inoculated with a mixed culture of SRB and SOB.

2.9 RESEARCH MOTIVATION

As can be seen from the literature reviewed, much research has been conducted on the use of microbial fuel cells as a method of wastewater treatment. In addition to this, integrated systems in which MFCs are incorporated into wastewater treatment reactors are possible. The integration of MFCs into wastewater treatment processes has been found to both improve the treatment of waste as well as produce electricity which could potential offset the energy costs of treatment.

A linear flow channel reactor (LFCR) is currently being investigated within CeBER for the treatment of sulphate-rich wastewater. The reactor makes use of a mixed community of sulphate reducing bacteria (SRB) to perform biological sulphate reduction (BSR) and sulphide oxidising bacteria (SOB) which oxidise sulphide to form elemental sulphur in a floating sulphur biofilm (FSB) on the surface of the bulk liquid.

SRB and SOB have been shown to successful produce electricity from sulphur species rich waste in microbial fuel cells. A clear opportunity exists for the investigation into an integrated linear flow channel reactor and microbial fuel cell system. The LFCR itself is a novel system and an integration of a microbial fuel cell into a semi-passive reactor of this type has never been attempted.

2.9.1 Research Objectives and Key Questions

The overall aim of this research is to construct an integrated linear flow channel reactor and microbial fuel cell system (LFCR-MFC). The original LFCR (van Hille *et al*., 2015) was designed for combined biological sulphide reduction and sulphide oxidation to yield a sulphur product. This research aims to modify the existing LFCR to incorporate the elements of a MFC to achieve an integrated system which functions as both a wastewater treatment reactor and generates electricity through the MFC.

An additional aim is to test the ability of the microbial community, selected for use in the linear flow channel reactor (LFCR), to produce electricity. This can be achieved through the construction of a single-chambered MFC from literature, which operates using the microbial community and substrate used in the LFCR (presented in Chapter 5). The performance of the mixed community in the single-chambered MFC provides a basis to which the integrated system could be compared and can be used to determine whether an integrated system is likely to produce electricity (presented in Chapter 6).

The following key questions are proposed:

1. To what extent does the constructed single-chambered microbial fuel cell behave as suggested by literature?
2. Is the microbial community present in the linear flow channel reactor capable of producing electricity in the constructed single-chambered MFC while utilising the same substrate being utilised in the LFCR?
3. Is it possible to produce electricity in a LFCR modified to incorporate the elements of a microbial fuel cell?

From the key questions posed, an additional aim is set to determine the shortfalls in the constructed single-chambered MFC, by determining to what extent it behaves as suggested in the literature. This will be achieved by operating the constructed MFC under the identical conditions to a study reported in literature (Chapter 4).

3 METHODOLOGY

This chapter presents the detailed experimental methods and materials used in this research to achieve the objectives discussed in Section 2.9.1. The experimental approach incudes the investigation into the electricity production and corresponding substrate utilisation by microorganisms in two different reactors. Some examination into the microbial community structure was also carried out.

3.1 CULTIVATION OF MICROORGANISMS

3.1.1 *Shewanella oneidensis* MR-1

S. oneidensis MR-1 (ATCC BAA-1096) was purchased from the ATCC. It was aerobically grown in Luria-Bertani medium (10 g tryptone, 5 g yeast extract and 5 g NaCl per liter) at 30°C in shake flasks at 125 rpm. After 24 hours, the cells were harvested by centrifugation at 4000 rpm for 10 minutes. The cell pellet was washed and re-suspended 3 times in PIPES biological buffer (50mM, pH 7 by NaOH). The washed cells were then re-suspended in *Shewanella* basal medium (Wu *et al*., 2013b) consisting of (per litre) 10 mM sodium lactate, 15.1 g PIPES, 1.5 g NH_4Cl, 0.6 g NaH_2PO_4, 3 g NaOH, 0.1 g KCl, 5.8 g NaCl, 100 µℓ 100x trace mineral solution and 1 mℓ of 10x trace vitamin solution, buffered to pH 7 with NaOH. The cell concentration was adjusted to an absorbance of 0.4 at 600 nm and 5 mℓ was inoculated into the MFC.

3.1.2 SRB and SOB

A stock culture comprising of a consortium of SOBs and SRBs was grown anaerobically at 30°C in a Schott bottle with constant low speed magnetic stirring in modified Postgate medium consisting of (per litre) 0.5 g KH_2PO_4, 1.0 g NH_4Cl, 2.0 g $MgSO_4.7H_2O$, 0.33 g Na_2SO_4, 1.0 g yeast extract, 0.3 g sodium citrate, 1.6 mℓ 60% sodium lactate (10 mM). For the single chambered MFCs, a 100 mℓ aliquot of modified Postgate medium was made to 1.25x concentration and 25 mℓ of the stock culture added, resulting in medium with the same concentration per litre as given above. The resultant cell concentration was found to be $1.18x10^9$ cells/mℓ by direct cell counting under a light microscope. This was then used for the setup of the four single-chambered MFCs.

For the LFCR-MFC, the same stock culture of SRBs and SOBs was used; however the culture was added directly to the reactor without dilution. This was done in an attempt to colonise the carbon microfiber anode rapidly and to provide a high concentration of sulphide necessary for the formation of the floating sulphur biofilm.

For the first 19 days after inoculation, the reactor was sampled and thereafter immediately seeded with 50 mℓ of effluent from an existing 2.125 ℓ LFCR operating at a 4 day residence time at 30°C and fed with the same modified Postgate medium as given above. This was done in an attempt to compensate for wash out of the SRB and SOB, and improve colonisation of the anode by adding an active SRB culture.

3.2 SINGLE-CHAMBERED MFC OPERATION

Four identical MFCs were constructed out of Perspex to have a chamber diameter of 3 cm and length of 4 cm, resulting in a working volume of 28 mℓ (Figure 3-1). Stainless steel discs were used as current collectors on the anode side and stainless steel rings were used on the cathode side to allow for diffusion of air. Two Perspex ends (Figure 3-1), were used to hold the electrodes and current

collectors in place when the assembly was bolted together. The cathode end had a hole 3 cm in diameter to allow for diffusion of air.

Carbon felt (10% wet proofed) was used for both the anode and cathode (7 cm^2). The air-cathode was coated with 0.2 mg/cm^2 of platinum unless otherwise stated. The platinum coating was prepared by dissolving 1340.7 mg of catalyst (40 wt.% Pt) in 28.27 mℓ of deionised water. This was stirred for 5 minutes before adding 2.44 mg each of ethylene glycol, glycerol and isopropanol and 3.75 mℓ of 15 wt.% Nafion binder stirring for 5 minutes between each addition. The mixture was then put in an ice bath and stirred at high speed with an overhead stirrer for 10 minutes three times with 10 minutes intervals for cooling. It was then sonicated for 20 minutes in a sonication bath. Two layers of the mixture were sprayed onto the cathode in a 5 cm x 5 cm area (five layers were used for a platinum loading of 0.5 mg/cm^2).

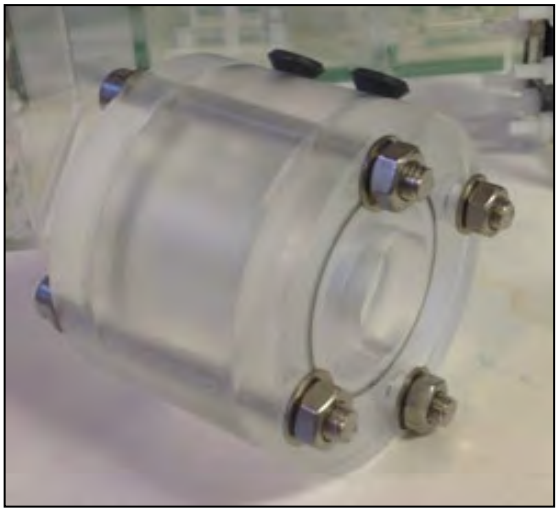

Figure 3-1: Photo of constructed single chamber microbial fuel cell

The MFCs were operated individually in parallel with a 100 kΩ resistor (unless otherwise stated) over which the cell voltage was measured (mV) every minute using a data logger (National Instruments USB-6009) and recorded to a personal computer. A schematic of this setup is seen in Figure 3-2 below.

MFCs were sterilised with 200 vol H_2O_2 overnight before inoculation, and temperature was maintained at 30°C by means of an incubator.

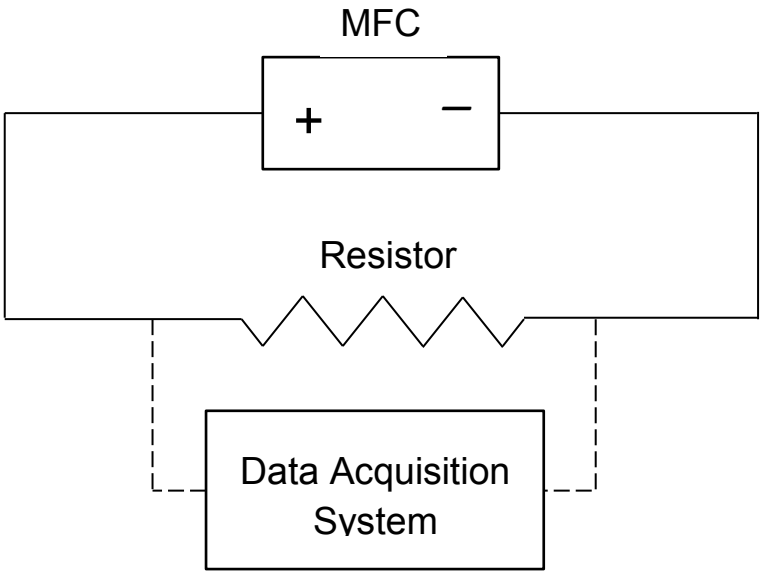

Figure 3-2: Schematic of electrical circuit setup

3.2.1 *Shewanella oneidensis* MR-1

After inoculation, biofilm formation was allowed by replacing 10 ml of spent media with fresh media every 2 days for 2 feeding cycles. The entire liquid content of the MFC was replaced every 2 days thereafter.

3.2.2 SRB and SOB

As a result of the poor attachment abilities of the SRB community, the MFC was fed by replacing 10 mℓ of spent media with fresh concentrated medium on average every 2 days. In this way complete washout of the SRB could be avoided. Concentrated medium was identical to the modified Postgate medium given above however the lactate and sulphate concentration was increased to 15 mM. Therefore by replacing 10 mℓ of medium, a fresh lactate and sulphate concentration of approximately 5 mM resulted throughout the cell.

In the first 3 feeding cycles, 1 mℓ of stock culture was added with the feed in an attempt to aid the colonisation of the MFC by the SRB and SOB community. The stock culture was high in sulphide concentration and depleted in lactate and sulphate.

The anode material was altered for one set of experiments on the SRB and SOB community. A carbon microfibre brush anode was constructed by manually attaching carbon microfibers to a stainless steel rod with stainless steel wire. The brush was 2.5 cm in length and 2.5 cm in diameter in accordance with the study conducted by Logan *et al*., (2007). As a result of it being impossible to determine to what extent the carbon microfibers would splay and therefore the surface area of microfibers, the ratio of mass of microfibers to cathode area was kept constant at 0.1 g/cm^2 of cathode.

3.3 INTEGRATED LFCR-MFC SYSTEM

3.3.1 LFCR Construction

The LFCR-MFC was a rectangular Perspex reactor which was open to the air at the top. The reactor was 110 mm long and 100 mm wide. An inflow and outflow valve was positioned at either end of the reactor 85 mm from the base. This essentially allowed for a working volume of 935 mℓ.

Sampling ports were located on each end of the reactor below the inlet and outlet ports and 50 mm from the base, as well as on the side panels 14 mm and 85 mm from the base, 18.5 mm from each end respectively. The experimental set-up of the reactor can be seen in Figure 3-3.

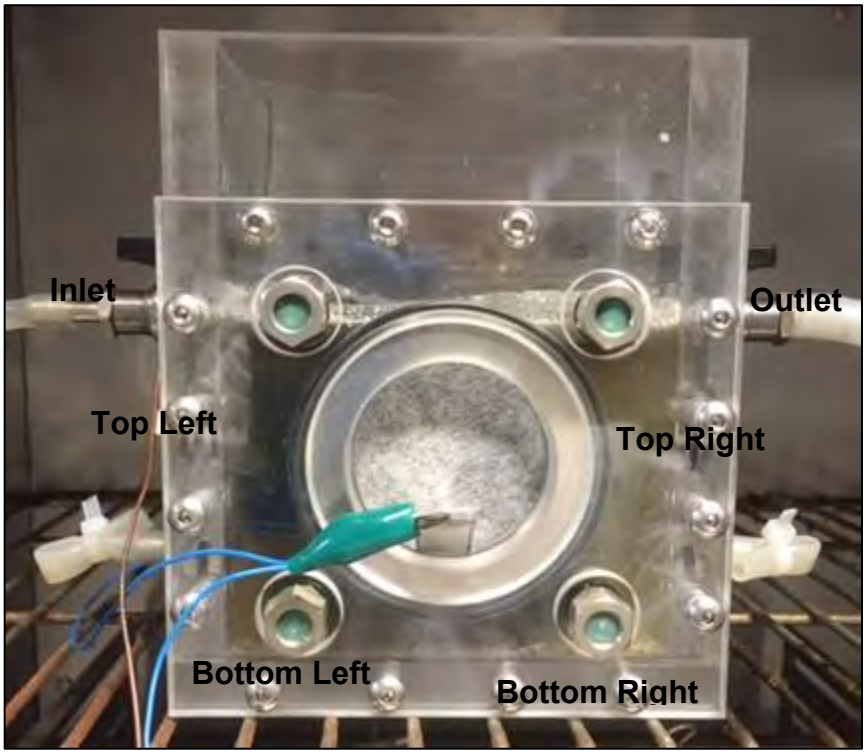

Figure 3-3: Photograph of LFCR-MFC experimental set-up

A cathode electrode 50 mm in diameter was located on each side of the reactor with its centre 50 mm from the base. The cathode electrodes were prepared using the same method as for the single-chambered MFCs as given by Section 3.2. Stainless steel rings were used as current collectors at the cathodes to allow for diffusion of air. Perspex clamps were used to hold the electrodes and current collectors in place when the assembly was bolted together. An anode electrode was constructed by manually attaching carbon microfibers to a stainless steel rod with stainless steel wire. The brush was 100 mm long and had a diameter of 80 mm (Figure 3-4). As a result of it being impossible to determine to what extent the carbon microfibers would splay and therefore the surface area of microfibers, the ratio of mass of microfibers to cathode area was kept constant at 0.1 g/cm^2 of cathode.

The LFCR-MFC was sterilised with 200 vol H_2O_2 overnight before inoculation. The reactor was operated at a four day residence time which corresponded to a flow rate of medium of 0.167 mℓ/min. The reactor was fed modified Postgate Medium with 10mM lactate concentration as specified above. The temperature was maintained at ambient laboratory temperature (approximately 25 °C).

The reactor was sampled as follows: 2 mℓ of sample was drawn using a syringe and needle from the sampling ports on either end of the reactor and the two lower sampling points on the side of the reactor daily. A further 6 mℓ of sample was drawn from the top of the reactor at the outlet.

Figure 3-4: Photograph carbon microfiber brush anode

3.3.2 Hydrodynamic study

A hydrodynamic study was performed on the LFCR in order to ascertain the mixing time and profiles of the integrated LFCR-MFC system. This was done by filling the reactor with 0.002 M sodium hydroxide solution (0.08 g in 1 ℓ of H_2O). A few drops of phenolphthalein tracer were added until the solution turned a bright pink colour. A 0.042 M hydrochloric acid solution (4.131 mℓ of 32% HCl in 1 ℓ of H_2O) was then pumped into the reactor at various flow rates. The mixing profile in the reactor was revealed by the solution, which as a result of the tracer is pink at pH 8.2 – 12, becoming colourless as the acid entered the reactor and the pH was lowered to below 8.2.

The time taken for the solution in the reactor to turn completely colourless was recorded for three different flow rates corresponding to residence times of 1 day, 2 days and 4 days. This was taken as the mixing time for the reactor. A photograph was taken every few minutes throughout the duration of the experiment in order to ascertain the mixing profile within the reactor.

3.4 ELECTRICAL ANALYSIS

3.4.1 Potential Difference

The data logger (National Instrument USB-6009) logged a potential difference value every minute for the duration of the experiment. The graphs of potential difference as a function of time in this document were plotted using the average of the of potential difference for 30 minute intervals i.e. for

each time point plotted, the potential difference for that point is and average of the 30 logged potential differences preceding it.

3.4.2 Polarisation Curves

Polarisation curves were obtained by plotting the recorded potential difference over the MFC in parallel with various resistors. The current and power density were calculated for each different resistance and a curve of current as a function of power density and current as a function of potential difference was plotted.

The values of potential difference for the polarisation curve were achieved as follows: the resistor in the external electrical circuit with the MFC was removed and the MFC was allowed it to stabilise at an open circuit voltage. The MFC was then placed in parallel with a 1 MΩ resistor. The potential difference over the cell was recorded by the data logger to the computer every minute. Once the potential difference had stabilised (changed less than 0.5mV for at least 5 readings) the resistor was replaced with a smaller resistor. This was continued until the potential difference over the cell was less than 10mV.

3.4.3 Cyclic Voltammetry

Cyclic Voltammetry (CV) was conducted using a 3 electrode setup. This consisted of a carbon paper and carbon rod electrodes used as the working and counter electrodes respectively and a double junction Ag/AgCl reference electrode (3 M KCl, 0.21 V versus SHE). A new working electrode was used for every CV. The carbon rod counter electrode and the reference electrode were rinsed thoroughly with deionised water between scans. A BioLogic SP-300 potentiostat was used to perform the CV.

CV was conducted in an electrochemical cell with working volume of 100 ml. The cell was cleaned with a mixture of sulphuric acid and hydrogen peroxide (30%) in a 4:1 ratio for 1 hour. The cell was then rinsed with deionised water 5 times and left to air dry. The electrochemical cell was covered with parafilm during the CV but remained aerobic. All CVs reported were conducted at room temperature at a scan rate of 1mV/s over different voltage ranges.

3.5 CHEMICAL ANALYSIS

3.5.1 Shewanella oneidensis MR-1 Samples

Samples were taken from the spent media at every feeding. Planktonic cells were removed by means of a 0.22 µm cellulose filter.

3.5.1.1 Volatile Fatty Acid Analysis

Samples were also analysed for volatile fatty acid content (lactate, acetate, propionate, butyrate, iso-butyrate, iso-valerate and valerate) using HPLC (Thermo Scientific AS3000) with a UV-VIS detector (Thermo Scientific UV1000). The column used was a Biorad Aminex HPX-87H ion exclusion column and the following conditions were maintained: filtered and degassed mobile phase of 5 mM H_2SO_4 (pH 1-3) with a flow rate of 0.5 ml/min, injection volume of 25 µℓ, column temperature of 45 °C and UV detection at 210 nm.

Samples taken from the MFCs were diluted in deionised water in a ratio of 1:4 and filtered again through a 0.22 µm cellulose filter. Standard solutions of known concentration (0-600 mg/ℓ) were run alongside samples with each new HPLC run. A new standard curve was plotted for each run. An example of a standard curve can be found in Appendix A.2.

3.5.1.2 Iron Assay

Samples to which ferric citrate had been added were tested for ferrous iron by means of a colorimetric iron assay in which 2 mℓ of 0.1 M 1-10 phenanthroline indicator solution, and 2 mℓ ammonium acetate buffer solution (250 g $NH_4C_2H_3O_2$, 700 mℓ concentrated glacial acetic acid, 150 mℓ deionised water) were added to 1 ml of appropriately diluted sample. The samples were read in a spectrophotometer at 510 nm. This assay is accurate below 1 mg/ℓ.

The spectrophotometer was auto-zeroed with a blank solution consisting of 1 mℓ of deionised water, phenanthroline indicator solution and ammonium acetate buffer solution. A stock solution of iron (497.629 g $FeSO_4.7H_2O$ dissolved in 20 mℓ of H_2SO_4 and 50 mℓ of deionised water diluted to 1000 mℓ of deionised water) was used to plot a standard curve of ferrous iron concentration as a function of absorbance at 510 nm. The standard curve can be found in Appendix A.3.

Total Iron was read using the same assay. A micro-spoon of hydroxylamine was added to all samples including the blank after the absorbance of the samples had been read. The samples were vortexed for 10-20 seconds to ensure all hydroxylamine was dissolved. The samples were allowed to stand for 5 minutes to allow for the colour to develop as ferric iron is reduced to ferrous iron. The absorbance was read again at 510 nm. The spectrophotometer was auto-zeroed with a blank solution to which the hydroxylamine had been added.

3.5.1.3 COD Assay

Samples were then analysed for COD content to be used for determining Coulombic efficiency (CE) using the following assay: 500 µℓ of appropriately diluted sample, 1100 µℓ COD reagent A (Merck 1.14679.0495) and 900 µℓ COD reagent B (Merck 1.4680.0495) heated for 2 hours at 150°C and read in a photo spectrometer at 605 nm. This assay is accurate between 500-10000 mg COD/ℓ.

The spectrophotometer was auto-zeroed with a blank solution of 500 µℓ of deionised water, COD reagent A and COD reagent B. A standard solution of potassium hydrogen phthalate was used to plot a standard curve of COD as a function of absorbance which can be found in Appendix A.1.

3.5.2 SRB-SOB Samples

In the case of the sample taken from the single-chambered MFCs, triplicate 2 mℓ samples were taken. A sulphide assay was done on each of the triplicate samples before being used for VFA measurement by HPLC, sulphate measurement by IC and COD assays to provide an indirect measure of available organic carbon respectively. The remaining volume was used to measure the redox potential with respect to the Ag/AgCl reference electrode and the pH of the sample.

In the case of the LFCR-MFC system, a sulphide assay was conducted on each 2 mℓ sample from each sampling port and effluent taken daily. The remaining sample was used for both VFA measurement by HPLC and sulphate measurement by IC. The remaining volume from the effluent sample was used to measure the redox potential and pH and to conduct a COD assay.

3.5.2.1 Colorimetric Sulphide Assay

A colorimetric sulphide assay was conducted on all SRB samples as follows (Cline, 1969): 200 µℓ of zinc acetate solution (10 g of zinc acetate dissolved in 1000 mℓ of deionised water) was added to a test tube followed by 4800 µℓ of sample diluted to sulphide concentration below 1 mg/ℓ. Thereafter, 500 µℓ of DMPD solution (2 g of N,N-dimethyl-p-phenylenediamine dihydrochloride dissolved in 500 mℓ of 6 M HCl) and 500 µℓ of ferric chloride solution (8 g of ferric chloride dissolved in 6 M HCl) was added. The test tube was vortexed for 10-20 seconds and allowed to stand for 5 minutes to allow for the methylene blue to form. The absorbance was read at 670 nm. This assay is accurate below 1 mg/ℓ.

The spectrophotometer was auto-zeroed with a blank solution consisting of the zinc acetate, DMPD and ferric chloride solution with 4800 µℓ of deionised water. A stock solution of sulphide (750 mg of $Na_2S.9H_2O$ in 1000 mℓ of deionised water) was used to plot a standard curve of sulphide concentration as a function of absorbance at 670 nm. The standard curve can be found in Appendix A.5.

3.5.2.2 Sample Preparation and Storage

After reading the redox potential and pH and conducting a sulphide assay on the samples, 40 µℓ of $ZnCl^2$ solution (100 g/ℓ) was added to precipitate out the hydrogen sulphide. Samples were centrifuged at 14500 rpm for 10 minutes and filtered through a 0.22 µℓ cellulose filter. These samples were then frozen until such time as HPLC, IC and COD assays could be conducted.

3.5.2.3 Sulphate Assay

Analysis for sulphate concentration was conducted either by ion chromatography or by a barium chloride assay.

Ion Chromatography (IC) was conducted using a Thermo Scientific Dionex ICS-1600. The column used was a Dionex IonPac AS16 RFIC column and a filtered and degassed 22 mM NaOH mobile phase was used at a flow rate of 1 mℓ/min and ambient temperature.

The barium chloride assay was conducted as follows (APHA, 1975): The sample was appropriate diluted to 5 mℓ and 250 µℓ of conditioning agent (300 mℓ of deionised H_2O, 100 mℓ absolute ethanol, 50 mℓ glycerol, 30 mℓ 32% HCl and 75 g NaCl) was added. A micro-spoon of barium chloride was then added to be in excess. The test tube was then vortexed for 10-20 seconds until all barium chloride was dissolved. The absorbance was read at 420 nm. This assay is accurate below 50 mg/ℓ.

The spectrophotometer was auto-zeroed with a blank solution consisting of the 5 mℓ of deionised water, conditioning agent and barium chloride salt. A stock solution of sulphate (0.1479 g Na_2SO_4 in 1 ℓ deionised water) was used to plot a standard curve of sulphate concentration as a function of absorbance at 420 nm.

3.5.2.4 Volatile Fatty Acid Analysis

Samples were also analysed for volatile fatty acid content using HPLC (Waters 717plus Autosampler) with a UV-VIS detector. A Biorad Aminex HPX-87H ion exclusion column was used with a filtered and degassed mobile phase of 10 mM H_2SO_4 at a flow rate of 0.6 mℓ/min. An injection volume of 25 µℓ was used. The column temperature was maintained at 60°C and UV detection of 210 nm was used.

Samples taken from the MFCs were diluted in deionised water in a ratio of 1:4 and filtered again through a 0.22 µm cellulose filter. Standard solutions of known concentration (0-600 mg/ℓ) were run alongside samples with each new HPLC. A new standard curve was plotted for each run. An example of a standard curve can be found in Appendix A.2.

3.5.2.5 COD Analysis

Samples were then analysed for COD content to be used for determining Coulombic efficiency (CE) using the following assay: a 1500 µℓ aliquot of the samples, 150 µℓ COD reagent A (Merck 1.14679.0065) and 1150 µℓ COD reagent B (Merck 1.4680.0495) was heated for 2 hours at 150°C for reaction to occur. Absorbance was measured spectrophotometrically at 605 nm. This assay is accurate between 100-1500 mg COD/ℓ.

The spectrophotometer was auto-zeroed with a blank solution of 1500 µl of deionised water, COD reagent A and COD reagent B. A standard solution of potassium hydrogen phthalate was used to plot a standard curve of COD as a function of absorbance which can be found in Appendix A.1.

3.6 BIOLOGICAL ANALYSIS

3.6.1 Scanning Electron Microscopy (SEM)

Electrodes from the single-chambered MFCs for both the *S. oneidensis* and SRB-SOB fuel cells were sent for scanning electron microscopy (SEM) in order to determine the cell morphology of the cells attached to surface. Samples were prepared by fixing in 2.5% glutaraldehyde for 8 hours. The samples were then rinsed with PIPES buffer (pH 7) before dehydrating in an alcohol series consisting of 30%, 50%, 70%, 90%, 95% and 100% ethanol. Samples were placed in each alcohol solution for 10 minutes. The samples were then critical point dried and mounted on an aluminium stub and covered in carbon clue. The stub was then sputter coated with carbon before SEM was conducted (FEI Nova Nanosem 230 with field emission gun).

3.6.2 DNA Extraction and Microbial Analysis

Cells were collected from the anode and cathode electrodes by scraping the cell mass into 15 mℓ polypropylene tubes using a sterile 1000 µℓ pipette tips with the addition of 1 mℓ 1x PBS buffer (137 mM NaCl; 2.7 mM KCl; 10 mM Na_2HPO_4; 2 mM KH_2PO_4; pH 7.4). Cells were harvested following centrifugation at 14,000 xg for 10 minutes after being transferred into 2 mℓ polypropylene tubes. Planktonic cells were collected from 10 mℓ sample by centrifugation (14,000 xg for 10 minutes) into sterile 2 mℓ micro-centrifuge tubes (Eppendorf) to obtain cell pellets. Cell pellets from the anode, cathode and planktonic samples were washed twice in 1 mℓ 1x PBS buffer and cells collected by centrifugation at 14,000 xg for 10 minutes following each wash step. Genomic DNA was extracted from the cell a pellet using the High Pure PCR Template Preparation Kit (Roche, Germany) according to the manufacturer instructions with minor modifications. The protocol for DNA extraction using this kit is as follows:

Cells were pelleted by centrifugation at 13 000 xg for 5 minutes. Supernatant was removed and the cell pellet was resuspended in 200 µℓ tissue lysis buffer (supplied with kit). Lysozyme (50 µg/mℓ in 10 mM Tris-HCl) and RNaseA (2 µg/mℓ) were added as per manufacturer instructions and the suspension was incubated at 37 °C for 30 minutes. Following the addition of 40 µℓ of reconstituted Proteinase K, the suspension was incubated at 55°C for 30 minutes. The DNA was eluted into 50 µℓ sterile elution buffer (supplied with kit). Quantity and quality of the DNA was analysed using a Nanodrop® 2000.

The purity of the electrode biofilms samples taken from the single-chambered MFC with *S. oneidensis* was analysed by quantitative real-time PCR. This was done using the universal primers for the 16S ribosomal RNA gene (UniBact 335 Forward and UniBact 937 Reverse primers). The region of DNA targeted by these primers is evolutionarily conserved across all species of bacteria. It is however possible to detect single nucleotide polymorphisms (SNPs), which differ between bacterial species or strains in the amplified region (amplicon), by melt curve analysis.

A melt curve analysis was performed on all samples taken from the single-chambered MFC with *S. oneidensis*. Fluorescence was measured over a temperature range was 75-95°C. The derivative of fluorescence with temperature (dF/dT) was plotted as a function of temperature in order to obtain the melt curves.

4 PERFORMANCE OF *SHEWANELLA ONEIDENSIS* MR-1 IN SINGLE-CHAMBERED MFC

4.1 INTRODUCTION

The overall aim of this study is to incorporate the elements of a MFC into a linear flow channel reactor (LFCR) designed for combined biological sulphide reduction and sulphide oxidation to yield a sulphur product. The integration aims to create a LFCR-MFC that functions as a wastewater treatment reactor yielding a sulphur product and electricity through the MFC. A constructed single-chambered MFC was used to test the ability of the microbial community, selected for use in the linear flow channel reactor (LFCR), to produce electricity. It can therefore be concluded if the community is capable of electricity production (presented in Chapter 5). The performance of the mixed community from the LFCR in the single-chambered MFC provides a basis to which the integrated system could be compared and can be used to determine whether an integrated system is likely to produce electricity (presented in Chapter 6).

The performance of the constructed MFC should be validated using a well know electrogenic microbial culture. Through this approach, it is possible to decouple the effects of the design elements of the integrated LFCR-MFC on electricity generation. In this way, if the chosen design of the MFC-LFCR was to perform poorly or not produce current at all, one could identify whether it was the design of the system or the microbial community and their wastewater substrate which had the largest effect on electricity generation performance.

This chapter details the investigation into the operation of a single-chambered MFC, originally designed by Liu and Logan (2004), operating with a pure culture of *Shewanella oneidensis* MR-1 and a lactate feed as was used by Wu *et al*. (2013b). The research in this chapter aims to determine the shortfalls in the constructed single-chambered MFC, by determining to what extent it behaves as suggested by literature. To do this the constructed MFC was operated under the identical conditions to the study performed by Wu *et al*. (2013b).

The single-chambered MFC was selected with the overall aim of this study in mind. The design of the LFCR is a single-chambered flow through system and lends itself to being modified into a single-chambered integrated MFC-reactor system. As a result of the expenses associated with proton exchange membranes (PEM) (Jang *et al*., 2004; Liu & Logan, 2004; Sukkasem *et al*., 2011; Zhu *et al*., 2011; Kokabian & Gude, 2015), their use in the MFC design were avoided. Further although the power densities produced by mixed community MFCs are typically considerably higher than that of pure cultures MFCs (Nevin *et al*., 2008), the use of a pure culture is much easier to interpret and more easily reproduced. Single-chambered MFCs operating with pure bacterial cultures were therefore considered to validate the reactor design.

The use of catholytes was ruled out by avoiding PEM use as the anolyte and catholyte could not be separated. Electrogenic pure cultures were considered in order to avoid making use of mediators as their use on an industrial scale is unfeasible and their addition to wastewater treatment reactors in not desirable in the case of MFC-reactor integration. Mediators constantly need to be replaced and are often toxic and expensive (Liu & Logan, 2004; Jang *et al*., 2004; Ghangrekar & Shinde, 2007; Cha *et al*., 2010). The waste produced from the fuel cell would need to be processed and this is impractical as a wastewater treatment method.

The single-chambered MFC originally proposed by Liu and Logan (2004) was chosen for construction and testing of the mixed community in the LFCR, owing to the significant amount of research conducted on the fuel cell (Liu & Logan, 2004; Liu *et al*., 2005a; Liu *et al*., 2005b; Cheng *et al*., 2006a; Cheng *et al*., 2006b; Cheng & Logan, 2007) and the various pure cultures tested in it (Xing *et al*., 2008; Wu *et al*., 2013b; Wu *et al*., 2013c). It has consistently produced reasonable power densities.

Shewanella oneidensis MR-1 was chosen as the pure culture to test the single-chambered MFC, as a result of the significant amount of research reported in microbial fuel cells, discussed in Section 2.8.1.1, and its use in the study by Wu *et al*. (2013b) in the same single-chambered MFC originally proposed by Liu and Logan (2004).

In this way many of the experimental conditions used by Wu *et al*. (2013b) could be replicated and the results obtained could be directly comparable to those reported in order to demonstrate expertise in MFCs and validate the reactor construction before investigating the potential of both the SRB microbial system in the CeBER laboratory and the design of the integrated LFCR-MFC

The specific objectives of the research presented in this chapter were as follows:

1. To construct a single-chambered MFCs in accordance with literature and replicate the study conducted by Wu *et al*. (2013b) using a pure culture of *Shewanella oneidensis* MR-1.
2. To evaluate the results of the study to determine to what extent the constructed single-chambered MFC behaved as suggested in literature and draw conclusions on the reasons for differences in electrical performance.

4.2 EXPERIMENTAL APPROCAH

4.2.1 Data Collection

For this investigation the experimental procedure used in the study by Wu *et al*. (2013b) was followed, using the single-chambered MFC of Liu and Logan (2004) and *Shewanella oneidensis* MR-1 cultured on lactate medium. A detailed experimental approach is provided in Section 3.2.1. For each experiment the potential difference over the MFC in parallel with a resistor was monitored throughout the duration of the experiment. A two day residence time was used. All samples taken were analysed for the concentration of COD and volatile fatty acids. Samples of the anodic and cathodic biofilms were taken from each of the MFCs researched. To confirm the microorganism present the DNA was extracted from the samples and a melt curve analysis was conducted, the details of which are given in Section 3.6.2. These melt curves were compared to that of a pure *Shewanella oneidensis* MR-1 sample in order to have an indication of the purity of the sample.

The experiments in this chapter were divided into three sections and are listed below.

1. A base case was investigated using 20 mM lactate medium. SEM was conducted on the anodic biofilm of the MFC.
2. The effect of lactate concentration was investigated by operating three microbial fuel cells with medium with a lactate concentration of 10 mM, 20mM and 40mM respectively. All other variables remained the same.
3. The effect of the addition of ferric citrate was investigated by operating two microbial fuel cells with medium with a lactate concentration of 10 mM and ferric citrate concentration of 6 mM. In addition to the COD and VFA analysis, samples were also analysed for ferrous iron concentration.

Analytic methods for the iron assay and COD assay were carried out in triplicate for all samples taken. HPLC was only conducted on one sample per sampling interval owing to constraints on HPLC

access and it being necessary to run a single sample for 45 minutes for resolution of all volatile fatty. acids. All standard curves and raw data obtained for these experiments can be found in Appendix A and Appendix B respectively.

4.2.2 Data Handling

4.2.2.1 Power Density Calculation

Power can be calculated from the current and resistance as follows (Equation 11):

$$P = I^2R = \frac{V^2}{R}$$ Equation11

where I is current (A or C/s), V is cell voltage (V), R is external resistance (Ohms) and P is power (W).

It is possible to calculate the power based on the electrode surface area or MFC volume (power density) by dividing by the chosen electrode surface area (Equation 12) or volume of the fuel cell or fuel cell compartments (Equation 13) respectively as follows:

$$P_A = \frac{V^2}{RA}$$ Equation 12

$$P_v = \frac{V^2}{Rv}$$ Equation 13

where P_A is power density (W/m^2), P_v is power density (W/m^3); A is surface area (m^2) and v is volume (m^3).

4.2.2.2 Coulombic Efficiency Calculation

Voltage (V) was measured at one minute intervals and recorded in millivolts for the duration of the experiment. Current (I) in amps was calculated using voltage and resistance with Ohm's law and converting millivolts to volts (Equation 14).

$$I = \frac{V \times 1000}{R}$$ Equation 14

The change in COD concentration (ΔCOD) was calculated for one feeding cycle (Equation 15) i.e. from the time fresh medium is added until it is replaced. The COD for the feed (COD_{feed}) and spent medium (COD_{spent}) was measured by a COD assay described in Section 3.5.1.3.

$$\Delta COD = COD_{feed} - COD_{spent}$$ Equation 15

The coulombic efficiency (E_c) is calculated by equation 16:

$$E_c = \frac{M \int_0^{tb} Idt}{FbV_{MFC}\Delta COD}$$ Equation 16

where M is molar mass of oxygen (32 g/mol), t_b is run time of the experiment, F is Faraday's constant (96485.34 C/mol), b is number of electrons exchanged per mole of oxygen (4), V_{MFC} is volume of the single-chambered MFC (m^3) and ΔCOD is the difference in COD between influent and effluent (g/m^3).

The integral of $\int_0^{tb} Idt$ is the total amount of charge produced (coulombs) for the duration of the feeding cycle. It is approximated by determining the difference in current between two recorded values and multiplying it by the time between those points (60 seconds). These values are added to determine total charge produced over one feeding cycle (Equation 17).

$$\int_0^{tb} Idt \cong \sum_{i=0}^{tb}(I_{i+1} - I_i) \times 60$$ Equation 17

4.3 RESULTS

4.3.1 Replication of Base Case MFC reported by Wu *et al*. (2013b)

4.3.1.1 Electrical Performance

While the experimental set-up used by Wu *et al*. (2013b) made use of a 1 kΩ resistor in parallel with the MFCs, a larger 100 kΩ resistor was chosen for most experiments in this research. Owing to internal resistances higher than reported in literature, a larger resistor was required in the external circuit in order for current generation to occur. A larger resistor demands lower current production by the MFC which results in higher potential differences and is more sensitive to changes in cell performance.

In initial experiments a cathode coated with 0.5 mg/cm^2 of platinum and 10 mM lactate medium feed was used. After each introduction of feed, the potential difference over the MFC increased to a maximum before decreasing again prior to the replacement of spent medium. This feeding cycle took approximately 2 days. The maximum potential obtained for a feeding cycle increased over the first 12 days of the experiment (Figure 4-1) during the colonisation of the reactor. Thereafter it remained fairly constant at around 580 mV for the remainder of the experiment.

The preparation of the cathode electrodes required spraying several layers a carbon and platinum onto the carbon felt. For a cathode with a platinum concentration of 0.5 mg/cm^2, five layers were required. During operation of the MFC, the platinum coating flaked off into the bulk solution. This was attributed to the thickness and poor drying of the base layers. Further, a platinum catalyst is expensive. To minimise costs and reduce the flaking of the catalyst coating, the platinum loading of the cathode was decreased from 0.5 mg/cm^2 to 0.2 mg/cm^2.

The experiments were repeated using a lactate concentration of 20 mM and Pt loading of 0.2 mg/cm^2. In the results presented in Figure 4-2, the cell potential increased to a point at which the peak became flat around 625 mV, owing to the potential achieved by the MFC being higher than the range the data logger. To lower the potential produced by the MFC, the resistor was changed to a 10 kΩ resistor. The cell potential continued to increase with time as shown in Figure 4-3.

The highest potential difference produced for various different MFC setups was used to determine the maximum power density for each case, reported in Table 4-1. The maximum power density achieved in these experiments was 13.7 ± 0.228 mW/m^2 of anode area.

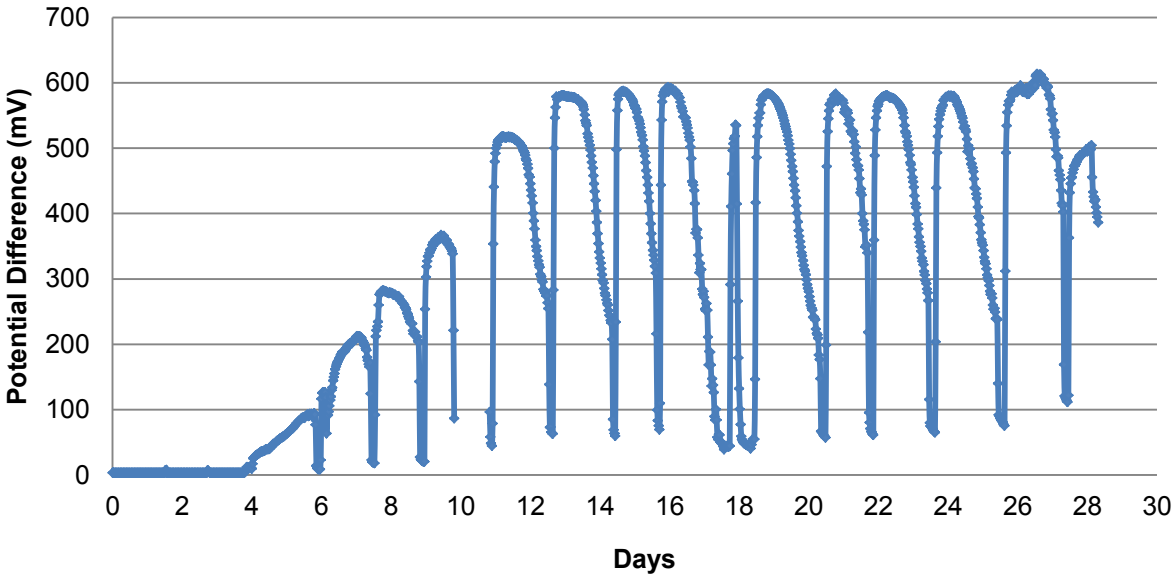

Figure 4-1: Cell potential as a function of time for a MFC fed 10 mM lactate in parallel with a 100 kΩ resistor and 0.5 mg/cm^2 of Pt on the cathode

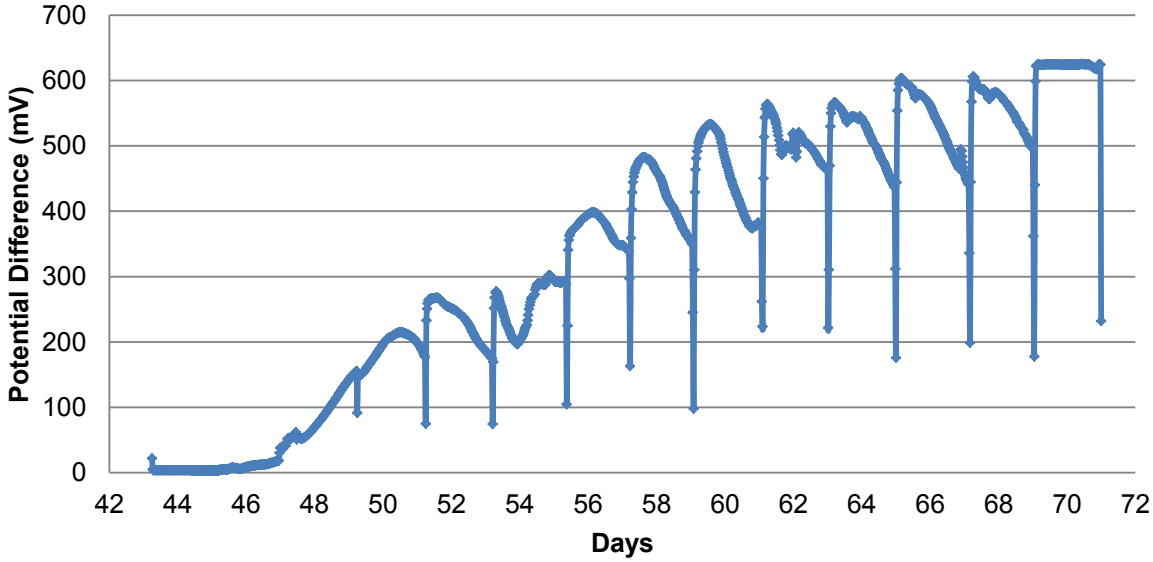

Figure 4-2: Cell potential as a function of time for a MFC fed 20 mM lactate in parallel with a 100 kΩ resistor and 0.2 mg/cm^2 of Pt on the cathode

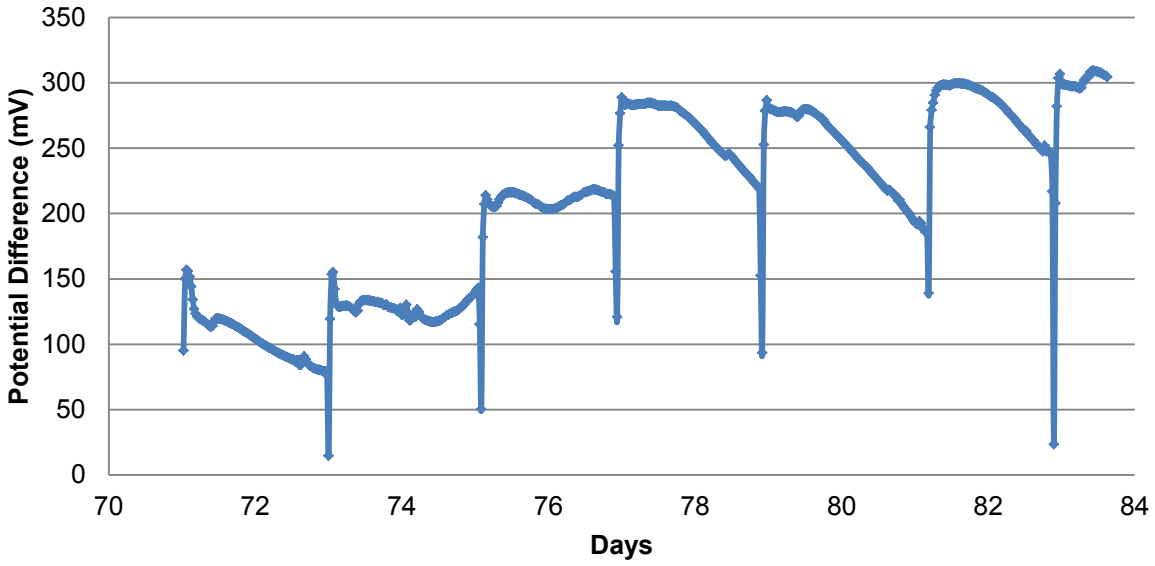

Figure 4-3: Cell potential as a function of time for a MFC fed 20 mM lactate in parallel with a 10 kΩ resistor and 0.2 mg/cm^2 of Pt on the cathode

4.3.1.2 Substrate Utilisation

The results of the HPLC analysis revealed the presence of lactate. Although some samples contained small amounts of acetate, most samples did not form a definitive acetate peak on the chromatogram. Lactate concentration, presented as a function of time in Figure 4-4, varied substantially between 100 and 1700 mg/ℓ across the experiment. Between day 51 and 71 the lactate concentration stabilised between 1400-1700 mg/ℓ. When the resistor was changed from 100 kΩ to 10 kΩ on day 71 the lactate concentration shifted to remain mostly between 1200-1500 mg/ℓ for the remainder of the experiment. A t-test was performed to compare the lactate concentration during operation with a 10 kΩ to 100 kΩ resistor. The t-value lay outside the critical range (Table A 3) and therefore the concentration usage was statistically different for operation with different resistors. The lactate concentration appeared to have a decreasing trend from day 51 to 89. Consequently the lactate usage exhibited an increasing trend over the same time period (Figure 4-5).

The COD concentration remained fairly constant between 15000-16000 mg/ℓ for the duration of the experiment (Figure 4-6). The high value of COD was as a result of the use PIPES of biological buffer. A t-test was also performed for COD concentration for different resistors. The t-value was found to lie within the critical range and P > 0.05 (Table A 3) which indicated that statistically there was little difference in COD concentration after each feeding cycle for different resistors. This is believed to be as a result of the high COD values which hide subtle changes in COD during analysis, as a significant difference in lactate concentration for the different resistors was noted.

As can be seen from Figure 4-7 presenting coulombic efficiency as a function of time, CE increased from almost 0 % on day 47 and stabilised at 0.3 % on days 67 to 71. After the changing of the resistor from 100 kΩ to 10 kΩ the CE increased further to a maximum of 1.45%. The trend observed for the maximum potential difference achieved (Figure 4-2 and Figure 4-3) closely followed that of the CE. The relatively small change in COD concentration implies that the potential difference affected the CE to a greater extent than the amount of COD degraded.

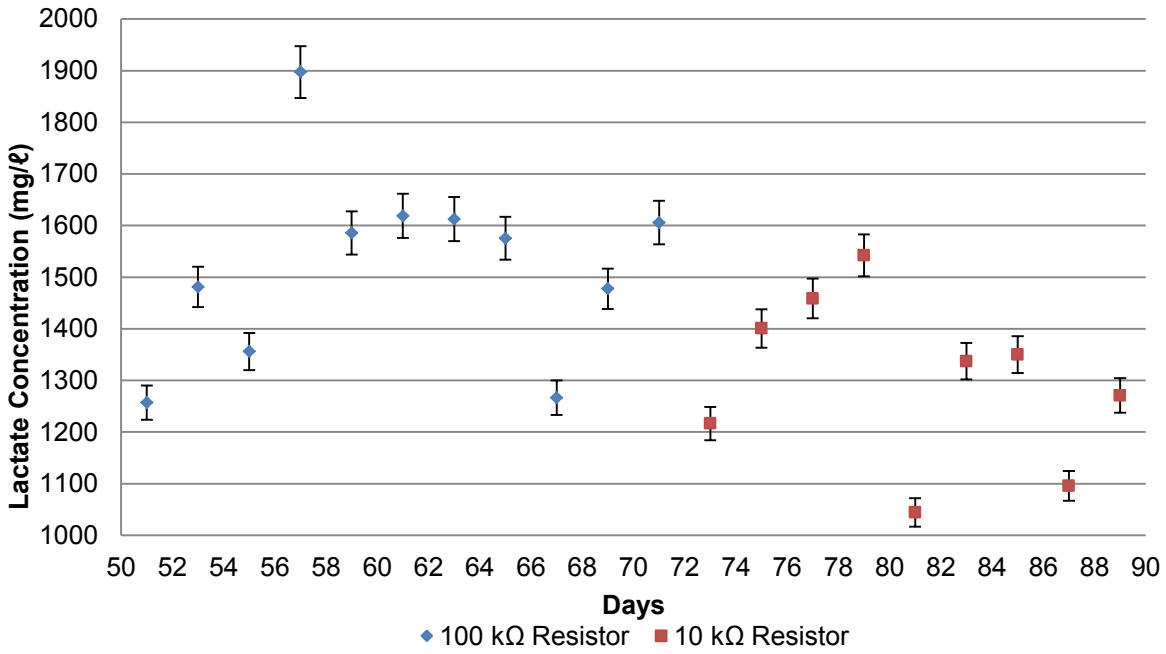

Figure 4-4: Concentration of lactate as a function of time in MFC fed 20mM lactate and in parallel with a 10kΩ and a 100kΩ resistor

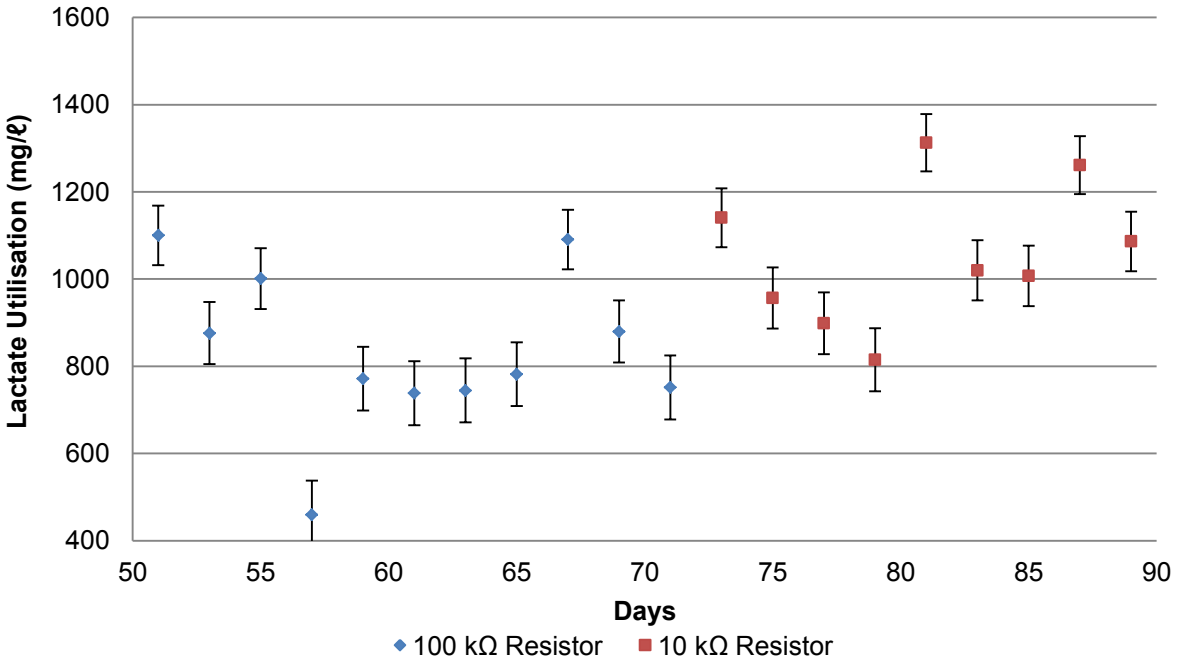

Figure 4-5: Lactate utilisation as a function of time for a MFC fed 20mM lactate and in parallel with a 10kΩ and a 100kΩ resistor

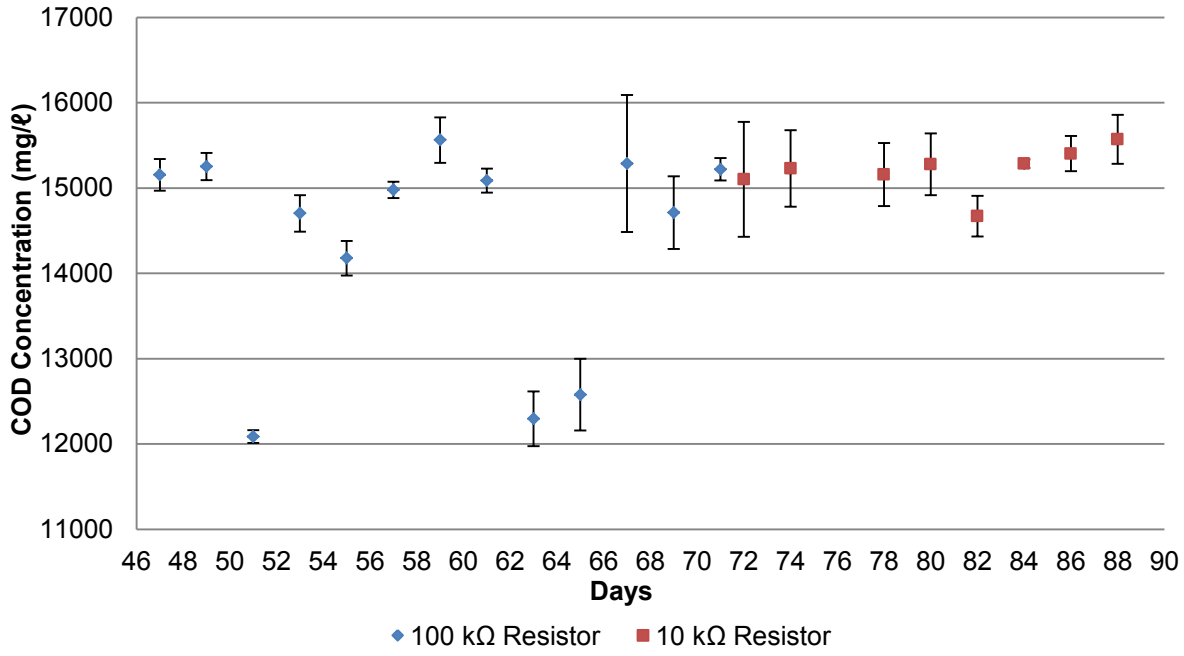

Figure 4-6: COD concentration as a function of time for a MFC fed 20mM lactate and in parallel with a 10kΩ and a 100kΩ resistor

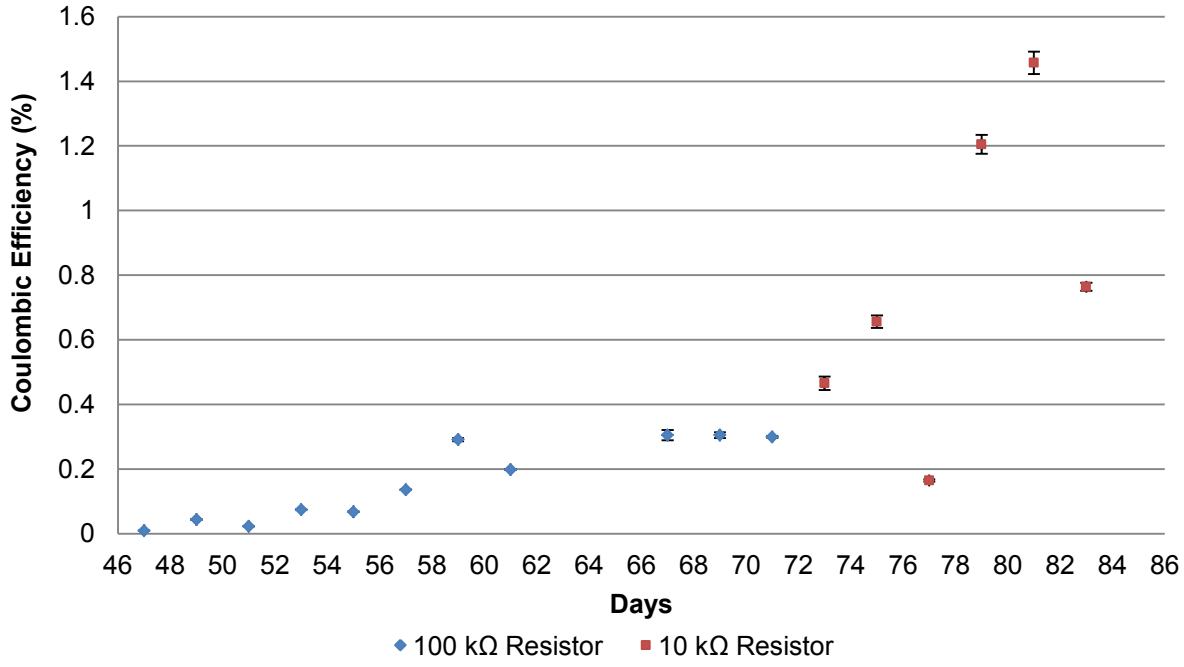

Figure 4-7: Coulombic efficiency as a function of time for MFCs fed 20mM lactate in parallel with a 10kΩ and a 100kΩ resistor

4.3.2 Effect of Lactate Concentration

4.3.2.1 Electrical Performance

The MFCs were operated with different concentrations of lactate in the feed medium. As can be seen in Figure 4-8 below, a lactate concentration of 40 mM resulted in an average potential difference higher than that of the 20 mM lactate concentration. The cell potential is only reported several days

after inoculation as a result of the negligible potential recorded until that point. In the case of both feed concentrations, the highest cell potential achieved in each feeding cycle increased to a maximum before it began to decrease. This maximum was achieved on days 34 to 38 and 28 to 29 for the MFCs with 20 mM and 40 mM lactate feed respectively.

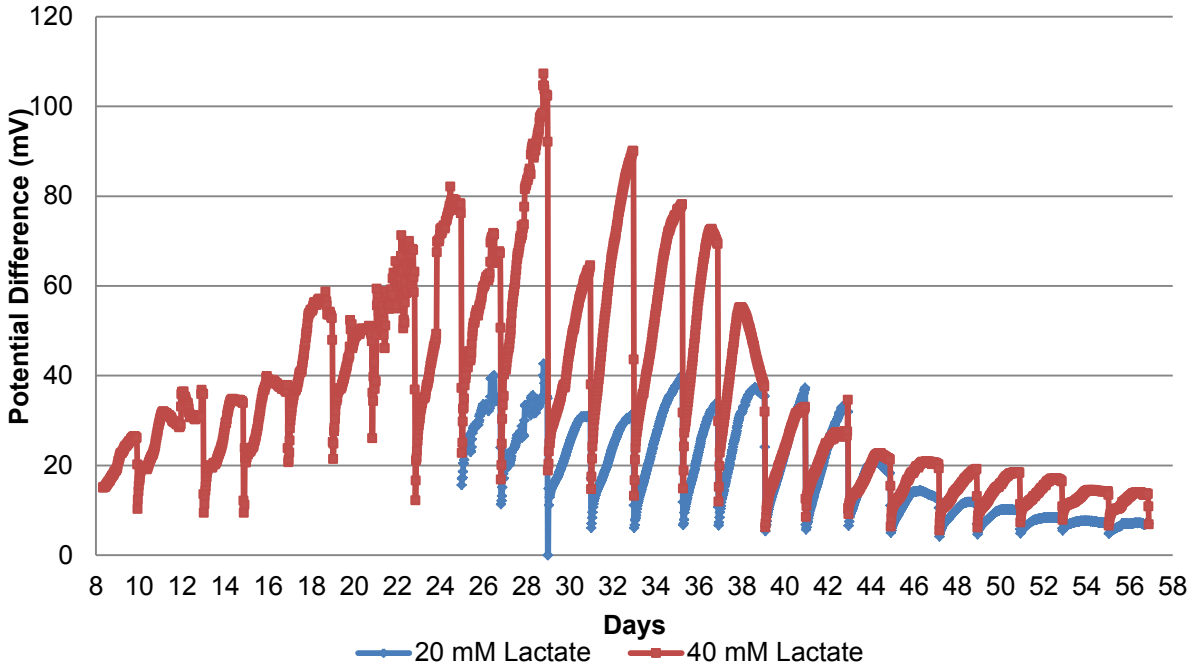

Figure 4-8: Potential as a function of time for MFCs fed different lactate concentrations in parallel with a 100 kΩ resistor

Table 4-1: Table of the maximum potential and corresponding power density achieved MFCs with different concentrations of lactate feed

MFC	Best Performance* 10 mM Lactate	Best Performance* 20 mM Lactate	
Resistor (kΩ)	100	100	10
Maximum Voltage Produced (mV)	613 ± 5.25	625 ± 8.56	310 ± 5.15
Power Density (mW/m^2 anode)	5.37 ± 0.044	5.58 ± 0.076	13.7 ± 0.228

* Best Performance refers to the MFC which produced the highest power density at the given lactate feed concentration

4.3.2.2 Substrate Utilisation

The lactate usage was very similar for both feed concentrations (Figure 4-9). For the range of coulombic efficiencies achieved, the lactate varied with no significant trend observed for both MFCs (Figure 4-12). Regression analysis indicated R^2 values of 0.024 and 0.002 respectively which supports this. Over time the lactate usage in the MFC fed 20 mM lactate remained mostly constant (between 1000-1500 mg/ℓ). The MFC fed 40 mM lactate had similar lactate usage, however larger variation in concentration was observed. The largest variation in lactate usage was observed from approximately day 35-45. The COD concentration remained fairly constant for both MFCs for the duration of the experiment (Figure 4-10). This is in keeping with the stable lactate usage observed.

The CE for each feeding cycle was found to decrease over time for both concentrations of lactate (Figure 4-11). This trend closely followed the trend seen in Figure 4-8. Again, cell potential appeared to have a larger effect on CE than the change in COD concentration as observed in Section 4.3.1.2.

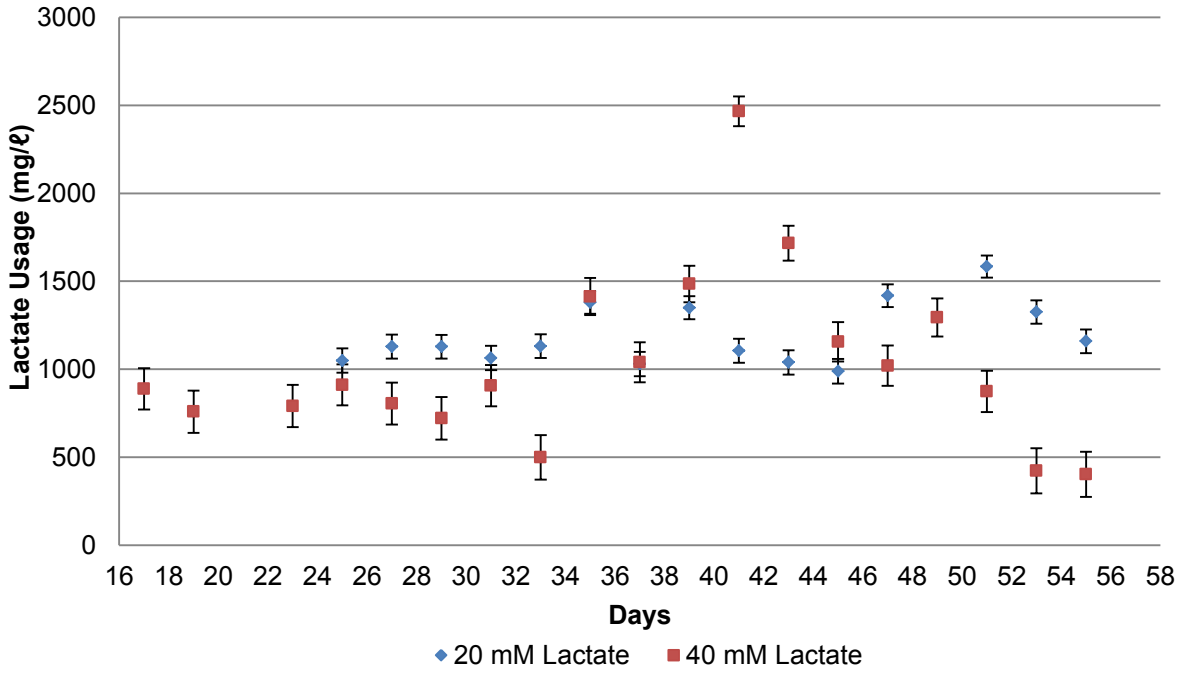

Figure 4-9: Lactate usage as a function of time for MFCs fed different concentrations of lactate in parallel with a 100 kΩ resistor

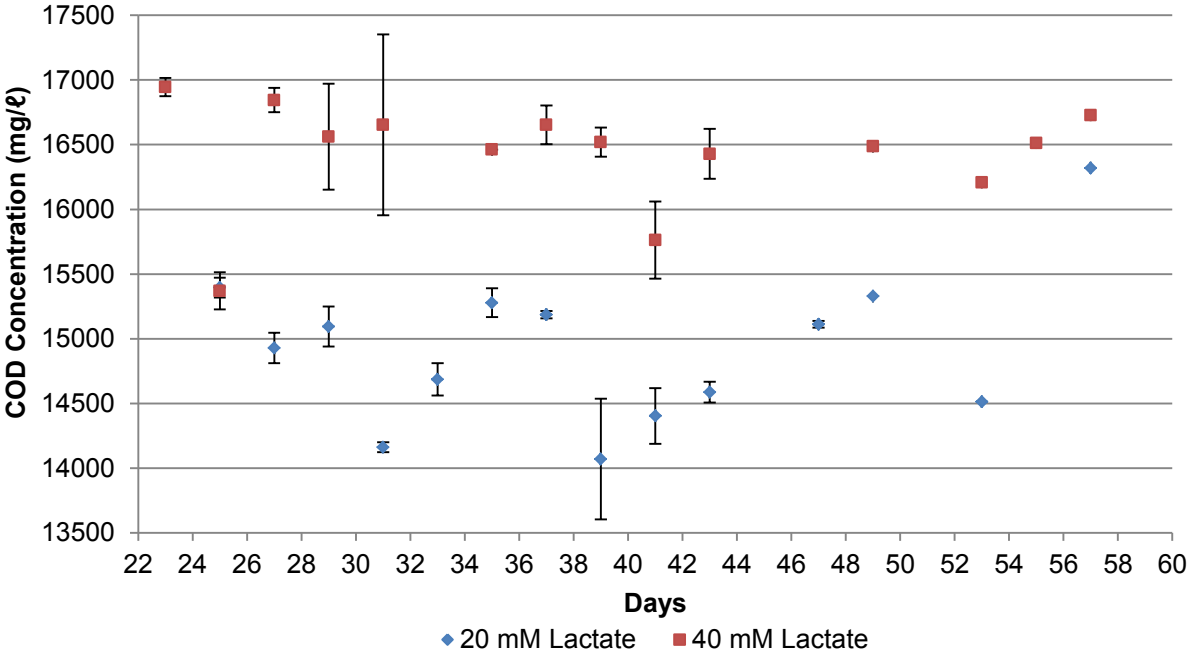

Figure 4-10: COD concentration as a function of time for MFCs fed different lactate concentrations in parallel with a 100 kΩ resistor

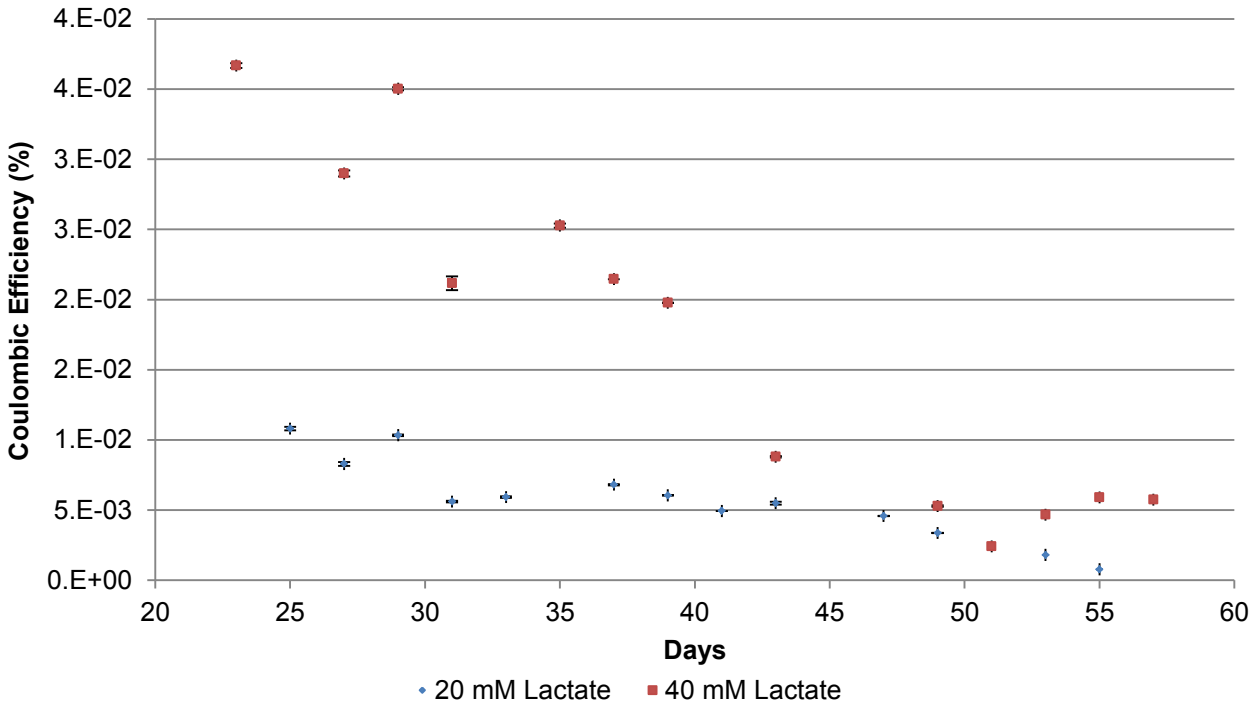

Figure 4-11: Coulombic efficiency as a function of time for MFCs fed different concentrations of lactate and in parallel with a 100kΩ resistor

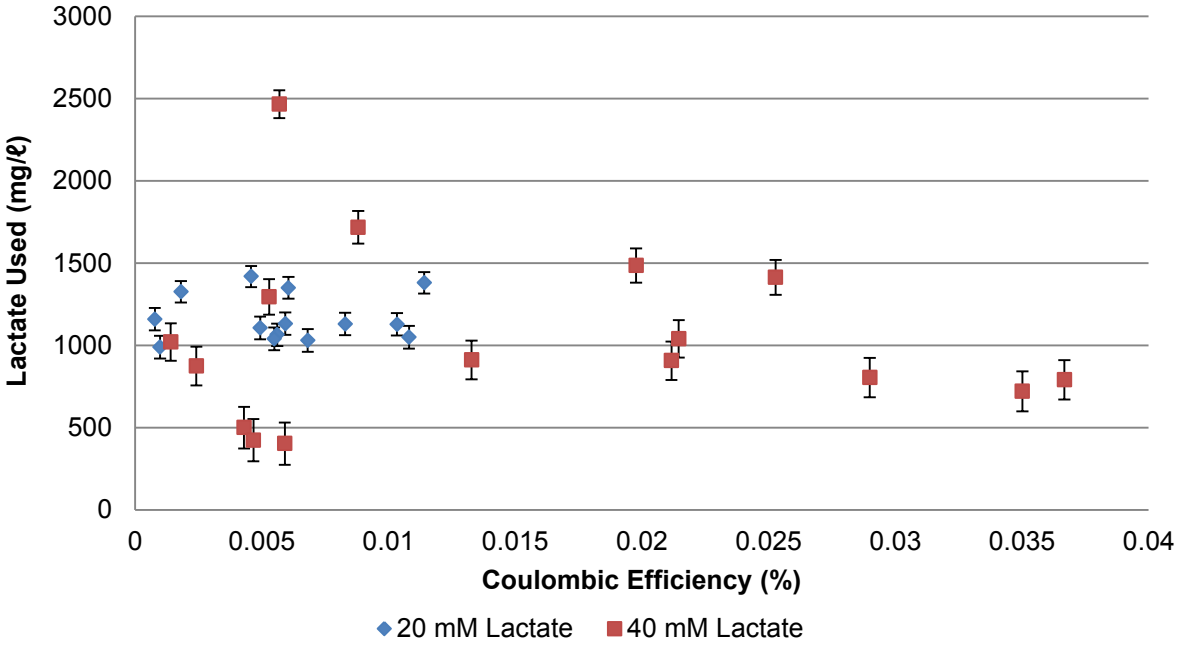

Figure 4-12: Lactate usage as a function of Coulombic Efficiency for MFCs fed different concentrations of lactate in parallel with a 100kΩ resistor

On day 57 of operation, the concentration of the lactate feed for the MFC being fed 40 mM lactate (henceforth called cell 2) was changed from 40 mM lactate to 20 mM lactate. The potential difference for the last feeding cycle with 40 mM lactate and the subsequent four feeding cycles with 20 mM for

Cell 2 are plotted in Figure 4-13. The last four feeding cycles for the 20 mM MFC (henceforth called Cell 1) are also given in Figure 4-13.

At this point in time the potential difference had dropped for both MFCs to the same order of magnitude (within 8 mV of each other) and was very low for both MFCs (below 14 mV). As can be seen in Figure 4-13, when Cell 2 was run on a lactate concentration of 20 mM the potential difference produced continued to decrease in the same trend observed in Figure 4-8 in the days preceding this change. It is therefore difficult to quantify how the change in concentration affected the potential difference, although it can be said that both MFCs had similar electricity generation at this point in time before the next stage of experiments.

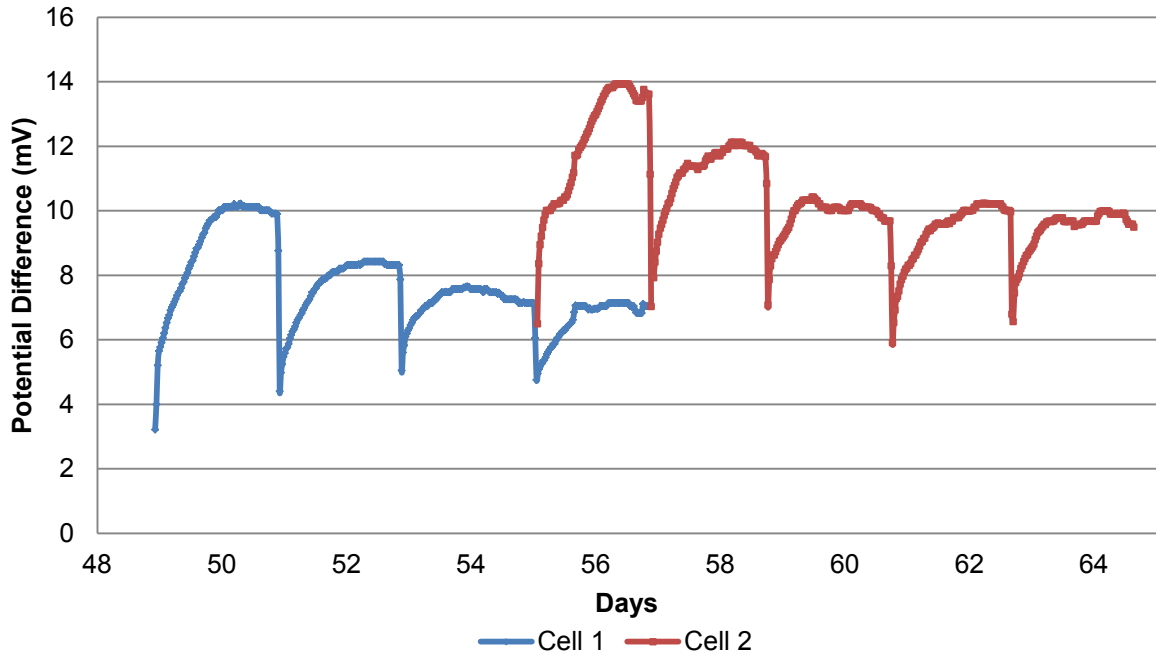

Figure 4-13: Potential as a function of time for MFCs operating with 20 mM lactate in parallel with a 100kΩ resistor

4.3.3 Addition of Ferric Citrate

4.3.3.1 Electrical Performance

Wu *et al.*, (2013b) noted that the addition of Fe(III) citrate into the feed medium resulted in improved power density produced and shortened the start-up period. With a gradual decline of the cell potential produced by the MFCs and no improvement expected, the lactate concentration of both MFCs was fixed at 20mM and the feed medium was altered to include 6mM Fe(III) citrate (Figure 4-14). Although the addition of Fe(III) did not occur at the same time after the initial inoculation for both Cell 1 and 2, the first addition of Fe(III) was marked as time zero for each MFC for this phase of the experiment in order to better compare the potential difference profiles.

As can be seen from Figure 4-14, the cell potential for both MFCs increased substantially upon the addition of the Fe(III) citrate from that produced before its addition (Figure 4-13). In the first feeding cycle with Fe(III), the maximum cell potential increased considerably before becoming more or less constant in subsequent feeding cycles. The maximum potential difference for the first peak after the addition of Fe(III) was similar for both MFCs (between 440 and 470 mV). Thereafter it decreased to approximately 300 mV for Cell 1 and 150 – 200 mV for Cell 2. The maximum power density achieved using Fe(III) citrate feed was 3.09 ± 0.028 mW/m^2 for Cell 1 (Table 4-2). Before the addition of Fe(III) citrate the power density had decreased as low as 7.24x10^{-4} ± 1.14 x10^{-5} mW/m^2.

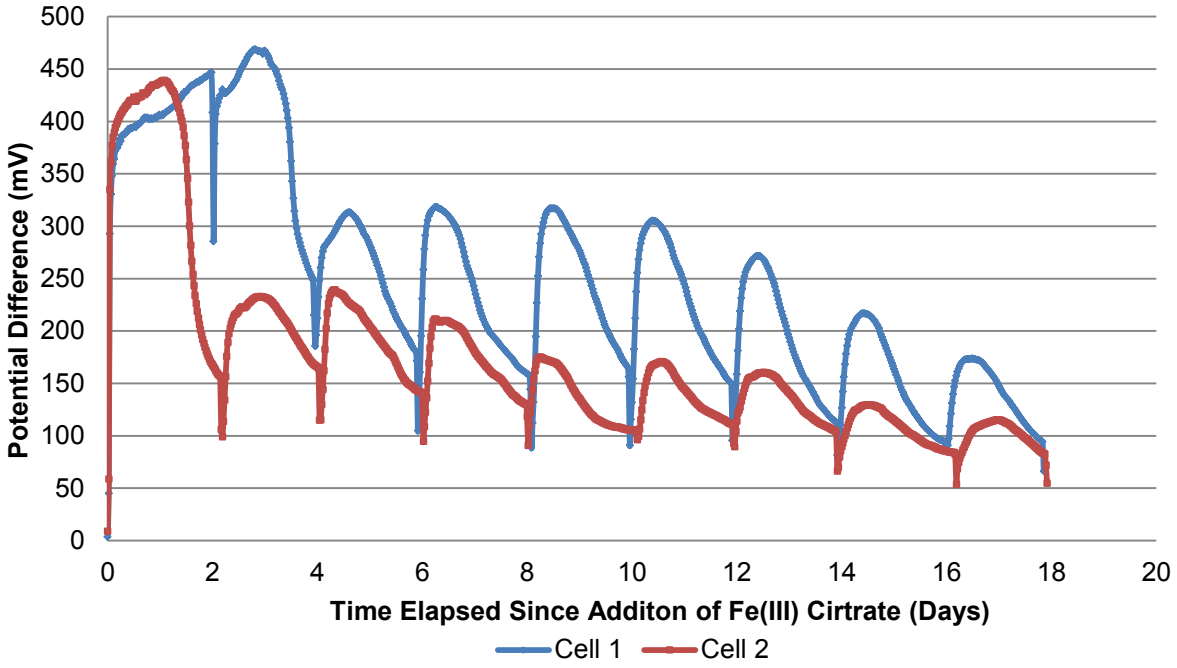

Figure 4-14: Potential as a function of time for MFCs operating with 20 mM lactate and 6 mM Ferric Citrate in parallel with a 100 kΩ resistor

Table 4-2: Table of the maximum potential and corresponding power density achieved for MFCs before and after the addition of ferric citrate to the lactate feed

MFC	Before Addition of 6 mM Ferric Citrate		Before Addition of 6 mM Ferric Citrate	
	Cell 1	Cell 2	Cell 1	Cell 2
Resistor (kΩ)	100		100	
Maximum Voltage Produced (mV)	7.12 ± 0.112	9.89 ± 0.452	465 ± 4.25	439 ± 2.56
Power Density (mW/m^2 anode)	$7.24x10^{-4}$ ± 1.14 $x10^{-5}$	$1.42x10^{-3}$ ± 6.49 $x10^{-5}$	3.09 ± 0.028	2.75 ± 0.016

4.3.3.2 Substrate Utilisation

S. oneidensis MR-1 is a metal reducing bacteria and capable of reducing ferric iron to ferrous iron. The concentration of the ferrous iron in solution at the end of each feeding cycle was therefore monitored over time and was plotted as a function of time for both MFCs in Figure 4-15. The ferrous iron concentration decreased over time for both MFCs. The fastest rate of decreased was observed for the first 8 days after Fe(III) addition

An increase in lactate concentration for both MFCs was observed (Figure 4-16) for the first 6 days after the addition of Fe(III) citrate. Thereafter the concentration remained fairly stable between 1300-1500 mg/ℓ and 1500-1800 mg/ℓ for Cell 1 and 2 respectively for the remainder of the experiment. The corresponding lactate usage during this time remained low for both MFCs (below 400 mg/ℓ for each

feeding cycle) (Figure 4-17). Figure 4-18 shows that for an increase in lactate usage, there is a higher concentration of ferrous iron and therefore higher reduction of ferric iron.

The profile of COD concentration as a function of time (Figure 4-19) followed a similar trend to that of lactate concentration as a function of time (Figure 4-16) i.e. there was a significant increase in COD concentration for the first 6 days after Fe(III) citrate and thereafter the concentration remained reasonably constant between 15500 and 16500 mg/ℓ for the remainder of the cell operation. The CE for both MFCs was found to be higher than that of the MFCs without added Fe(III) citrate and remained mostly constant with a small increase from day 10 until the end of the experiment as shown by Figure 4-20.

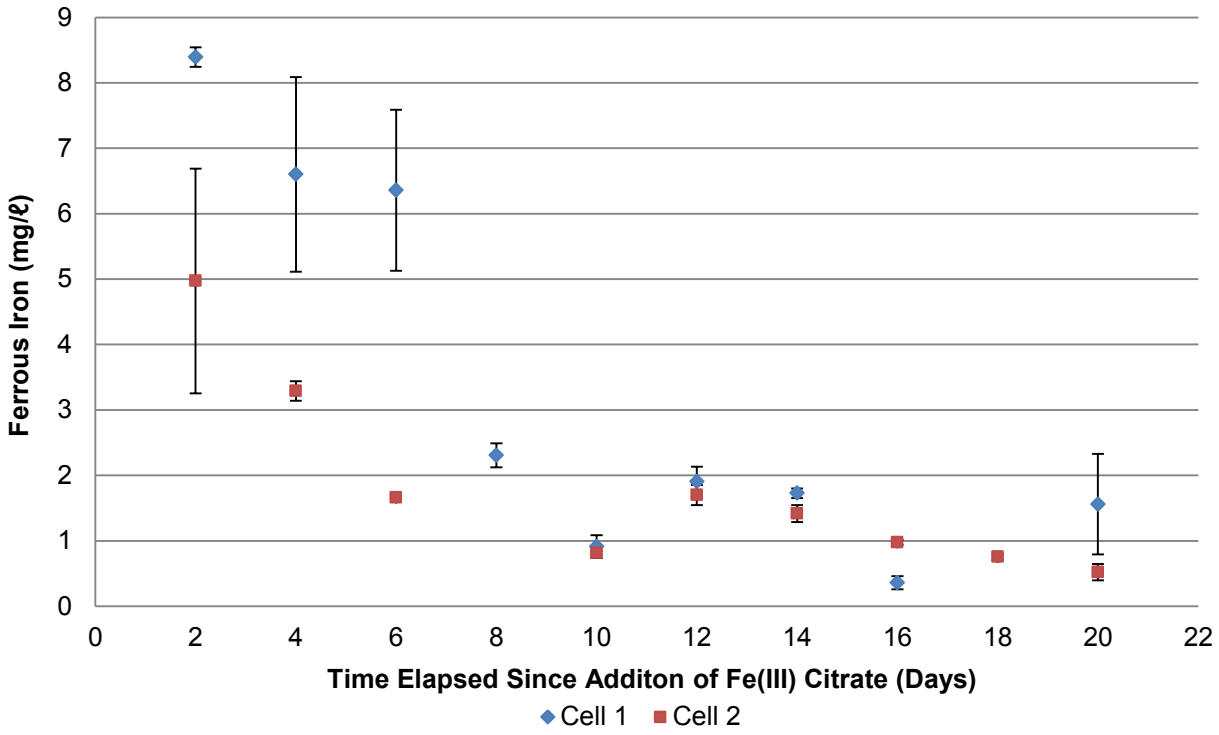

Figure 4-15: Ferrous iron concentration as a function of time for MFCs fed with 20 mM lactate and 6 mM ferric citrate in parallel with a 100 kΩ resistor

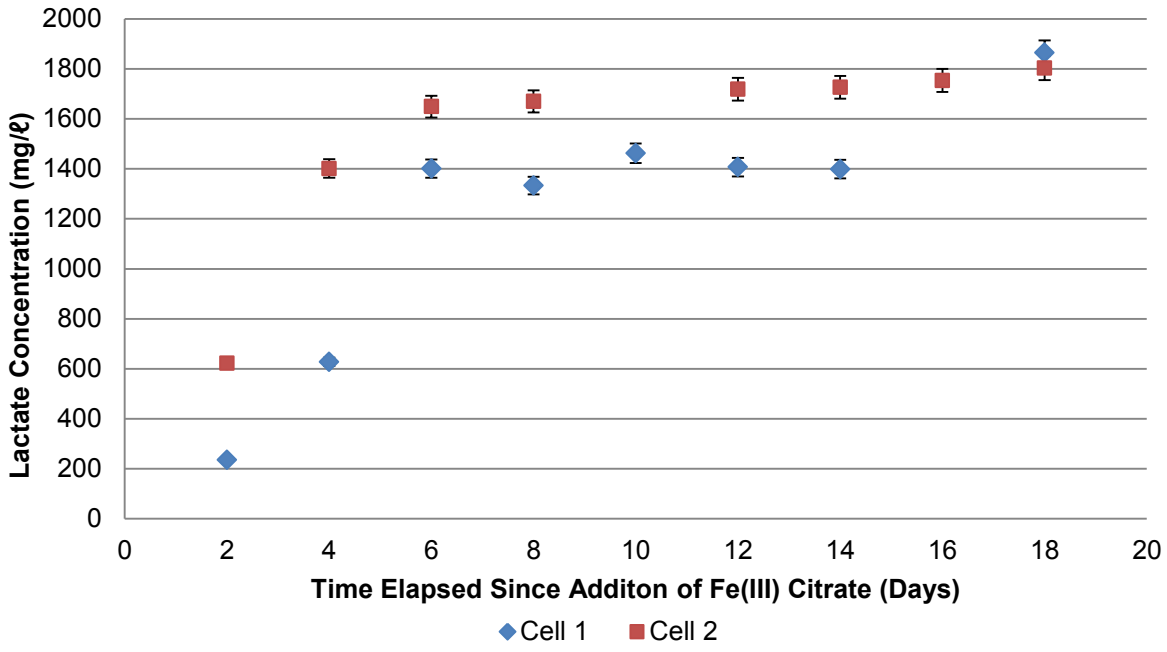

Figure 4-16: Concentration of lactate as a function of time in MFCs fed with 20 mM lactate (1782 mg/ℓ) and 6 mM ferric citrate in parallel with a 100 kΩ resistor

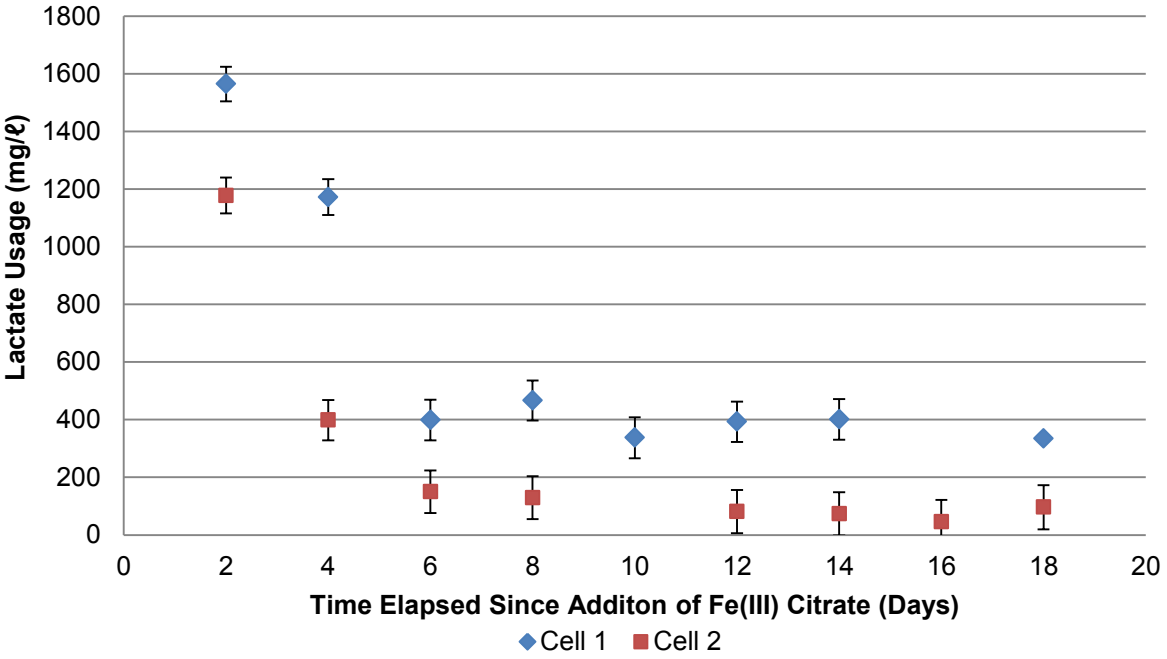

Figure 4-17: Lactate usage as a function of time for MFCs fed with 20 mM lactate (1782 mg/ℓ) and 6 mM ferric citrate in parallel with a 100 kΩ resistor

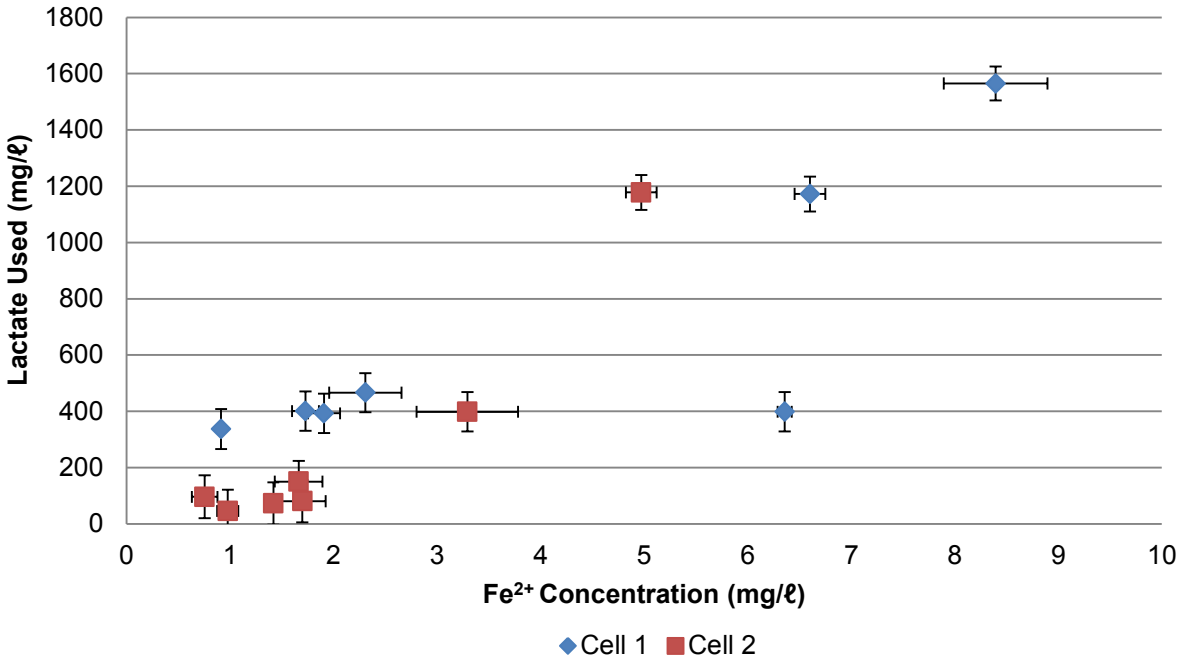

Figure 4-18: Lactate usage as a function of ferrous iron concentration for MFCs fed 20mM lactate (1782 mg/ℓ) and 6 mM ferric citrate medium and in parallel with a 100kΩ resistor

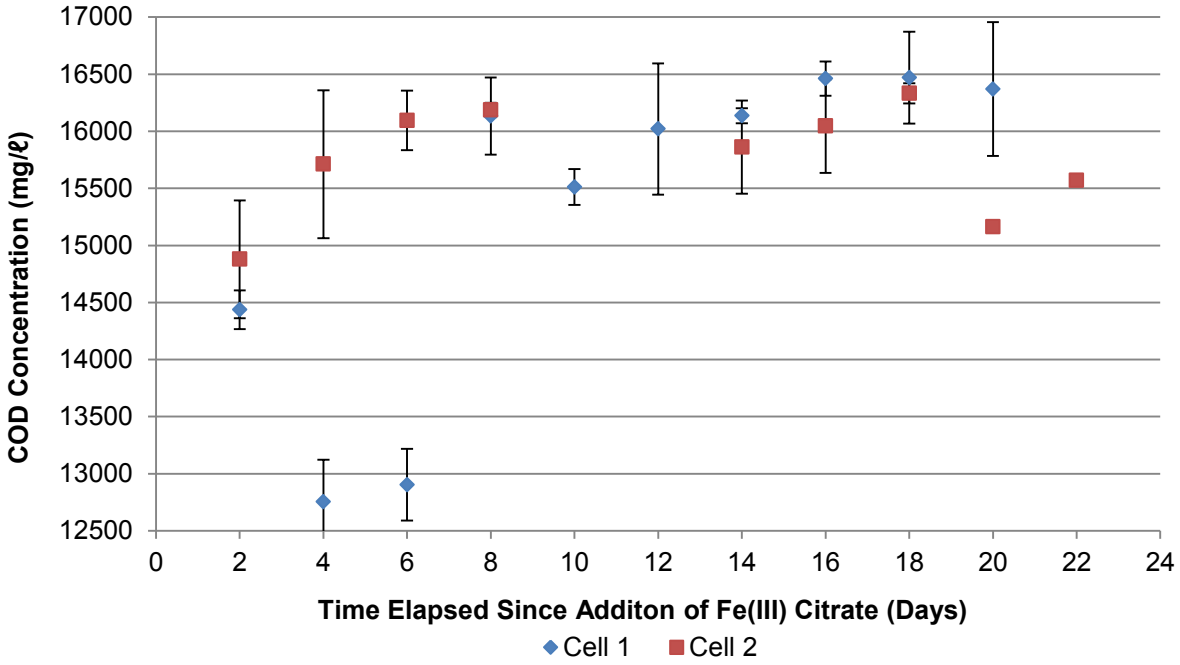

Figure 4-19: COD concentration as a function of time for MFCs fed 20mM lactate and 6 mM ferric citrate medium in parallel with a 100kΩ resistor

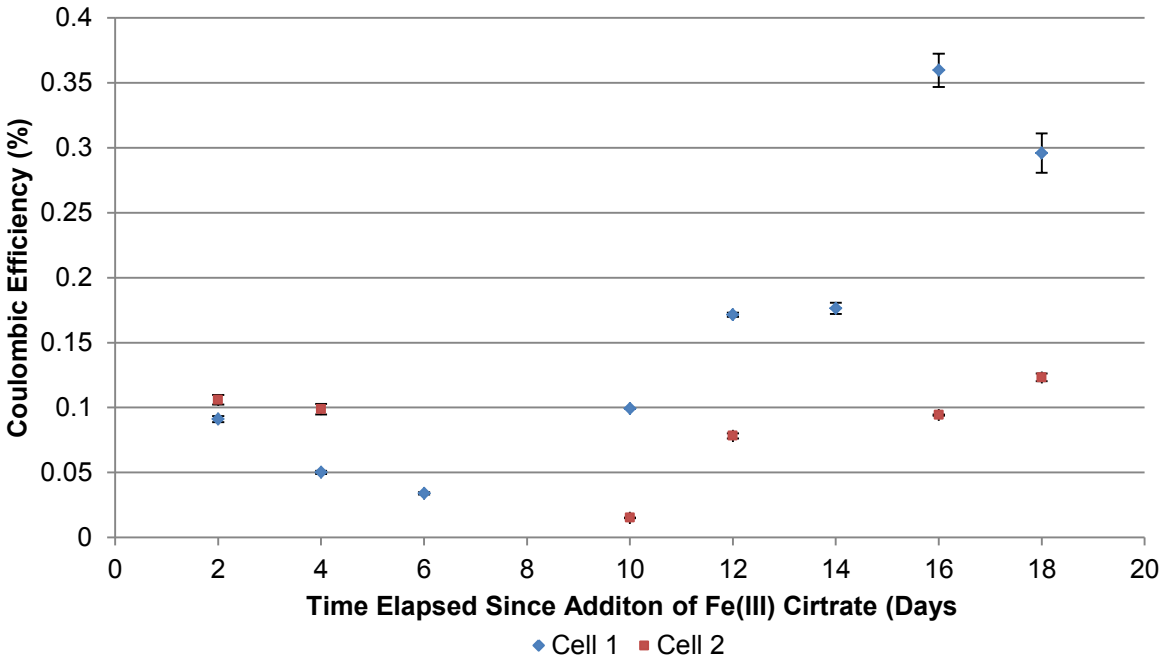

Figure 4-20: Coulombic efficiency as a function of time for MFCs fed 20mM lactate and 6mM ferric citrate medium in parallel with a 100kΩ resistor

4.3.4 Visualisation of the Anode Electrode Using SEM

A sample of the anode of the best performing MFC, producing 13.7 ± 0.228 mW/m^2, was taken for SEM analysis in an attempt to see any nanowires produced by the bacteria colonising the electrode. As discussed in Section 2.8.1.2, *S. oneidensis* MR-1 has been reported in literature to produce nanowires in an anaerobic environment in the absence of dissolved electron acceptors. The MFC operates anaerobically after a biofilm on the cathode had formed, therefore removing oxygen as an electron acceptor. In addition, the MFC demonstrated steady current production.

The carbon electrode itself appeared as closely packed particulate matter (Figure 4-21A). The SEM images clearly show the rod-like *S. oneidensis* MR-1 cells colonising the carbon electrode (Figure 4-21B, Figure 4-21C, Figure 4-21D). Extracellular polymeric substances (EPS) surrounded the cells. During the biofilm dehydration process in preparation of SEM, the biofilm and carbon coating on the cathode cracked and pulled apart clearly revealing the growth of filamentous structures from several of the cells (Figure 4-21C). These structures were comparable with those identified as nanowires on *S. oneidensis* MR-1 by Logan & Regan (2006), who described them as being a “bundles of nanowires containg many individually conductive fillament (like a cable) that together have the appearance of a thick pilus”. The filamentous structures in these images touch both the electrode and other cells in the biofilm as is reported in literature (Logan & Regan, 2006).

Considering their appearance and the oxygen limiting environment in which the cells were grown that is necessary for nanowires to form, these structures are likely nanowires. Figure 4-21D clearly shows nanowires growing from the end of an *S. oneidensis* cell towards the anode.

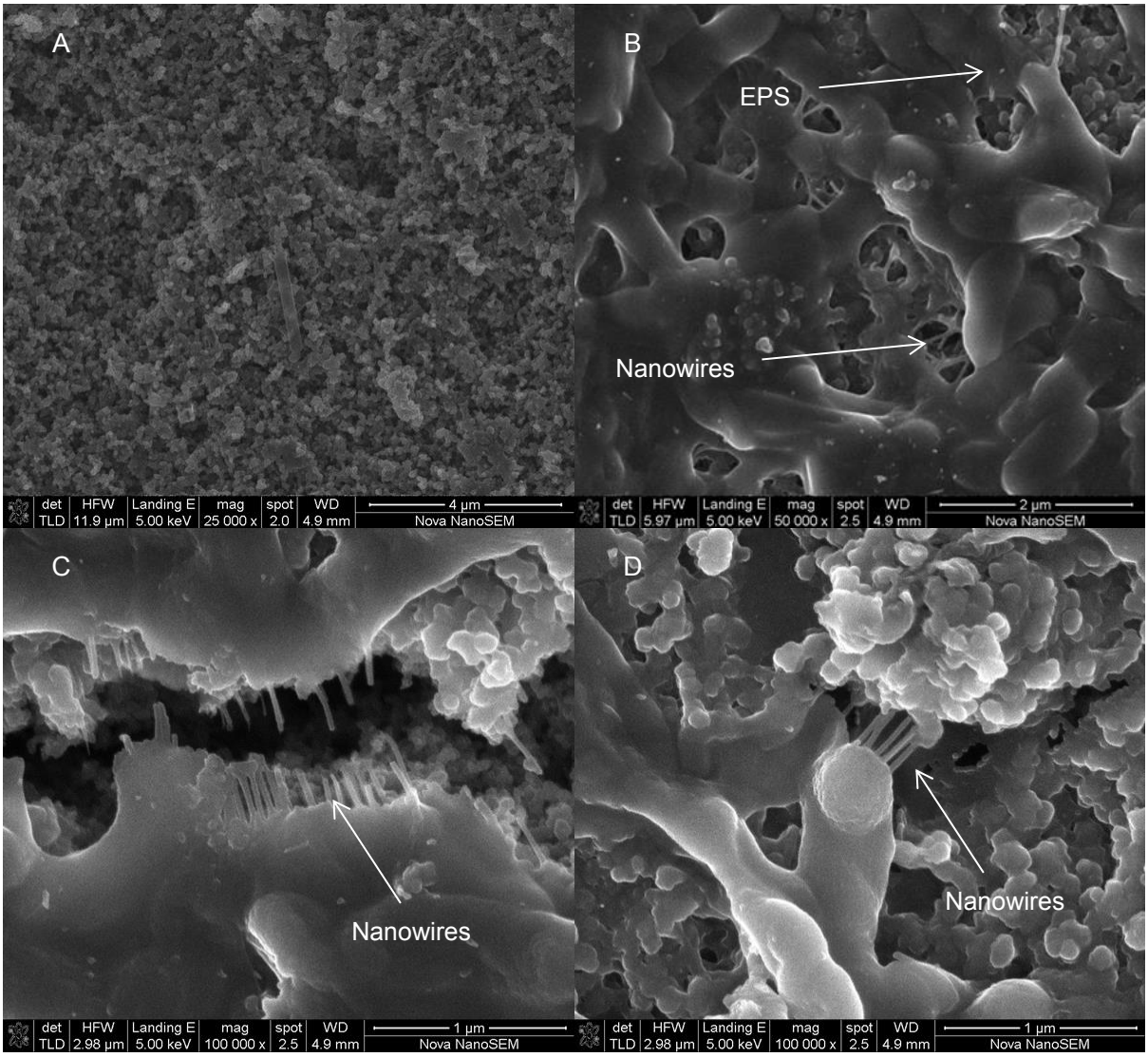

Figure 4-21: SEM pictures of *S. oneidensis* MR-1 producing nanowires on the carbon anode electrode of a MFC fed 20 mM lactate in parallel with a 10 kΩ resistor and 0.2 mg/cm^2 of Pt on the cathode

4.3.5 Microbial Analysis

A melt curve analysis was performed on DNA extracted from the biofilms taken from the anode and cathode of the different single-chambered MFCs operated with *S. oneidensis* MR-1. On observing the de-coupling of DNA strands as a function of temperature (dF/dT), a single peak normally indicates the presence of a single amplicon or bacterial species (unique GC profile), while multiple peaks can indicate that there is more than one bacterial species (or strain) in the sample.

As can be seen from the graph of dF/dT as a function of time for the MFC fed 10 mM lactate with a 0.5 mg/cm^2 coating of platinum on the cathode (Figure 4-22A), the melt curve analysis of the DNA extracted and amplified from the anode and cathode both revealed a single peaks. Both peaks occurred within 0.5°C degrees of the peak of the pure culture of *S. oneidensis* MR-1 and are interpreted as pure *S. oneidensis* biofilms.

The melt curve analysis of the MFC fed 20 mM lactate with a 0.2 mg/cm^2 coating of platinum on the cathode (Figure 4-22B) revealed a single peak from the anodic biofilm within 0.5°C of the pure *S.*

oneidensis culture, however the cathodic biofilm yielded two peaks. This indicates that there was likely more than one bacterial culture present in the cathodic biofilm.

The same trend was observed for Cell 1 and 2 fed 20 mM lactate medium containing 6 mM ferric citrate (Figure 4-23A and Figure 4-23B). These MFCs were originally fed 20 mM and 40 mM lactate medium respectively. Two peaks were observed for the melt curve analysis of the DNA amplified from the cathodic biofilm for both MFCs. In addition, the melt curves of the anodic biofilm from Cell 1 (Figure 4-23A) had two peaks and the peak for Cell 2 (Figure 4-23B) has a notable shoulder. This indicates that contaminating bacteria were likely present in both the anodic and cathodic biofilm on Cell 1 and Cell 2.

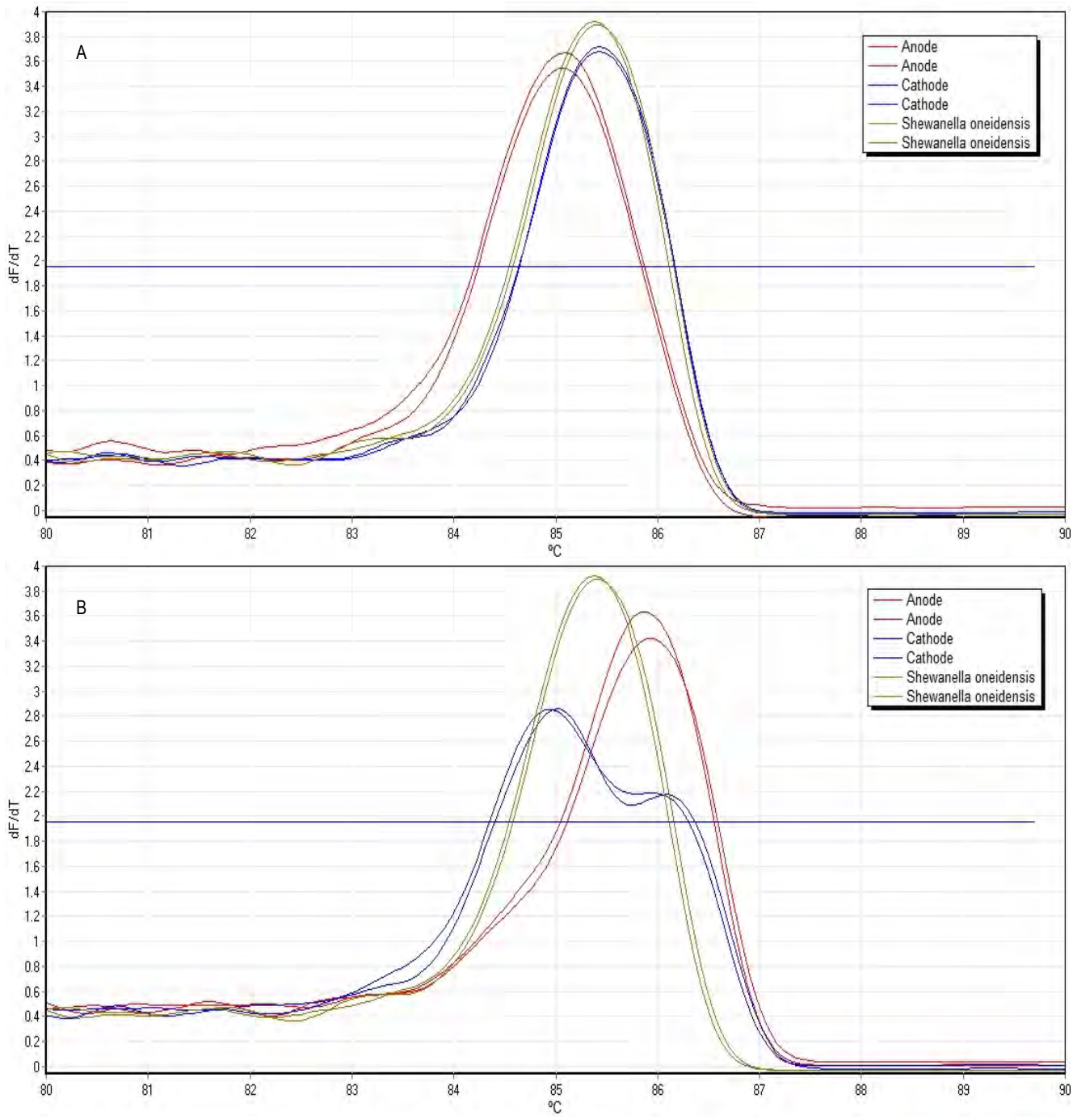

Figure 4-22: Results of melt curve analysis conducted on MFC fed 10 mM lactate with 0.5 mg/cm^2 Pt loading on the cathode and MFC fed 20 mM lactate with 0.2 mg/cm^2 Pt loading.

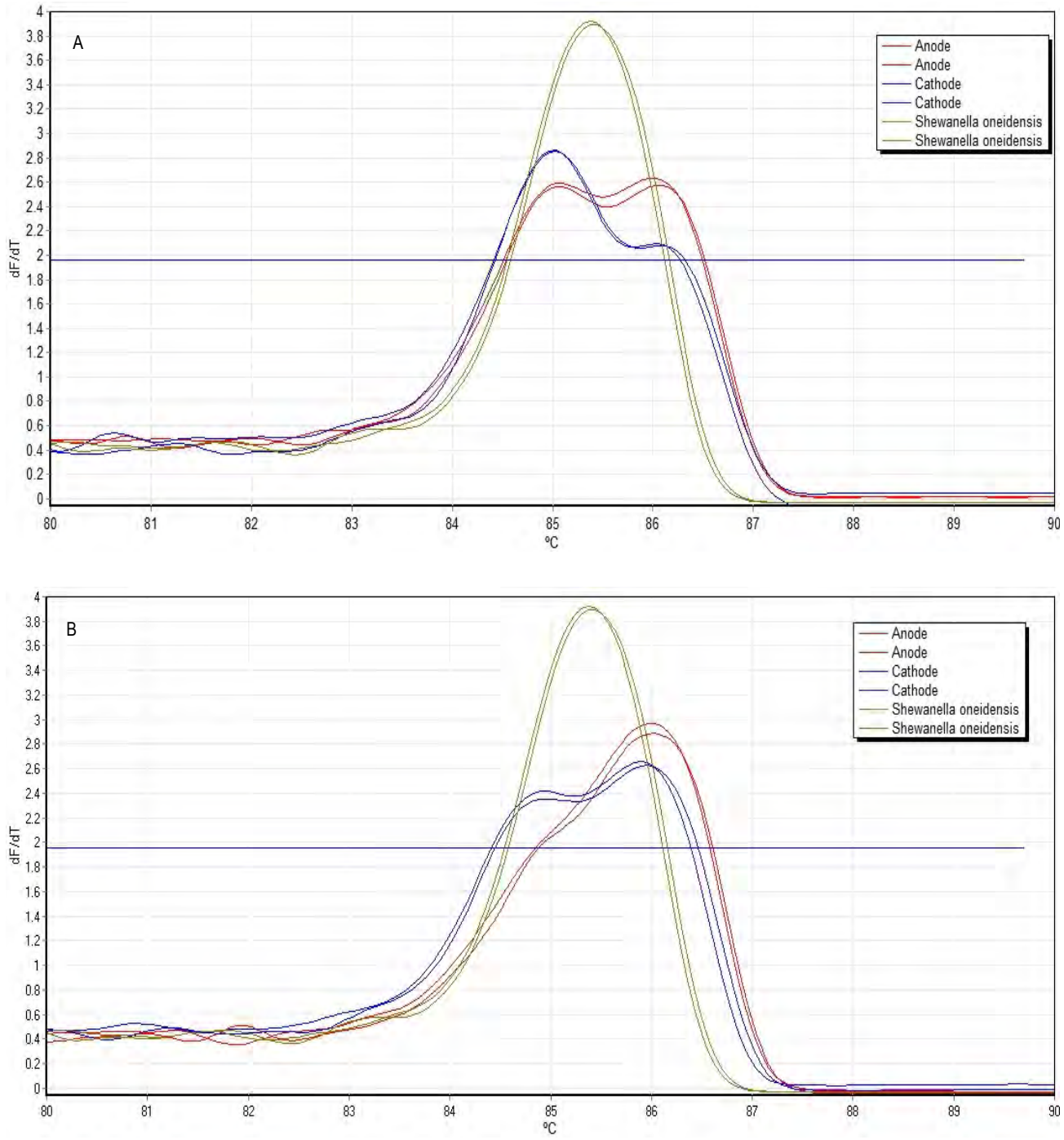

Figure 4-23: Results of melt curve analysis conducted on MFCs A: fed 20 mM and B: fed 40 mM lactate

4.4 DISCUSSION

The long period of time necessary for the MFCs to begin producing notable electricity resulted from the need for both anodic and cathodic biofilm formation as well the adaptation time necessary for the bacteria to adjust to digesting lactate in place of LB medium.

As discussed in Section 2.8.1, *S. oneidensis* MR-1 is only capable of electricity generation under anaerobic conditions (Kim *et al*., 1999). As a result of the MFC being a single chamber with an air breathing cathode, oxygen was able to diffuse through the bulk liquid to the anode. In order to

efficiently produce electricity, the anode must remain anaerobic to avoid loss of electrons to the aerobic oxidation of substrate.

The cathodic biofilm can contribute to preserving the anaerobic state of the anode by consuming oxygen entering through the porous cathode as well as physically inhibiting oxygen diffusion (Crisitiani *et al*., 2013). Some aerobic microbes are capable of adopting the cathode as an electron donor and as a result catalyse the oxygen reduction reaction (Clauwaert *et al*., 2007; Cha *et al.,* 2010; Wang *et al*., 2014). Therefore the electricity production is hindered before a substantial cathodic biofilm is formed. Further, good colonisation of the anode is required for electricity production.

Under normal MFC operation, it is expected that *S. oneidensis* growing on the anode digests lactate anaerobically to produce acetate which it will not digest any further (Ringø *et al*., 1984; Lovley *et al*., 1989). As a result of the MFC being a single chamber, *S. oneidensis* also grew on the cathode where aerobic digestion of substrate occurred for the bacteria in immediate contact with the electrode. It is possible that these aerobic bacteria degraded the acetate produced by the anaerobic bacteria. Mass transfer limitations of substrate may have arisen depending on the thickness of the biofilm and therefore, despite a strong preference for lactate, acetate was degraded. It is also possible that the cathodic bacteria digested some lactate which did not contribute to electricity production.

4.4.1 Performance of MFCs

Electricity Production

As stated in the Section 4.1, the experiments were conducted on constructed single-chambered MFCs operating with pure culture of *S. oneidensis* MR-1 to assess the assembly of the MFCs and compare its performance to that reported in literature. The experiments conducted by Wu *et al*., (2013b) found the maximum power density production by *S. oneidensis* MR-1 to be 73.9 ± 2.8 mW/m^2 (±227 mV; 1 kΩ resistor) in the absence of Fe(III) and 158.1 ± 4.8 mW/m^2 (±332 mV; 1 kΩ resistor) in a MFC with 6 mM ferric citrate added. Therefore, using a platinum loading of 0.5 mg/cm^2 on the cathode and 10 mM lactate substrate, the MFC should produce a power density of approximately 74 mW/m^2. The highest power density achieved in these experiments was 13.73 ± 0.228 mW^2. This was substantially lower (18.6%) than that reported in literature, however this may be as a result of several factors.

For the same MFC design, Cheng *et al*. (2006a) noted that a carbon cloth cathode with 0.5 mg/cm^2 platinum loading made with a 5% Nafion binder performed 19% better on average than the same cathode with a 0.1 mg/cm^2 platinum loading. Cheng *et al*. (2006b) noted that, in the same MFC, the performance of the MFC could be improved by coating the air facing side of the cathode with polytetrafluoroethylene (PTFE), to decrease water flooding of the catalyst. The power density produced by the MFC was found to increase by 15% on addition of the first diffusion layer of PTFE (30 wt%). Four diffusion layers (base layer of 30 wt% PTFE with 60 wt% for successive layers) were found to increase the power density by 42% and improve the CE by 171%.

The cathode used by Wu *et al*. (2013b) had a platinum loading of 0.5 mg/cm^2, 30% wet proofing and was coated with 40% PTFE on the air facing side, whereas the cathode used in these experiments had only 0.2 mg/cm^2 Pt loading, 10% wet proofing and no PTFE diffusion layers. In addition, the connection of the electrodes to the current collectors and external circuits was very crude compared to that used in literature. The original MFC setup made use of platinum wires (Liu and Logan, 2004) soldered to the electrodes, whereas these MFCs used only the pressure of the bolted MFC chamber and ends to ensure connection between the electrodes and the external circuit. This increased the internal resistance of the MFC considerably and resulted in lower potential differences and power densities produced by the MFC.

Therefore, taking into account the many inadequacies of the cathodes used in these experiments, it is likely that the power density of 13.7 ± 0.228 mW/m^2 recorded in these experiments was appropriate for the setup. The single chamber MFC could therefore be said to be adequately constructed for further testing with other microorganisms. It is hypothesised that improvements in cell performance could be made through improvements to the connection and construction of the cathode.

It is unclear as to why one MFC run so significantly outperformed the others. The experiments conducted, in which different concentrations of lactate were used, should have revealed similar potential differences to those produced by the MFC fed 20 mM lactate (0.2 mg/cm^2 platinum on the cathode) used in the replication study. However, this was not the case.

As can be seen from the melt curve analysis of the anode and cathode of the MFC fed 10 mM (0.5 mg/cm^2), single peaks with no shoulders were observed for both electrodes (Figure 4-22A). The melt curves for both electrodes were very similar to that of the pure *S. oneidensis* melt curve and the biofilms are believed to have been pure cultures of *S. oneidensis*. As can be seen from the melt curves of the cathodic biofilm for the Cell 1 and 2 fed ferric citrate, two peaks were clearly visible (Figure 4-23A and B). Two peaks were also observed for the anodic biofilms. It is therefore very likely that one or more contaminating bacteria were present in the anodic and cathodic biofilms.

The melt curve of the cathodic biofilm of the MFC fed 20 mM lactate (0.2 mg/cm^2 platinum on the cathode) which produced 13.7 ± 0.228 mW/m^2, exhibited two peaks (Figure 4-22B). This MFC outperformed both Cell 1 and 2 despite the likely presence of contaminating bacteria in the cathodic biofilm. The anodic biofilm produces electricity and the presence of contaminating bacteria in this biofilm likely negatively affected the electricity generation by Cell 1 and 2, whereas a MFC was capable of good electricity production when only the cathodic biofilm was contaminated.

Although the MFCs and all relevant components were chemically sterilised on setup and hygienically operated, the system as a whole was not operated sterilely. The MFC was made from Perspex which cannot be heat-sterilised. Autoclaving can also potentially cause the platinum coating on the cathode to crack and chemical sterilisation of the cathode was not possible due to fouling or compromising of the platinum layer.

4.4.2 Effect of Lactate Concentration

A higher potential difference was observed for the MFC fed 40 mM lactate than for the 20 mM lactate (Figure 4-8). This was expected as several studies have tested the effects of a range of COD loading rates on the electrical performance of MFCs and found that the power density produced increased with an increase in COD for the tested range (Clauwaert *et al.,* 2007; Jiang and Li, 2009; Zhu *et al*., 2011; Wang *et al*., 2014).

It is evident that the lactate usage was similar for both MFCs (Figure 4-9) despite the difference in concentration and potential difference. It has been previously noted that an increase in COD loading resulted in decreased internal resistance of the MFC (Jiang and Li, 2009; Wang *et al*., 2014). This was attributed to the increase in ionic strength at high substrate concentration which reduces ohmic losses. It is possible improved ionic strength resulted in improved electricity generation for the 40 mM instead of higher lactate usage.

The lactate usage remained fairly constant throughout the experiment although there was notable increased lactate usage for the 40 mM MFC from approximately day 35 to 45. The CE decreased during this period (Figure 4-11) which implies that the increased lactate use was not aiding current generation, but used elsewhere. On day 33 the cathodic biofilm of the 40 mM MFC was disrupted and began to peel off the cathode. It was fully dislodged by day 39. It is hypothesised that the increase in lactate usage was therefore contributing to the growing of a new biofilm on the cathode during this time.

The CE was very low for both lactate concentrations. This is postulated to result from the very low potential difference for the duration of this experiment. It is evident from the relationship of lactate usage and CE that the lactate usage remains fairly constant throughout the range of CEs achieved (Figure 4-12). It is therefore assumed that the decrease in CE for both MFCs is a result of the decrease in electricity production by the bacteria.

4.4.3 Addition of Ferric Citrate

After the addition of ferric citrate to the feed medium of the MFCs, there was initially a substantial increase in maximum cell potential achieved for both MFCs in the first feeding cycle (Figure 4-14). Subsequent feeding cycles produced lower and more reproducible cell potentials that remained improved substantially by the addition of ferric citrate. Both MFCs had decreasing cell potentials prior to the addition of Fe(III) citrate (Figure 4-8 and Figure 4-13). This likely resulted from contaminating bacteria outcompeting *S. oneidensis* which continued after the Fe(III) addition as seen in the gradual decrease in cell potential seen in Figure 4-14.

The reduction reaction at the cathode has often been found to be the limiting step in electricity generation (Jang *et al.*, 2004; Du *et al.*, 2007; Jiang and Li, 2009; Wang *et al.*, 2014). It is hypothesised that the initial increased maximum cell potential achieved was a result of a surplus of available electrons in solution contributing to the reduction reaction with Fe(III). This is also seen in the initially higher values of ferrous iron in solution after Fe(III) was added, which decreased over the duration of MFC operation (Figure 4-15). As can be seen from Figure 4-18, increased lactate usage corresponded to increased reduction of ferric iron.

The maximum cell potential produced decreased gradually over the duration of the experiment, although still improved by the addition of the ferric citrate. As is discussed in Section 2.8.1.2, *S. oneidensis* MR-1 is able to produce flavins which act as soluble redox mediators which effectively shuttle electrons between the microbe and the metal to be reduced or the anode in the case of MFCs (von Canstein *et al.*, 2008). The production of flavins results in both reduction of insoluble electron acceptors and improved electron transfer from the microbe to the anode, resulting in improved electricity production (Wu *et al.*, 2013a; Wu *et al.*, 2013b). The increased potential difference observed for the MFCs after the addition of ferric citrate in these experiments supports this.

The CE initially decreased over the first 6 days of operation (Figure 4-20) in correspondence with the decreasing and increasing trends observed for ferrous iron and lactate concentration respectively over the first 6 days of the experiment. This implies that the increased lactate usage during this time did not result in the generation of electricity. From day 6 onwards the CE increased with time for MFC 1 but remained fairly constant below 0.15% for MFC 2. The CE achieved with the addition of ferric citrate was higher than that of the other MFCs investigated. The presence of flavins possibly aided electron transfer and therefore improved CE.

4.5 CONCLUSIONS

The single-chambered MFC operating with a pure culture of *S. oneidensis* MR-1 and a lactate feed produced a maximum power density of 13.7 ± 0.228 mW/m^2. This was 18.6% of that reported in literature and thought to have resulted from the many inadequacies of the cathodes used in these experiments. It is hypothesised that improvements in cell performance could be made through improvements to the connection and construction of the cathode. However, the single chamber MFC was deemed to be adequately constructed and suitable for further testing with other microorganisms.

SEM conducted on the anode of the MFC fed 20 mM lactate in parallel with a 10 kΩ resistor and 0.2 mg/cm^2 of Pt on the cathode, revealed the presence of nanowires growing from the *S. oneidensis* cells in the anodic biofilm. This is indicative of electricity production.

Contaminating bacteria were present in the MFCs despite efforts to avoid contamination. Contaminating bacteria in the anodic biofilm negatively affected the electricity production. The MFC was capable of producing electricity with contaminating bacteria present in the cathodic biofilm.

An increase in the lactate concentration improved the electricity production for the range of concentrations tested. The addition of 6 mM ferric citrate to the feed medium improved the electricity generation and coulombic efficiency produced by the MFC via the production of flavins which aided electron transport.

5 PERFORMANCE OF SULPHATE REDUCING AND SULPHIDE OXIDISING BACTERIAL COMMUNITIES IN SINGLE-CHAMBERED MFCs

5.1 INTRODUCTION

This chapter details the investigation into the operation of a single-chambered MFC, originally designed by Liu and Logan (2004), operating with a mixed community of SRB and SOB cultured on lactate medium. The investigation aims to determine the ability of the community to produce electricity. The mixed microbial community is similar to that present in a linear flow channel reactor (LFCR) established for treatment of acid mine drainage. In Chapter 6, the integration of a MFC into the LFCR is investigated. The integrated LFCR-MFC is designed for combined biological sulphide reduction and sulphide oxidation to yield a sulphur product and generate electricity.

The single-chambered MFC chosen for the testing of the microbial community from the LFCR was selected based on several factors discussed in Section 4.1. The MFC constructed at UCT was tested by replicating a study performed by Wu *et al*. (2013b) with a pure culture of *Shewanella oneidensis* MR-1 cultured on lactate, reported in Chapter 4, prior to being used in this investigation where it was operated with the same substrate and microbial community used in the LFCR. Investigations could therefore be conducted on the ability of the mixed microbial community to produce electricity the potential of an integrated system for electricity production.

The specific objectives of the research presented in this chapter were as follows:

1. To operate the constructed single-chambered MFC with the same microbial community and substrate used in the LFCR investigated by van Hille *et al*. (2015).
2. To evaluate the ability of the mixed community to produce electricity and treat sulphate-rich wastewater in order to determine the feasibility of an integrated reactor.
3. To determine the effects of using a carbon microfibre brush anode in place of the standard carbon felt anode used in literature to understand the effects carbon microfibres (used in the LFCR) might have on the electricity production in the constructed LFCR-MFC.

5.2 EXPERIMENTAL APPROACH

5.2.1 Data Collection

The detailed experimental procedure used in these experiments is given in Section 3.2.2. The potential difference over MFCs in parallel with a resistor was monitored throughout the duration of the experiment using a data logger and computer. Samples taken were analysed for the concentration of sulphate, sulphide, COD and volatile fatty acids. The concentration of lactate and sulphate in the standard feed used in these experiments was maintained at 15 mM. The experiments conducted were divided into four sections and are listed below:

1. A base case of electricity production by the microbial community was investigated in four MFCs (MFC 1-4) with a 15 mM lactate and sulphate feed medium. Scanning Electron Microscopy (SEM) was conducted on the anode and cathode of a well performing single-

chambered MFC, the details of which are given in Section 3.6.1, to assess the microbial community.

2. The effect of using a carbon microfibre brush anode was investigated (MFC-CBA). Carbon microfibre was used as the anode in the integrated LFCR-MFC (Chapter 6).This was done in an attempt to minimise differences between the single-chambered MFC and the integrated LFCR-MFC system. The details of the carbon microfibre brush anode are given in Section 3.2.2. The cathode was unchanged.
3. The effect of the concentration of lactate and sulphate in the feed medium was investigated. Two MFCs were fed concentrated medium (28 mM lactate and sulphate). One MFC was placed in parallel with a resistor (MFC-CFC) and the potential difference over the MFC was monitored. The other remained in an open circuit (MFC-CFU) and was not monitored. In order to determine the effect of a change in substrate concentration, a MFC with a carbon felt anode (MFC 5) and the MFC with a carbon microfibre brush anode (MFC-CBA) were operated with standard feed medium until a reproducible pattern in potential difference and stable power density was observed. The fed medium was then changed to concentrated medium.
4. Cyclic voltammetry (CV) was conducted on abiotic fresh medium, abiotic spent medium, planktonic cells in spent medium and the biofilm in fresh medium in order to decouple the electricity generation by the cells in the biofilm and planktonic cells present in the MFCs. CV was also conducted on the anode and cathode of the MFC fed concentrated medium and connected in circuit. The details of the procedure are given in Section 3.4.3.

Details of the MFCs and their operation used in these experiments is summarised in Table 5-1. Letters are used to denote a change in inoculum i.e. the inocula were taken at different points in the lifetime of the stock culture. Sulphide and COD determination were carried out in triplicate for all samples taken. Sulphate concentration was determined through ion chromatography (IC). IC and HPLC were only conducted on one sample per sampling interval owing to constraints on equipment access and the run time required for resolution of all components. All standard curves and raw data obtained for these experiments can be found in Appendix A and Appendix C respectively.

Table 5-1: Table of details of the operation of various single-chambered MFCs

<table>
<tr><th>Name</th><th>Description</th><th>Inoculum</th><th>Feed</th></tr>
<tr><td>MFC 1</td><td rowspan="3">Carbon Felt Anode</td><td rowspan="3">A</td><td rowspan="3">Standard (15 mM Lactate and Sulphate)</td></tr>
<tr><td>MFC 2</td></tr>
<tr><td>MFC 3</td></tr>
<tr><td>MFC 4</td><td>Carbon Felt Anode</td><td>B</td><td>Standard (15 mM Lactate and Sulphate</td></tr>
<tr><td>MFC 5</td><td>Carbon Felt Anode</td><td rowspan="2">C</td><td rowspan="2">Standard (15 mM Lactate and Sulphate) and Concentrated (28 mM Lactate and Sulphate)</td></tr>
<tr><td>MFC-CBA</td><td>Carbon Brush Anode</td></tr>
<tr><td>MFC-CFC</td><td>Carbon Felt Anode – Connected in Circuit</td><td>D</td><td>Concentrated (28 mM Lactate and Sulphate)</td></tr>
</table>

Name	Description	Inoculum	Feed
MFC-CFU	Carbon Felt Anode – Unconnected in Circuit		

5.2.2 Data Handling

Calculations performed to determine power density and coulombic efficiency are given in detail in Section 4.2.2. Calculations for the balancing of VFAs are given in Section C.3.2.

5.2.2.1 Internal Resistance

Internal resistance (R_{int}) can be approximated by either calculating the slope of the linear region of the polarisation curve (current (I) as a function of voltage (V)) (Equation 18) or from the maximum power density (P_{max}) (Logan, 2008).

$$R_{int} = \frac{V_2 - V_1}{I_2 - I_1} \quad \text{Equation 18}$$

The maximum power density is achieved when the internal resistance of the MFC is equal to the resistance in the external circuit. The maximum power density can be approximated by fitting a trendline (in this case a second order parabola) to the power density curve (Equation 19). The first derivative is determined and set equal to zero (Equation 20) to get the x coordinate of the turning point of the curve, corresponding to the current (I_{max}) at the maximum power density (Equation 21). The maximum power density (y coordinate of the turning point) is determined by substituting the I_{max} into Equation 22. The internal resistance at the maximum power density can then be determined by Equation 23.

$$y = ax^2 + bx + c \quad \text{Equation 19}$$

$$\frac{\partial y}{\partial x} = 0 = 2ax + b \quad \text{Equation 20}$$

$$x = I_{max} = \frac{b}{2a} \quad \text{Equation 21}$$

$$y = P_{max} = a\left(\frac{b}{2a}\right)^2 + b\left(\frac{b}{2a}\right) + c \quad \text{Equation 22}$$

$$R_{int} = \frac{P_{max}}{I_{max}^2} = \frac{y}{x^2} \quad \text{Equation 23}$$

5.3 RESULTS

5.3.1 Electrical Performance

5.3.1.1 Carbon Felt Anode

Four single chambered MFCs were operated with a mixed SRB / SOB consortium growing on lactate and sulphate with intermittent media replenishment. A general trend in the maximum potential difference was noted for three of the single-chambered MFCs. The maximum potential for each feeding cycle increased with time over the first few days after inoculation until a maximum was reached (Figure 5-1, Figure 5-2 and Figure 5-3). For all three MFCs the potential difference peaks in the first 4 days of the experiment are defined and narrow which corresponded to spiking with a stock culture high in sulphide concentration. In the case of both MFC 1 and MFC 2, the maximum potential was maintained for a few feeding cycles before decreasing. In the case of MFC 1 (Figure 5-1) the decrease was slow, whereas for MFC 2 (Figure 5-2) the potential dropped substantially on day 27 without recovery.

MFC 3 achieved a reasonably stable maximum cell potential within 6 days after inoculation (Figure 5-3). As a result of its reproducibility the cell was placed in parallel with a smaller resistor (10 kΩ) between days 14 and 18. As a result of the very low potential difference achieved during this time and the decrease in maximum cell potential achieved, the resistor was changed back to 100 kΩ for the remainder of the experiment.

A polarisation curve plotted for MFC 3 is given in Figure 5-4. A maximum power density of 2.86 ± 0.009 mW/m^2 of cathode area was achieved. As mentioned in Section 5.2.2.1, an estimation of the internal resistance of the cell can be made by using the slope of the linear region of the polarisation curve and from the maximum power density (Logan, 2008). The calculation of the slope of the linear region of the curve of potential difference as a function of current (Figure 5-4) revealed that the internal resistance of the MFC was approximately 20 600 ± 571 Ω.

Data was only recorded for MFC 4 from day 13 of the experiment onwards. This was due to data loss and logging difficulties arising from electricity supply interruptions. The MFC was in parallel with a 100 kΩ resistor until day 30 of the experiment (Figure 5-5). In this initial stage the potential difference remained largely constant for the duration of each feeding cycle. Decrease in the potential was as a result of feeding. On day 30 the resistor in the external circuit was changed to 10 kΩ (Figure 5-6). A common trend was noted for subsequent feeding cycles in which the potential increased slowly followed by a dramatic increase before a maximum was reached and the potential began to decrease. As this point the MFC was fed and a dramatic drop in potential was noted. This trend was most evident for days 30 to 48 of the experiment. Data is missing between days 42 to 45 due to electricity cuts. From day 48 until the end of the experiment, a double peaked trend for a feeding cycle was still observed however, the peaks become smaller and are similar in amplitude. There is also a general trend of decreasing maximum cell potential was observed from approximately day 26 of the experiment.

A polarisation curve was plotted for MFC 4 on day 44 of the experiment and is presented in Figure 5-7. A maximum power density of 0.926 ± 0.057 mW/m^2 of cathode area was achieved. The internal resistance of the MFC was calculated to be approximately 21 600 ± 846 Ω.

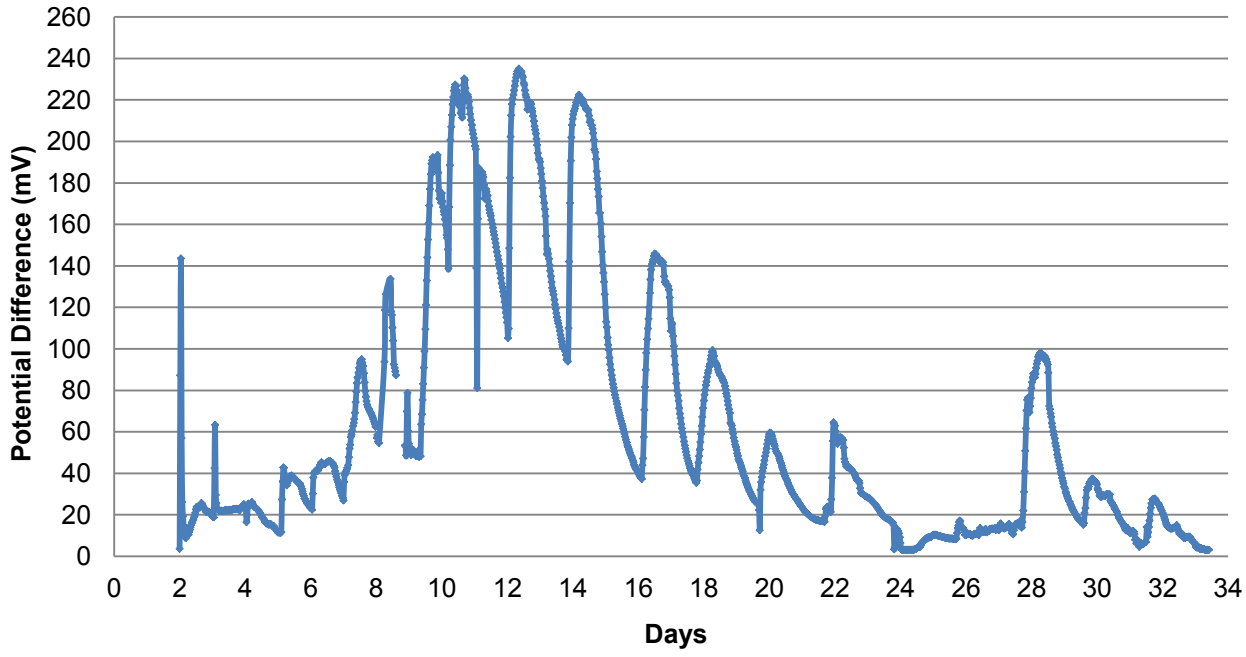

Figure 5-1: Cell potential as a function of time for MFC 1 with carbon felt anode fed standard medium and in parallel with a 100 kΩ resistor

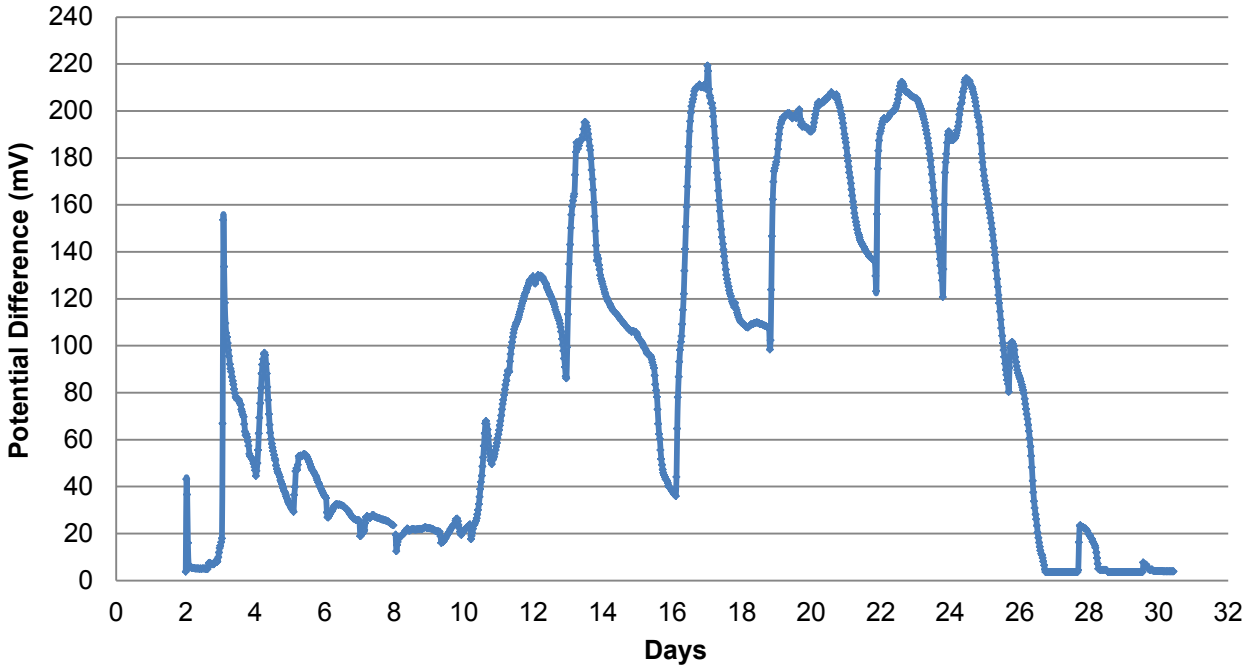

Figure 5-2: Cell potential as a function of time for MFC 2 with carbon felt anode fed standard medium and in parallel with a 100 kΩ resistor

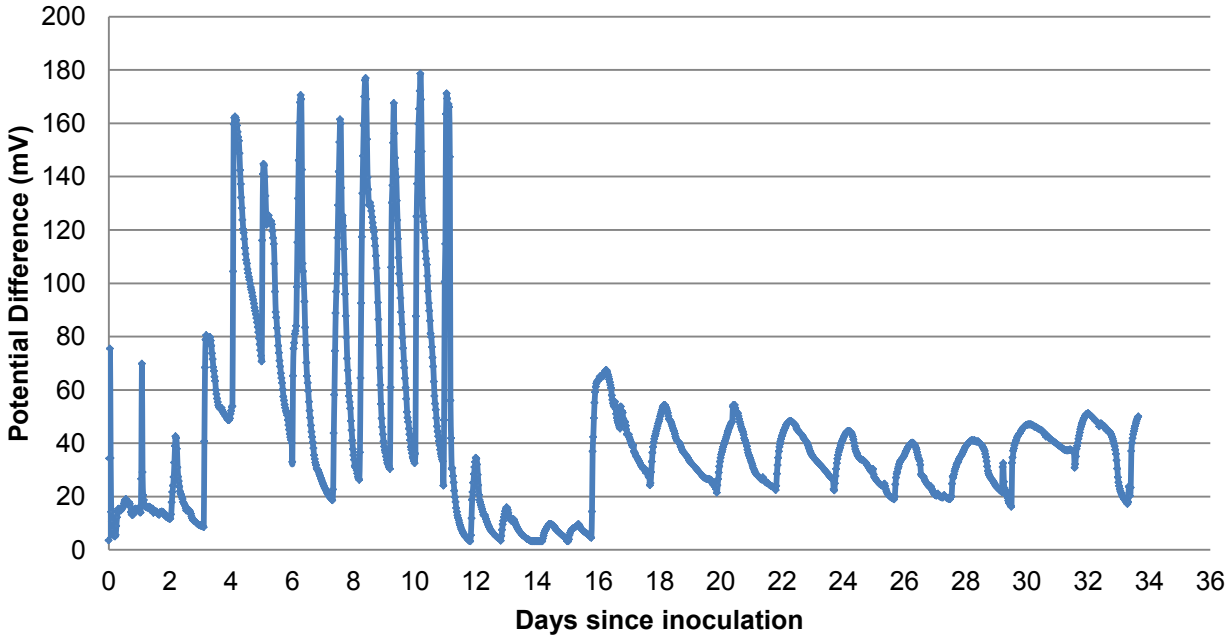

Figure 5-3: Cell potential as a function of time for MFC 3 with carbon felt anode fed standard medium and in parallel with a 100 kΩ resistor

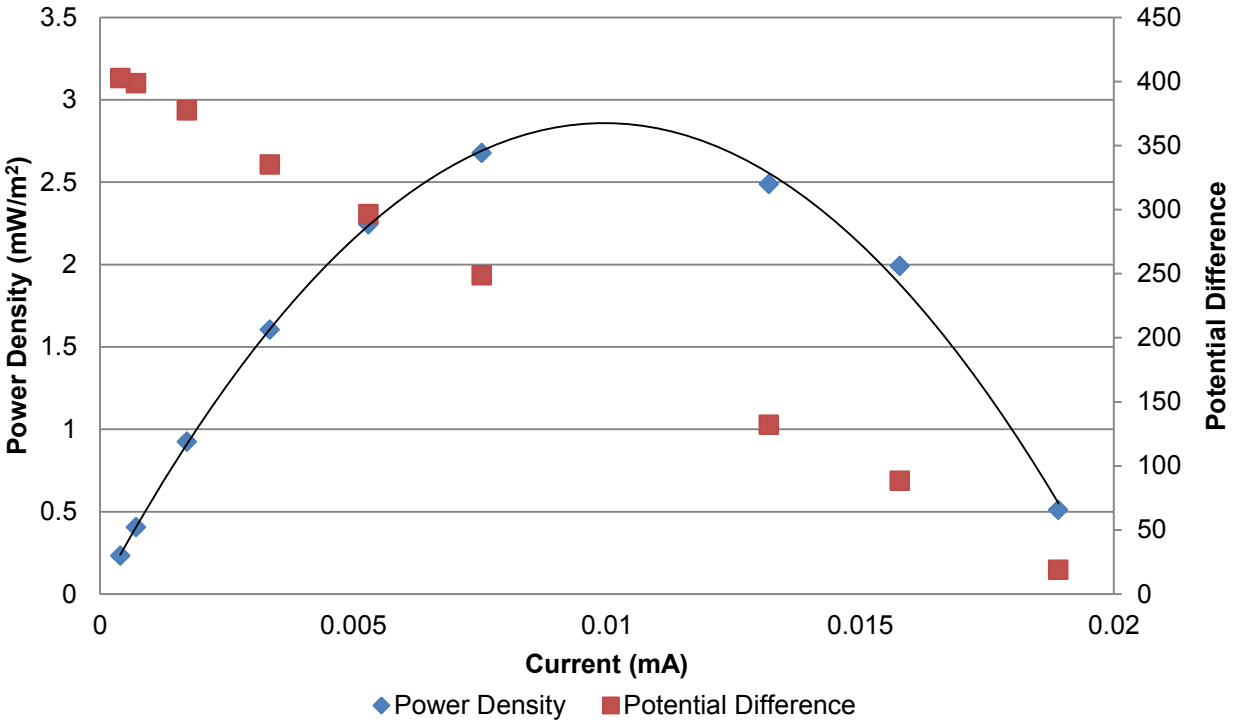

Figure 5-4: Power density and potential difference as a function of current for MFC 3

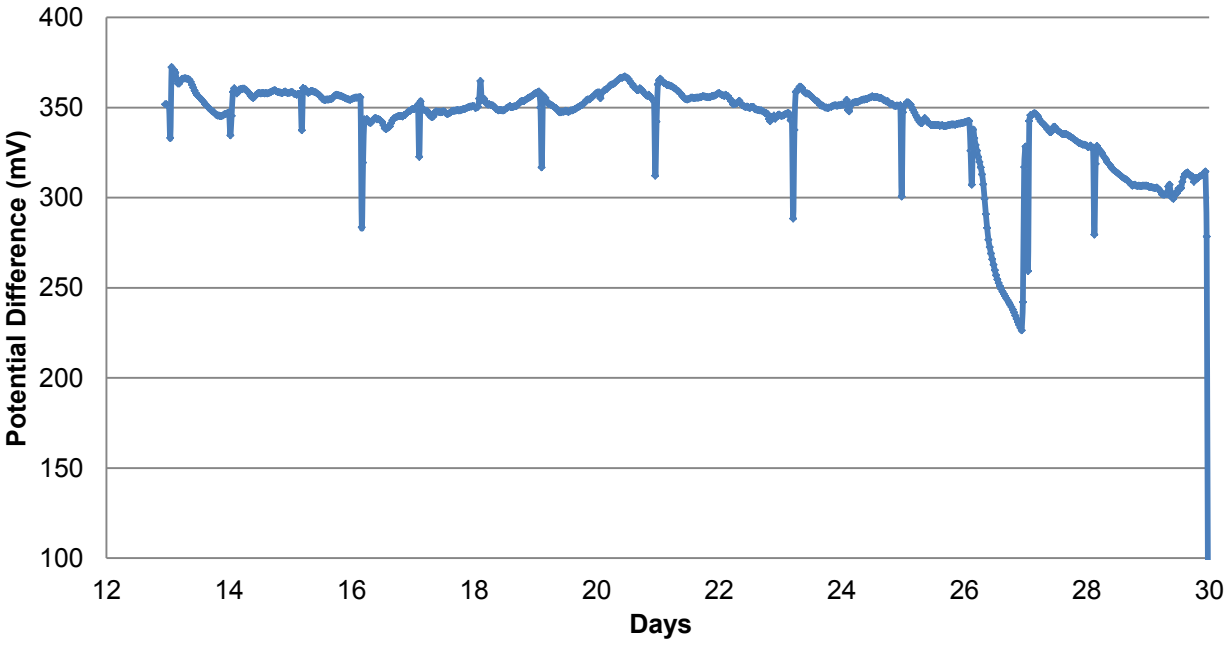

Figure 5-5: Cell potential as a function of time for MFC 4 with carbon felt anode fed standard medium and in parallel with a 100 kΩ resistor

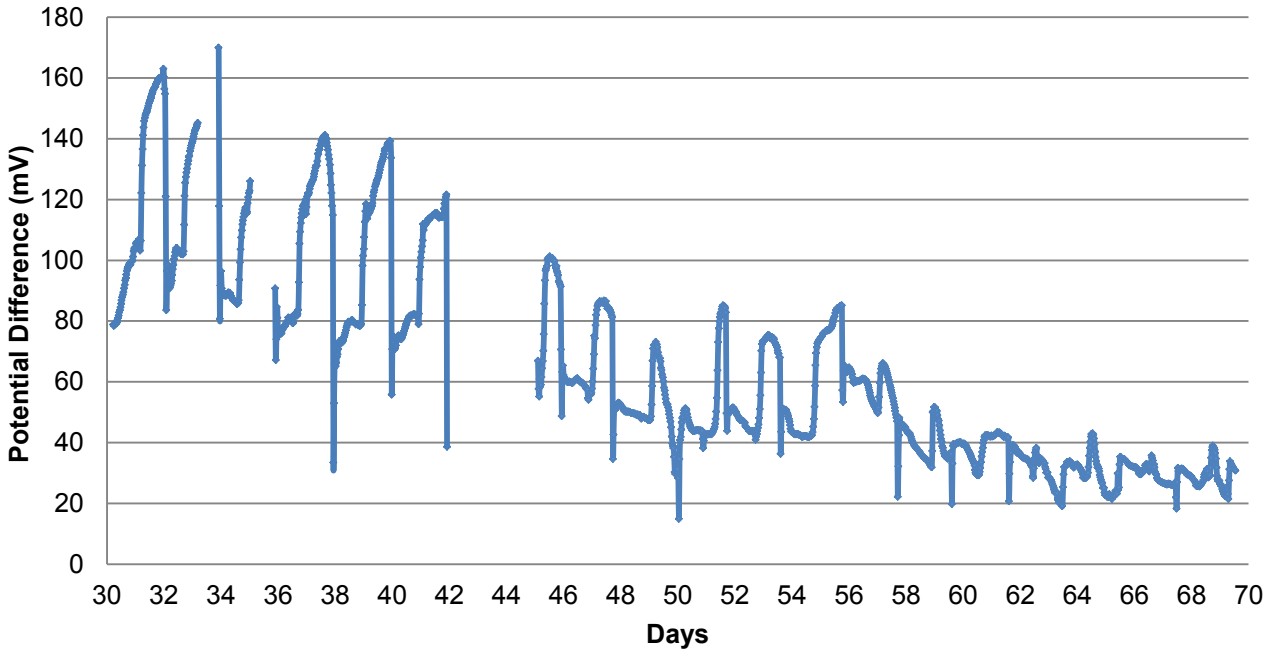

Figure 5-6: Cell potential as a function of time for MFC 4 with carbon felt anode fed standard medium in parallel with a 10 kΩ resistor

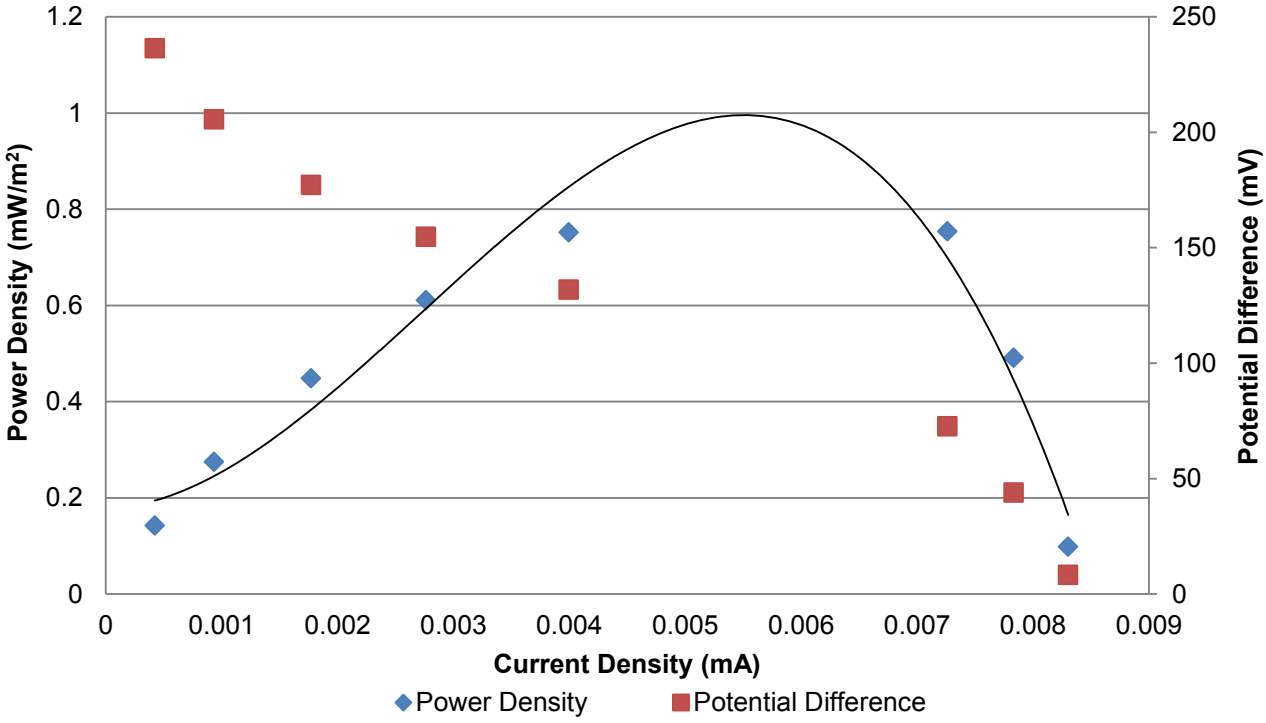

Figure 5-7: Power density and potential difference as a function of current for MFC 4 on day 44

5.3.1.2 Carbon Fibre Brush Anode

A single-chambered MFC with a carbon microfibre brush anode (MFC-CBA) was operated with a mixed SRB / SOB consortium growing on lactate and sulphate medium with intermittent media

replenishment. For the first 6 days of the experiment the MFC was kept in parallel with a 100 kΩ resistor which was replaced with a 10 kΩ resistor for the remainder of the experiment (Figure 5-8).

From day 6 onwards a trend was evident following each feeding point whereby, after feeding, the potential difference over the cell increased substantially, reached a maximum and decreased to approximately the same potential at which feeding took place. It then remained fairly constant for several days before the MFC was fed again. As a result the MFC was fed less frequently than the MFCs with carbon felt cathodes which were fed on average every two days. The potential difference decreased over time from between 150 and 200 mV from day 6 to 22, to between 50 and 100 mV in the last 10 days of the experiment. Although the concentration of the feed was altered on day 35 of the experiment (increased to 28mM lactate and sulphate), no notable change in potential difference is observed.

A polarisation curve was plotted for the MFC on day 54 (Figure 5-9). The maximum power density achieved was 0.966 ± 0.002 mW/m^2 of anode area and the internal resistance was calculated to be approximately 7 720 ± 253 Ω. This resistance is considerably lower than the resistances calculated for MFCs 3 and 4 (20 600 ± 571 Ω and 21 600 ± 846 Ω respectively).

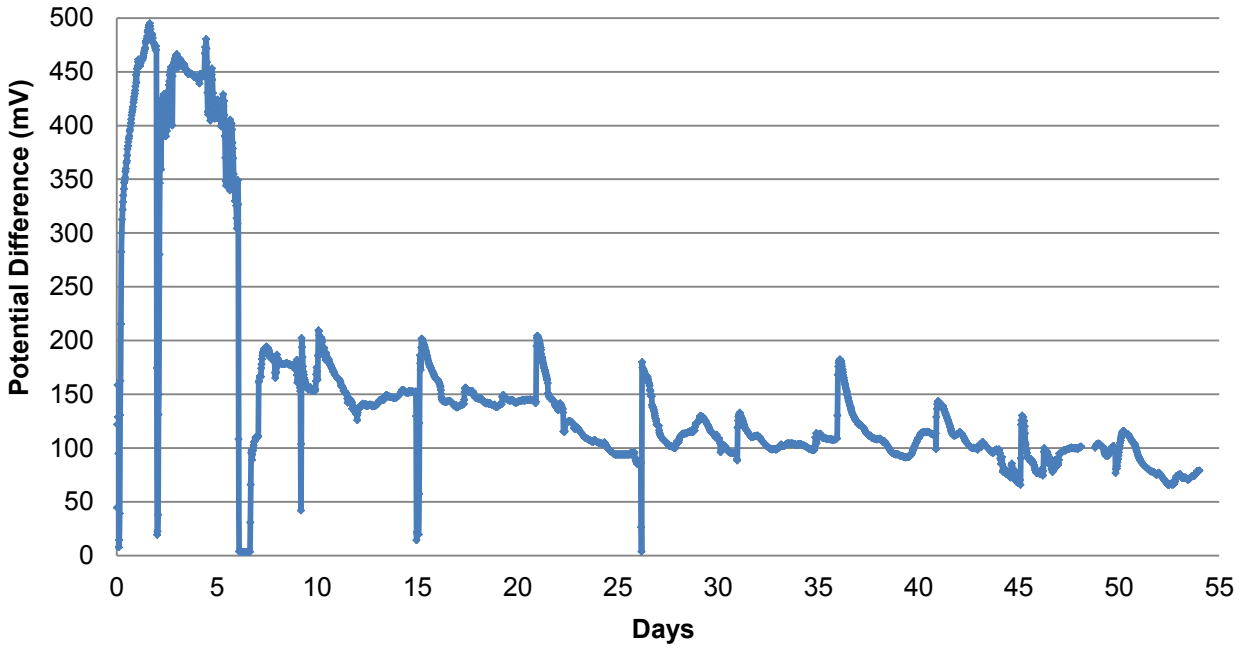

Figure 5-8: Cell potential as a function of time for MFC with carbon fibre brush anode fed standard and concentrated medium and in parallel with a 10 kΩ resistor

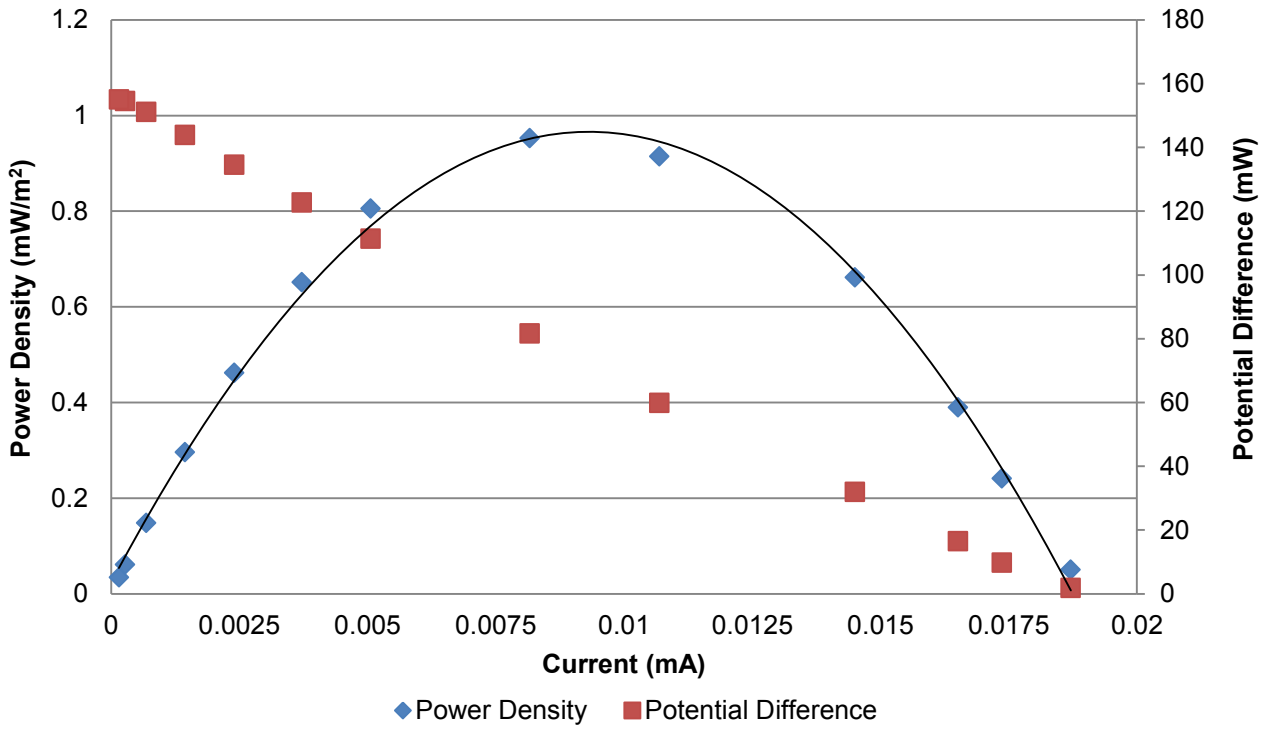

Figure 5-9: Power density and potential difference as a function of current for MFC with carbon fibre brush anode

5.3.1.3 Concentrated Feed

Two single-chambered MFCs were operated with a concentrated lactate and sulphate feed (28 mM lactate and 2.8 g/ℓ sulphate). One MFC was left unconnected to an external circuit and the other was put in parallel with a 100 kΩ resistor. The potential difference over the connected cell initially spiked to reach a maximum of between 200 and 250 mV in the first 3 days of the experiment (Figure 5-12). Thereafter, the maximum potential difference dropped dramatically and increased for the subsequent feeding cycles. After feeding on day 14, the potential difference increased to a maximum and stabilised until it was fed 5 days later. The subsequent feeding cycles also resulted in a fairly constant potential difference for the duration of the feeding cycle.

A further experiment was conducted on a single-chambered MFC (MFC 5) with a carbon felt cathode. It was initially operated in the same way as MFCs 1-4 with a change in feed concentration (28 mM lactate and 2.8 g/ℓ sulphate) on day 37. The potential difference over the MFC (Figure 5-10) initially spiked after each feeding in the same way as for MFCs 1-3 (Figure 5-1, Figure 5-2 and Figure 5-3) and the MFC with concentrated feed (Figure 5-12). From days 14 to 37 a trend was observed wherein the peaks become broader and regular in size with maximum potentials between 50-100 mV. On day 37 after the change in feed concentration, the peak observed with each feeding cycle became steeper and from day 43 until the end of the experiment, two peaks were visible for a feeding cycle. The addition of the concentrated feed on day 37 resulted in an increase in maximum cell potential observed.

Polarisation curves were plotted for the MFC with concentrated feed on day 16 (Figure 5-13) and 29 (Figure 5-14) of the experiment. The maximum power densities produced were 1.11 ± 0.004 mW/m^2 and 1.87 ± 0.005 mW/m^2 respectively. The polarisation curve plotted on day 29 exhibits an overshoot phenomenon which is observed in the bending inwards of the curve. This implies a system limitation (Winfield *et al.*, 2011). The internal resistance was 26 900 ± 4260 Ω on day 16 and in the region of 9000 ± 4850 Ω on day 29 although this is difficult to estimate from the curves as a result of the

overshoot phenomenon. The percent error (54%) for this value is therefore higher than recorded for other MFCs.

The polarisation curve of MFC 5 (Figure 5-11) revealed that the maximum power density produced at that time was 0.91 ± 0.001 mW/m^2 and the internal resistance was calculated to be 71 700 ± 6560 Ω. A summary of the maximum power densities achieved and the internal resistances of the MFC in these experiments are given in

Table 5-2.

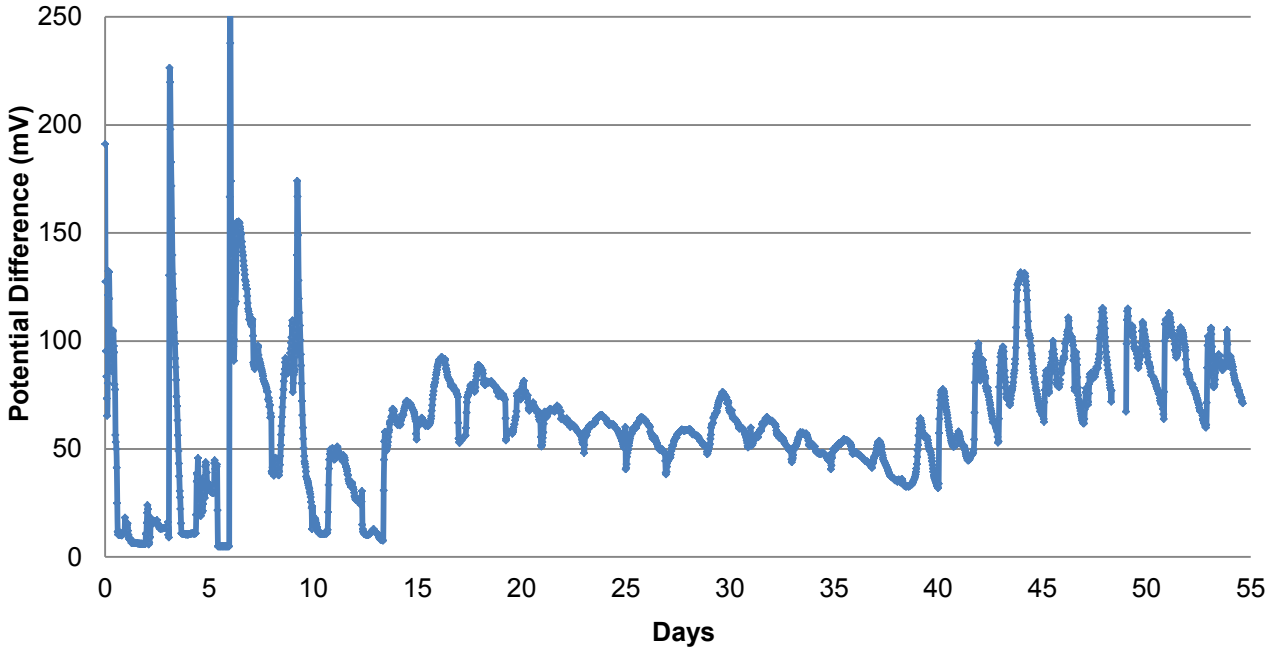

Figure 5-10: Cell potential as a function of time for MFC 5 with carbon felt anode fed standard and concentrated medium and in parallel with a 10 kΩ resistor

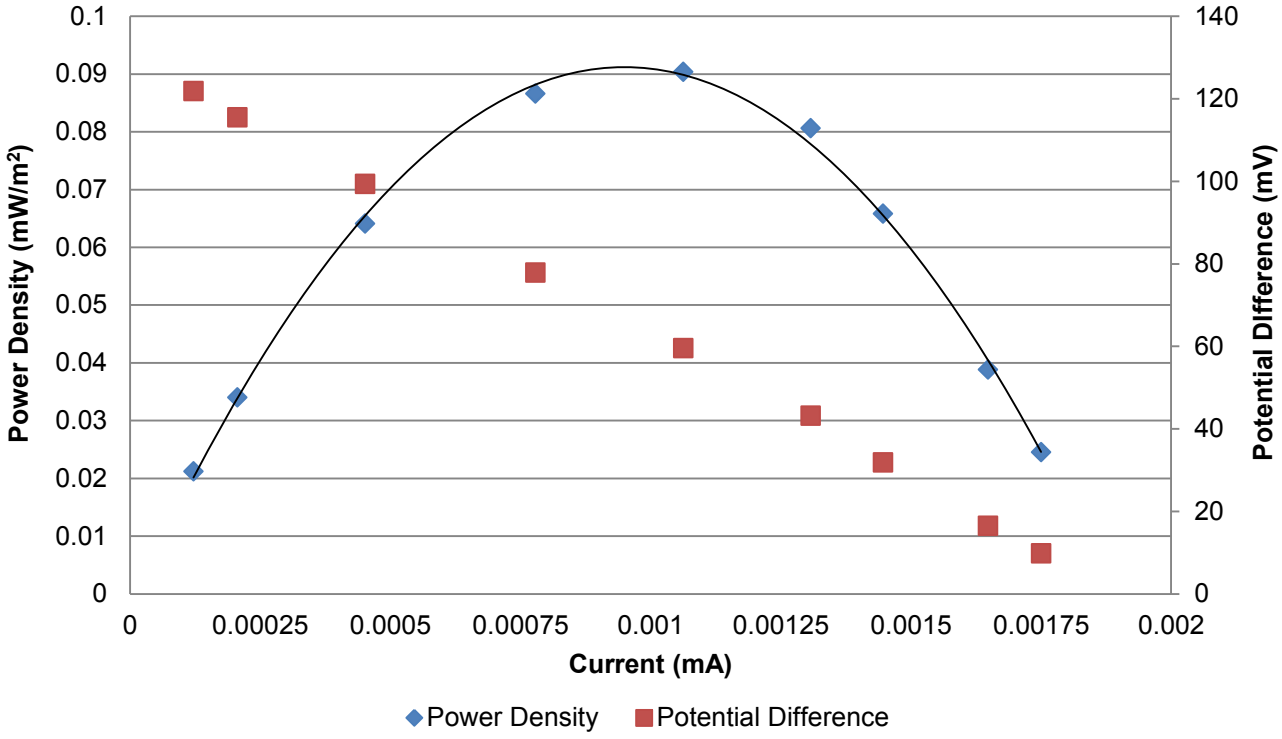

Figure 5-11: Power density and potential difference as a function of current for MFC 5, operated with a carbon felt anode at day 55

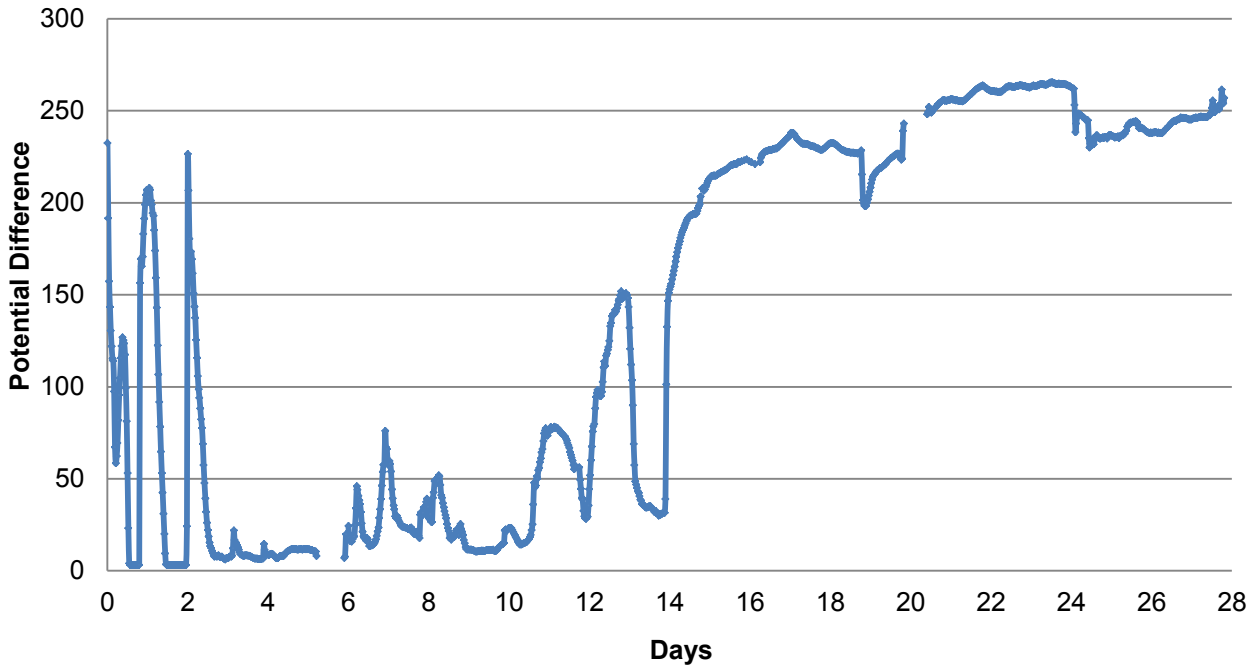

Figure 5-12: Cell potential as a function of time for a MFC-CFC fed intermittently with concentrated medium and in parallel with a 100 kΩ resistor

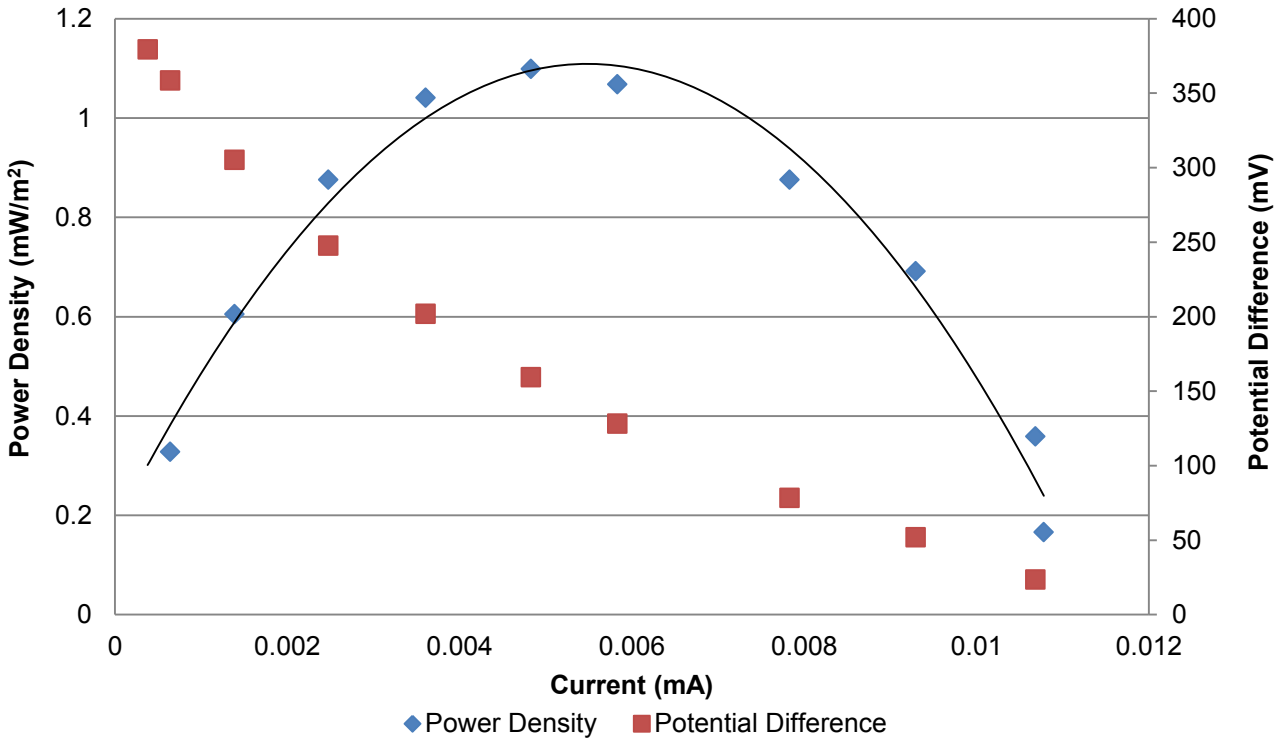

Figure 5-13: Power density and potential difference as a function of current for MFC-CFC with concentrated feed on day 16 of operation

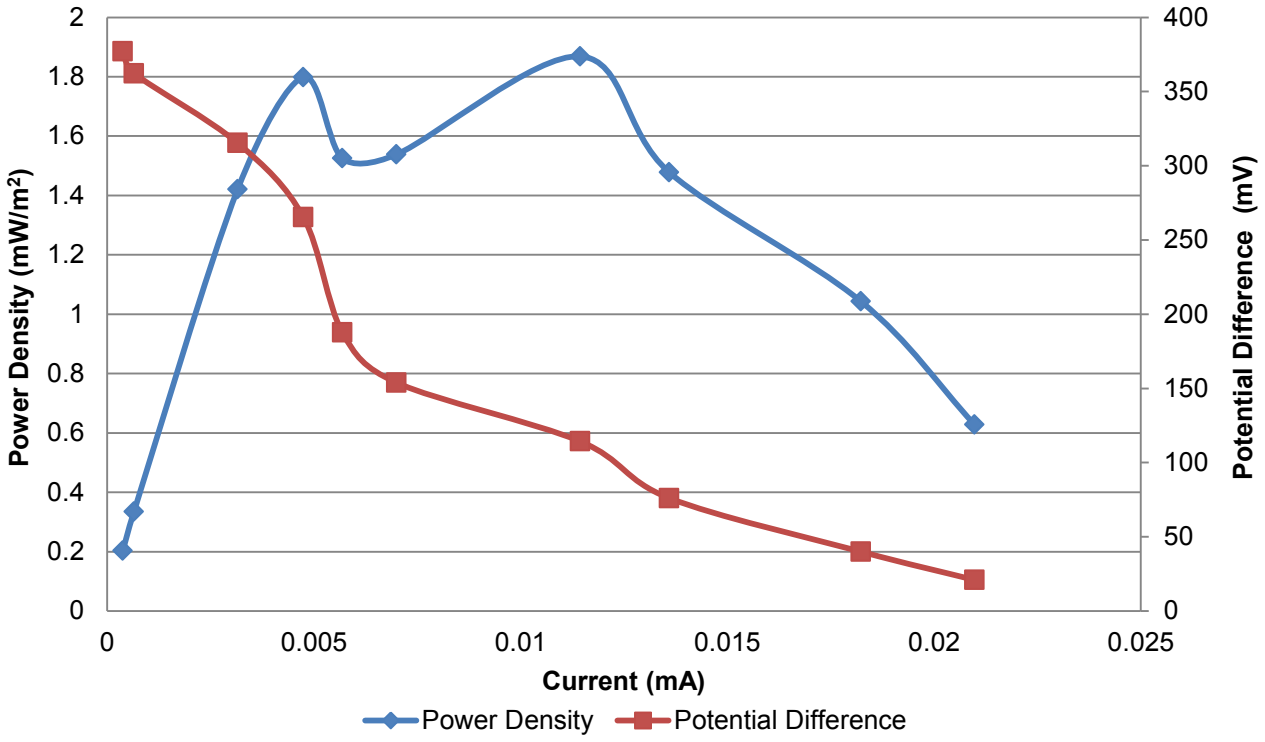

Figure 5-14: Power density and potential difference as a function of current for MFC-CFC with concentrated feed on day 29 of operation

Table 5-2: Maximum power density achieved and internal resistance for different MFCs

MFC Type	MFC	Maximum Power Density (mW/m^2)	Internal Resistance (Ω)	Days Since Inoculation
Carbon Felt Anode	MFC 3	2.86 ± 0.009	20600 ± 571	4
	MFC 4	0.926 ± 0.057	21600 ± 846	44
Carbon Fibre Brush Anode	MFC-CBA	0.966 ± 0.002	7720 ± 253	54
Carbon Felt Anode Concentrated Feed	MFC-CFC	1.11 ± 0.004	26900 ± 4260	16
	MFC-CFC	1.87 ± 0.005	9000 ± 4850	29
	MFC 5	0.091 ± 0.001	71700 ± 6560	55

5.3.2 Substrate Utilisation

5.3.2.1 Carbon Felt Anode

Concentration of Sulphur Species

The single-chambered MFCs with carbon felt anodes were fed with standard medium (15 mM lactate and sulphate) which resulted in a pulse of an additional concentration of approximately 500 mg/ℓ to the bulk liquid when 10 mℓ of liquid contents was replaced with fresh medium.

It was found that for the duration of the experiment, the sulphate concentration within the MFCs 1-4 decreased (Figure 5-15, Figure 5-16). The rate at which the concentration decreased was calculated for the period from day 3 to 10 (Appendix C.1.1) and was found to be similar for MFCs 1, 2 and 3 (84.8, 85.1 and 69.7 mg/ℓ/day respectively). The results of a t-test analysis indicated that that the t-value lay well within the critical range and close to zero for all cases and P>0.05 was true for all cases (Table A 10) therefore indicating that the average rate of sulphate reduction was similar for MFC 1-3.

The initial rate of sulphate reduction was much faster for MFC 4 (158 mg/ℓ/day). The sulphate concentration of MFC 1-3 was higher than the feed concentration for approximately the first 10 days of operation and the rate of decrease in sulphate concentration was slower than that of the dilution rate. This may be as a result of the complete oxidation of sulphide back to sulphate as a result of the high concentration of oxygen in the system in the first few days of the experiment before a mature biofilm formed on the cathode. It is also possible that the spiking of the MFCs with inoculum for the first 3 feeding cycles resulted in increased sulphate concentration as a result of residual unoxidised sulphate in the inoculum.

If no sulphate was reduced in the system, the sulphate concentration would tend towards that of the feed and become 15 mM (approximately 1500 mg/ℓ) within 8 feeding cycles, as can been seen in Figure 5-15 and Figure 5-16. The sulphate concentration was reduced below the feed value for all

MFCs, providing evidence for biological sulphate reduction by SRBs in the system. This occurred on approximately day 11-12 for MFCs 1 and 3, but only at around day 19 for MFC 2.

MFC 4 had a general trend of decreasing sulphide concentration over the duration of the experiment. On day 19 the sulphate concentration began to increase from approximately 1100 mg/ℓ to above the concentration of the feed, likely as a result of complete oxidation of sulphide, but returned to 1100 mg/ℓ by day 35. This indicates that during this time little or no sulphate reduction was taking place.

Sulphide assays were conducted on every sample taken from each of the MFCs. In many cases, the sulphide concentration was too low to be detected by the assay. Only MFC 3 and MFC 4 had detectable sulphide concentrations. The sulphide concentration as a function of time is plotted in Figure 5-17 and Figure 5-18. Sulphide was only detected in the spent medium at day 10 after inoculation for both MFCs. The concentration for MFC 3 remained below 30 mg/ℓ until day 29, before increasing substantially in the last few days of the experiment to reach a maximum of 111 mg/ℓ. The concentration of sulphide in MFC 4 remained below 35 mg/ℓ for the duration of the experiment.

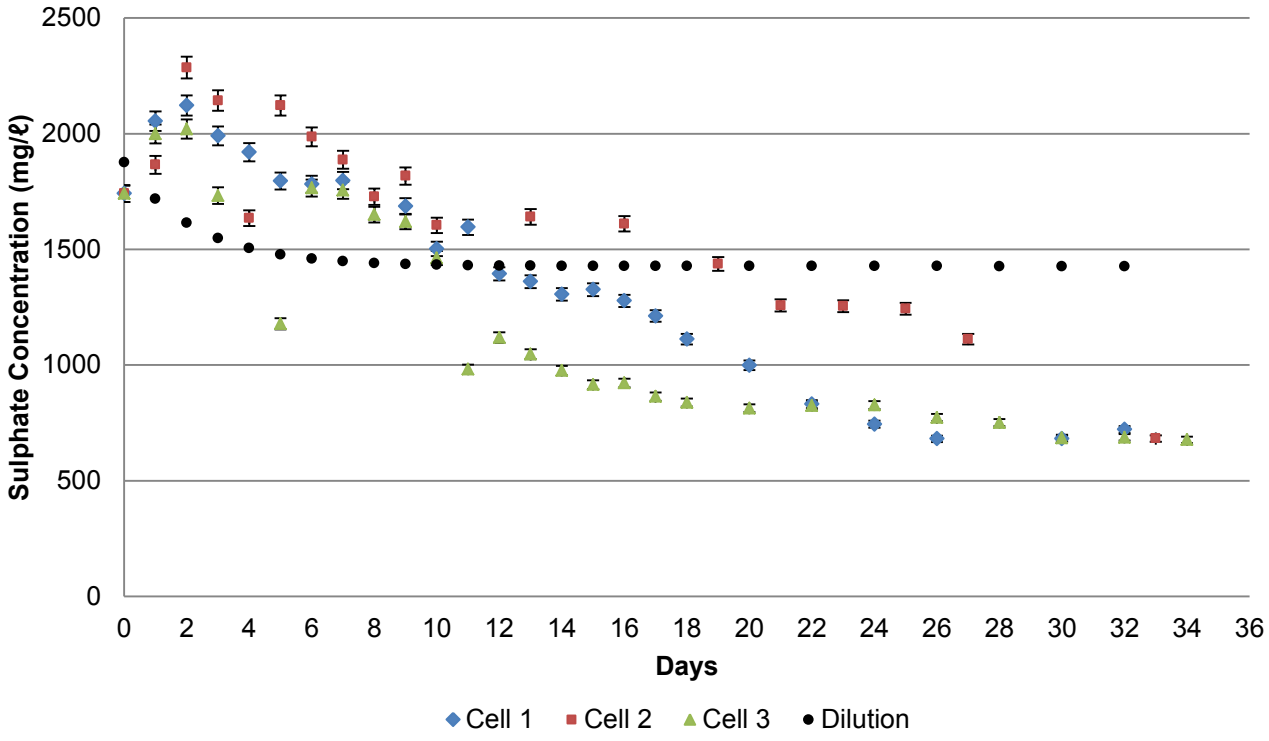

Figure 5-15: Sulphate concentration as a function of time for 3 MFCs fed standard medium

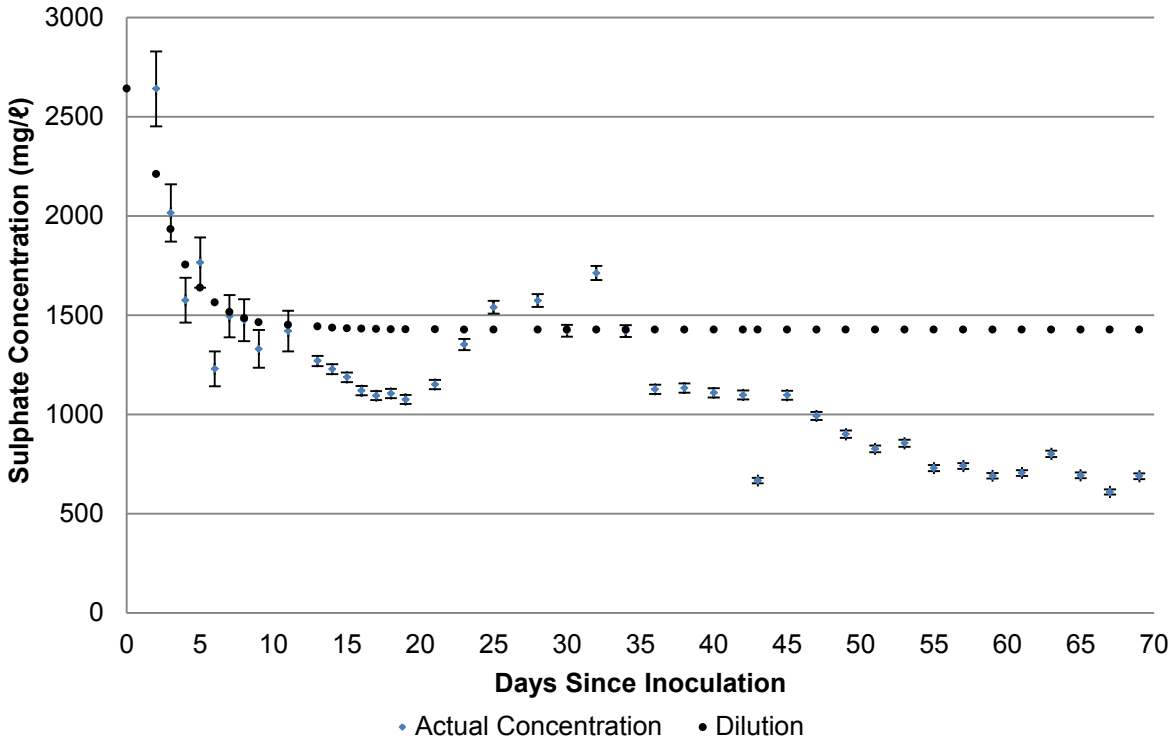

Figure 5-16: Sulphate concentration as a function of time for MFC 4 fed standard medium

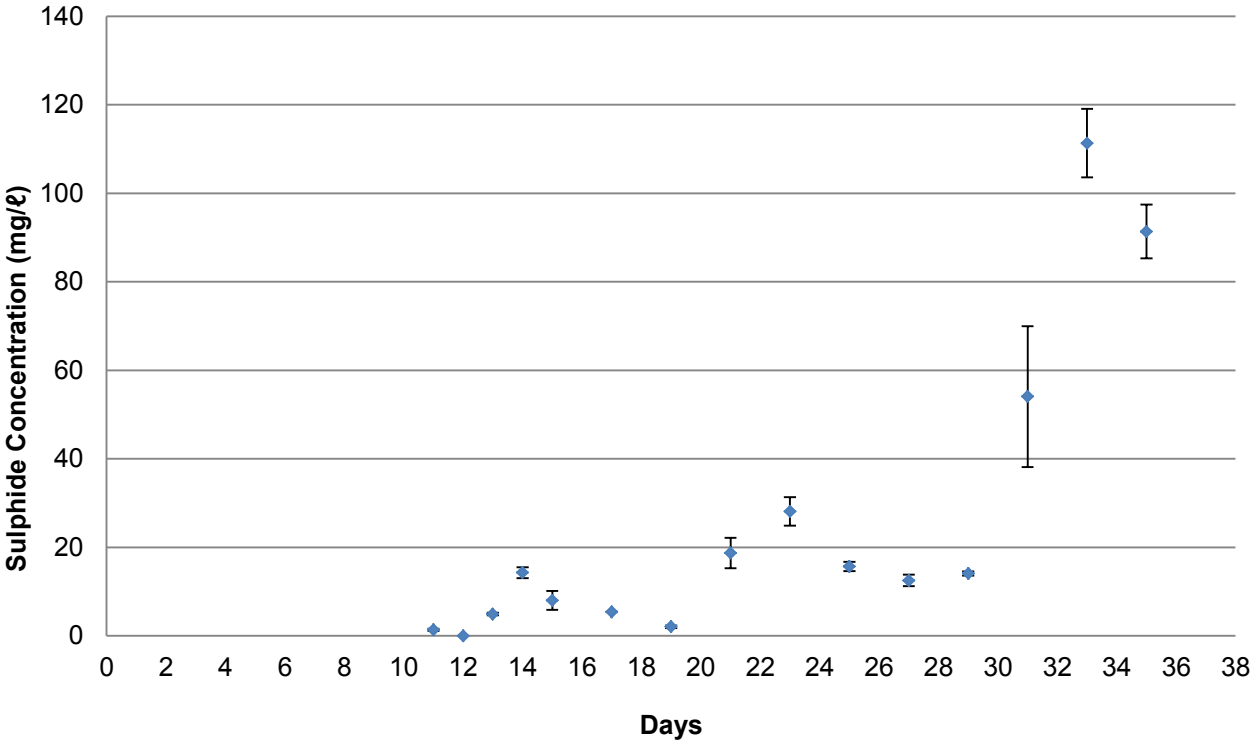

Figure 5-17: Sulphide concentration as a function of time for MFC 3 fed standard medium

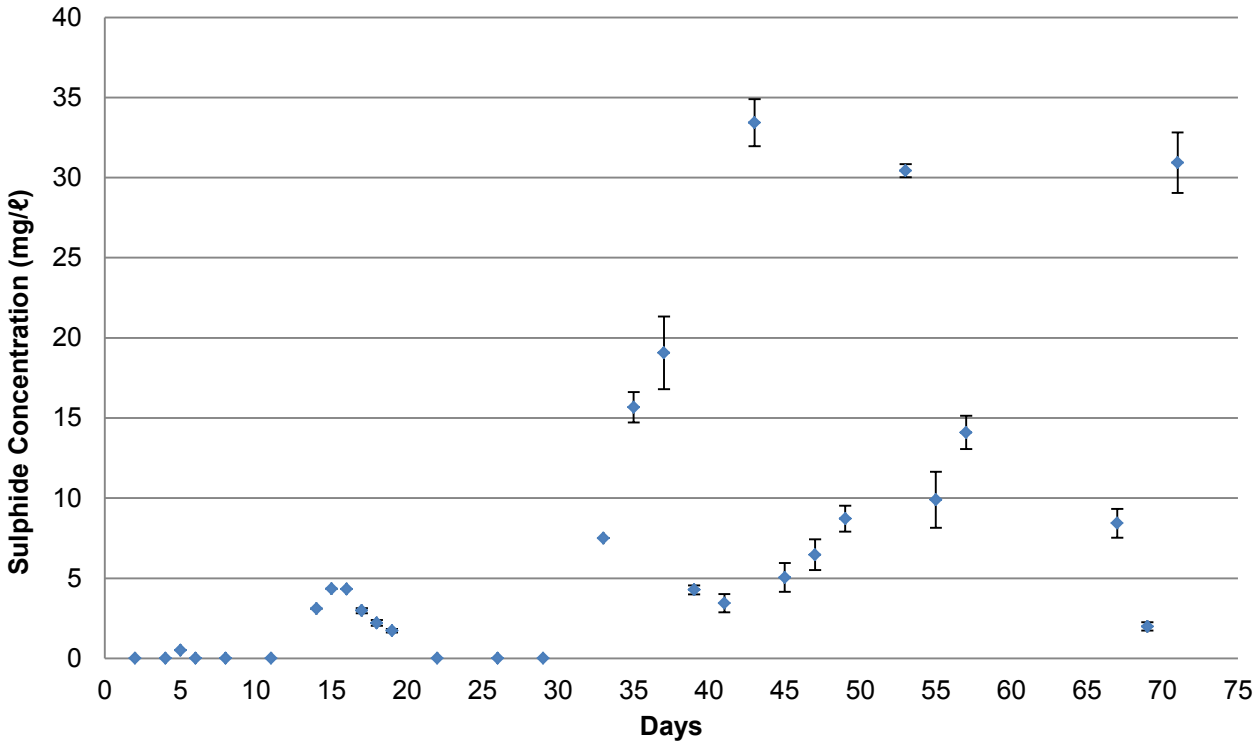

Figure 5-18: Sulphide concentration as a function of time for MFC 4 fed standard medium

Concentration of Volatile Fatty Acids

Although lactate, acetate, propionate, butyrate, iso-butyrate, valerate and iso-valerate were detected with HPLC in many of the samples taken from the MFCs, only the concentration of lactate, acetate and propionate are shown. Concentrations of the remaining volatile fatty acids were typically much lower than that of acetate and propionate (collectively less than 10 % of carbon fed), and remained fairly constant throughout the duration of the experiment. They were also not present in earlier samples.

As can be seen from the profile of VFA concentration as a function of time for MFC 1-4 (Figure 5-19, Figure 5-20, Figure 5-21 and Figure 5-22), the lactate concentration decreased rapidly for all four MFCs to almost 0 mg/ℓ within the first 5 days for MFCs 1-3 and within 10 days for MFC 4. It remained low for the remainder of the experiment. Acetate was present initially as a result of it being present in the inoculum, but also decreased to very low concentrations within 2 or 3 days after inoculation.

Between approximately days 12 to 14, the concentration of acetate and propionate began to increase for MFCs 1-3. This increase in VFA concentration corresponds to the increase in COD concentration seen in Figure 5-23. MFCs 2 and 3 (Figure 5-20 and Figure 5-21) had similar concentrations of acetate and propionate and both increased for the remainder of the experiment.

MFC 1 (Figure 5-19) exhibited a substantial increase in propionate from days 16 to 24, reaching a maximum at around 1100 mg/ℓ before decreasing again to below 150 mg/ℓ by day 30. It then remained low for the remainder of the experiment.

As can be seen from the curve of potential difference as a function of time for MFC 1 (Figure 5-1), the maximum cell potential reached with each feeding cycle began to decrease on day 12 and reached a minimum on day 14. This corresponded directly to the increase in propionate in the system during this time as shown by Figure 5-19. The maximum cell potential reached by MFC 1 increased after day 24, which corresponded to the lower concentration of propionate.

MFC 4 (Figure 5-22) exhibited an initial increase in both acetate and propionate from approximately day 5 to 18. Both reached a maximum at around 500 mg/ℓ before decreasing until day 31. At this point the acetate concentration began to increase to between 1000-1200 mg/ℓ by day 47 where it largely remained for the remainder of the experiment. The concentration of propionate, however, continued to decrease to below 200 mg/ℓ by day 33 and remained there for the remainder of the experiment. The resistor in parallel with the MFC was changed from 100 kΩ to 10 kΩ on day 30 which corresponded to the increase in acetate concentration and decrease in propionate concentration.

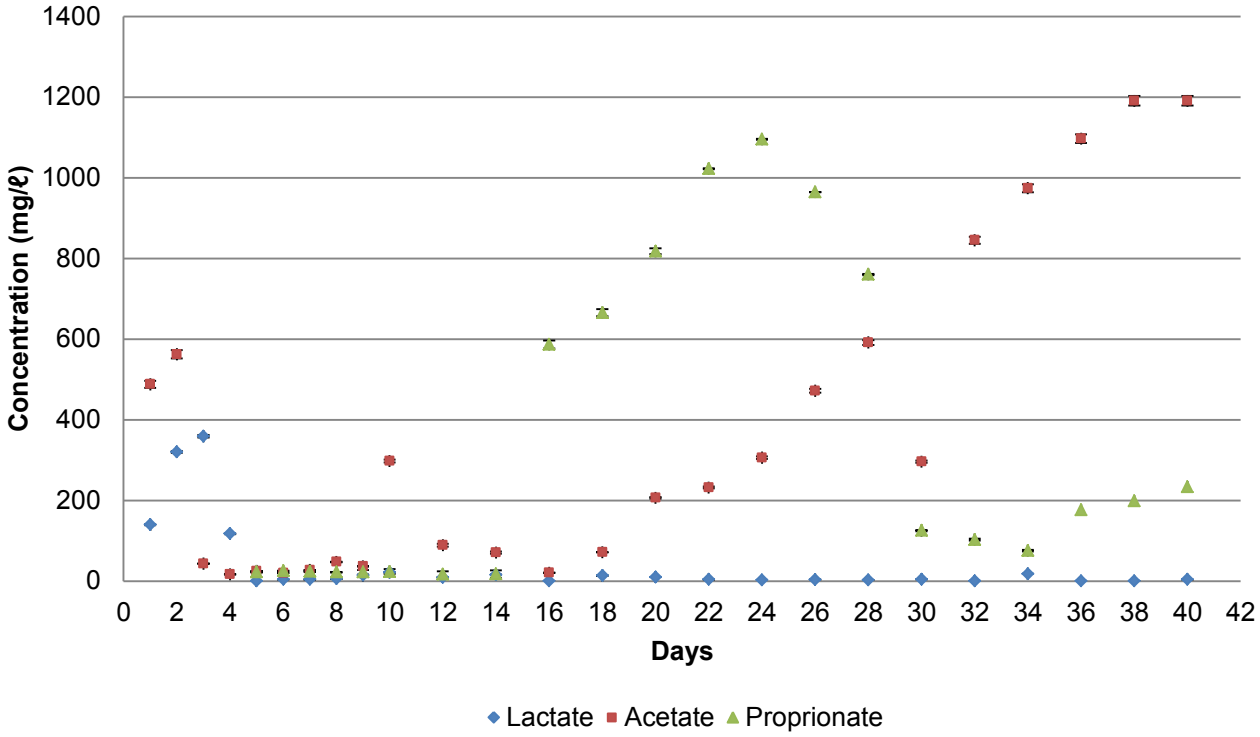

Figure 5-19: Concentration of volatile fatty acids as a function of time for MFC 1 fed standard medium

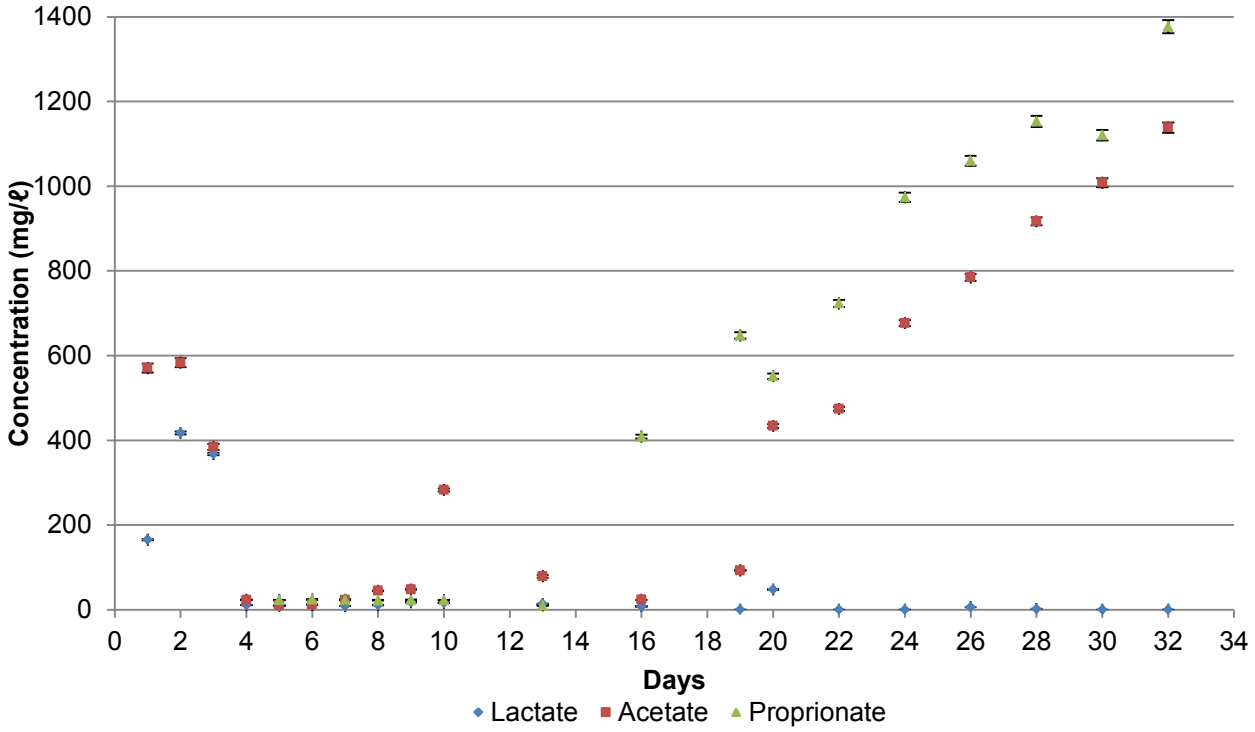

Figure 5-20: Concentration of volatile fatty acids as a function of time for MFC 2 fed standard medium

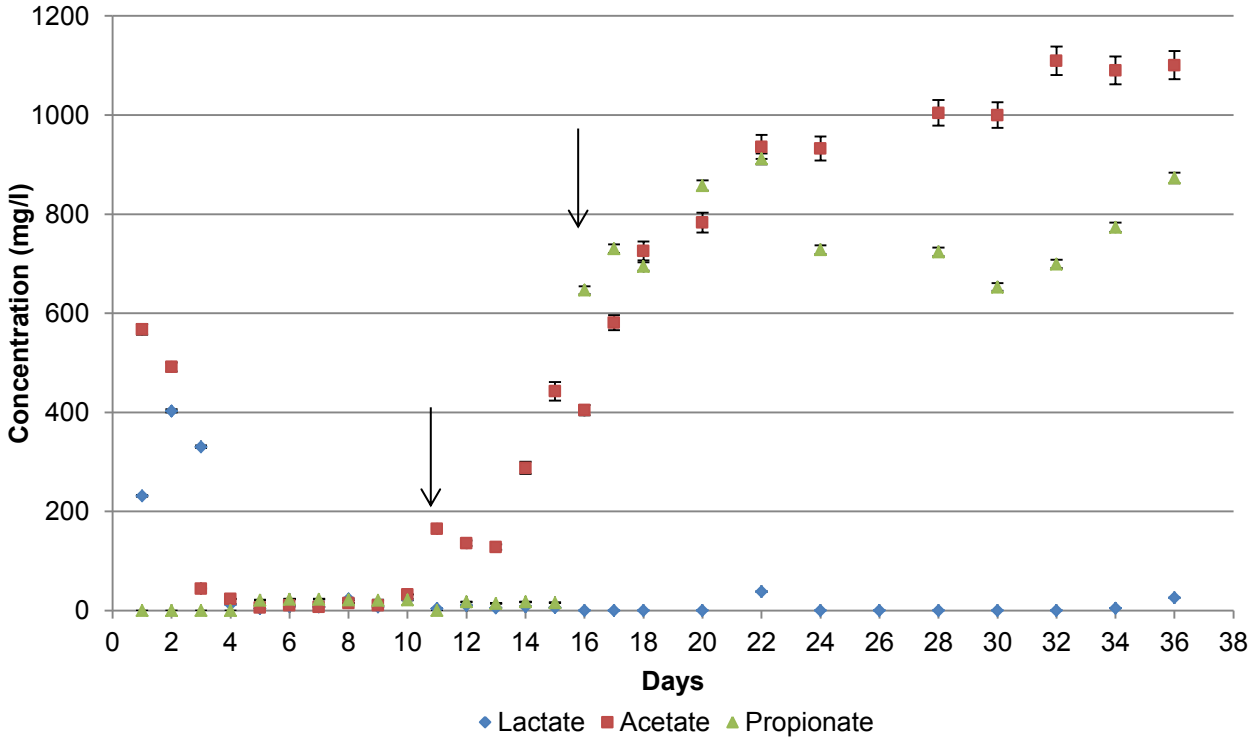

Figure 5-21: Concentration of volatile fatty acids as a function of time for MFC 3 fed standard medium with arrow marking the change in resistor

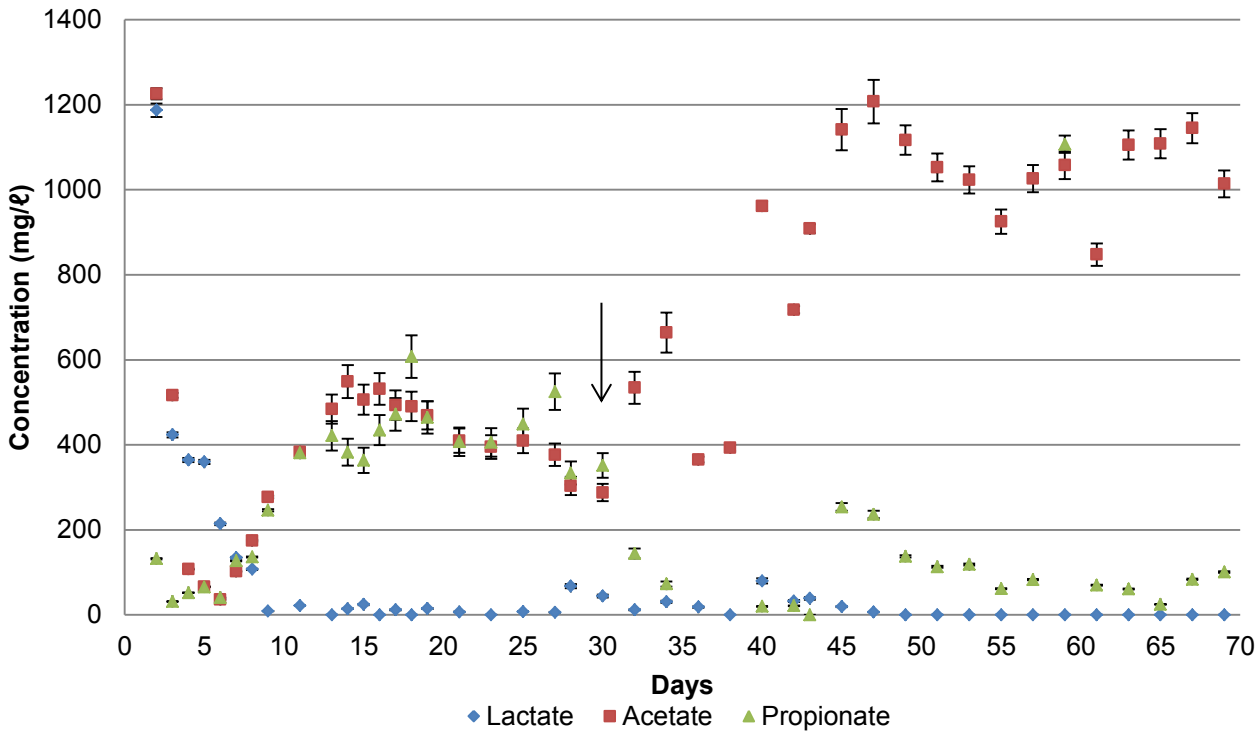

Figure 5-22: Concentration of volatile fatty acids as a function of time for MFC 4 fed standard medium with arrow marking the change in resistor

COD Degradation and Coulombic Efficiency

Initially the COD in MFCs 1-3 decreased rapidly before gradually increasing for the remainder of the experiment (Figure 5-23). The rate of increase was similar for all three MFCs. The minimum concentration of COD occurred approximately from days 4 to 16 for all 3 MFCs. During this time the COD remained below 500 mgO_2/ℓ. The percent of COD degraded was also similar for all three MFCs (Figure 5-24). Maximum degradation was observed between days 6 to 12 in correspondence with the minimum concentration of COD during this time. The percent of COD degraded decreased for the remainder the experiment to below 30% for the last 8 days.

The COD concentration of MFC 4 remained fairly constant between 1500-2000 mg/ℓ for most of the experiment (Figure 5-26). An increase in COD was observed for the last 6 days of operation. The percent of COD degraded was highest for the first 6 days of operation (Figure 5-27). It then remained between 10-30% for most of the experiment with a drop below 10% observed in the last few days of the experiment.

The coulombic efficiency achieved for MFCs 1 and 3 remained below 0.15% for the duration of the experiment (Figure 5-25). MFC 2 achieved slightly higher CE but remained below 0.3% for most its operation. The trends observed for all 3 MFC CE curves correspond with the trends observed for maximum potential difference (Figure 5-1, Figure 5-2 and Figure 5-3) indicating that cell potential has the largest effect on CE achieved. The CE of MFC 4 was on average higher than that of MFCs 1-3 (between 0.5-1.5%) (Figure 5-28) and remained fairly stable for the period over which potential difference data are available.

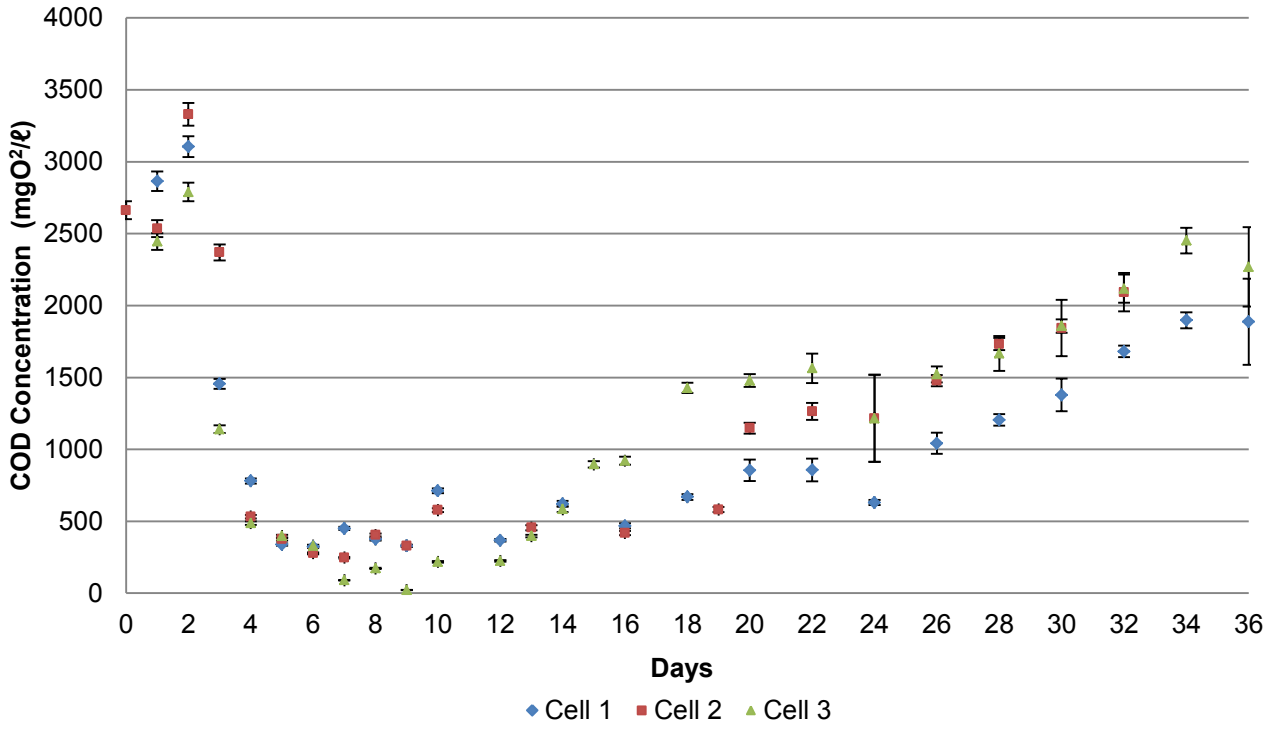

Figure 5-23: Soluble COD concentration as a function of time for 3 MFCs fed standard medium

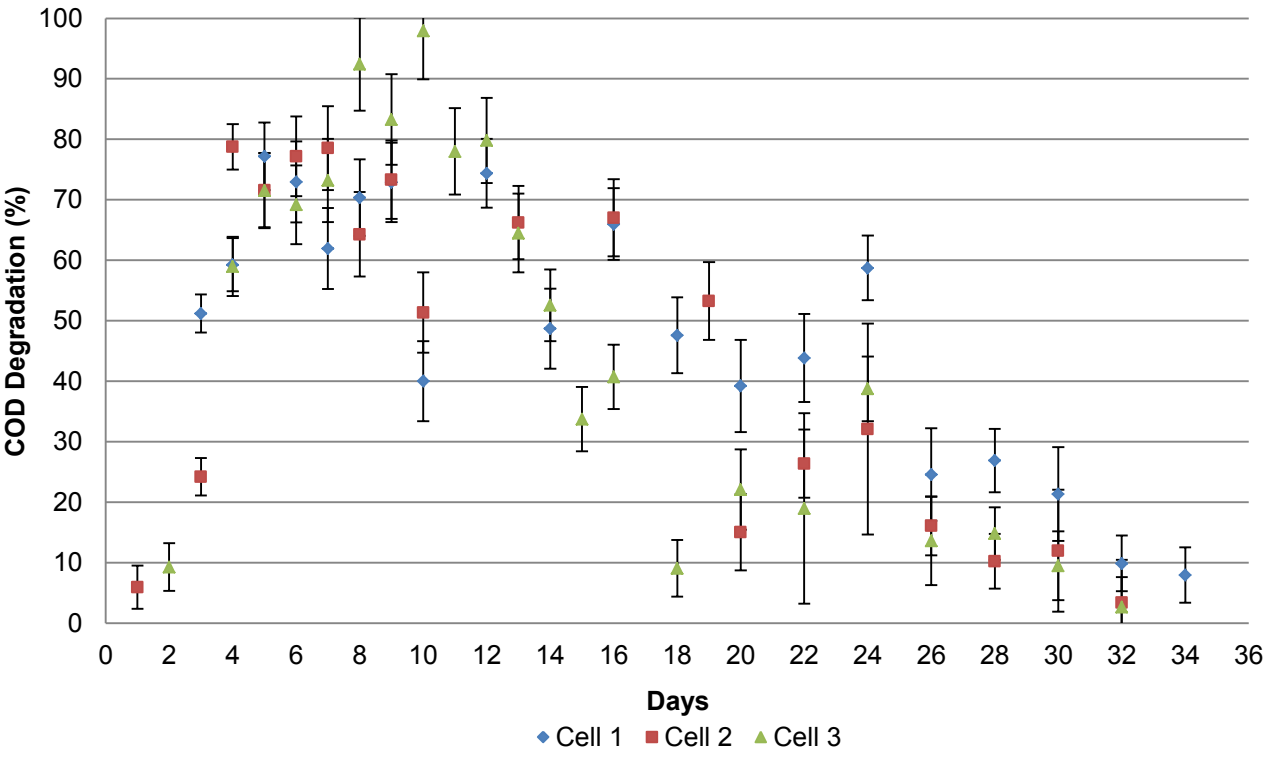

Figure 5-24: Percent of soluble COD degraded as a function of time for 3 MFCs fed standard medium

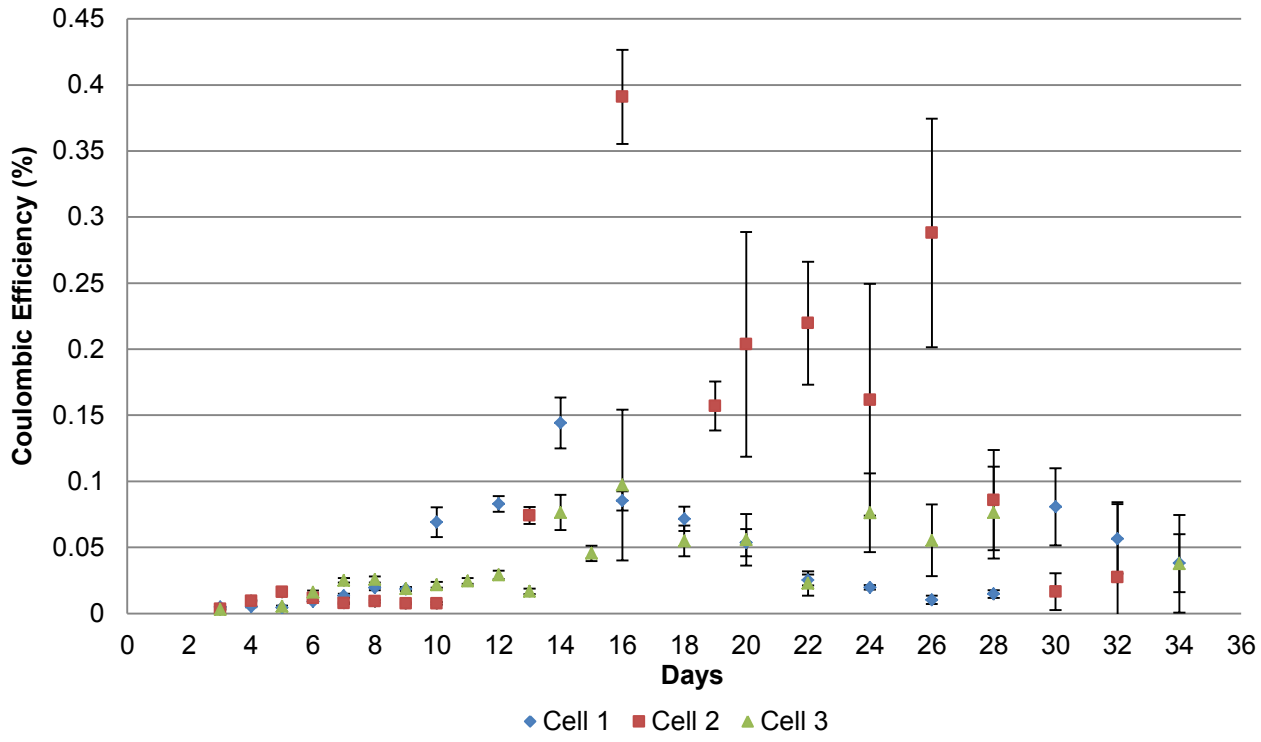

Figure 5-25: Coulombic efficiency as a function of time for 3 MFCs fed standard medium

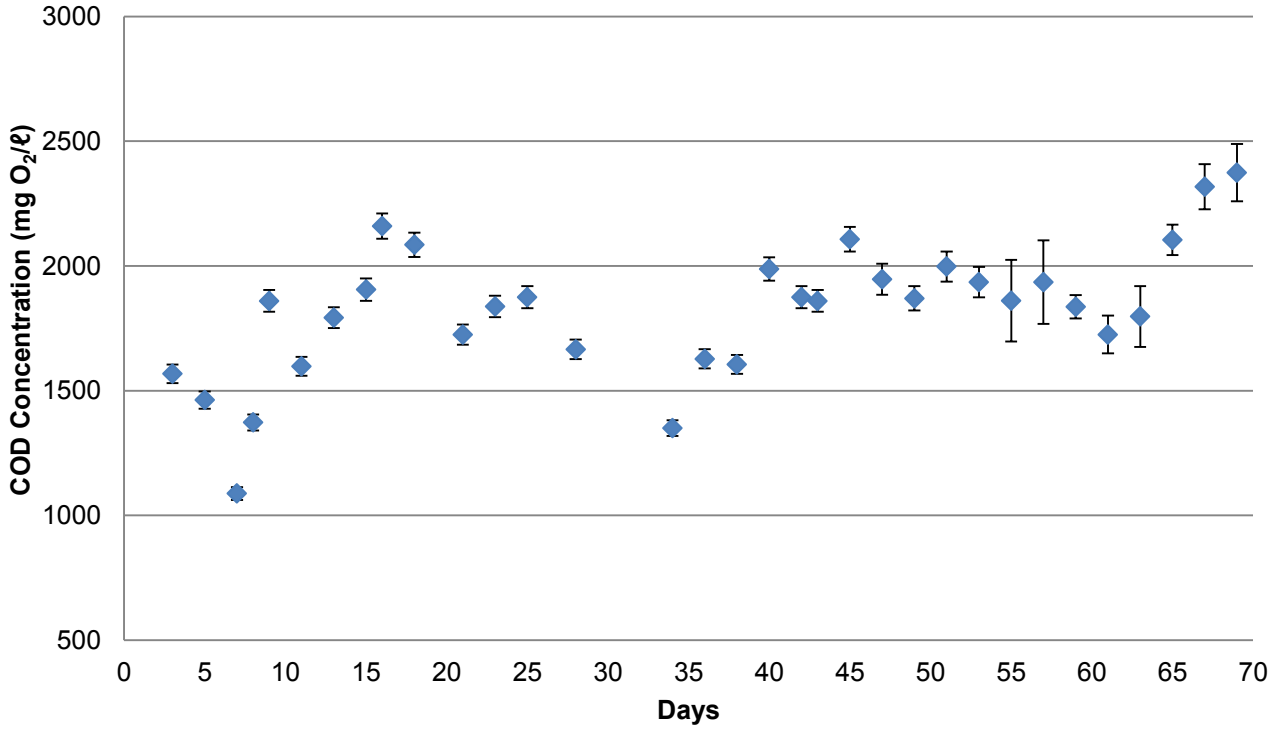

Figure 5-26: Soluble COD concentration as a function of time for MFC 4 fed standard medium

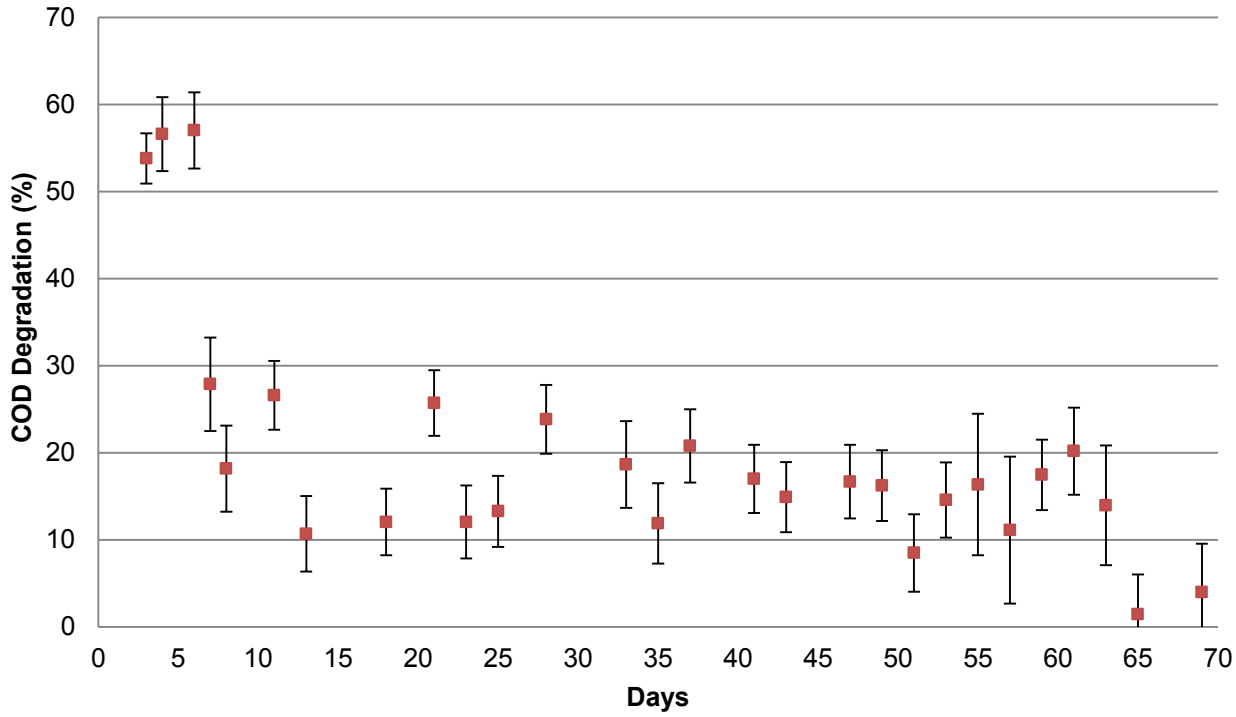

Figure 5-27: Percent of soluble COD degraded as a function of time for MFC 4 fed standard medium

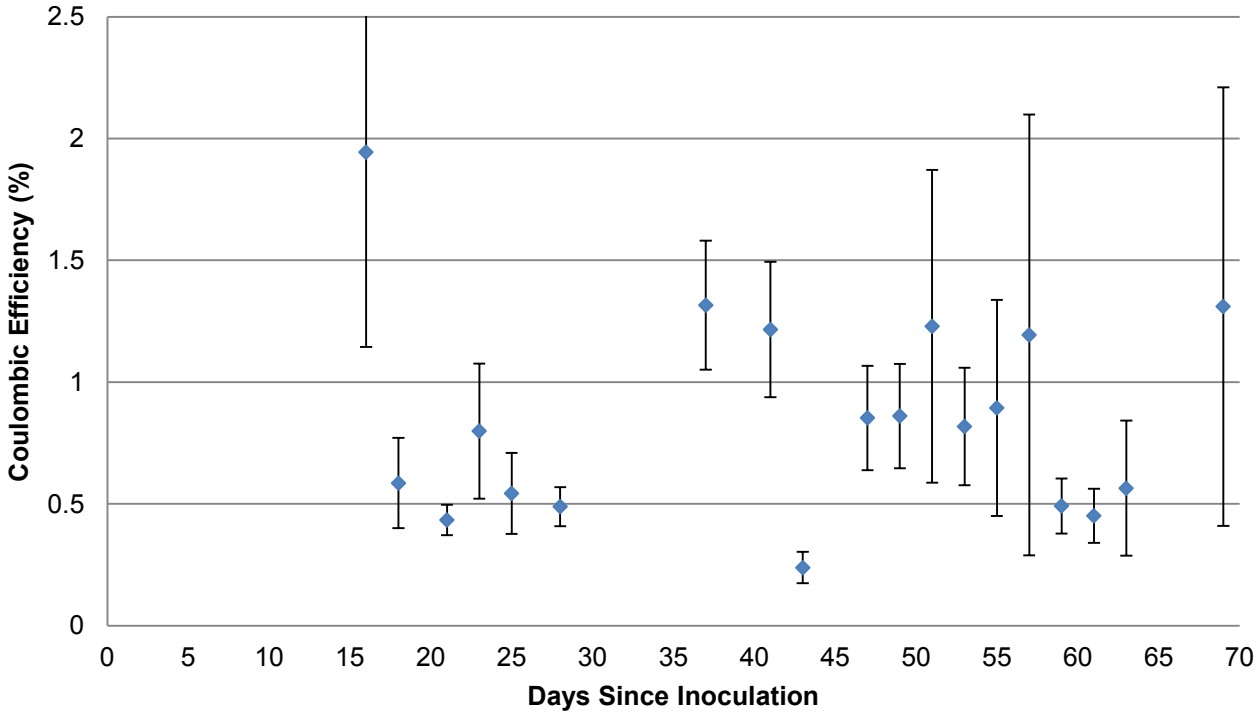

Figure 5-28: Coulombic Efficiency as a function of time for MFC 4 fed standard medium

5.3.2.2 Carbon Fibre Anode Brush

Concentration of Sulphur Species

MFC-CBA was fed with standard medium containing 15 mM lactate and sulphate at two day intervals. On each draw and fill of 10 mℓ in a 28 mℓ reactor, an additional sulphate concentration of approximately 500 mg/ℓ in the MFC resulted. On day 35 of the experiment the feed was changed for concentrated medium (28 mM lactate and sulphate) which resulted in the addition of a concentration of 1000 mg/ℓ of sulphate when 10 mℓ of spent medium was replaced.

In the first 35 days, the presence of sulphide in the spent medium (Figure 5-30) and the decrease in sulphate concentration below the fed concentration (1500 mg/ℓ) indicated that sulphate reduction took place (Figure 5-29). The sulphide concentration however was very low (less than 15 mg/ℓ). When the concentration of feed was changed on day 35, a jump in sulphate concentration was noted, after which it continued to decrease for the remainder of the experiment. An increase in sulphide concentration was also observed which indicated that the increase in sulphate concentration may also have triggered increased sulphate reduction.

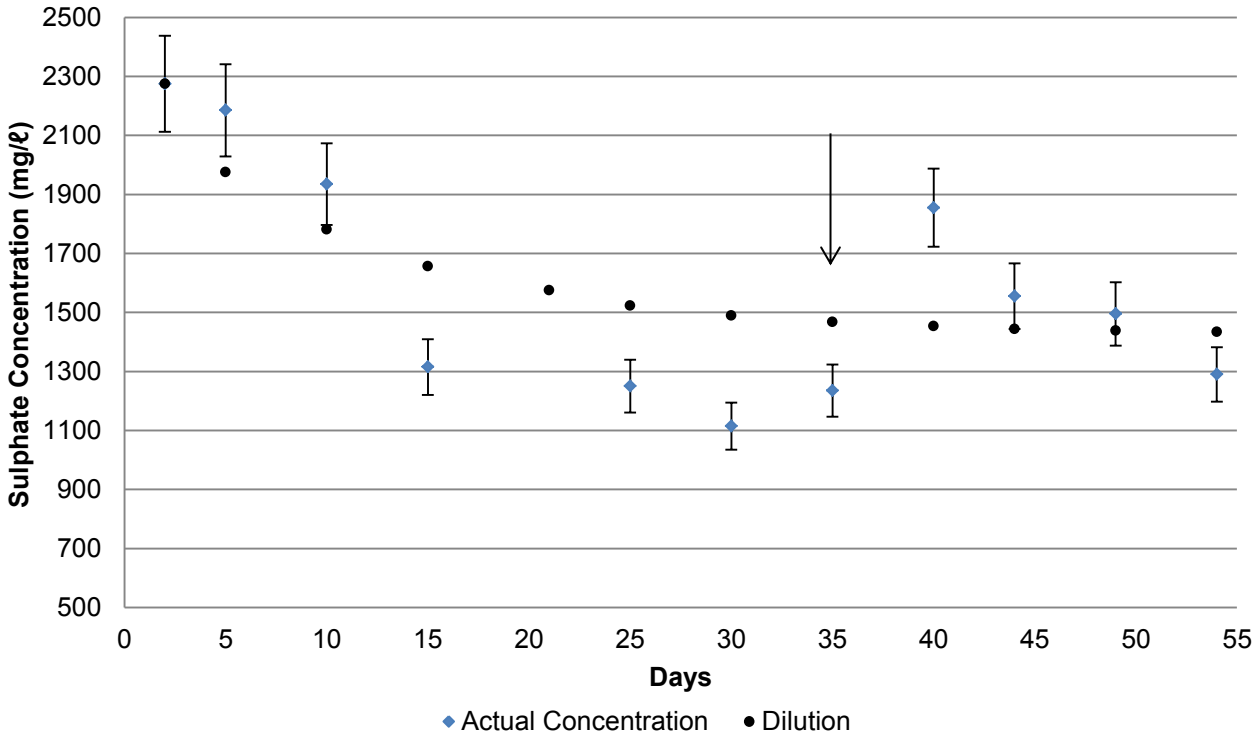

Figure 5-29: Sulphate concentration as a function of time for MFC with carbon fibre brush anode and change in feed marked by arrow

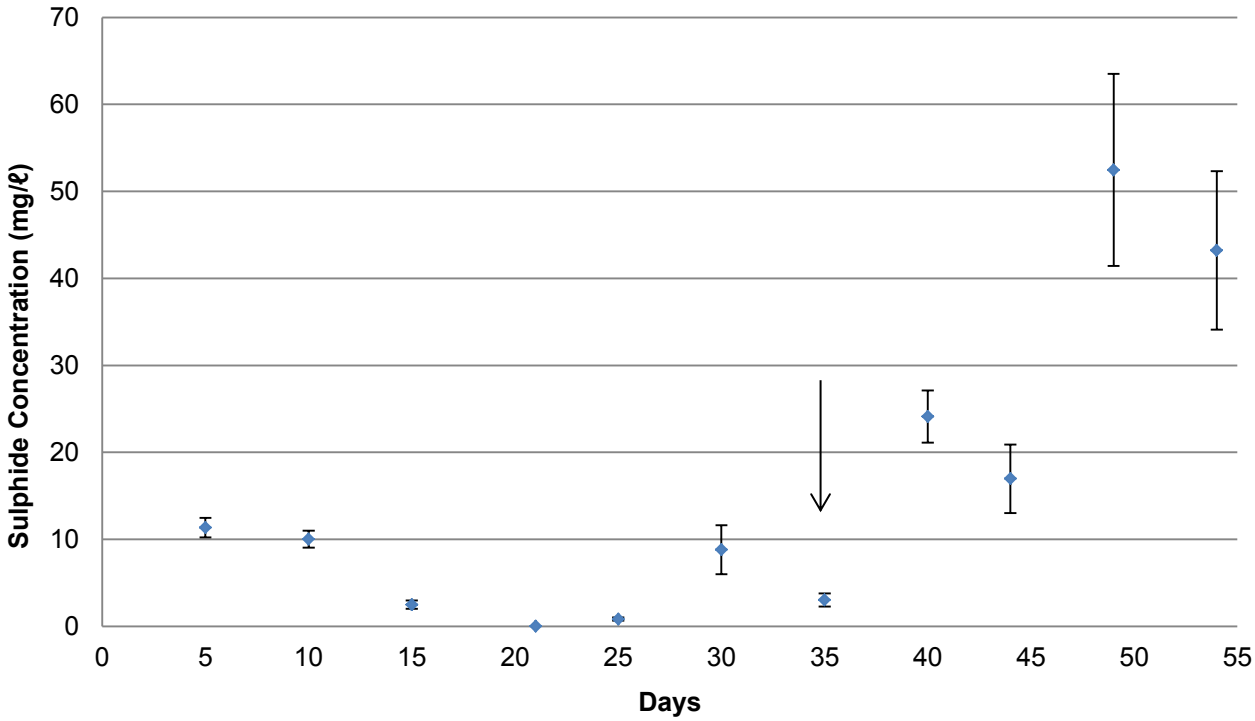

Figure 5-30: Sulphide concentration as a function of time for MFC with carbon fibre brush anode and change in feed marked by arrow

Concentration of Volatile Fatty Acids

As can be seen from the curve of VFA concentration as a function of time (Figure 5-31), the concentration of lactate dropped to almost 0 mg/ℓ within the first feeding cycle of the MFC-CBA. It remained at almost 0 mg/ℓ for the remainder of the experiment. Acetate and propionate were present in the inoculum. The concentration of acetate initially decreased in the first 15 days of the experiment before increasing to approximately 1700 mg/ℓ by the end of the experiment. The concentration of propionate initially deceased to almost 0 mg/ℓ at day 35 before increasing for the remainder of the experiment. This corresponds with the increase in feed concentration on day 35.

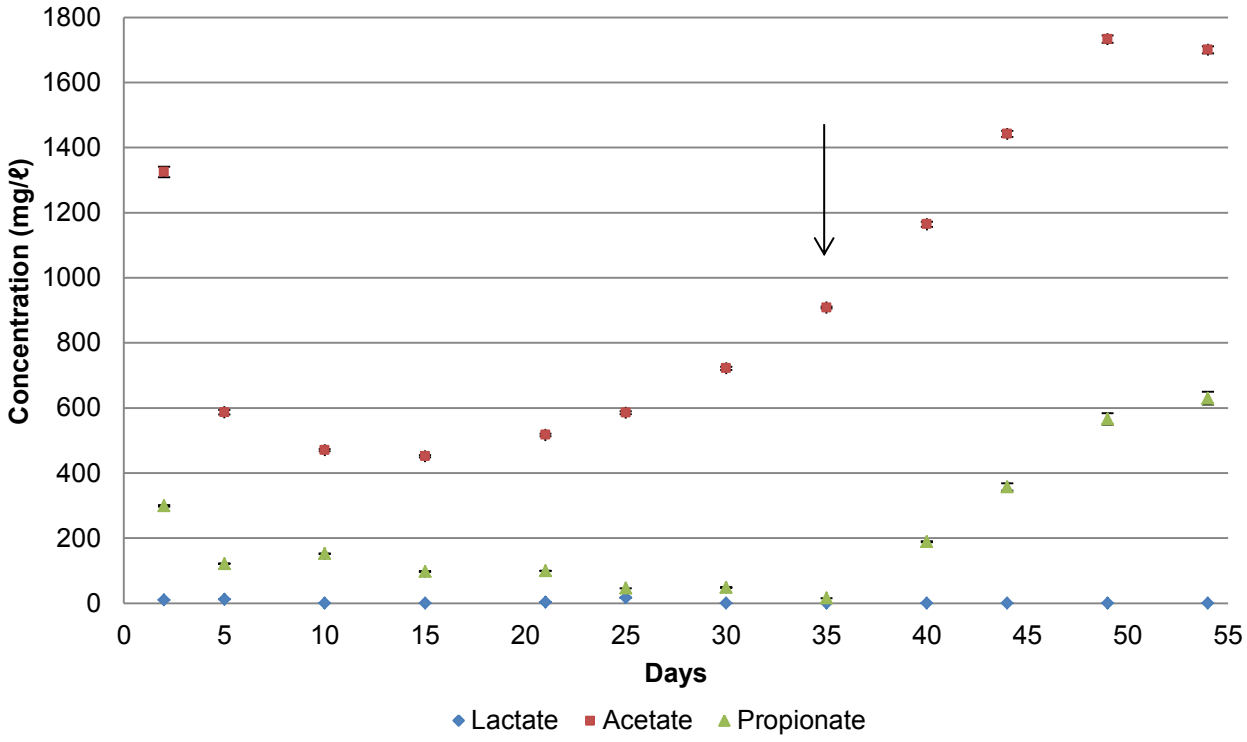

Figure 5-31: Concentration of volatile fatty acids as a function of time for MFC with carbon fibre brush anode and change in feed marked by arrow

COD Degradation and Coulombic Efficiency

The COD concentration of the spent medium decreased rapidly over the first 10 days of the experiment (Figure 5-32). It remained between 1000-1500 mg/ℓ until day 30 and decreased further to below 500 mg/ℓ by day 35. This corresponds with the general increase in the percent of COD degraded which was observed for the first 35 days of the experiment (Figure 5-33).

After day 35, a jump in COD concentration was noted in correspondence to the increase in lactate concentration in the feed and remained high for the remainder of the experiment. A continued increase in the percent of COD degraded was noted for the remainder of the experiment, although a dramatic initial decrease was observed after the feed was changed.

The coulombic efficiency was observed to increase in the first 15 days of the experiment and reached a maximum of almost 4% before decreasing for the remainder of the experiment (Figure 5-34). The coulombic efficiency associated with MFC-CBA is higher than the CE calculated for the MFCs with carbon felt anodes (Figure 5-25 and Figure 5-28).

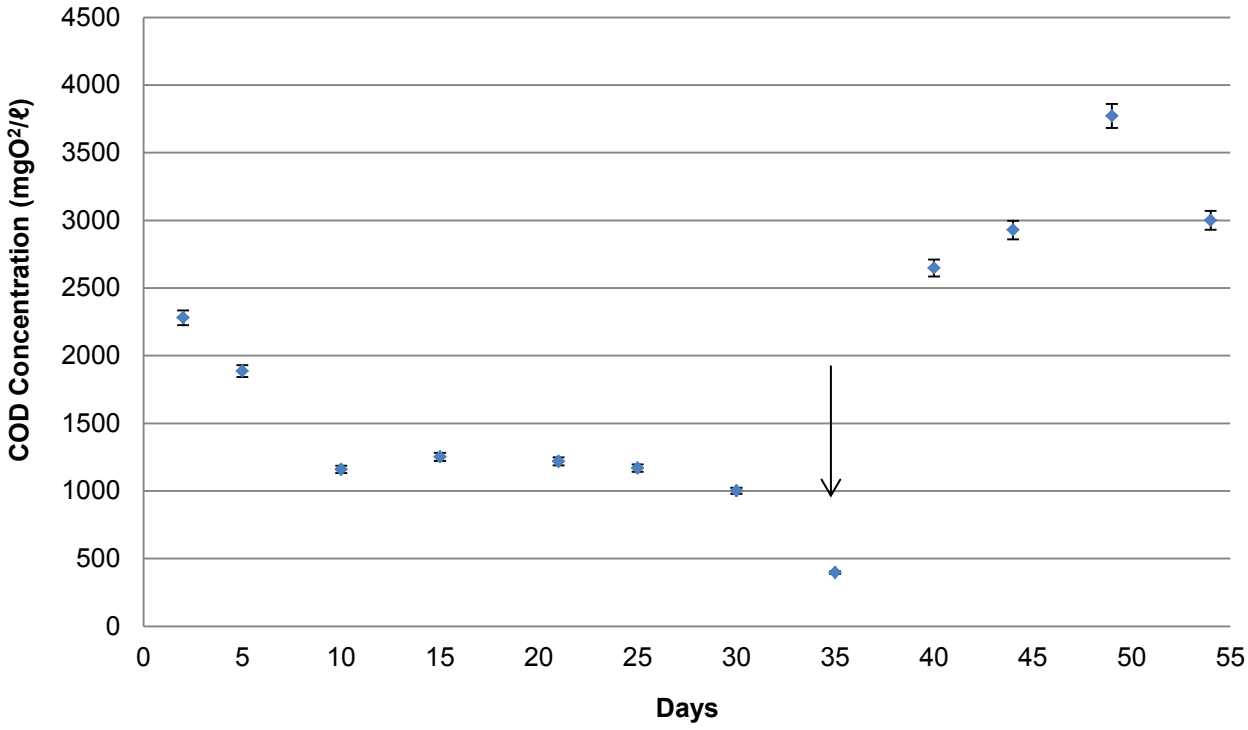

Figure 5-32: Soluble COD concentration as a function of time for MFC with carbon fibre brush anode and change in feed marked by arrow

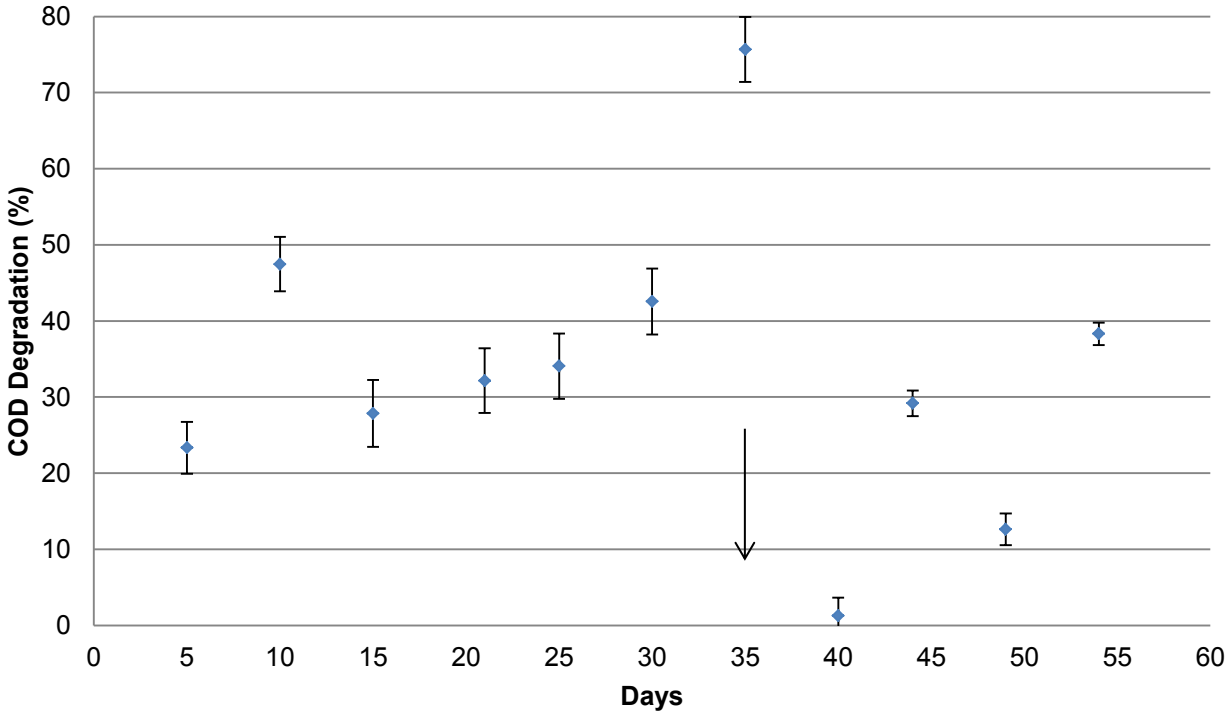

Figure 5-33: Percent of soluble COD degraded as a function of time for MFC with carbon fibre brush anode and change in feed marked by arrow

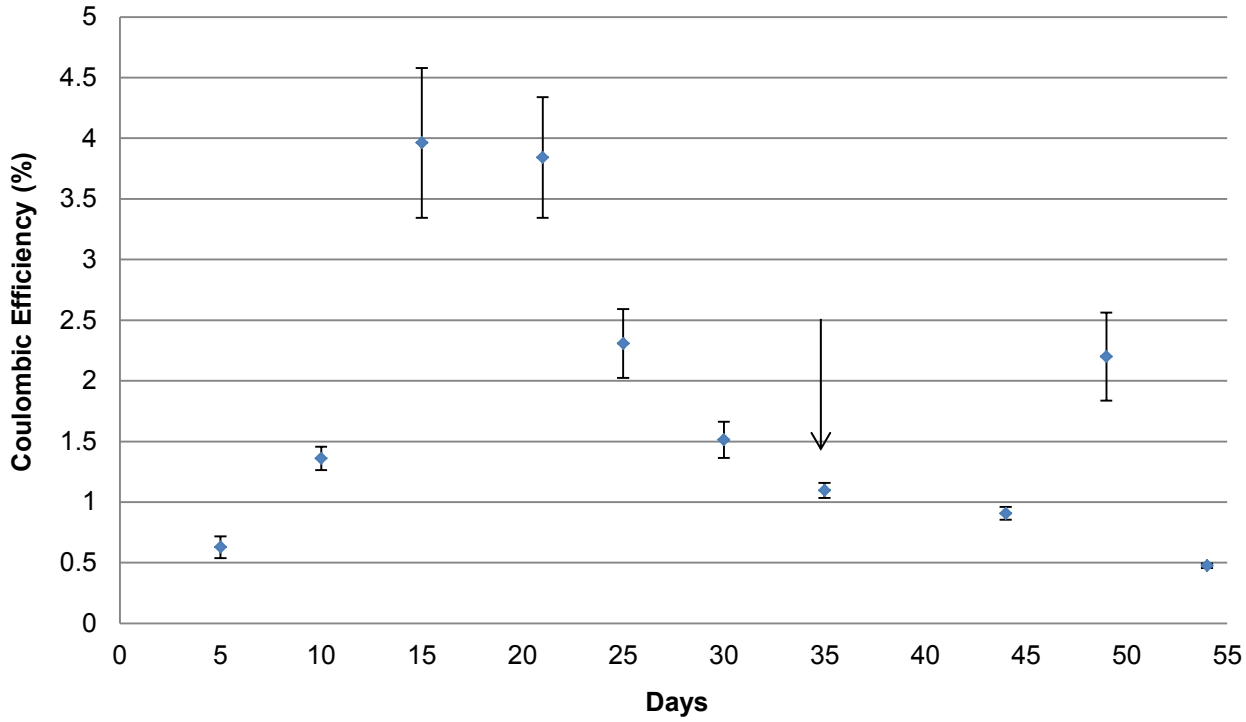

Figure 5-34: Coulombic efficiency as a function of time for MFC with carbon fibre brush anode and change in feed marked by arrow

5.3.2.3 Concentrated Feed

Concentration of Sulphur Species

The sulphate concentration of the MFC 5 initially increased for approximately the first 15 days of operation (Figure 5-35). This may have resulted from the complete oxidation of sulphide back to sulphate as a result of the high concentration of oxygen in the system in the first few days of the experiment before a mature biofilm formed on the cathode. It is also possible that the spiking of the MFCs with inoculum for the first 3 feeding cycles resulted in increased sulphate concentration as a result of residual un-oxidised sulphate in the inoculum. Sulphate concentration then decreased to between 1000-1500 mg/ℓ between day 25 and 37 before increasing again and remaining between 2000-2500 mg/ℓ for the last 13 days of the experiment which corresponded to the increase in feed concentration on day 37.

The sulphate concentration of both MFC-CFC and MFC-CFU decreased over the course of the experiment (Figure 5-37). The rate of decrease appears to be similar for both MFCs initially but deviated around day 10 with the connected cell demonstrating a higher rate of sulphate removal.

The sulphide concentration of MFC 5 remained low (below 20 mg/ℓ) for the duration of the experiment (Figure 5-36). Both MFC-CFC and MFC-CFU also had low sulphide concentration (below 30 mg/ℓ) for the duration of the experiment (Figure 5-38). A general increase in concentration throughout the operation of the MFC is noted for MFC 5 and both concentrated feed MFCs. The concentration was similar for both MFC-CFC and MFC-CFU.

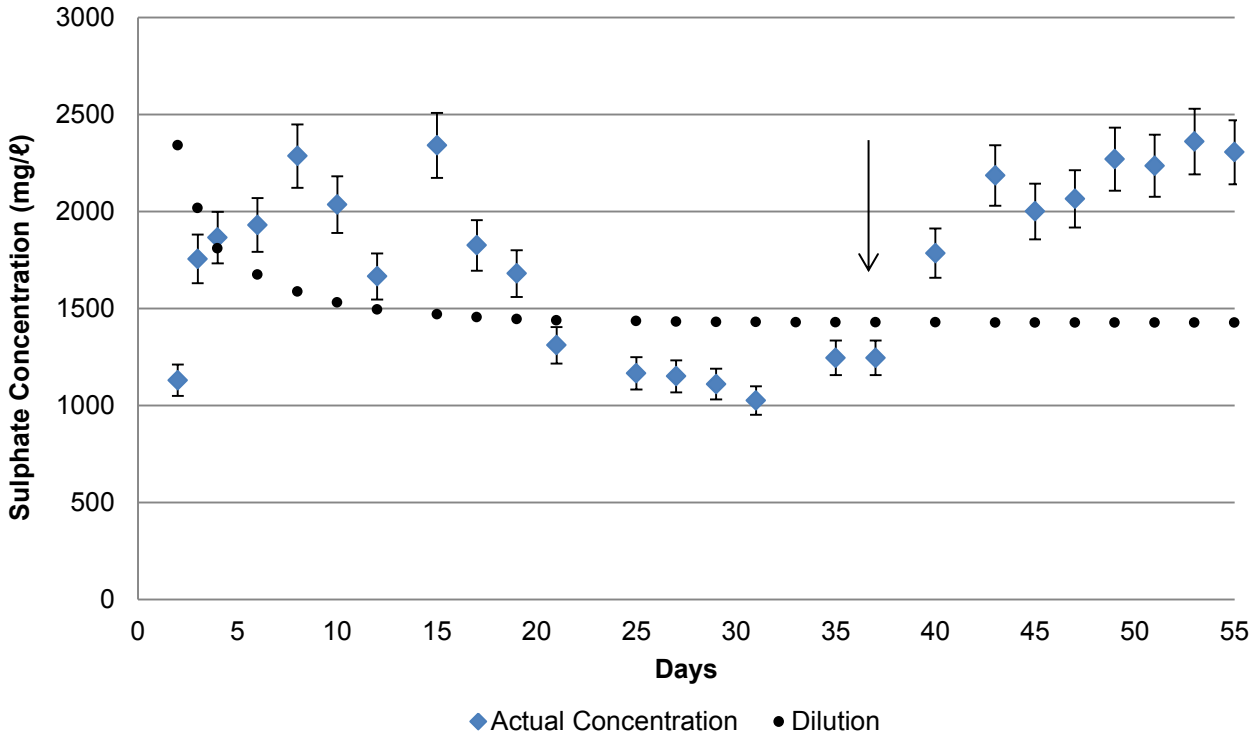

Figure 5-35: Sulphate concentration as a function of time for MFC 5 with standard and concentrated feed and change in feed marked by arrow

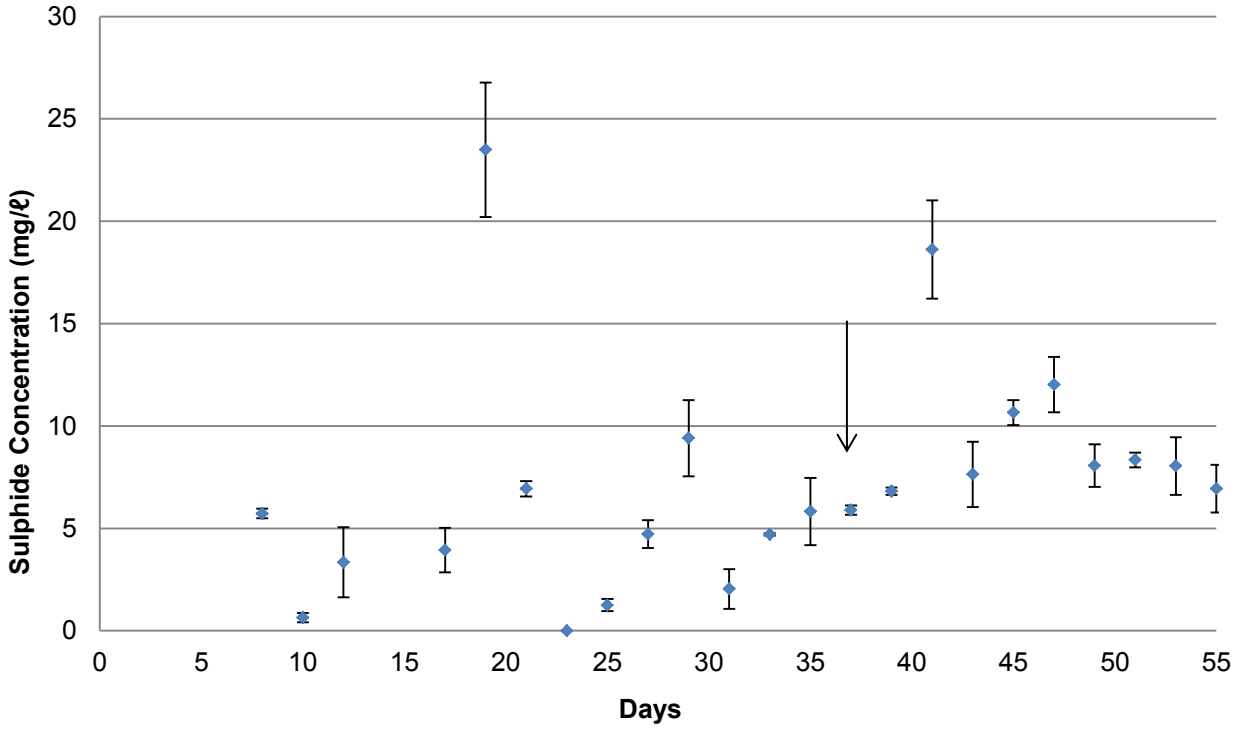

Figure 5-36: Sulphide concentration as a function of time for MFC 5 with standard and concentrated feed and change in feed marked by arrow

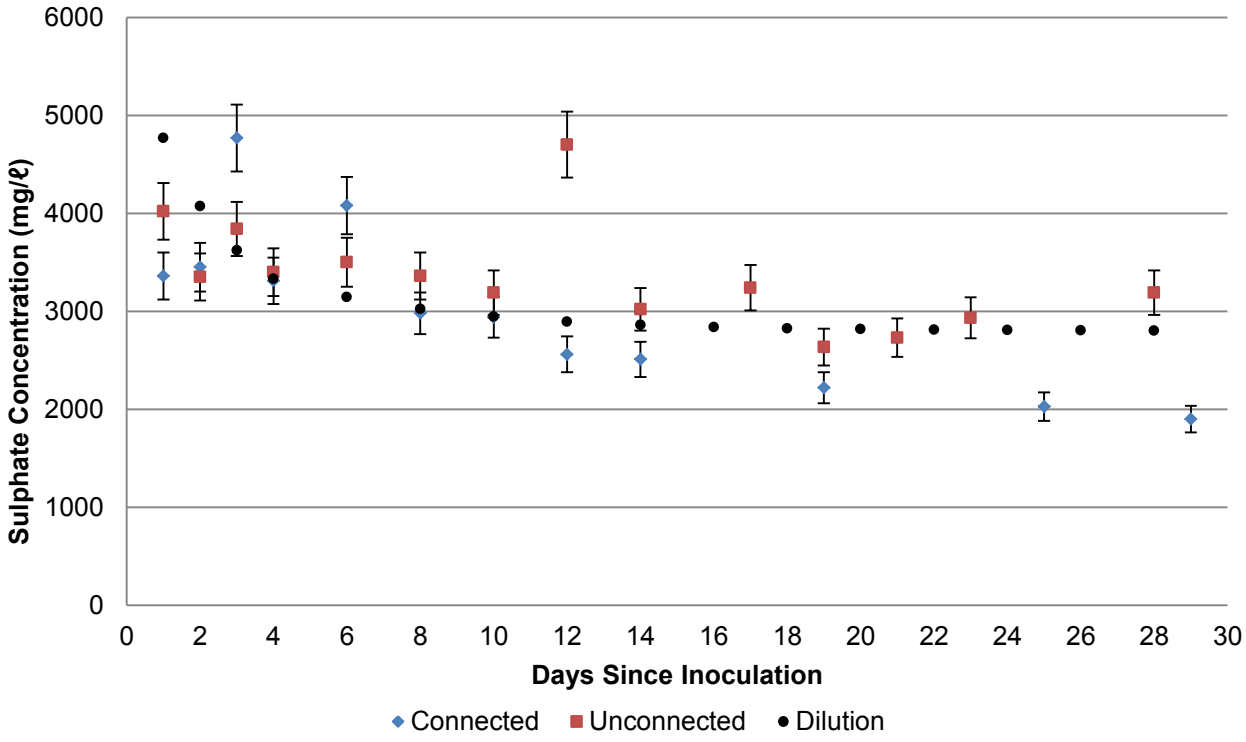

Figure 5-37: Sulphate concentration as a function of time for two MFCs fed concentrated feed

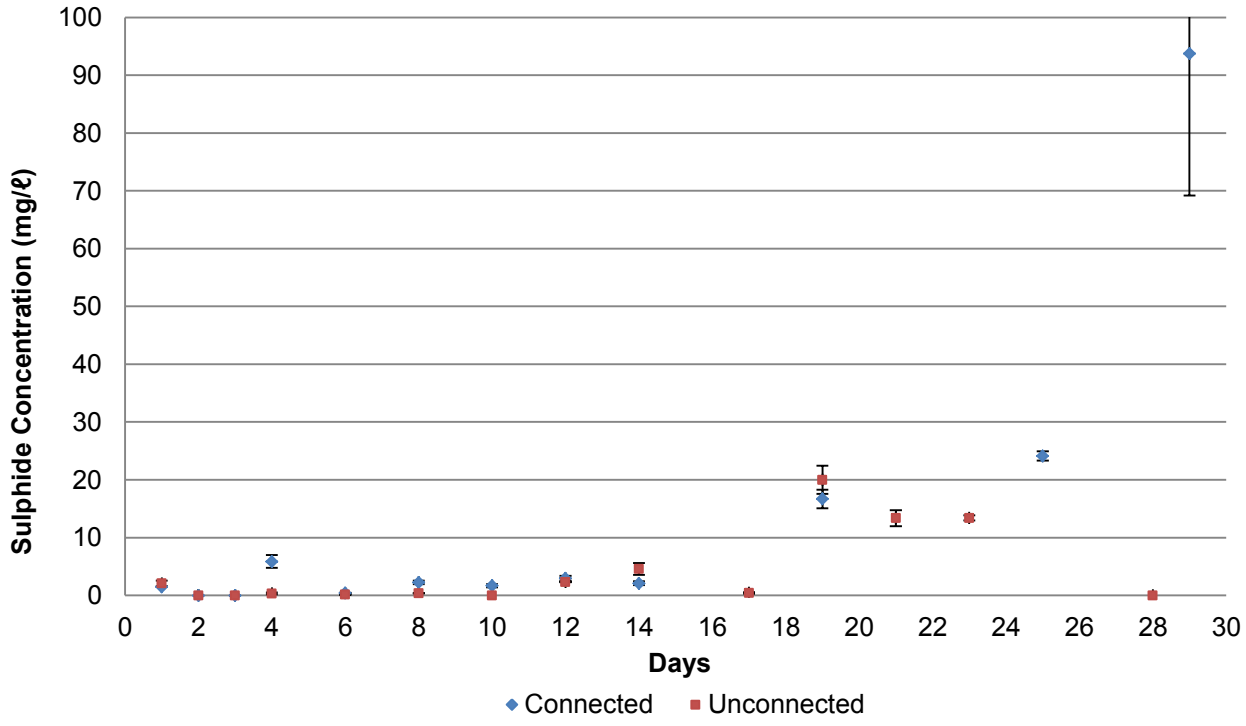

Figure 5-38: Sulphide concentration as a function of time for two MFCs fed concentrated feed

Concentration of Volatile Fatty Acids

The concentration of acetate in MFC 5 increased steadily for the first 35 days of operation (Figure 5-39). The propionate concentration remained low (less than 100 mg/ℓ) during this time. On day 37, in

correspondence with the increased feed concentration, the rate of increase in acetate concentration increased before becoming constant between 1500-1600 mg/ℓ in the last 10 days of the experiment. The propionate concentration also increased from day 37 until the end of the experiment. The propionate concentration was used to determine the concentration of acetate produced as a result of the metabolism of SRBs. The concentration of this acetate as a function of time had a similar profile to that of the measured acetate (Figure A 8 in Section C.3.2). Between 80-100% of the total measured acetate comprised of acetate from BSR indicating that BSR also increased with time. Over time a gradual decrease in the fraction of total acetate made up by acetate arising from BSR was observed.

The concentration of acetate increased similarly for both the connected and unconnected MFCs with concentrated feed (Figure 5-40 and Figure 5-41). The propionate concentration remained below 400 mg/ℓ for the unconnected MFC duration of experiment. An increase in propionate until day 10 was observed for the connected MFC. Thereafter the concentration decreased for the remainder of the experiment.

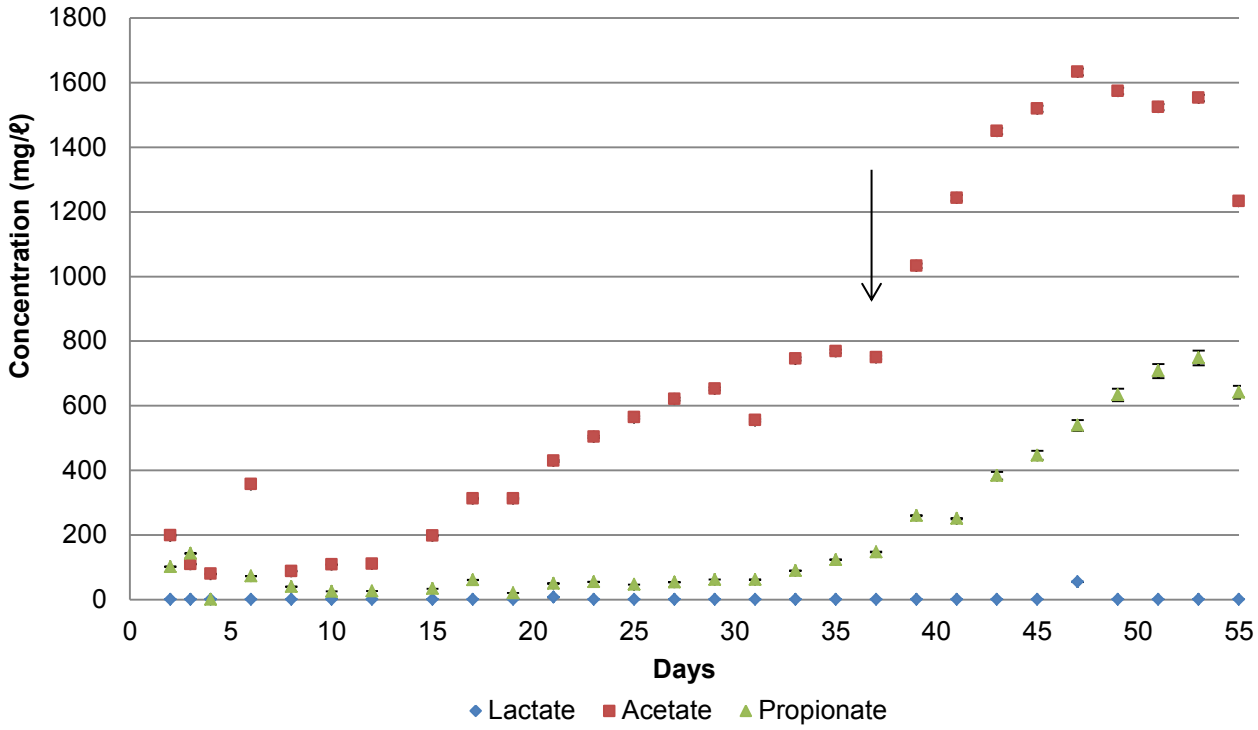

Figure 5-39: Concentration of volatile fatty acids as a function of time for MFC 5 with standard and concentrated feed and change in feed marked by arrow

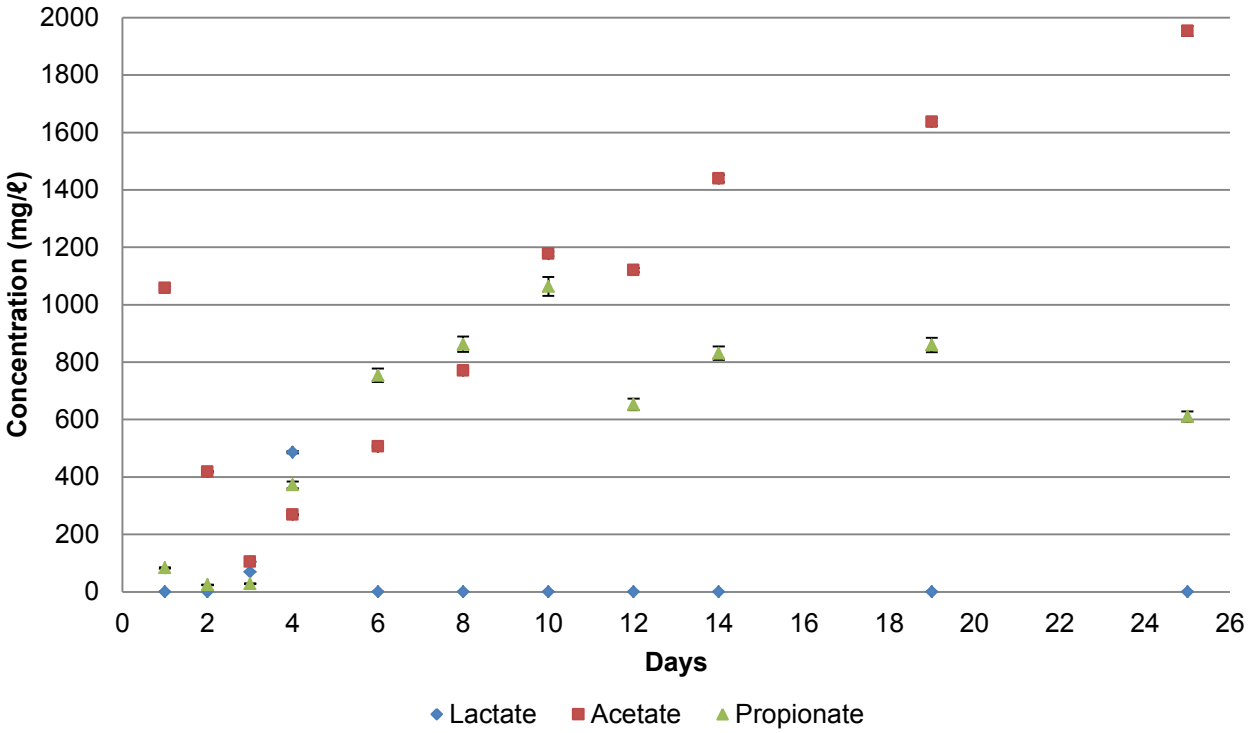

Figure 5-40: Concentration of volatile fatty acids as a function of time for MFC-CFC with concentrated feed

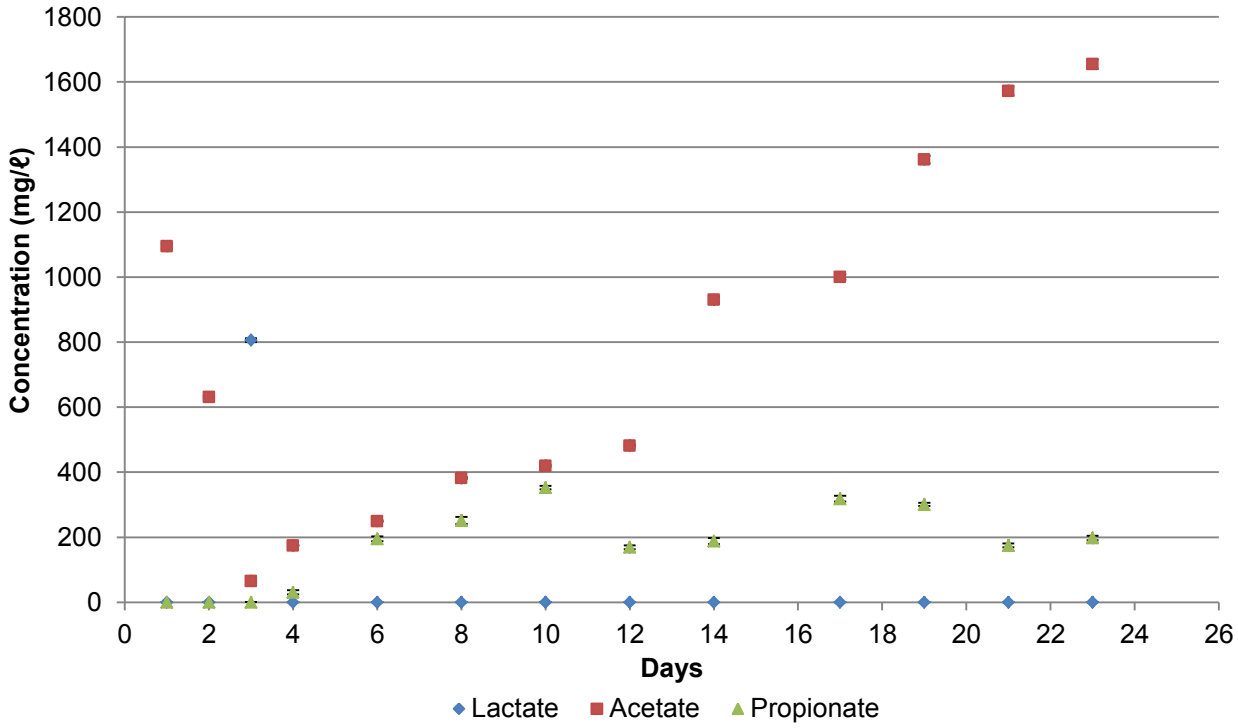

Figure 5-41: Concentration of volatile fatty acids as a function of time for MFC-CFU with concentrated feed

COD Degradation and Coulombic Efficiency

The COD concentration of MFC 5 (Figure A 9 in Section C.3.3) initially decreased over the first 8 days of operation which corresponds to the decrease of VFA concentration observed in Figure 5-39. The

COD increased slowly until day 37 before increasing dramatically after the addition of concentrated feed. It remained between 4000-4500 mg/ℓ for the 5 days of operation. This corresponds with a decrease in the percent of COD degradation from between 50-70 % in the first 15 days of operation to between 10-20% for the last 15 days of operation (Figure A 10 in Section C.3.3).

Both MFCs fed concentrated medium demonstrated an increase in COD concentration (Figure 5-42) and a decrease in the percent of COD degraded (Figure 5-43) over time. Although similar rates were observed for both MFCs, the unconnected MFC had a lower COD concentration for the duration of the experiment. The COD of the connected MFC increased as high as 5000 mg/ℓ by the end of the experiment whereas the COD in the unconnected MFC only reached 3000 mg/ℓ.

The CE for MFC 5 varied on a day to day basis and remained very low (below 0.08%) for the duration of the experiment (Figure A 11 in Section C.3.3). The connected MFC with concentrated feed also had low CE (below 0.2%) for the first 14 days of operation before increasing as high as 1.5% by the end of the experiment (Figure 5-44).

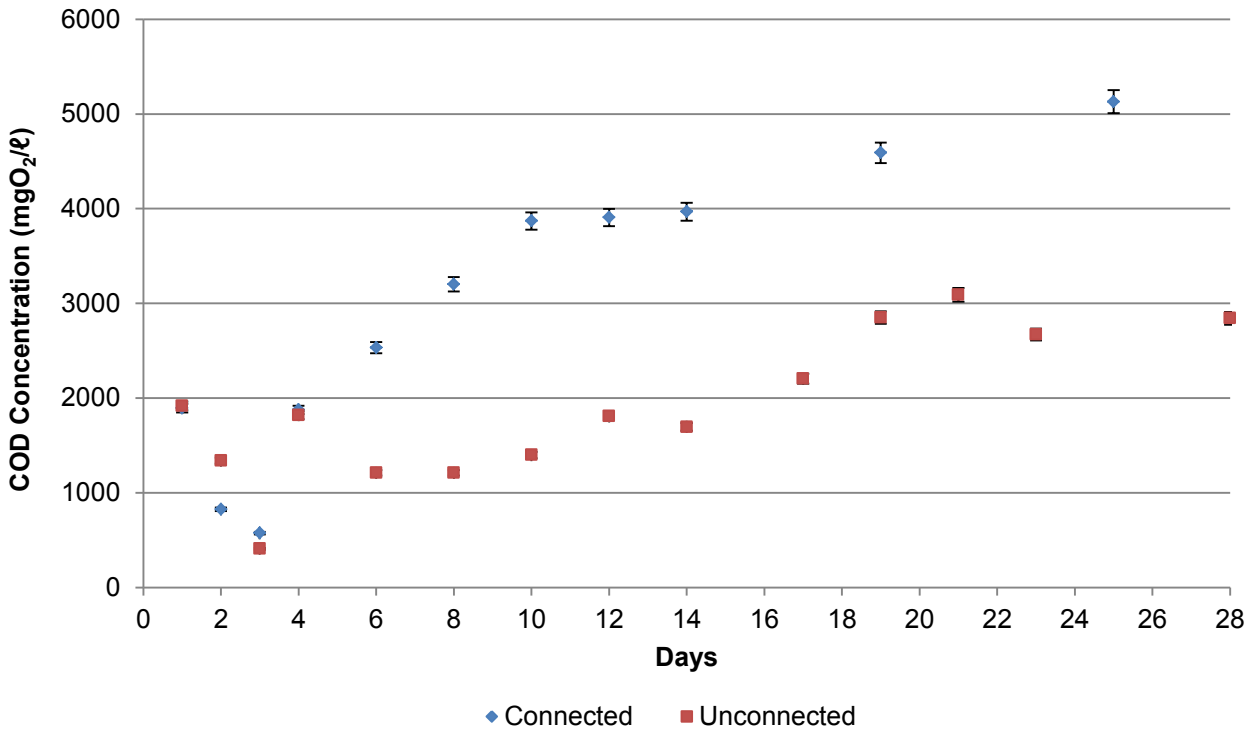

Figure 5-42: Soluble COD concentration as a function of time for MFC-CFC and MFC-CFU fed concentrated feed

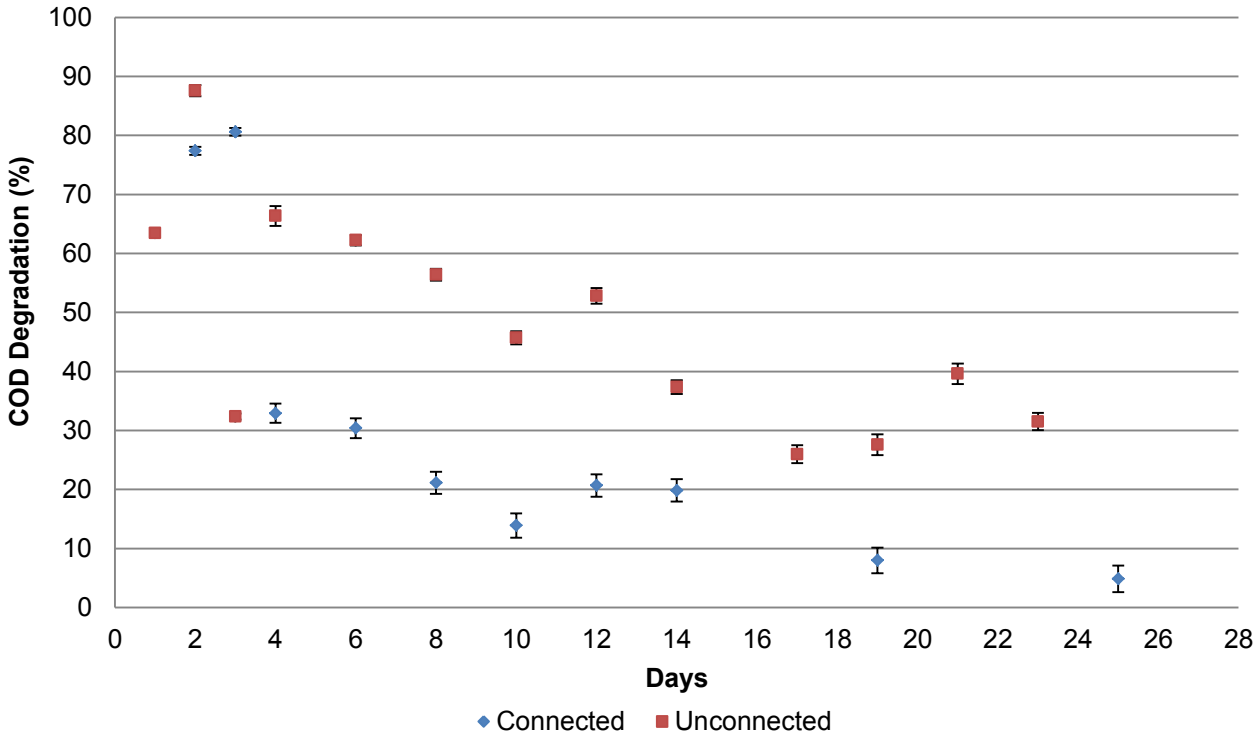

Figure 5-43: Percent of soluble COD degraded as a function of time for MFC-CFC and MFC-CFU with concentrated feed

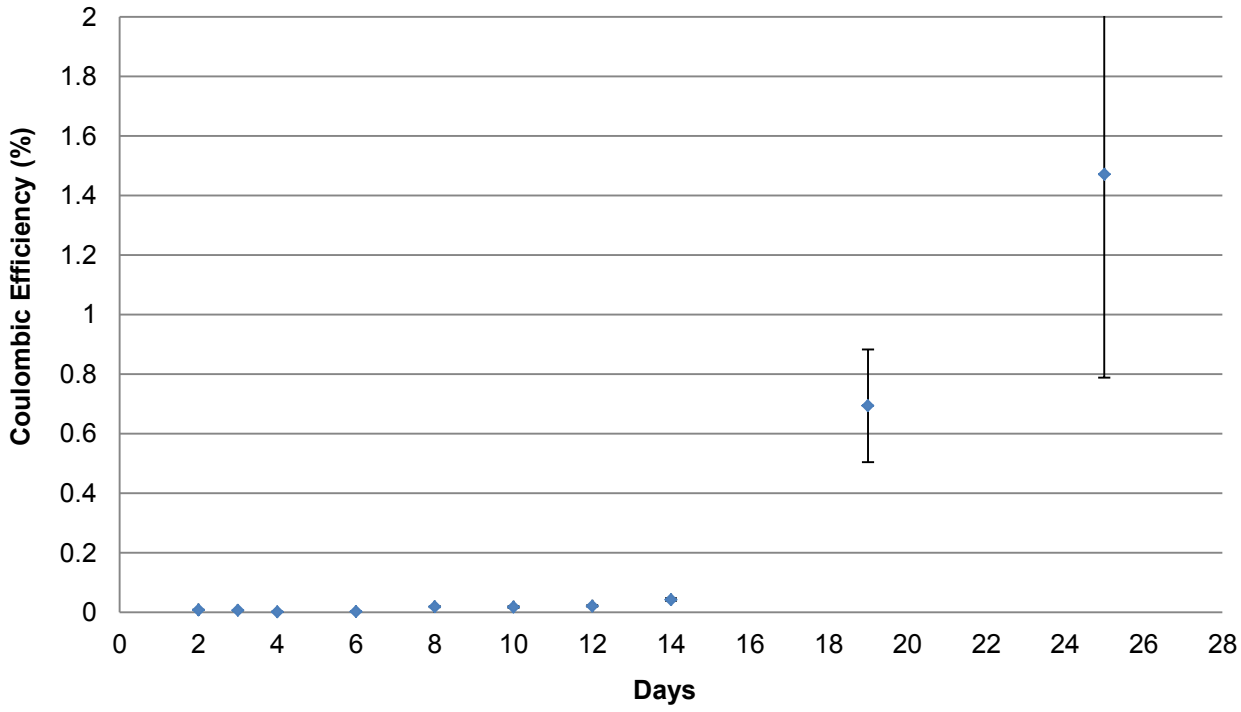

Figure 5-44: Coulombic efficiency as a function of time for MFC-CFC connected in circuit with concentrated feed

5.3.3 pH and Redox Potential

5.3.3.1 Carbon Felt Anode

As can be seen from Figure 5-45, the pH value of the spent medium taken from the single-chambered MFCs decreased over the course of the experiment. This trend was strongest for MFC 3. MFC 4 only has pH and redox potential data available from day 14 to 54. The pH of the spent medium increased during this time but remained between pH 6.8 and 7.5 (Figure 5-47).

The redox potential of MFCs 1-3 decreased for approximately the first 7 days of the experiment (Figure 5-46). The redox potential of cell 3 stabilised around -350 mV from day 9 until the end of the experiment. The redox potential of MFC 1 and 2 increased gradually over remainder of the experiment. The redox potential of MFC 4 increased between days 14 to 23 before deceasing to around 350 mV until day 54 (Figure 5-48).

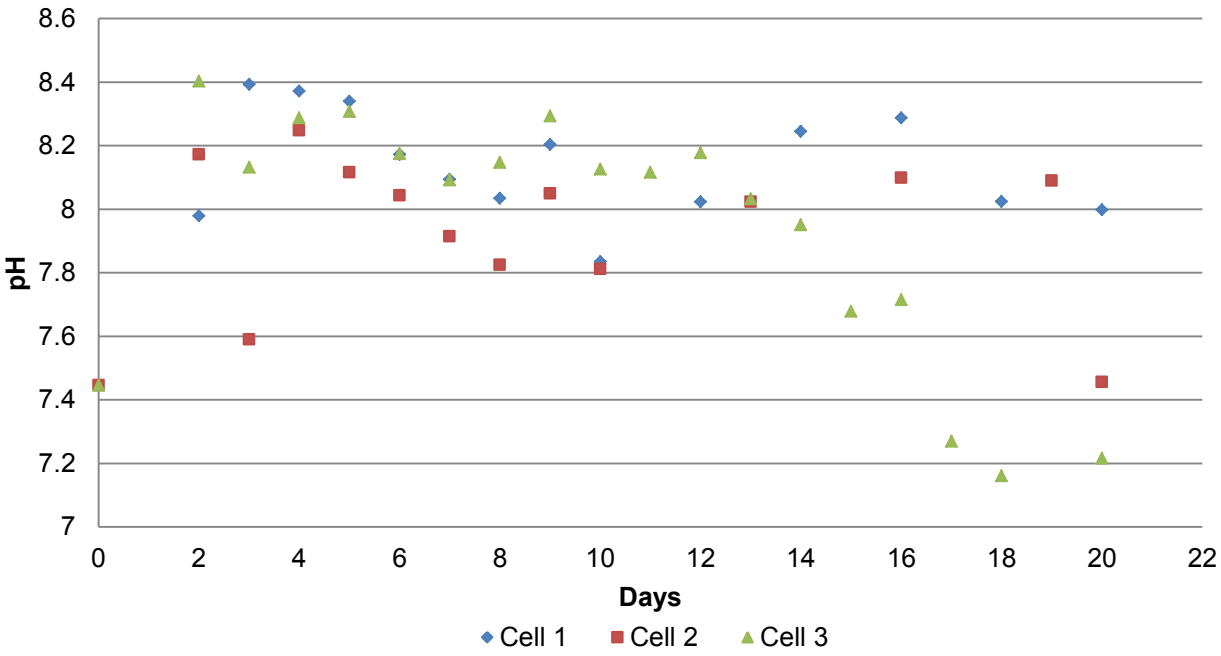

Figure 5-45: pH as a function of time for 3 MFCs with carbon felt anode

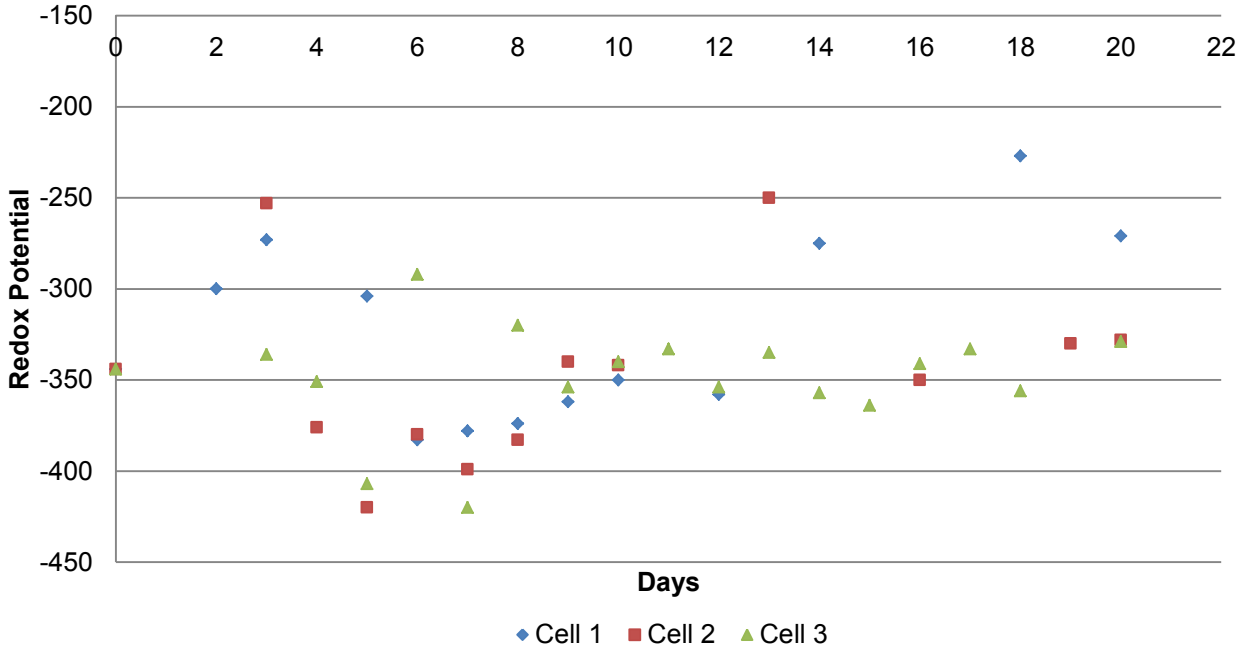

Figure 5-46: Redox potential (wrt Ag/AgCl reference electrode) as a function of time for 3 MFCs with carbon felt anode

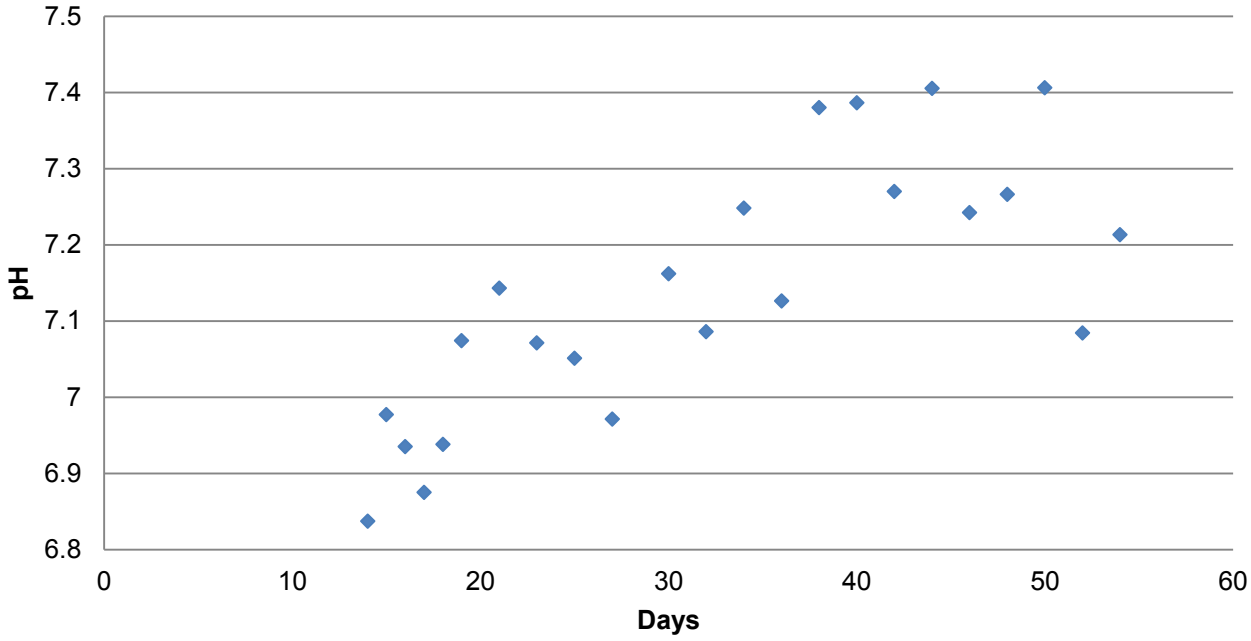

Figure 5-47: pH as a function of time for MFC 4 with carbon felt anode

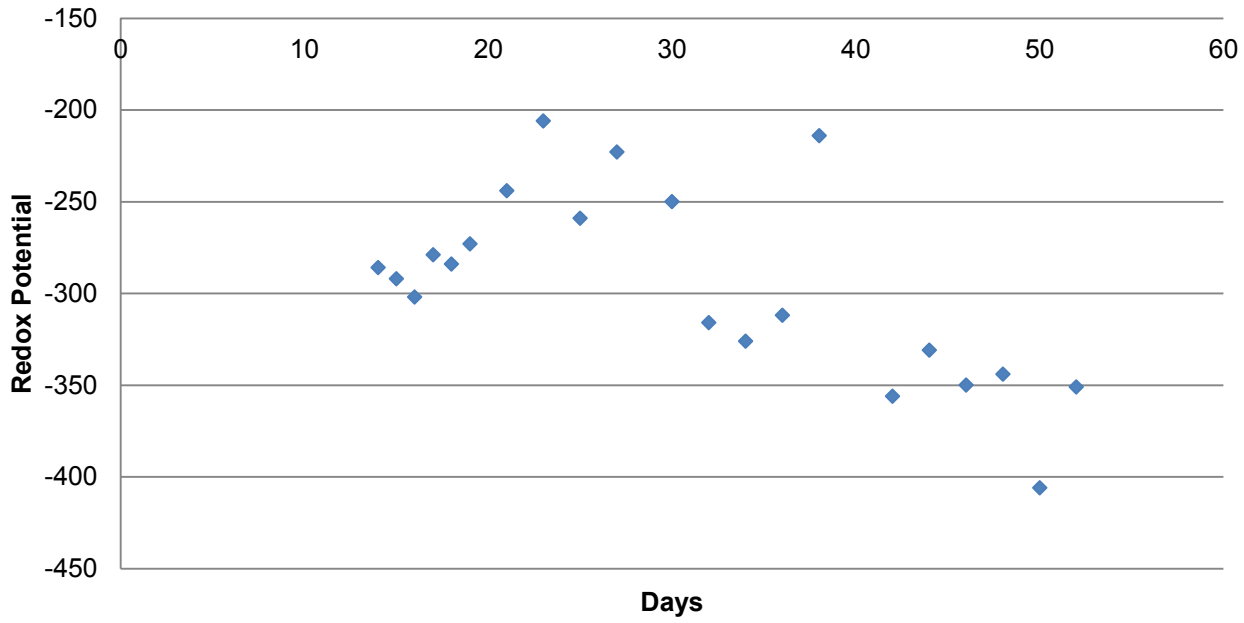

Figure 5-48: Redox potential (wrt Ag/AgCl reference electrode) as a function of time for MFC 4 with carbon felt anode

5.3.3.2 Carbon Fibre Brush Anode

The pH of the MFC-CBA decreased over the course of the experiment from around pH 8.5 to around pH 7 (Figure 5-49). As can be seen from Figure 5-50, the redox potential initially increased over the first 15 days and stabilised between -330 mV and -370 mV for the remainder of the experiment.

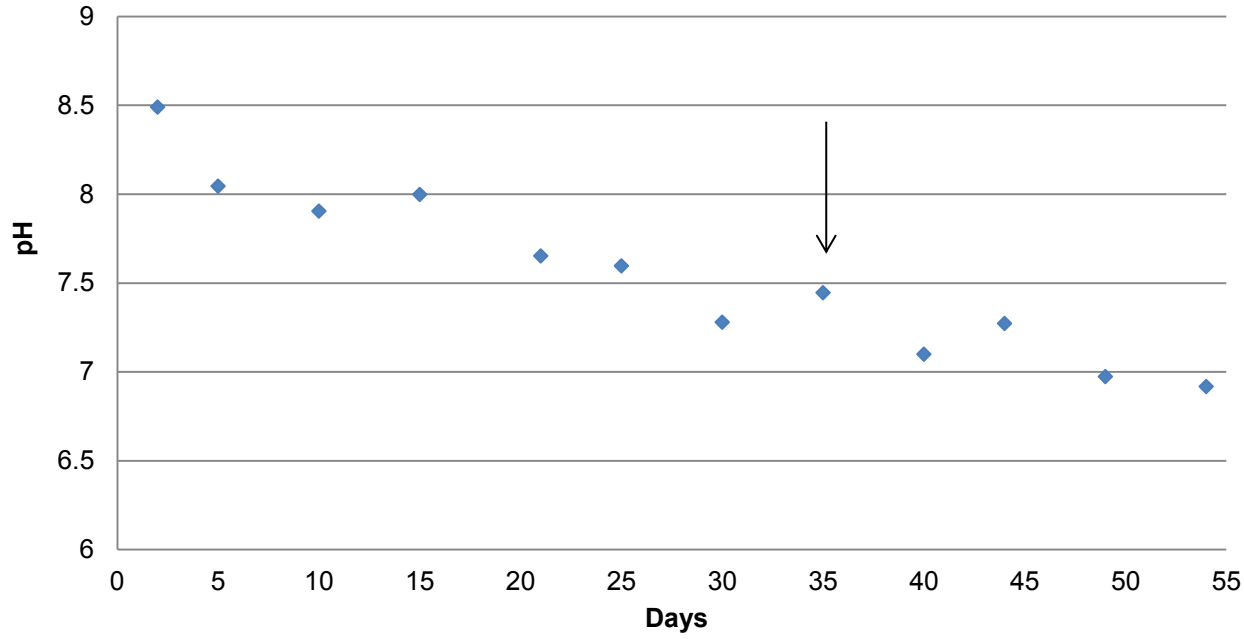

Figure 5-49: pH as a function of time for MFC with carbon fibre brush anode and change in feed marked by arrow

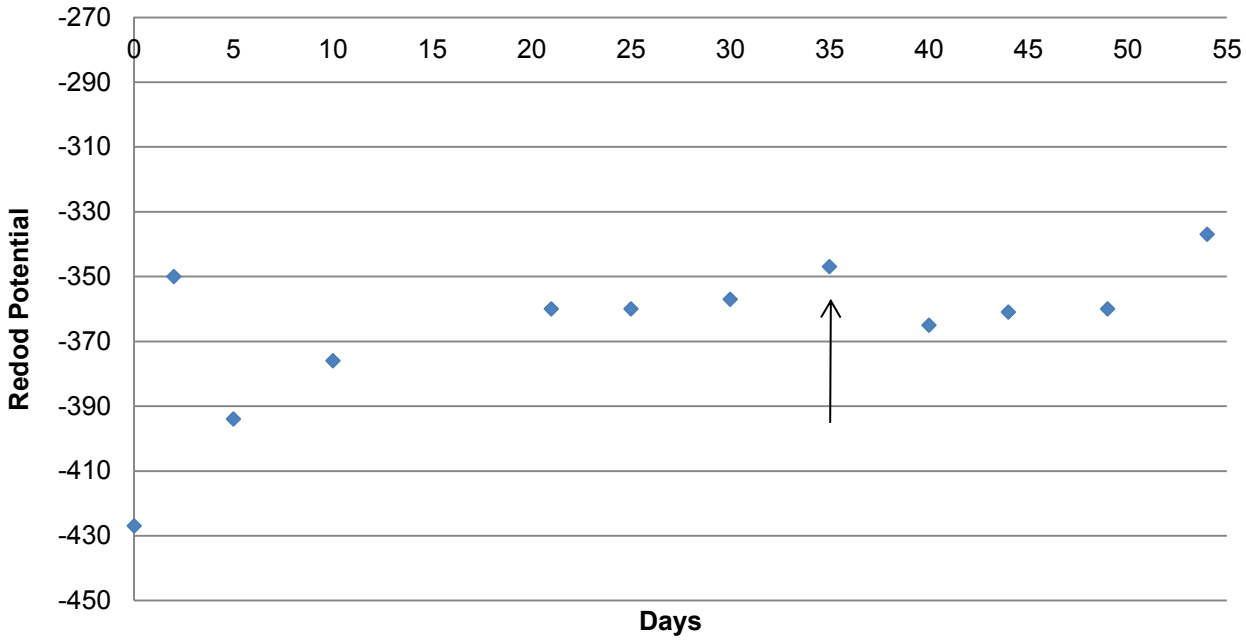

Figure 5-50: Redox potential (wrt Ag/AgCl reference electrode) as a function of time for MFC with carbon fibre brush anode and change in feed marked by arrow

5.3.3.3 Concentrated Feed

The pH of MFC 5 decreased from approximately pH 8.5 to pH 7 over the first 37 days of the experiment (Figure A 12 in Section C.3.4). It then stabilised at around pH 7 for the remainder of the experiment. Figure 5-51 indicates that the pH decreased over the course of the experiment for both MFC-CFC and MFC-CFU. The rate of decrease for MFC-CFC was faster than that of MFC-CFU. MFC-CFC reached pH 7 in approximately 10 days where it stabilised for the rest the operation of the MFC. MFC-CFU only decreased to pH 7.5 by the end of the experiment.

The redox potential of MFC 5 initially increased for the first 15 days of the experiment before stabilising between -330 mV and -360 mV for the remainder of the experiment (Figure A 13 in Section C.3.4). The potential of the MFC-CFU remained mainly between -340 mV and -400 mV for the duration of the experiment Figure 5-52. MFC-CFC demonstrated an increase in redox potential to around -330 mV over the first 12 days of the experiment but remained between -360 mV and -380 mV for the rest of the experiment.

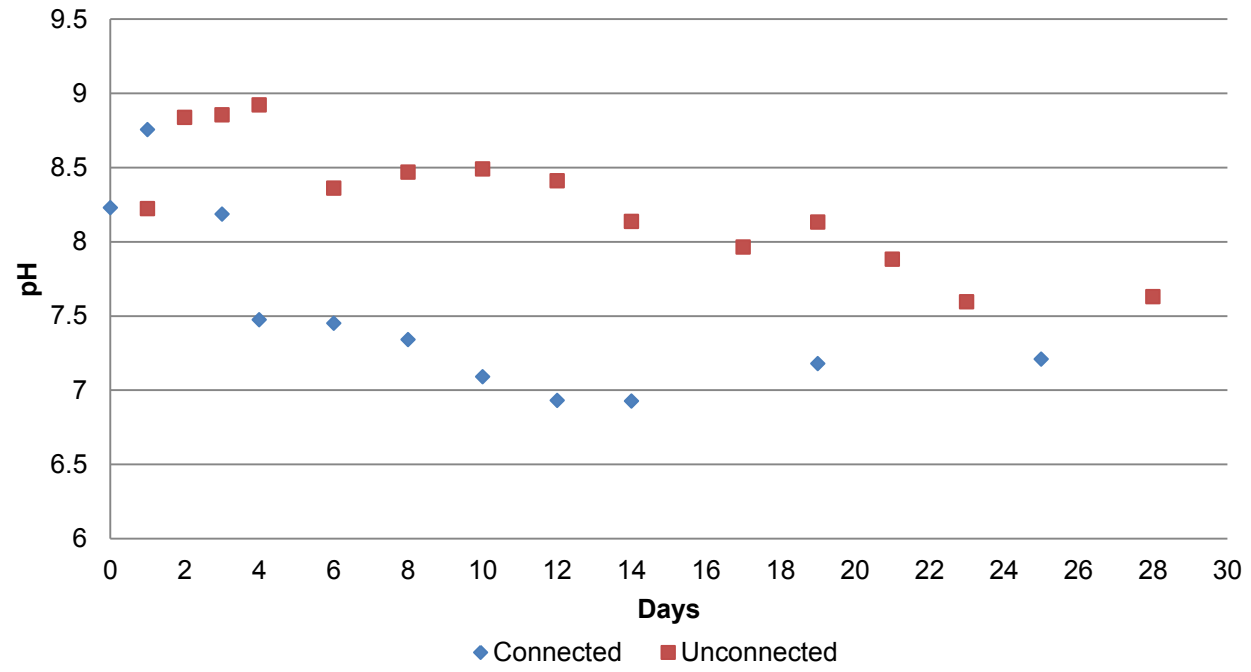

Figure 5-51: pH as a function of time for two MFCs fed concentrated feed

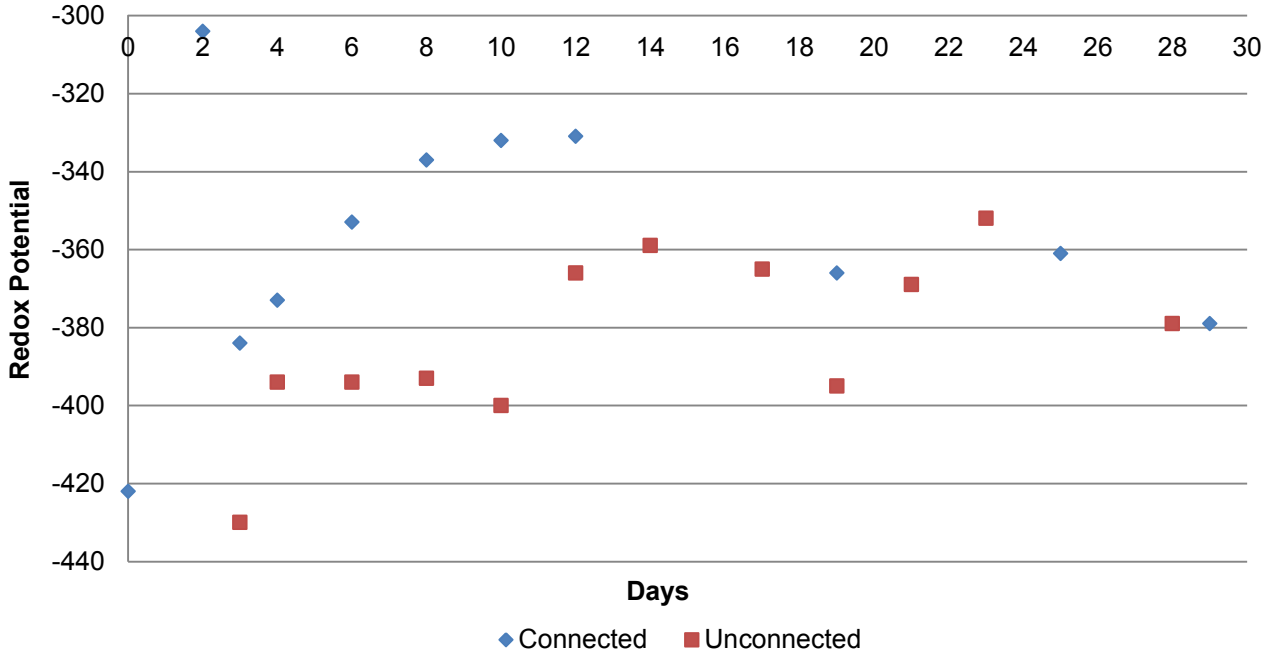

Figure 5-52: Redox potential (wrt Ag/AgCl reference electrode) as a function of time for two MFCs fed concentrated feed

5.3.4 Scanning Electron Microscopy (SEM)

While very little quantitative detail can be gathered from SEM images of anodic and cathodic biofilms, it is possible to determine the morphology of the microorganisms colonising the electrodes. Differences in morphology between the microorganisms on the anode and cathode provide evidence of their different roles in the MFC. The growth of nanowires from bacterial cells in the biofilm can also confirm the presence of exoelectrogenic bacteria in the system. It cannot, however, determine how prolific exoelectrogenic bacteria are in the community or how much of the current produced is as a result of the action of microorganisms. Exoelectrogenic bacteria which do not produce nanowires cannot be reliably identified using this methodology.

SEM was performed on the anode and cathode of MFC 5. As can be seen Figure 5-53, there was visible sulphur deposition on the anode. In the process of removing the electrodes from the MFC, flakes of sulphur were dislodged. Small amounts of sulphur are also evident on the cathode. Salt crystals were also present on both anode and cathode but in larger amounts on the cathode electrode. These crystals are seen in Figure 5-55A.

SEM images of the anode were taken both above and below the sulphur layer (Figure 5-54A). As can be seen from Figure 5-54E and Figure 5-54F, a complex biofilm was present on the top of the sulphur layer. Different cell morphologies and extracellular polymeric substance (EPS) were observed. Underneath the sulphur layer in direct contact with the carbon anode, the bacteria present appear to be largely the same as can be seen in Figure 5-54B, Figure 5-54C and Figure 5-54D. The bacteria are rod-like and appear to form clusters with one end in contact with the carbon and the other end angled to touch the ends of the other bacteria in the cluster. As can be seen from Figure 5-54D, thin strands stretch between some of the bacteria. *Geobacter sulfurreducens* is a species that is likely present in the microbial community of the MFC and is known to produce nanowires which have been described as “long thin filamentous strands” (Logan & Regan, 2006). The nanowires produced by *G. sulfurreducens* are also thinner than those produced by *S. oneidensis* MR-1 (Logan & Regan, 2006).

The filamentous strands in Figure 5-54D match the description of nanowires given in literature and are thinner relative to cell size than those produced by *S. oneidensis* in Figure 4-21. These filaments are therefore believed to be nanowires and indicative of the electricity producing abilities of these bacteria. An enlarged view of the nanowires is given in Figure 5-56A.

Figure 5-55B, Figure 5-55C and Figure 5-55D show the complex biofilm present on the cathode. Both the SEM images taken of the biofilm in contact with the carbon electrode (Figure 5-55C and Figure 5-55D) and the salt crystals on it (Figure 5-55B), indicate that many different cell morphologies are present as well as EPS. The cathode biofilm is dominated by rounded, coccial cells interspersed with elongated cells. As can be seen from Figure 5-55C, threadlike structures believed to be nanowires are also present in the cathodic biofilm. An enlarged view of the nanowires is given in Figure 5-56A. Although the nanowires appear to grow from rod-like cells, they touch many other cells in the biofilm and it cannot be concluded that the cocci cells do not produce nanowires.

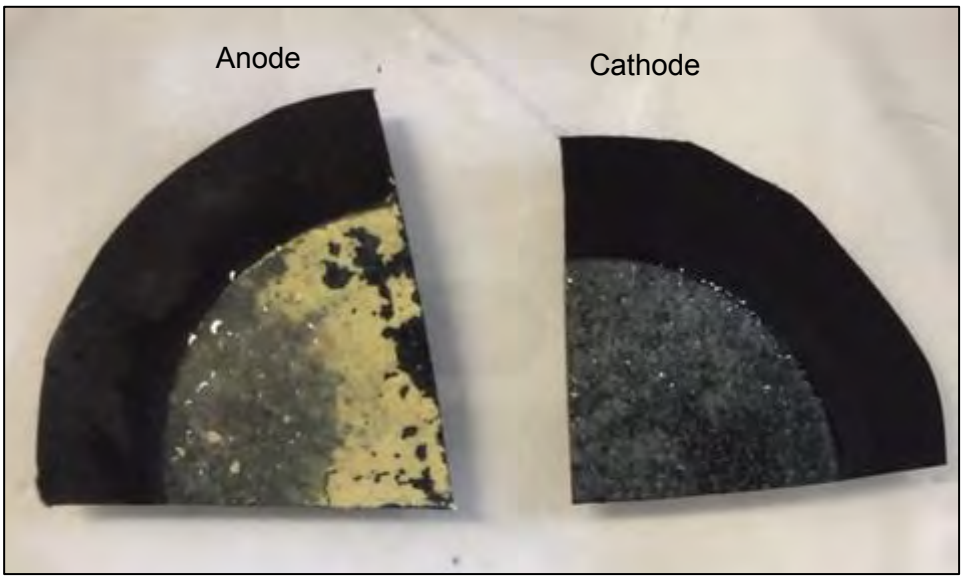

Figure 5-53: Photograph of section of the anode and cathode of MFC 5 at the end of its operation on which SEM was performed

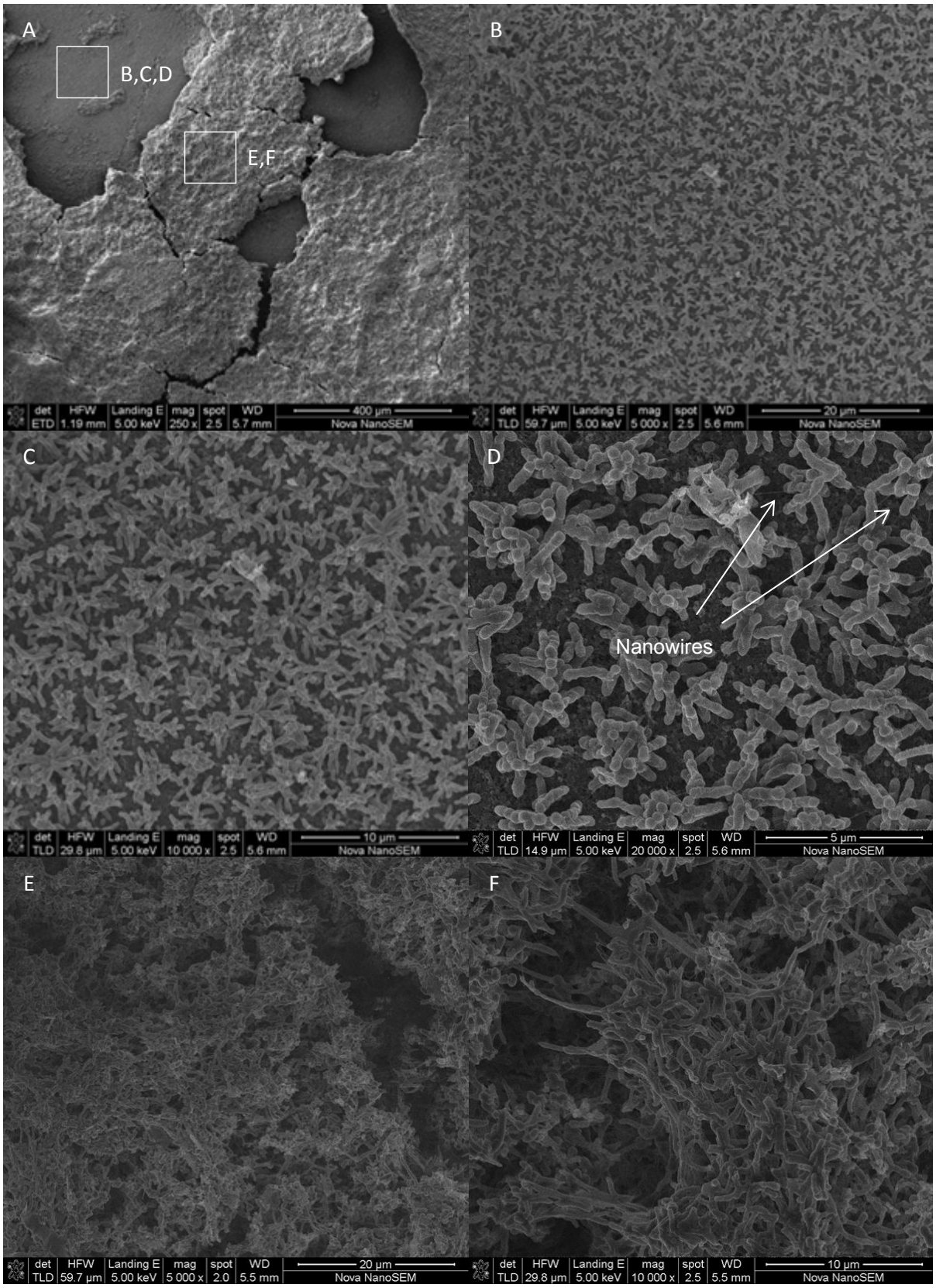

Figure 5-54: SEM of anodic biofilm of single-chambered MFC with SRB and SOB community

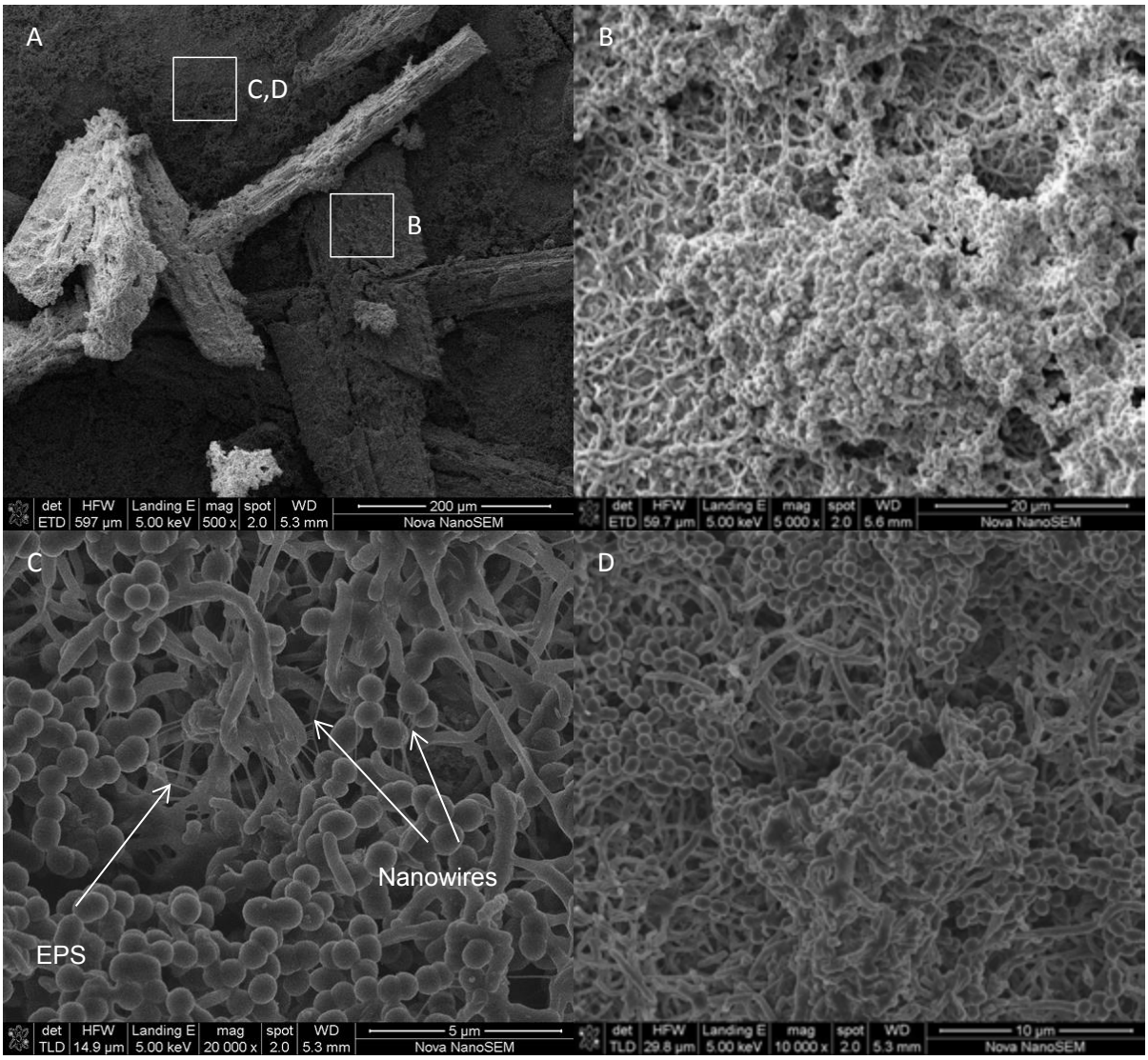

Figure 5-55: SEM of cathodic biofilm of single-chambered MFC 5 with SRB and SOB community

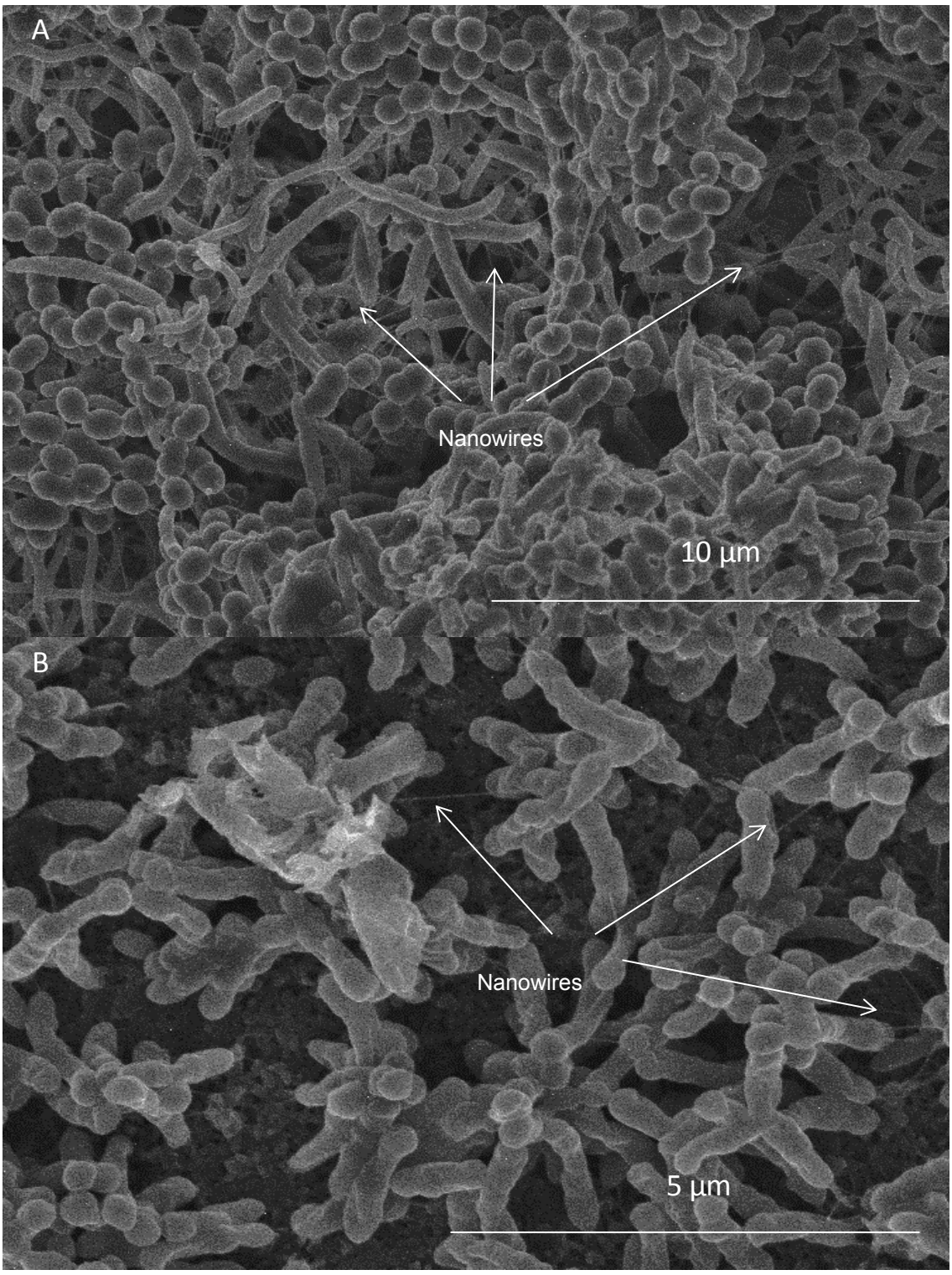

Figure 5-56: Enlarged SEM image of A: Cathode from Figure 60D at 20 000x magnification and B: Anode from Figure 59D at 20 000x magnification

5.3.5 Cyclic Voltammetry

All potentials are reported with reference to a Ag/AgCl reference electrode. Cyclic voltammetry was conducted using fresh 10 mM lactate and sulphate medium at scan rates of 1 mV/s and 5 mV/s (Figure 5-57). An oxidation and reduction peak at approximately 0.19 V and -0.33 V respectively was observed at a scan rate of 1 mV/s. At a scan rate of 5 mV/s, the oxidation and reduction peaks were less distinct but occurred at approximately 0.19 V and -0.44 V respectively. For reversible redox couples where mass transfer is limiting, peak separation is equal to 59/z mV at 25°C, where z is the number of electrons transferred between species. This is not affected by the scan rate (Harnisch & Freguia, 2012). The peaks observed in the CV of the medium at 1 mV/s were similar in height and within 52 mV of each other however, the peak separation is larger at 5 mV/s (approximately 0.63 V). This suggests that the reactions occurring may not be reversible.

This CV was conducted over a range of -0.9 V to 0.9 mV. CV was conducted on planktonic cells in medium over the same range. As can be seen from the voltammogram, no strong oxidation or reduction peaks were produced. A very small reduction peak at approximately -0.75 V was observed. Despite this, the current produced was higher than that of medium. A similar trend was noted for the voltammogram of spent abiotic medium. A small oxidation peak at around -0.22 V was observed. A smaller scan range was used for the CV on the spent medium (-0.9 V to 0.4 V) as a result of no peaks being visible for the planktonic cells in medium and no separation of current produced for the oxidative and reductive cycles above 0.5 V in normal medium.

The high current produced for the CV of both planktonic cells and spent medium is likely as a result of double layer charging. Double layer charging occurs when ions in solution (of opposite charge to the electrode) migrate and adsorb to the electrode surface due to electrostatic forces. One of the most common models to describe double layer charging is the Stern model. In this model the layer adjacent to the electrode is called the Stern layer and is static and the width of the radius of solution particles. Beyond the Stern layer is the diffuse layer in which the movement of ions is controlled by both diffusion and electrostatic forces (Wang & Pilon, 2012). This double layer essentially functions as a capacitor and therefore as the potential of the electrode changes, charge is reassigned from the solution at the electrode to the electrode surface and vice versa. This is called capacitive current. No actual transfer of electrons which results in the oxidation or reduction of species in solution occurs, and therefore no faradaic current flows.

Any peak produced by the CV of planktonic cells in medium or spent medium is likely to indicate the presence of mobile cell-membrane associated mediators produced by the microorganism (Logan, 2008). The small peaks produced could indicate that mediators are present but it is likely that they are present in small enough quantities to not contribute significantly to electricity production.

CV was conducted on the anode and cathode of a single-chambered MFC over a range of -0.7 V to 0.4 V at a scan rate of 1 mV/s (Figure 5-59). No strong peaks are observed for either the anode or cathode. Upon enlarging the voltammogram of the cathode a small oxidative peak around 0.15 V is observed (Figure 5-60). At a scan rate of 1mV/s it is thought that the masking of faradaic current by capacitive current would be reduced however, in the case of electrodes sparsely covered with biofilm, capacitive current may always mask faradaic current even at very low scan rates (Harnisch & Freguia, 2012). As a result of the cathode being placed in fresh medium for the CV, mediators in solution would have been removed. It therefore is likely that microorganism growing on the cathode produce cell-membrane associated mediators or conductive nanowires. The SEM conducted on the cathode (Figure 5-56A) reveals that microorganisms producing nanowires are present.

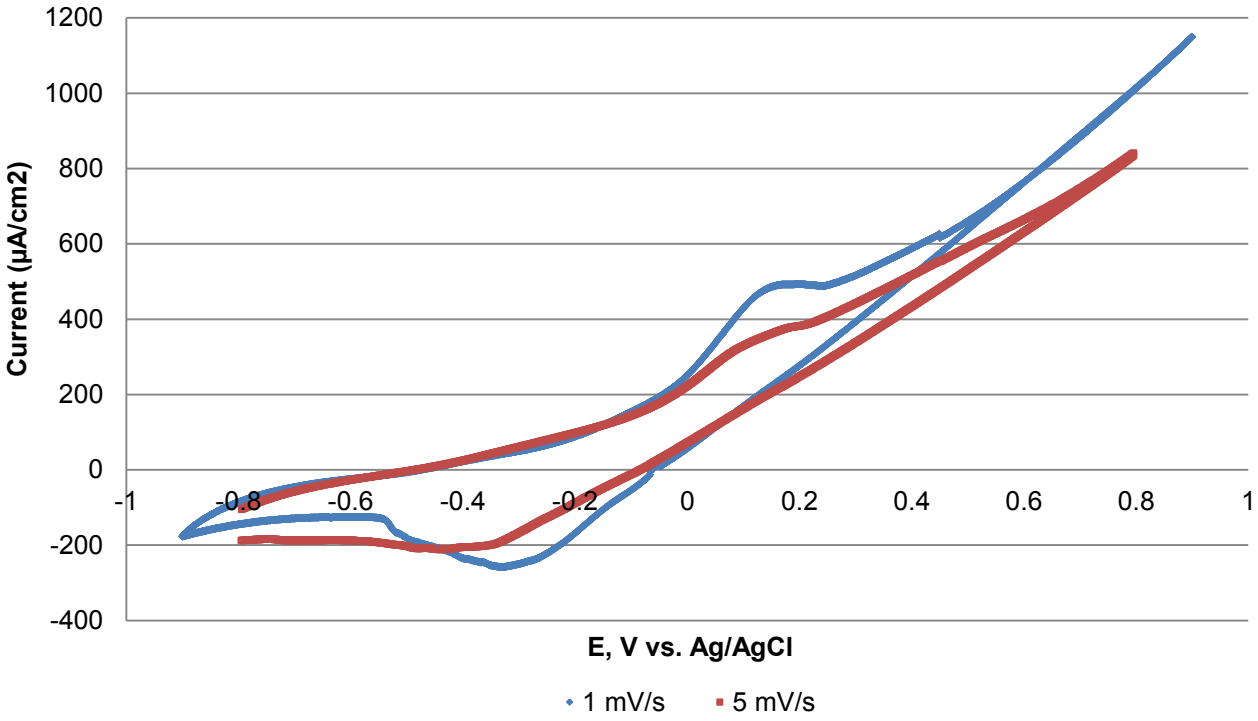

Figure 5-57: Cyclic voltammograms of fresh medium conducted at a scan rate of 1 mV/s and 5 mV/s

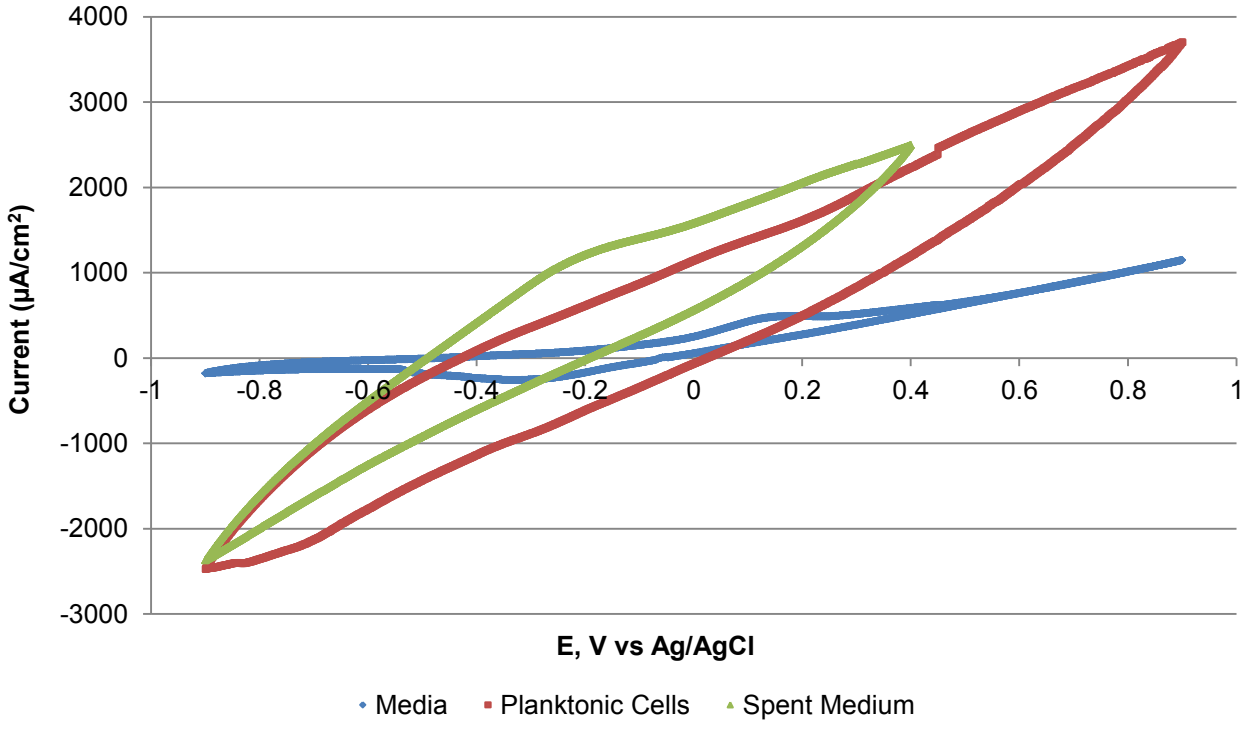

Figure 5-58: Cyclic voltammograms of various aspects of the single-chambered MFCs conducted at a scan rate of 1 mV/s

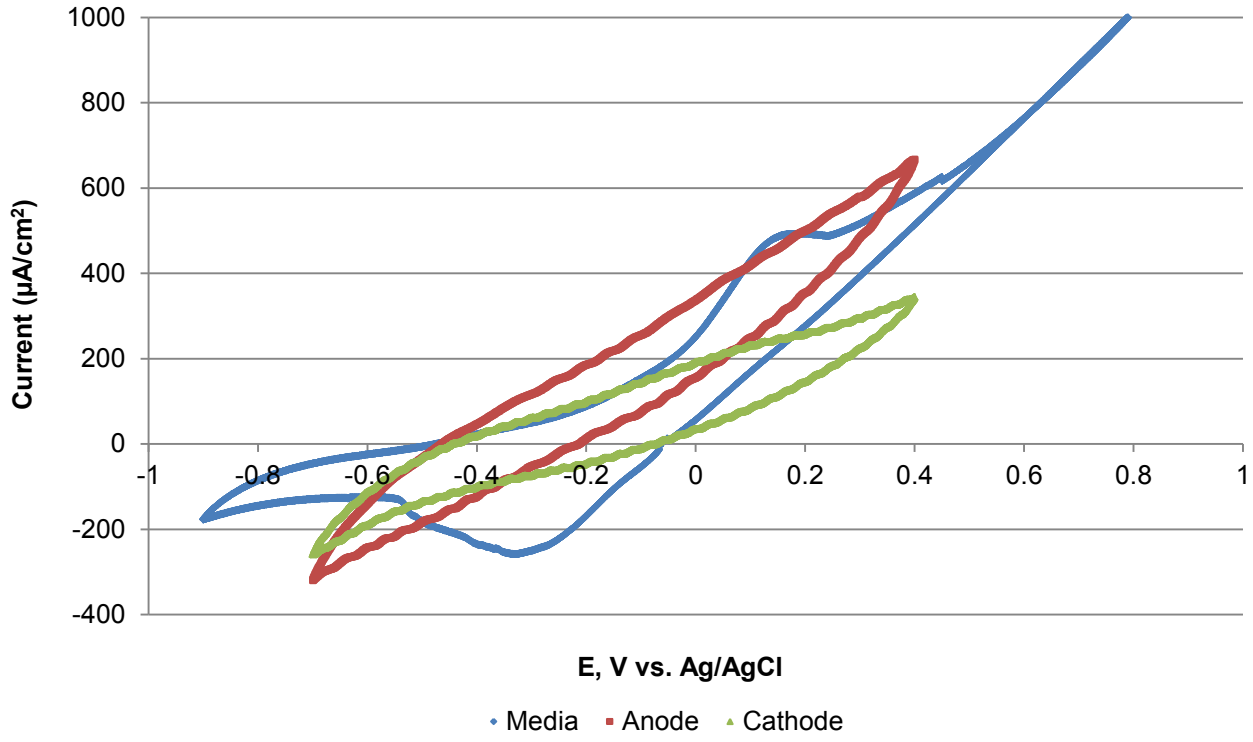

Figure 5-59: Cyclic voltammograms of the anode and cathode of a single-chambered MFC

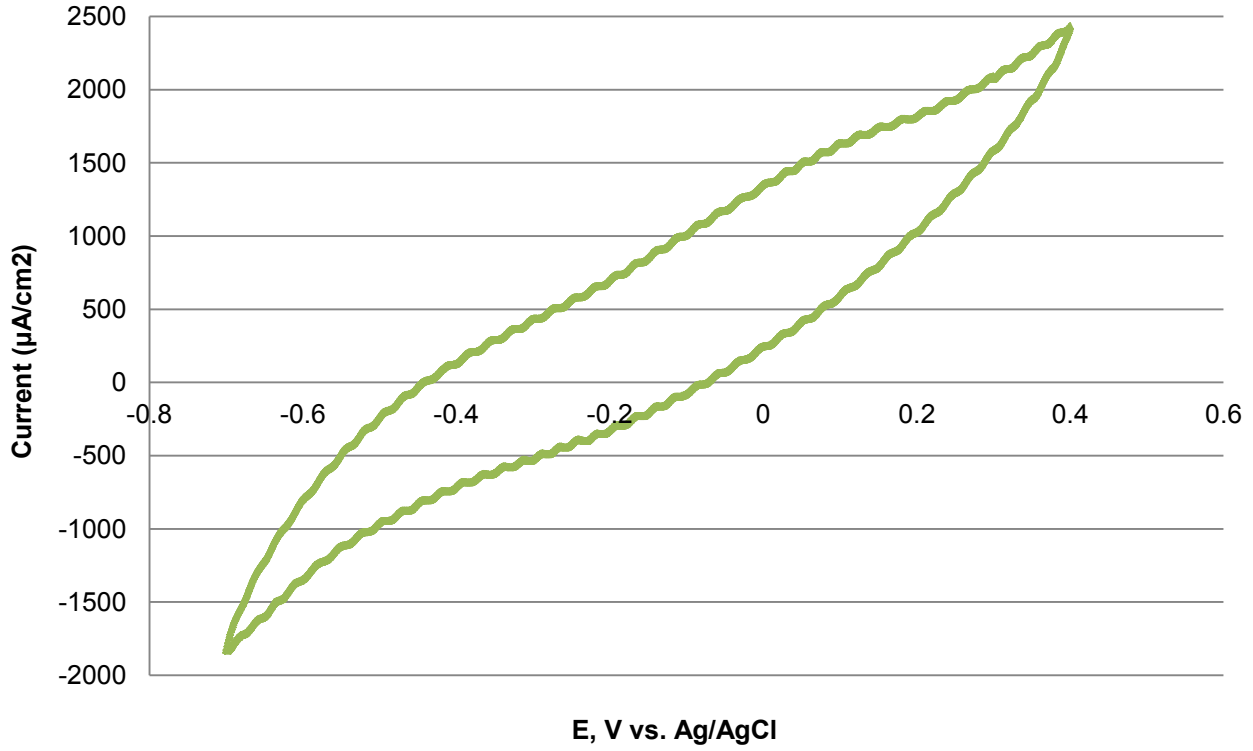

Figure 5-60: Cyclic voltammogram of cathode of a single-chambered MFC at a scan rate of 1 mV/s

5.4 DISCUSSION

5.4.1 Start-up of Single-Chambered MFCs

These experiments were conducted over several months. During this time, subtle changes in the microbial community of the stock culture are expected to have occurred, causing small changes in the inoculum community across experiments. MFC 1-3 were inoculated with the same inoculum. MFC 4 was inoculated at a different time. MFC 1-3 have similarly shaped potential difference peaks (Figure 5-1, Figure 5-2 and Figure 5-3). The peaks observed for MFC 4 (Figure 5-5 and Figure 5-6) differ. From day 30 until the end of the experiment, two peaks were observed in each feeding cycle. This may be due to a difference in the microbial communities in MFC1-3 and MFC 4.

As discussed in Section 2.8.2.5, electricity generation in a sulphate-fed MFC containing SRB and SOB is proposed to occur in one of two ways (Sangcharoen *et al*., 2015). The BSR by SRB either in the anodic biofilm or as planktonic cells, with concomitant oxidation of organic compounds produces sulphide. Sulphide is then either oxidised abiotically or by SOB to sulphur or polysulphide at the anode with concurrent electricity production. Organic compounds may also be removed by exoelectrogenic microorganisms (EEM) at the anode with concurrent electricity production. The initial spikes in potential difference noted in the first few days of most of the experiments in this study are likely due to the presence of sulphide in the inoculum.

When the single-chambered MFC is inoculated, the system is open and aerobic. Further, the absence of biofilm on the cathode facilitates oxygen diffusion through the cathode. This hinders electricity production. The chemical oxidation of sulphide is expected to be dominant at this point. The initial absence of sulphide in the spent media supports this.

All single-chambered MFC investigated with carbon felt anodes exhibited a slow increase in the maximum potential difference achieved for each feeding cycle and a lag phase before a regular pattern was observed. It is postulated that good colonisation of the MFC is needed before steady electricity production can take place.

Almost complete oxidation of substrate occurred for the first 12-16 days for MFC 1-3 (Figure 5-19, Figure 5-20, Figure 5-21, Figure 5-23). This substrate was likely used largely for cell growth. Once the electrodes were colonised, the substrate was used mainly for cell maintenance and sulphate reduction.

An initial decrease in COD and VFA concentration is also observed for MFC 4 (Figure 5-22 and Figure 5-23), MFC 5 (Figure 5-39 and Figure A 9), MFC-CFC and MFC-CFU (Figure 5-40, Figure 5-41 and Figure 5-42). The COD and VFA concentration decreased over the first 6 to 8 days for MFC 4 and 5 and for the first 3 days for the MFCs fed concentrated feed. However, the concentrations increased thereafter and no period of complete oxidation of substrate was noted as for MFC 1-3. The shortened colonisation period for the MFCs fed concentrated feed is most likely the result of more substrate being available for cell growth.

An initial colonisation period with gradually increasing potential was not observed for the MFC with the carbon microfibre brush anode. As can be seen from Figure 5-8, the potential difference increased from the time of inoculation. Over the first 10-15 days of the experiment a decrease in the concentration of VFAs and COD was observed (Figure 5-31 and Figure 5-32) which is likely due to the use of substrate for biomass growth for colonisation of the MFC. It is hypothesised that the planktonic cells are more readily captured onto microfibres due to improved contacting, allowing for faster colonisation. The higher surface area resulted in a larger number of cells being able to transfer electrons directly to the anode. The presence of microfibres in the system also possibly hindered the diffusion of oxygen into areas of the MFC chamber through the cathode as a result of its dense

packing. The system therefore remained more anaerobic than MFCs with carbon felt anodes and the oxidation of sulphide occurred more slowly resulting in broader potential difference peaks. The anaerobic nature of the MFC allowed for the generation of electricity to take place sooner as the unproductive aerobic metabolism of substrate was limited.

Decrease in Potential Difference with time

As can be seen from Figure 5-53, deposition of element sulphur occurred mainly on the anode electrode of the single-chambered MFCs. This is in keeping with the theory of sulphide oxidation to sulphur being an electricity producing reaction. As can be seen from the SEM images in Figure 5-54D and Figure 5-56A, bacteria with nanowires had colonised the anode and sulphur deposition occurred on top of the biofilm. Nanowires are suggestive of direct electron transfer from the cells to electrode. It is therefore likely that these bacteria were EEM.

Over time the thickness of the sulphur increases and limits the mass transfer of substrate to the bacteria in direct contact with the anode. The increased thickness of the sulphur layer is also likely to limit the transfer of electrons to the electrode by the sulphide oxidation reaction.

The deposition of sulphur and salt crystals on the cathode is also apparent in Figure 5-53. Over time this was likely to foul the platinum catalyst on the cathode and to reduce the rate of the reduction reaction with oxygen. This in conjunction with deposition on the anode ultimately results in the reduced electricity production with time. This was the case for most of the single-chambered MFCs investigated in this study.

5.4.2 Electrical Performance

As a result of the draw-and-fill feeding scheme of the MFCs, the residual concentration of substrate in the system changes considerably through a feeding cycle. The potential difference is a function of the concentration of substrate within the system and therefore the cycling in substrate concentration results in the cycling of potential difference. The cycle consists of the increase of potential when fresh medium is added until a maximum is reached, followed by a decrease in potential as substrate is used. This occurs for each feeding cycle. The constant change in potential difference makes plotting polarisation curves difficult. The time at which the polarisation curve is plotted in the feeding cycle affects the maximum potential difference achieved. The MFC must be given enough time to stabilise before the resistor in parallel with MFC can be changed. This often takes several hours. During this time the concentration of substrate in the MFC also changes

Sun *et al*. (2011) and Sangcharoen *et al*. (2015) both conducted studies on sulphidogenic systems in single-chambered MFCs with air cathodes. Sun *et al*. (2011) used a sulphide fed system which produced a maximum power density of 13 mW/m^2. The power density in the sulphate fed system investigated by Sangcharoen *et al*. (2015) varied significantly with time. It produced a maximum of 7.74 mW/m^2, 0.43 mW/m^2 and 14.4 mW/m^2 on days 13, 73 and 94 respectively. A maximum power density of 2.86 ± 0.009 mW/m^2 was achieved for the single-chambered MFCs with the carbon felt anode using standard medium (15 mM lactate and sulphate). This was comparable with that reported in literature. The internal resistance of the MFC with the carbon microfibre brush anode was considerably lower than that of the standard MFC with carbon felt anode (7720 Ω and 20600 Ω respectively). This may be a result of the reduced distance between the anode and the cathode. The shorter distance results in the improved transfer of protons between the electrodes and reduces ohmic losses and internal resistance. This trend has been noted in numerous studies (Jang *et al*., 2004; Ghangrekar & Shinde, 2007; Jiang & Li, 2009; Zhu *et al*., 2011).

The power density produced by the carbon fibre brush anode MFC (0.966 mW/m^2) was not improved over the carbon felt anode material. This may have been mainly a result of the time at which the power density curve was plotted. This was comparable with the maximum power density produced for

MFC 4 on day 44 of its operation (0.926 ± 0.057 mW/m^2). Over time, the internal resistance of the MFC increased as a result of mass transfer limitation arising from the deposition of elemental sulphur on the anode and the fouling of the platinum catalyst on the cathode, as well as decreased activity of SRB. A decrease in maximum power density with time has been noted in several studies (Chou *et al*., 2013; Chou *et al*., 2014; Dutta *et al*., 2008; Sangcharoen *et al*., 2015).

The narrow distance between the anode and cathode may have resulted in the aerobic oxidation of substrate as a result of oxygen diffusion from the cathode to the anode (Jiang & Li, 2009; Zhu *et al*., 2011). However, this was unlikely in this experiment as a result of the mature biofilm developed on the cathode. The same MFC with carbon fibre brush anode was researched by Logan *et al*. (2007) who found that power density improved with the brush anode compared to carbon cloth. The corresponding internal resistances were 8 Ω and 31 Ω for carbon fibre and carbon cloth respectively, a reduction of 74 %. The improvement in internal resistance achieved in these experiments with carbon fibre was 63%, comparable to that found by Logan *et al*. (2007). The considerably higher internal resistances found in these experiments are postulated to have resulted from cathode preparation and electrical circuit connects, as discussed in detail in Section 0.

An increase in the organic substrate did not result in a notable increase in the power density produced by a MFC with carbon felt anode (1.11 ± 0.004 and 1.87 ± 0.005 mW/m^2 on day 19 and 29 of operation of the connected MFC with concentrated feed respectively). While an increase in the COD loading has previously been reported to result in an increase in power density, in some cases a maximum in power density as a function of COD loading was observed (Rabaey *et al*., 2005; Wang *et al*., 2014). It is therefore possible that the COD concentration at which the maximum power density was achieved had been exceeded at a lactate concentration of 28 mM for this MFC and microbial community.

The overshooting phenomenon was observed for the polarisation curve plotted for the concentrated feed MFC on day 29 (Figure 5-14). Overshooting is thought to be as a result of several factors, namely: an underdeveloped biofilm, a sample rate which is too fast for the capabilities of the anodic biofilm, the introduction of toxic compounds to the system or the use of feedstock which is insufficient in terms of its organic loading or conductivity (Winfield *et al*., 2011). In this experiment the biofilm was well developed as a result of the extended period of operation. The feedstock was also more concentrated than in previous experiments and believed to have sufficient organic loading and conductivity. It was therefore possible that either the sampling rate was too fast or the concentration of sulphide, which was considered to be the most toxic component in the system, was high at the time at which the curve was plotted. The sulphide concentration was approximately 94 mg/ℓ at the time at which the curve was plotted (Figure 5-38). This concentration was much higher than any other single-chambered MFC during normal operation and could therefore have caused the overshooting phenomenon observed in the polarisation curve.

The internal resistance on day 16 of the MFC fed concentrated feed (26900 Ω), was comparable to that of the other MFCs operated with carbon felt anodes. The decreased internal resistance from day 16 to 29 (9000 Ω) may have resulted from improved biofilm development and the increased feed concentration. The concentrated feed has been reported to increase the conductivity of the solution and therefore decrease the internal resistance of the MFC (Jiang & Li, 2009; Wang *et al*., 2014).

5.4.3 Substrate Utilisation

It is assumed that both complete and incomplete SRB oxidisers are present in the microbial community. In addition, methanogenic bacteria (MB) and fermentative bacteria (FB) are prolific in wastewater treatment systems and could have been present in the stock cultures used as the inoculum for the MFCs. The MB and FB compete actively for substrate with the SRB and play a role

in the performance of the MFC in terms of both its electricity production as well as its ability to treat the sulphate-rich wastewater (Lens *et al*., 1998).

As discussed in Section 2.8.2.1, higher rates of BSR and substrate utilisation are exhibited when lactate is used as a substrate in mixed SRB communities (Postgate 1984; Purdy *et al*., 1997; Brandt *et al*., 2001; Kuo & Shu, 2004). The rate of oxidation of lactate is therefore faster than the rate of utilisation of acetate produced. The regular addition of lactate feed is likely to favour partial oxidation. The concentration of lactate in the spent medium decreased in all experiments over the first few days after inoculation and remained very low for the remainder of the experiment, illustrating effective lactate utilisation.

The use of lactate as a substrate results in either carbonate as a product of complete oxidation or acetate as a product of partial oxidation by SRB. Some SRB have the ability to use fermentative pathways in sulphate limiting conditions resulting in the production of propionate (Heimann *et al*., 2005). Further, fermentative bacteria may compete with SRB under these conditions. The sulphate concentration remained above 500 mg/ℓ in all experiments and was unlikely to be limiting. The presence of propionate and other VFAs was therefore most likely as a result of FB, since sulphate and lactate were added in stoichiometric ratio.

When the draw and fill volume of 10 mℓ was used for the MFC, it resulted in a pulse equivalent to a concentration of approximately 5 mM (10 mM for the concentrated feed) being added to the bulk liquid. However, as a result of the un-metabolised organics in the solution remaining in the MFC, the concentration of organics in the bulk liquid was above 5 mM after feeding. The feeding scheme was such that over time the acetate concentration in the MFC at the end of a feeding cycle would tend towards the pseudo steady state concentration of acetate remaining after conversion of the lactate in the feed (between 0 and 5 mM) under constant operation. Conversely, the concentration of acetate in the spent medium was observed to increase with time for all of the experiments conducted in the single-chambered MFC. This may indicate a decrease in complete oxidation or increased partial oxidation of lactate by SRB, or an increase in fermentation of lactate or decrease in the utilisation of lactate by FB.

An increase in propionate results from increased fermentation and is coupled to a decrease in activity of SRB and SOB, owing to reduced availability of organic substrate, with a concomitant decrease in electricity generation. As can be seen from the VFA concentration as a function of time for MFCs 1-3 (Figure 5-19, Figure 5-20 and Figure 5-21), there was an increase in the concentration of propionate in the MFCs. A decrease in propionate concentration for MFC 1 was followed by improved potential difference over the cell (Figure 5-1).

The concentration of propionate and acetate were observed to increase for the first 14 -18 days for MFC 4 (Figure 5-22), suggesting the presence of fermenters or incomplete oxidisers. Thereafter a decrease in the concentration of both acetate and propionate was observed until day 30. On day 30 the resistor in parallel with the MFC was changed from 100 kΩ to 10 kΩ. Thereafter the propionate concentration remained low (0-200mg/ℓ) for the remainder of the experiment. The use of a smaller resistor in effect requires the MFC to produce more electricity (in the form of current). It is likely that this favours the electrogenic microorganisms and supresses the action of fermenters. The acetate concentration increased after day 30 until day 45 where it remained constant between 1000-1200 mg/ℓ for the remainder of the experiment. The increase in acetate coupled with the decrease in propionate suggested an increase in the partial oxidation of lactate by SRB. This increased activity is accounted for the change of resistor.

MFC 3 also exhibited a change in propionate concentration with a change in resistor. The propionate concentration in MFC 3 remained very low (less than 20 mg/ℓ) for the first 16 days of the experiment (Figure 5-21). Between days 11 and 16 a 10 kΩ resistor was in parallel with the MFC. This was

changed for a 100 kΩ resistor on day 16. An immediate increase in propionate concentration was observed. It is possible that the activity of the fermenters was supressed at 10 kΩ but was able to compete with the SRB at 100 kΩ. The concentration of propionate remained high for the remainder of the experiment (between 600-800 mg/ℓ). The maximum potential difference over the MFC did not recover to the same potential difference which was observed before the changing of the resistors (Figure 5-3) when no propionate was present. The MFC produced current steadily for the remainder of its operation. The propionate concentration did not rise as high as for MFC 1 and 2 (maximum concentrations of approximately 1100 and 1380 mg/ℓ respectively). It is thought that the activity of FB remained low enough in MFC 3 to ensure its prolonged current generation whereas fermenters potentially outcompeted the SRB in MFC 1 and 2 for lactate. Dissolved sulphide was only present in notable concentrations for MFC 3 (Figure 5-17) indicating that the SRB are more active in that MFC.

As discussed in Section 2.8.2, acetate utilising SRB have been shown to have higher growth rates than acetate utilising MB. The SRB also gain more energy from the consumption of acetate than MB, both of which give them an advantage over the MB (Oude Elferink *et al*., 1994; Lens *et al*., 1998). However, it has been suggested that MB have a better capacity for attachment than SRB (Omil *et al*., 1996). As a result of their better attachment abilities, it is likely that MB attach first to the carbon paper electrodes in the MFCs making it harder for SRB to attach. This coupled with removal of 10 mℓ of liquid when the MFC is fed could result in the gradual wash out of the SRBs from the system. MB may therefore outcompete the SRB if a system variable is changed which favours them or aids washout of SRB.

As can be seen from the profile of VFAs as a function of time for the single-chambered MFC with the carbon microfibre brush anode (Figure 5-31), an increase in the propionate concentration was observed after day 35. This corresponded to an increase in the concentration of the feed on day 35. The additional feed available to fermenters in the MFC is likely to have resulted in an increase in their activity. An increase in potential difference is expected for an increase in the concentration of feed. This was observed for MFC 5 (Figure 5-10). However, a slow decrease of potential difference with time was observed for the MFC-CBA (Figure 5-8). It is likely that the increased activity of the fermenters outweighed the increase in lactate concentration available to the SRB and SOB community for electricity generation. It is also possible that the surface area of the brush anode was such that the anodic reaction was improved to a point that the reduction reaction at the cathode was limiting. Further improvement of the anode reaction therefore did not improve electricity generation. This is discussed further below.

MFC 5 exhibited a similar increase in propionate concentration after the feed was altered to be more concentrated on day 37 of its operation (Figure 5-39). This corresponded to an increase in both acetate concentration and potential difference (Figure 5-10). The calculated acetate concentration arising from BSR demonstrated an identical increase after the change in feed concentration on day 37 (Figure A 8). It is therefore likely that both an increase in SRB and fermentative activity occurred. The fraction of total acetate which was made up of acetate from BSR decreased gradually over time after day 37. It is possible that, although SRB were able to outcompete fermenters and improve electricity generation, the increased availability of substrate allowed FB to compete more actively.

The concentration of propionate in the MFC with concentrated feed and connected in circuit with a resistor (MFC-CFC) increased for the first 10 days of the experiment to a maximum concentration of approximately 1060 mg/ℓ (Figure 5-40). It then decreased for the remainder of the experiment. The decrease corresponded to an increase in the potential difference over the MFC (Figure 5-12). This is in agreement with the theory of the increased activity of fermenters affecting the power generation of the MFC.

The sulphide concentration of the spent medium for all MFCs remained low for the duration of the experiment (typically lower than 30 mg/ℓ). As is mentioned above, the oxidation of sulphide either

abiotically or by SOB to sulphur or polysulphide is an electricity-producing reaction (Lee *et al*., 2014; Sangcharoen *et al*., 2015). The decrease in sulphate concentration in the effluent with respect to the feed indicated that sulphate reduction was occurring. This was found for all of the MFCs: MFC 1-5 (Figure 5-15, Figure 5-16 and Figure 5-35), MFC-CBA (Figure 5-29) and the MFCs fed concentrated feed MFC-CFC (Figure 5-37). The absence of sulphide is therefore likely as a result of it being oxidised to elemental sulphur.

pH and Redox

The pH of the inoculum was generally in the range of pH 8-9. It had residual sulphate and was high in bicarbonate as a result of biological sulphate and therefore fairly basic. The redox potential was very low as a result of the stock culture being anoxic and having a high sulphide concentration (Postgate, 1984). Over time the pH of the MFC decreased and stabilised around pH 7 for the remainder of the experiment. This is true of all MFCs tested except MFC 4. Data are only available from day 14 to 54 however over this time the pH increased.

A decrease in pH was coupled with an increase in the redox potential of the spent medium. All of the MFCs remained in the region of -330 mV to -370 mV for the bulk of the experiment. SRB require a redox potential below -200 mV for growth (Postgate, 1984) and are therefore likely to be active in the MFCs. Data for MFC 4 are only available from day 14 to 54 (Figure 5-47). This corresponded to a decrease in the redox potential for the same time period (Figure 5-48).

5.5 CONCLUSIONS

The microbial community, similar to that present in the LFCR, was capable of electricity generation and produced a maximum power density of 2.86 ± 0.009 mW/m^2 of anode area in the single-chambered MFC with a carbon felt anode. Hence an integrated LFCR-MFC is likely to produce electricity. The shortfalls associated with the construction of the single-chambered MFC are discussed in Section 4.4.1. It was concluded that the single-chambered MFC as constructed and operated in these experiments was producing only 18.6% of the power density reported in literature when *S. oneidensis* MR-1 was used to test it. Taking this into account the maximum power density could potentially be improved to approximately 15.3 mW/m^2 in a sulphidogenic system if the method of cathode preparation and electrical connection was improved. This is comparable with the power density reported by Sangcharoen *et al*. (2015) for a similar system (14.4 mW/m^2).

A power density of 0.996 ± 0.002 mW/m^2 was produced by the MFC with a carbon fibre brush anode. The use of the brush anode resulted in significant reduction of internal resistance and more stable potential difference. The potential difference was not improved by changing the feed concentration in the MFC with a carbon fibre brush anode but did improve in a MFC with felt anode.

Deposition of sulphur on both the anode from the electricity producing sulphide oxidation reaction and the chemical sulphide oxidation reaction at the cathode was observed. This was a challenge in long term electricity generation as a result of the mass transfer limitations of substances to and from the electrodes which arose. Deactivation of the catalyst coating on the cathode also occurred.

The presence of propionate in the spent medium is indicative of the presence of the fermentative bacteria in the microbial community which compete actively with the SRB and SOB for lactate. This competition negatively affects the electricity production by the MFC. Altering system variables which favour the SRB over the FB may improve electricity production. The use of a smaller resistor in the external circuit favoured the microorganisms which made use of the anode as an electron acceptor and therefore favoured the SRB and SOB community.

Cyclic voltammetry revealed that electricity production in the MFC may be contributed to both by mobile cell-membrane associated mediators and by the direct electron transfer in the biofilm. Electrogenic bacteria with nanowires growing in both the anodic and cathodic biofilms were observed with SEM which confirmed that direct electron transfer occurred.

6 PERFOMANCE OF THE INTEGRATED LINEAR FLOW CHANNEL REACTOR – MICROBIAL FUEL CELL (LFCR-MFC)

6.1 INTRODUCTION

This chapter details the investigation into the operation of an integrated linear flow channel reactor and microbial fuel cell system (LFCR-MFC). The original LFCR was designed for combined biological sulphide reduction and sulphide oxidation to yield a sulphur product (van Hille *et al*., 2015). The overall aim of this study is to incorporate the elements of a MFC into the LFCR, in order to create an integrated system which functions as both a wastewater treatment reactor and a MFC.

The LFCR makes use of a combination of BSR in the bulk liquid and biological sulphide oxidation in a floating sulphur biofilm (FSB). The FSB forms on the surface of the reactor where the air-liquid interface has both sufficient nutrients and a controlled oxygen supply required by the aerobic SOB (Mooruth, 2011). Both microbial and abiotic sulphide oxidation can occur simultaneously within the biofilm as a result of the complex redox conditions within the reactor and biofilm (Mooruth, 2011). In the oxygen limited conditions, sulphur is the major product of bacterial sulphide oxidation (Janssen *et al*., 1997; Janssen *et al*., 1998). The biofilm also acts as a barrier which limits the mass transfer of oxygen into the bulk liquid at the surface of the reactor and therefore ensures the correct sulphide to oxygen ratio for sulphur formation (Mooruth, 2011). The anaerobic environment necessary in the bulk liquid for effective BSR is maintained.

LFCRs have been researched in CeBER at a scale of 2.1, 8.0 and 24 litres (Mooruth, 2011; van Hille *et al*., 2015). The smallest laboratory scale LFCR in question is a Perspex reactor which has a working volume of 2.125 ℓ. It is rectangular with the dimensions 0.1 m wide, 0.25 m long and 0.15 m high. There is an inlet and outlet port at each end of the reactor 95 mm and 85 mm from the base respectively. The LFCR uses a mesh catchment device placed just below the surface of the reactor to collect the biofilm when it becomes too thick and collapses. Carbon microfibers are submerged in the bulk liquid of the reactor to provide a large surface area for bacterial adhesion and achieve a high cell concentration from improved efficiency of sulphate reduction.

SRB and SOB have been shown to have the ability to use carbon electrodes as external electron acceptors and therefore produce electricity in MFCs, discussed in detail in Section 2.8.2.5 and demonstrated in Chapter 5. The potential for an integrated MFC waste treatment system was therefore presented in which the carbon fibres could function as the anode electrode and the LFCR could be altered to include a cathode and therefore function as both a wastewater treatment reactor and a MFC.

The design and operation of the LFCR was reviewed and a new design was developed to include improved connection of the carbon microfibres to an external circuit and the addition of two cathode electrodes. The volume was also reduced to 935 mℓ. The design of the integrated LFCR-MFC is given in detail in Section 3.3.1. The integrated system was operated under the same conditions as used for the LFCR.

The specific objectives of the research presented in this chapter were as follows:

1. To operate the LFCR-MFC using the same conditions as van Hille *et al*. (2015) to test its functioning as both a microbial fuel cell and as a reactor treating sulphate-rich wastewater.

2. To determine key operating variable of the LFCR-MFC and define the further research that should be conducted on the LFCR-MFC for its improved operation.

6.2 EXPERIMENTAL APPROCAH

6.2.1 Data Collection

This investigation establishes a base case for conversion of sulphate to sulphur and electricity production by the integrated reactor which was investigated with a feed containing 10 mM lactate and sulphate at a flow rate of 0.167 mℓ/min, corresponding to a residence time of four days. The detailed experimental procedure used is given in Section 3.3. The potential difference over the LFCR-MFC in parallel with a resistor was monitored throughout the experiment. Samples were analysed for sulphate, sulphide, COD and volatile fatty acids.

Samples were taken from five points of the reactor at each sampling time: namely, top left, bottom left, top right, bottom right sample points and the effluent. Samples were not analysed in triplicate as a result of the resources and time necessary to do so. However, reproducibility of assays was already established in earlier experiments (Section 5.3.2). Further, by taking five samples at each sampling time, sufficient data were generated for confidence to be established in component concentrations within the reactor. Sulphate concentration for this set of experiments was determined through the turbidimetric barium sulphate assay. All raw data is presented in Appendix A and Appendix D.

Additional experiments were conducted for this study in order to gain insight into the novel system and are as follows:

1. In order to gather insight into its mixing profile, a hydrodynamic study was performed on the LFCR-MFC, the details of which are given in Section 3.3.2.. A hydrodynamic study performed by van Hille *et al*. (2011) on a 23.5 ℓ LFCR revealed that no turbulent mixing took place and that partitioning of the solution into stagnant and mobile zones occurred. The mixing profile in the modified LFCR-MFC is likely to demonstrate similar patterns to that of the LFCR investigated by van Hille *et al*. (2011) and Marais (unpublished data for 2.125 ℓ system).
2. Cyclic voltammetry (CV) was conducted on fresh abiotic media, spent abiotic media, planktonic cells in media, the anode electrode in fresh media and the LFCR-MFC itself in order to decouple the contribution by planktonic cells and cells in the biofilm to electricity generation. Details of the procedure used are given in Section 3.4.3.

6.2.2 Data Handling

Calculations performed to determine power density are given in Section 4.2.2. Calculations for the balancing of VFAs are given in Section D.2.

6.2.2.1 Coulombic Efficiency Calculation

Voltage (V) was measured at one minute intervals and recorded in millivolts for the duration of the experiment. Current (I) in amps was calculated using voltage and resistance with Ohm's law and converting millivolts to volts (Equation 14).

The difference in COD concentration between the feed and the effluent at the sampling time was calculated. The value of the COD for the feed and effluent medium was obtained by a COD assay as described in Section 3.5.1.3.

$$\Delta COD = COD_{feed} - COD_{effluent} \qquad \text{Equation 24}$$

The coulombic efficiency (E_c) is calculated by Equation 26:

$$E_c = \frac{MI}{Fbv\Delta COD}$$ Equation 25

where M is the molar mass of oxygen (32 g/mol), t_b is s run time of the experiment, F is Faraday's constant (96485.34 C/mol), b is number of electrons exchanged per mole of oxygen (4), v is volumetric flow rate of feed (m^3/s) and ΔCOD is difference in COD between influent and effluent (g/m^3).

The current (I) is taken as the average current between the two sampling times (t_0 and t_i).

$$I \cong \frac{\sum_{i=0}^{ti} I_i}{i}$$ Equation 26

6.2.2.2 Sulphur Species Balance Calculations

The theoretical sulphide concentration ($H_{Theoretical}$) was determined by assuming the sulphate used was converted to sulphide (Equation 29). The average sulphate usage (S_{Usage}) was calculated by determining the difference between the concentration of sulphate in the incoming feed (S_{Feed}) and the average sulphate concentration ($S_{Average}$) throughout the reactor (Equation 28). Average sulphate concentration was determined as the average of the concentrations between the five sampling areas of the reactor (Equation 27).

$$S_{Average} = \frac{S_{TL}+S_{BL}+S_{TR}+S_{BR}+S_E}{5}$$ Equation 27

$$S_{Usage} = S_{Feed} - S_{Average}$$ Equation 28

$$H_{Theoretical} = \frac{S_{Average}}{M_{Sulphate}} \times M_{Sulphide}$$ Equation 29

where S_{TL}, S_{BL}, S_{TR}, S_{BR} and S_E are the sulphate concentrations of the samples taken from the top left, bottom left, top right, bottom right ports and effluent respectively.

Seeding of the LFCR-MFC was stopped on day 19 on the experiment. As a result of the seeding the sulphate concentration within the reactor was higher than that of the feed medium. This is discussed in detail in Section 6.3.3.1. From day 19 onwards the concentration in the reactor dropped both as a result of dilution by incoming feed and BSR. The calculations for sulphate usage were therefore adjusted.

The concentration of sulphate expected in the reactor effluent on a given day (S_i) if dilution was the only method of sulphate removal was calculated as follows: The average sulphate concentration in the reactor was calculated on day 19 of the experiment (S_{19}) using Equation 28. This was used as the starting concentration for the dilution series. The equations below are given in terms of "i" where "i" is an integer between 20 and 31. The amount of sulphate washed out of the reactor over a 24 hour day ($S_{removed,i}$) was calculated (Equation 30). The sulphate concentration on a given day (between 20-31) (Si) as a result of BSR only is calculated by Equation 31.

$$S_{Removed,i} = F \times (S_{i-1} - S_{Feed}) \times 24 \qquad i \in [20,63]$$ Equation 30

$$S_i = S_{i-1} - S_{Removed,i}$$ Equation 31

where F is the flowrate at a 4 day residence time (ℓ/h).

The concentration S_i tended to the concentration of the feed (1 g/ℓ). This was achieved by day 30. Therefore between day 19 and 30, the sulphate used within the reactor was calculated as follows: The sulphate reduction occurring at a particular area or port in LFCR-MFC on a particular day ($S_{Usage,i}$) was determined by Equation 32.

$$S_{Usage,i} = (S_{Feed} - S_i)$$ Equation 32

6.3 RESULTS

6.3.1 Hydrodynamic Study

A hydrodynamic study was conducted on the LFCR-MFC at three different residence times: 1, 2 and 4 days. Similar mixing patterns were observed for all three conditions. As incoming feed entered the reactor it sank to the bottom and displaced the bottom layer of liquid in the reactor (Figure 6-1, Figure 6-2 and Figure 6-3). Some short circuiting of the feed across the top of the reactor occurred, visually demonstrated from the clearing of the liquid on the surface of the reactor. Diffusion appeared to take place from both the top and bottom liquid layers into the stagnant liquid in the middle of the reactor. The liquid in the centre of the reactor mixed fastest from the inlet to the outlet. The last liquid element to mix was in the middle layer of liquid on the right hand side just below the outlet.

Table 6-1 gives the mixing times of the reactor at the various flow rates investigated. The mixing time in this study is defined as the time necessary for the entire liquid contents of the reactor to become transparent. The mixing times at a 1 and 2 day residence time were approximately 84 minutes and 145 minutes respectively. The residence time used in the biological experiments was four days (flow rate of 0.167 mℓ/min). The reactor was found to have mixed completely within five hours. If short cutting of feed across the reactor had not occurred, the mixing time may have been reduced by increased displacement of the bottom liquid by incoming feed as opposed to loss of feed in the effluent. There were definite concentrations gradients within the reactor. The liquid in the centre at the same level as the top right and top left sampling ports was poorly mixed and remained in the reactor for the longest time. As a result of the short circuiting of feed, the effluent in the biological experiments was likely to contain higher quantities of un-oxidised lactate and unreduced sulphate than normally expected.

Table 6-1: Results of hydrodynamic study on the LFCR-MFC showing mixing times at various flow rates

Residence Time (Days)	Flow Rate (mℓ/min)	Mixing Time (mins)
1	0.667	84 ± 6.6
2	0.334	145 ± 3.8
4	0.167	302 ± 10.1

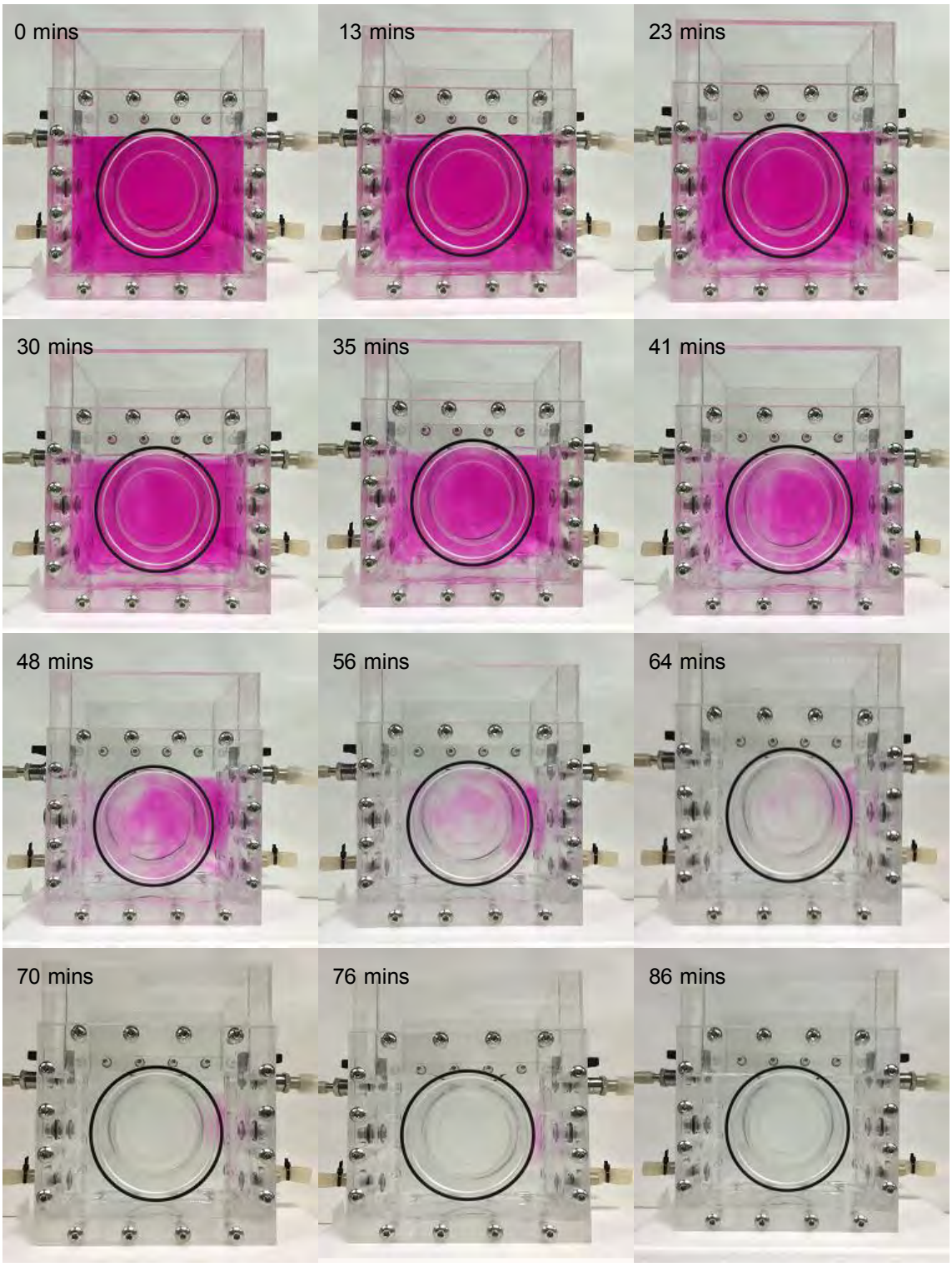

Figure 6-1: Hydrodynamic study conducted on the LFCR-MFC conducted at a 1 day residence time. Influent enters at the top port on the left of the reactor.

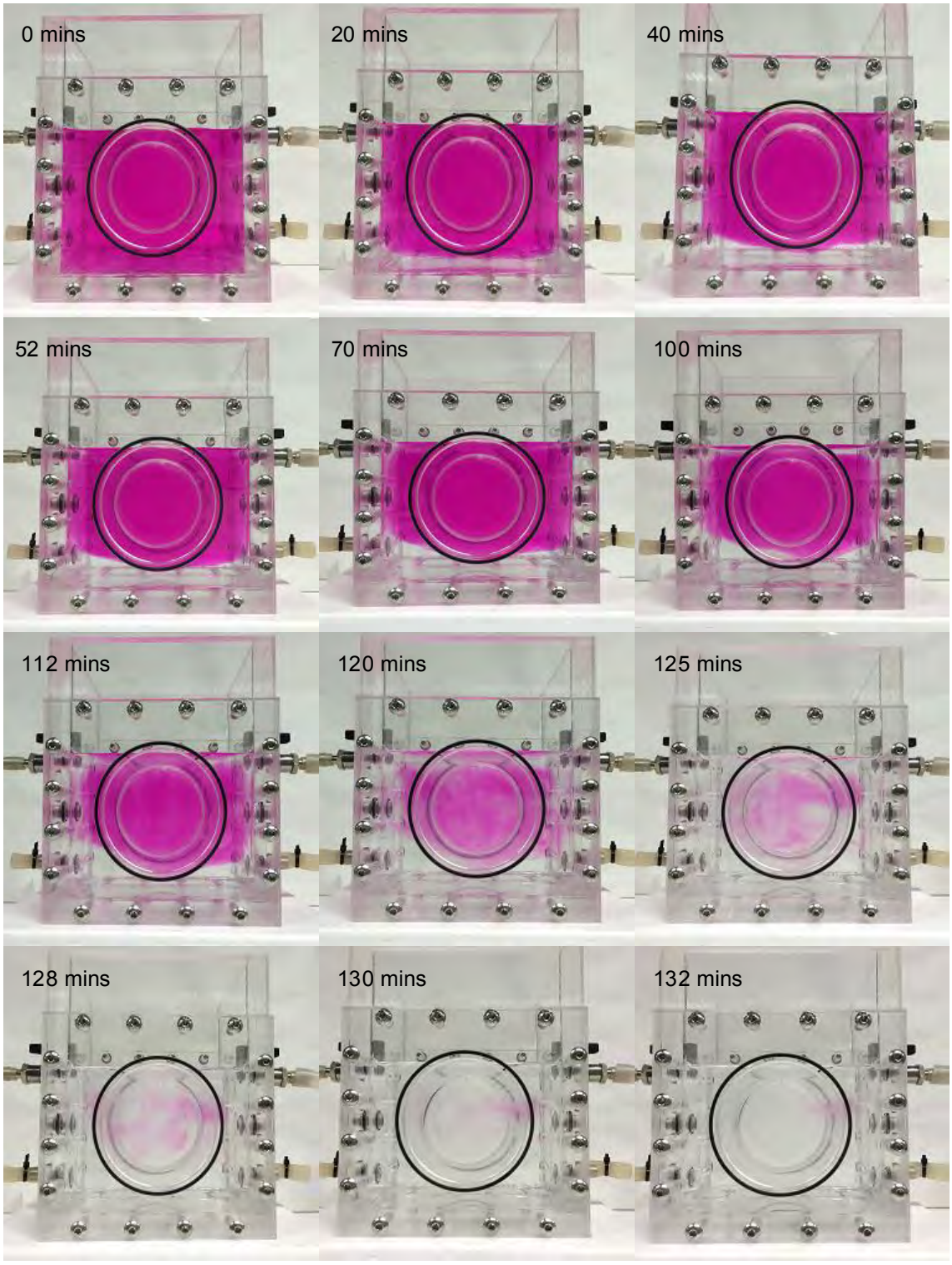

Figure 6-2: Hydrodynamic study conducted on the LFCR-MFC conducted at a 2 day residence time. Influent enters at the top port on the left of the reactor.

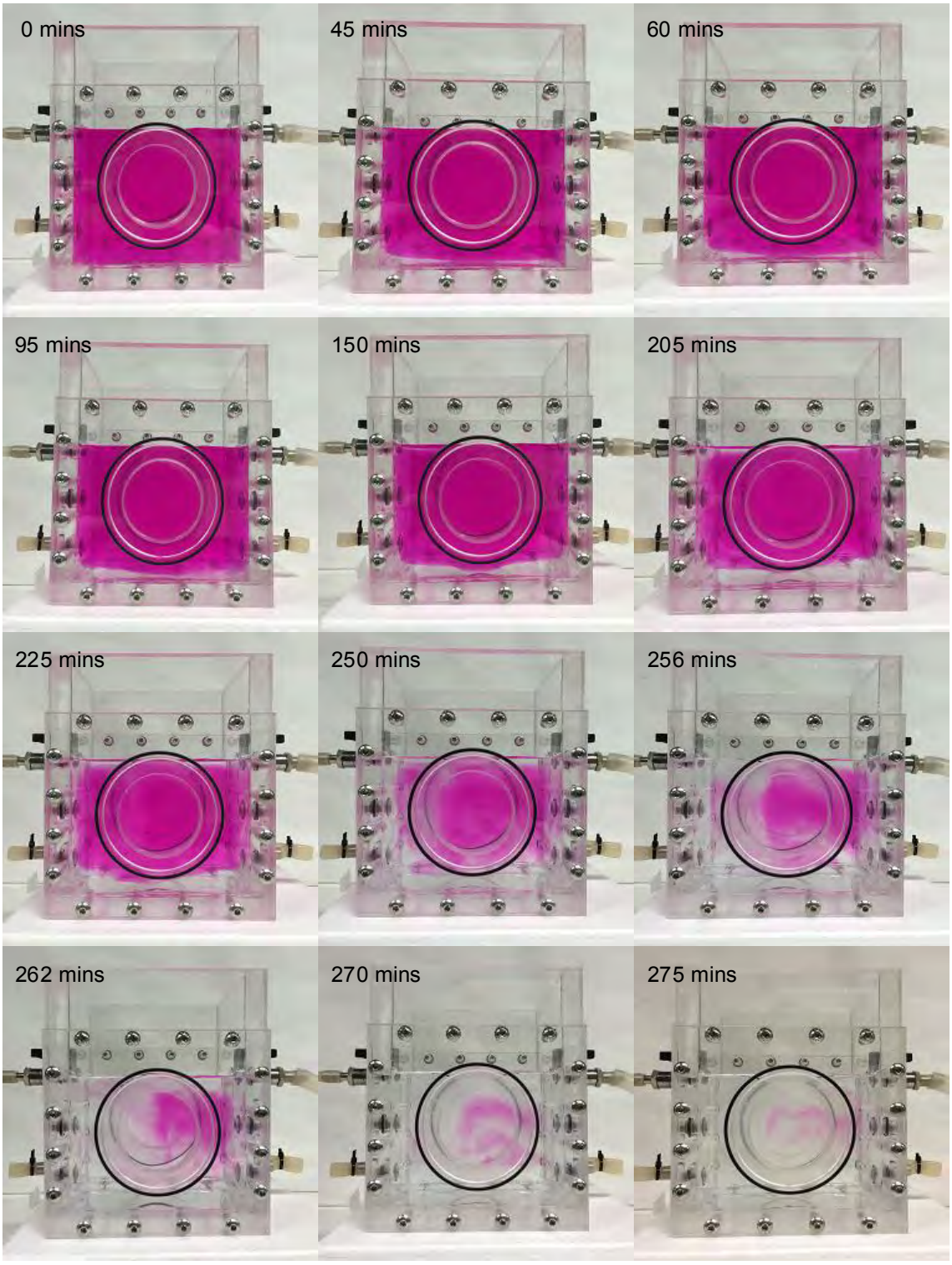

Figure 6-3: Hydrodynamic study conducted on the LFCR-MFC conducted at a 4 day residence time. Influent enters at the top port on the left of the reactor.

6.3.2 Electrical Performance

After inoculation and commencement of continuous operation at a 4 day residence time with a 10 mM feed concentration (lactate and sulphate), the potential difference over the LFCR-MFC increased rapidly before reaching a maximum on the 4th day at almost 450 mV. Thereafter, it decreased gradually before remaining fairly stable around 200 mV from day 19 to day 43 (Figure 6-4). This corresponded to the seeding of the reactor which was stopped after day 19. On day 43 the FSB began to collapse and collapsed fully on day 46, sinking to the bottom of the reactor. The potential difference remained between 100-150 mV between day 45 and 55.

On day 34 of the experiment, once the potential difference had stabilised at 200mV, a polarisation curve was plotted as described in Section 3.4.2. A maximum power density of 2.56 ± 0.005 mW/m^2 of cathode area (9.10 ± 0.017 mW/m^3) was achieved using a 1 kΩ resistor. The gradient of the curve of potential difference as a function of time for the LFCR-MFC (Figure 6-5) revealed that the internal resistance of the MFC was approximately 980 ± 118 Ω.

Potential difference data are only available until day 55 of the experiment as a result of the reactor being disconnected from the data logger and computer to perform cyclic voltammetry on the system. The sampling of the reactor was continued until day 63.

Figure 6-4: Potential difference as a function of time for the LFCR-MFC in parallel with a 10kΩ resistor and fed 10mM lactate

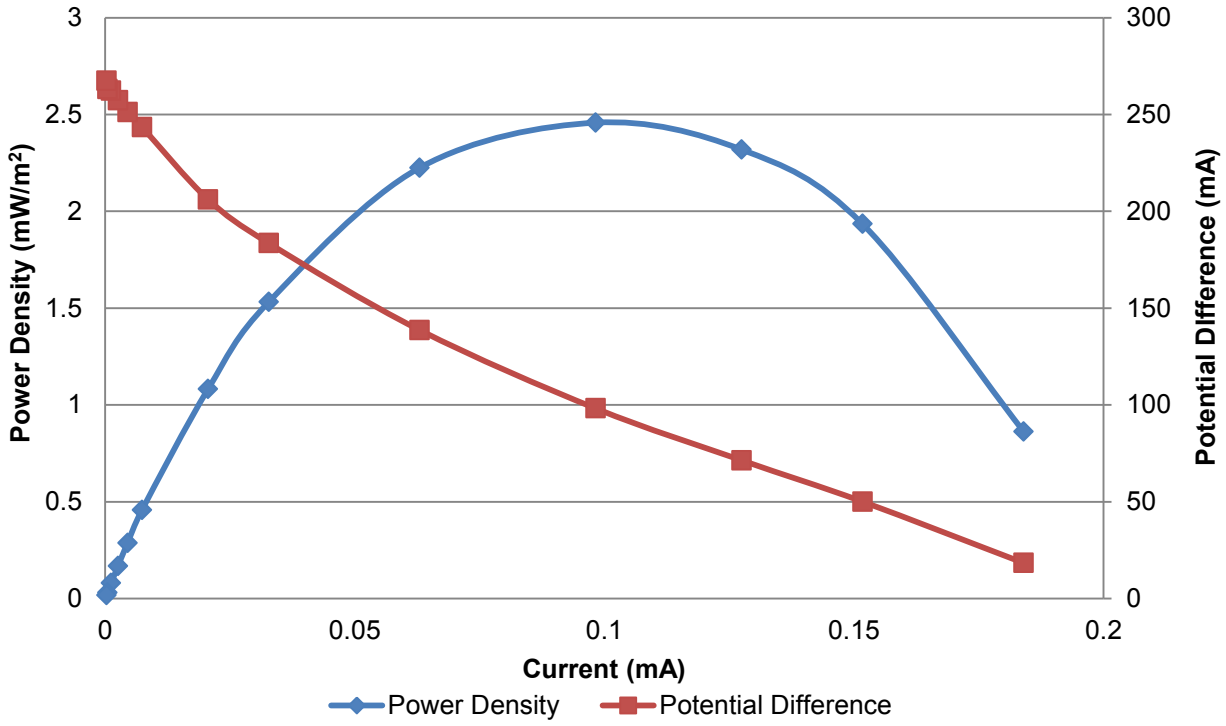

Figure 6-5: Power density and potential difference as a function of current for the LFCR-MFC fed 10mM lactate

6.3.3 Substrate Utilisation

6.3.3.1 Concentration of Sulphur Species

The sulphate concentration in solution was initially higher than that of the feed (1 g/ℓ) as a result of the seeding of the reactor with effluent from another LFCR containing residual sulphate above 1 g/ℓ. After day 19, from which point the reactor was no longer seeded, the sulphate concentration decreased across all sample points and trends in sulphate concentration became evident (Figure 6-6). The sulphate concentration in the bulk liquid decreased from between 1500-2000 mg/ℓ to between 500-1000 mg/ℓ where it remained for the last 30 days of operation.

The collapse of the FSB occurred on day 46. Between day 19 and 46, i.e. before collapse of the FSB, the sulphate concentration was most frequently higher in the lower level of the reactor, with the bottom right corner having the highest sulphate concentration. The top left and right corners of the reactor were found to have very similar sulphate concentrations. After day 46 the top level of the reactor had a slightly higher concentration of sulphate than the lower levels, owing to oxygen availability. A minimum in sulphate concentration of around 450-700 mg/ℓ was observed for the reactor on approximately day 46-50. From approximately day 50 until the end of the experiment, the sulphate concentration increased slightly throughout the reactor.

In addition to the decrease in residual sulphate concentration to below the feed concentration, the measured sulphide concentration provides evidence of sulphate reduction within the system. After day 19, trends in sulphide concentrations also formed (Figure 6-7). The concentration of sulphide in the lower level of the reactor was consistently higher than that of the levels above it. The bottom left corner of the reactor was found most frequently to have the highest concentration of sulphide, followed by the bottom right hand corner. The top left corner also had a higher concentration than the top right corner. Medium was fed on the left hand side of the reactor. The concentration of sulphide in the effluent was consistently low (approximately 20-30 mg/ℓ) compared to the sulphide concentration

in the reactor (50 – 150 mg/ℓ). In the last 30 days of the experiment, the sulphide concentration remained reasonably consistent between 50-100 mg/ℓ.

The theoretical sulphide concentration in the reactor was calculated by determining the average sulphate usage in the reactor and assuming all sulphate was converted to hydrogen sulphide (HS^-) ions. This and the average measured sulphide concentration in the reactor are plotted against time in Figure 6-8. The calculated theoretical sulphide concentration was mostly higher than that of the average measured sulphide concentration throughout the reactor i.e. there was less sulphide present than expected from the amount of sulphate reduced. Data are only shown from day 20 onwards, as the concentration of sulphur species in the seeded liquid was not measured and therefore a sulphur balance could not be completed.

The propionate concentration was used to determine the concentration of acetate as a result of BSR. This acetate concentration was used to calculate the amount of sulphate reduced by partial oxidation and therefore the concentration of sulphate which should theoretically be present in the reactor. This sulphate concentration as a function of time is given by Figure 6-9. Data are shown from day 20 onwards, however dilution occurred after seeding until day 32. After day 32 the reactor was thought to have reached a pseudo steady state. The predicted sulphate concentration after day 32 was very similar to the measured sulphate concentration (Figure 6-6). The top right and top left hand points of the reactor most closely represented the measured concertation.

Figure 6-6: Sulphate concentration as a function of time for the LFCR-MFC in parallel with a 10 kΩ resistor and fed 10mM lactate

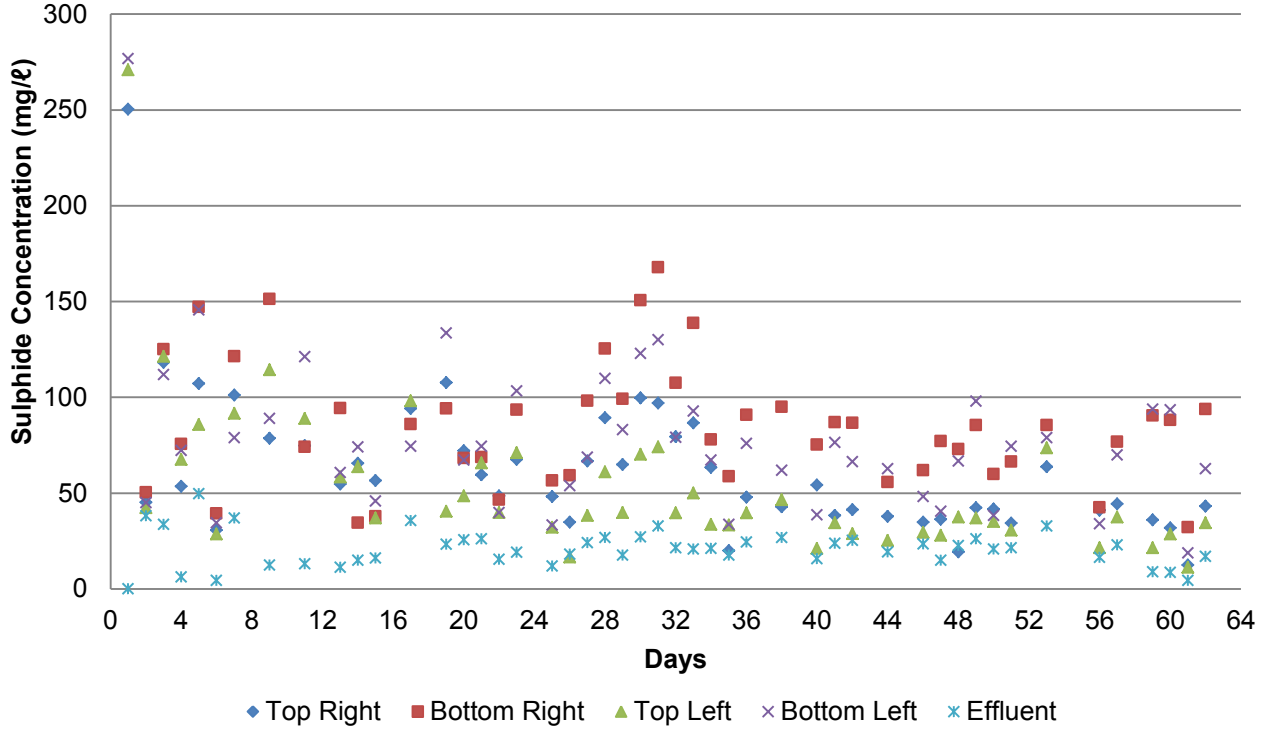

Figure 6-7: Sulphide concentration as a function of time for the LFCR-MFC in parallel with a 10 kΩ resistor and fed 10 mM lactate

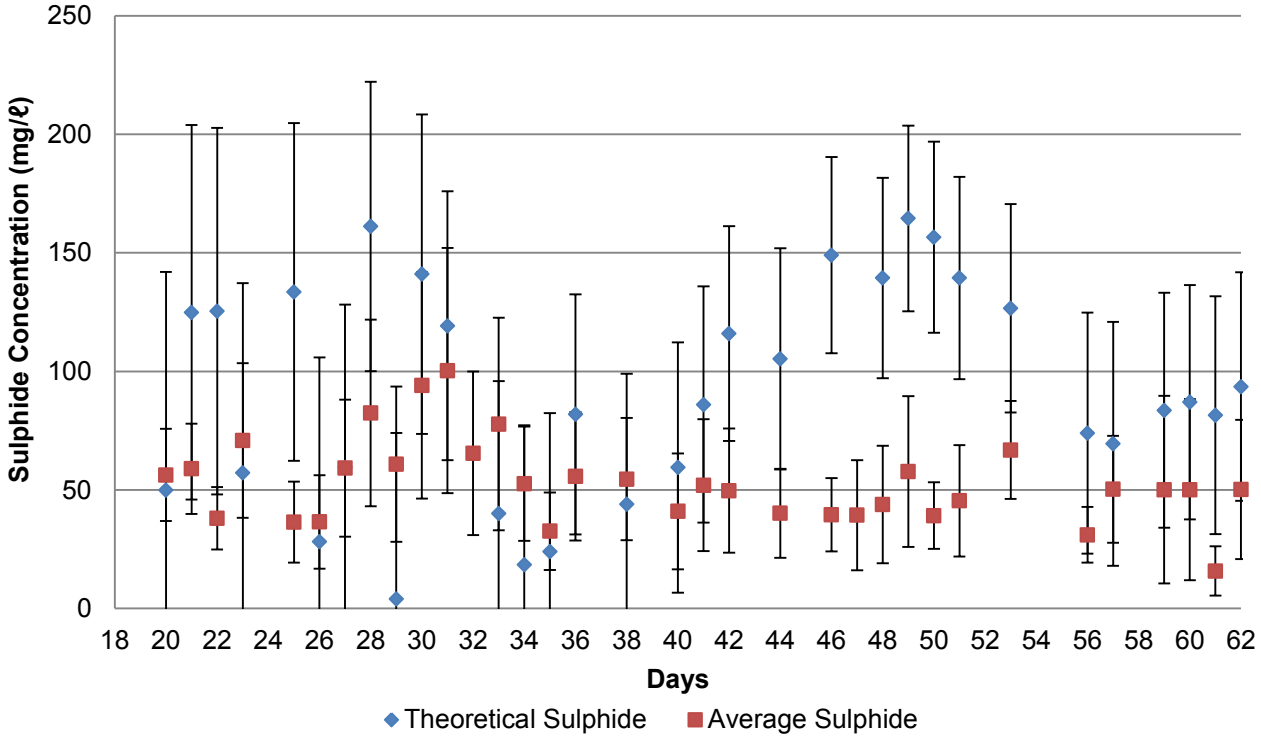

Figure 6-8: Concentration of theoretical and average sulphide concentration as a function of time for the LFCR-MFC in parallel with a 10 kΩ resistor and fed 10 mM lactate

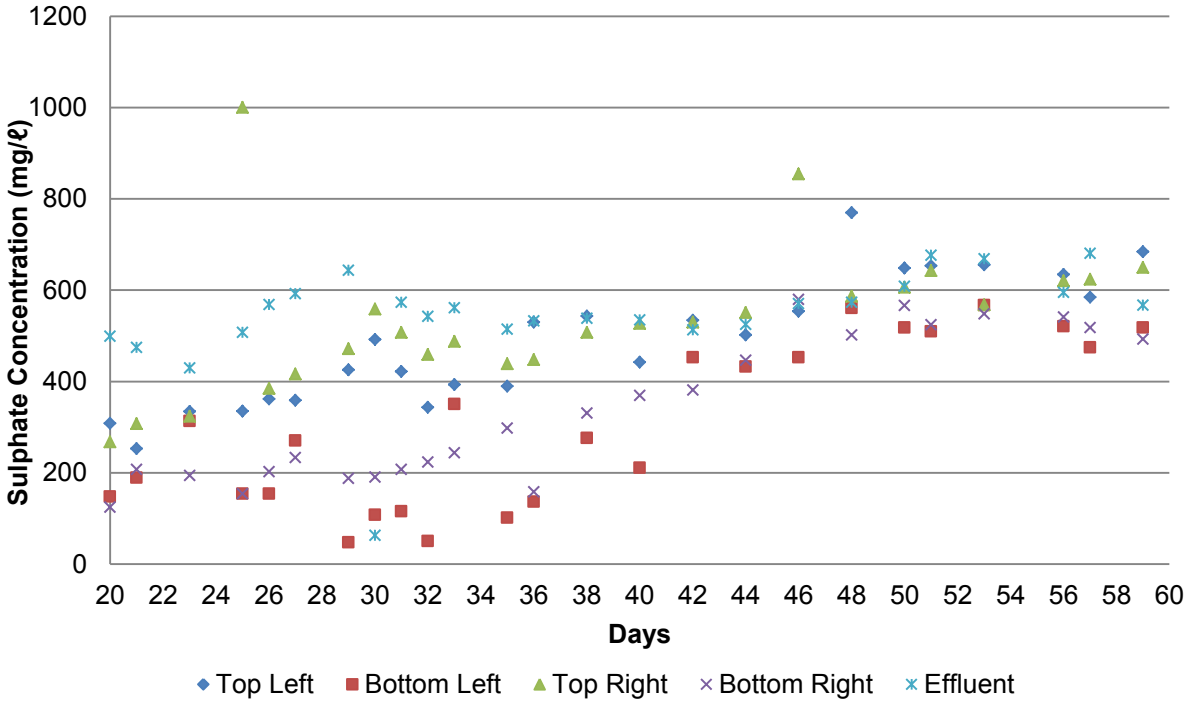

Figure 6-9: Sulphate concentration as a function of time for the LFCR-MFC in parallel with a 10 kΩ resistor and fed 10 mM lactate, calculated based on acetate concentration produced by SRB.

6.3.3.2 Concentration of Volatile Fatty Acids

Although lactate, acetate propionate, butyrate, iso-butyrate, valerate and iso-valerate were detected by HPLC in the samples taken from the LFCR-MFC, only the concentration of lactate, acetate and propionate are shown. Concentrations of the remaining volatile fatty acids were typically lower than 50 mg/ℓ (collectively less than 15 % of the carbon fed) and remained fairly constant throughout the experiment. They were also not present in earlier samples.

The concentration of lactate throughout the reactor decreased to approximately 0 mg/ℓ within the first 5 days of operation. Lactate was present in many effluent samples whereas it had been depleted throughout the rest of the reactor (Figure 6-10). This supported the short circuiting of the feed stream indicated by the hydrodynamic study. The presence of lactate in the effluent became less frequent and lower in concentration (below 50 mg/ℓ) after 30 days of operation. From day 48 until the end of the experiment, lactate was present in concentrations as high as 170 mg/ℓ in all areas of the reactor but most frequently in the top level and effluent. This suggested a change in activity of the consortium following the collapse of the FSB.

Acetate concentration was observed to differ significantly between the different sampling ports in the reactor (Figure 6-11). The concentration was consistently higher in the bottom level of the reactor. The concentration difference between ports on the same level was smaller than that of ports on different levels. There was generally a decrease in acetate concentration areas across all sampling points of the reactor with increased duration of the experiment. As can be seen from Figure 6-13, a positive relationship exists between acetate concentration and potential difference whereby an increased acetate concentration in the bulk liquid resulted in increased potential difference over the LFCR-MFC. No relationship existed for the effluent as a result of short circuiting of feed. The acetate produced by SRB with concomitant sulphate reduction was calculated. This acetate concentration as a function of time is given by Figure A 14 in Section D.2. The same positive relationship between this acetate concentration and potential difference is noted in Figure A 15.

The overall propionate concentration of the reactor decreased over time for the first 30 days of the experiment (Figure 6-12). The concentration then increased to approximately the same concentration as in the beginning of the experiment (300-350 mg/ℓ). During the first 30 days of operation, the propionate concentration of the lower level of the reactor was higher than the upper levels. From day 30 onwards the concentration was highest for the upper levels of the reactor. The concentration difference between ports on the same level was smaller than that of ports on different levels.

The trend of propionate concentration initially decreasing for the first 30 days followed by an increase for the remainder of the experiment was strongest for samples taken from the bottom left port of the reactor.

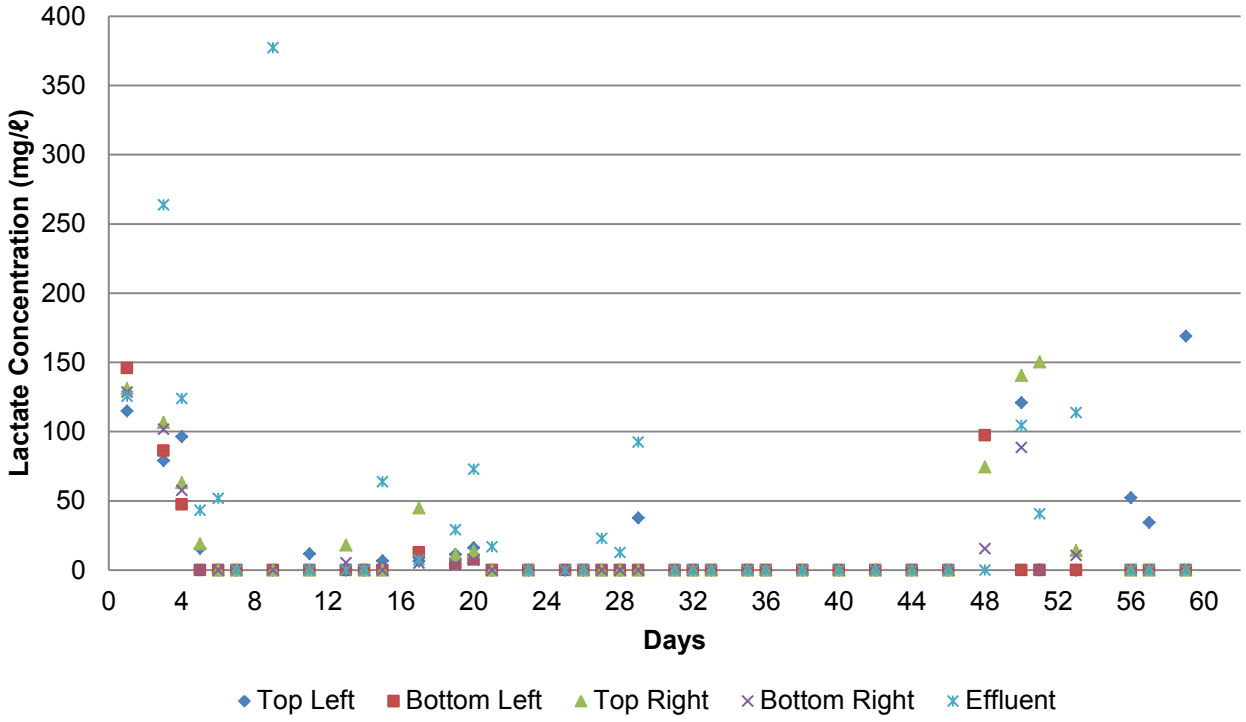

Figure 6-10: Lactate concentration as a function of time for the LFCR-MFC in parallel with a 10 kΩ resistor and fed 10 mM lactate

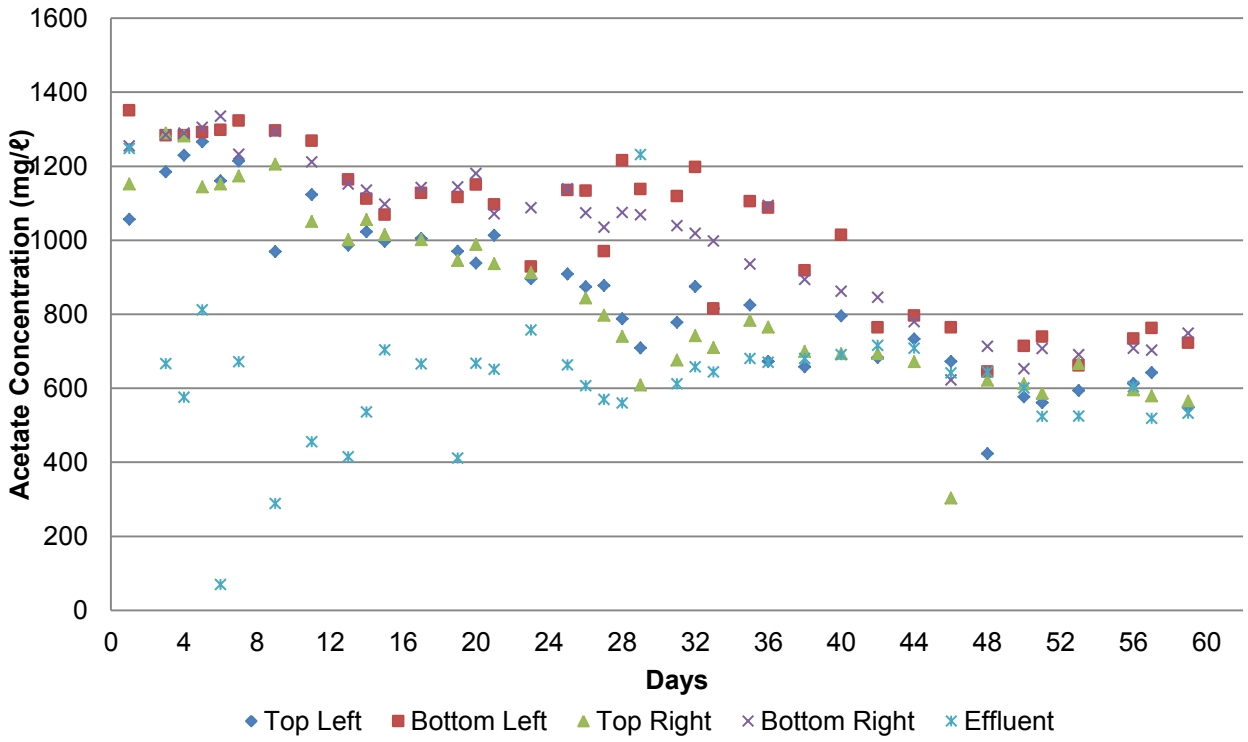

Figure 6-11: Acetate concentration as a function of time for the LFCR-MFC in parallel with a 10 kΩ resistor and fed 10 mM lactate

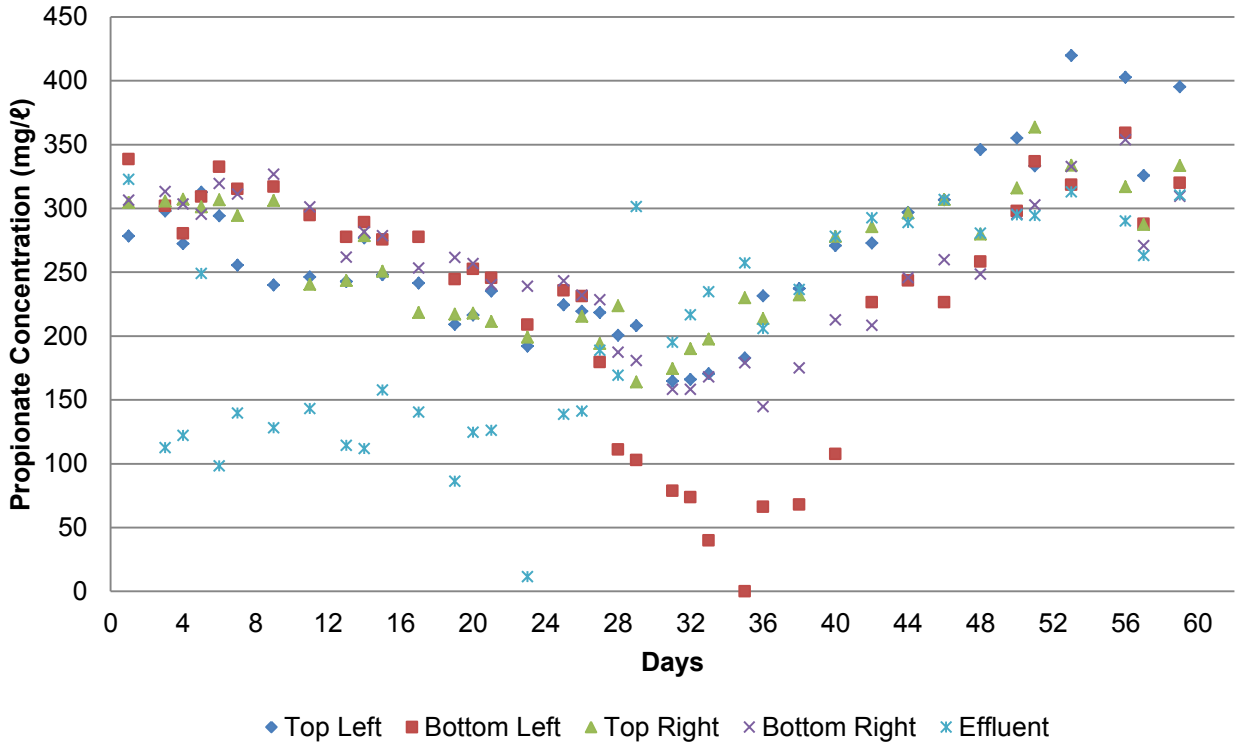

Figure 6-12: Propionate concentration as a function of time for the LFCR-MFC in parallel with a 10 kΩ resistor and fed 10 mM lactate

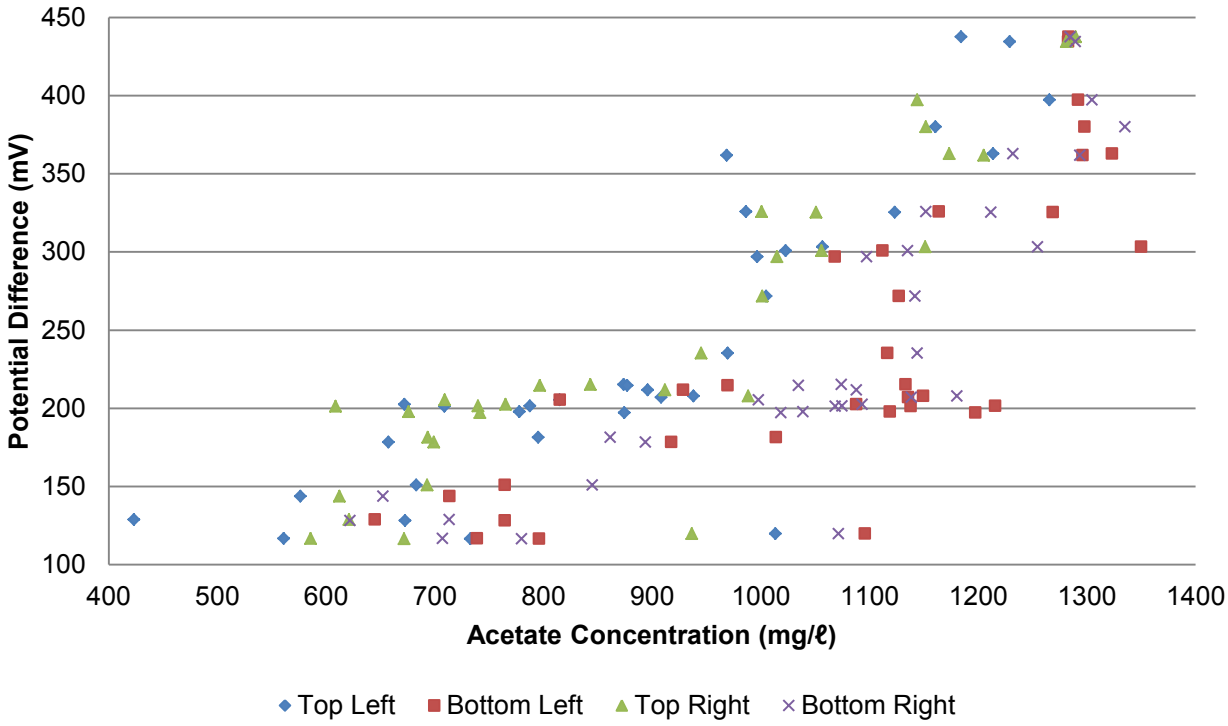

Figure 6-13: Acetate concentration as a function of potential difference for the LFCR-MFC in parallel with a 10kΩ resistor and fed 10mM lactate

6.3.3.3 COD Degradation and Coulombic Efficiency

The concentration of COD in the effluent from the LFCR-MFC remained fairly constant between 1200-1800 mg/ℓ from day 19 until the end of the experiment (Figure 6-14). This corresponds to a 35-55 % degradation of the COD in the incoming feed (Figure 6-15). The coulombic efficiency of the fuel cell remained lower than 0.1 % for the duration of the experiment (Figure 6-16). A gradual decrease with time was observed. This is most likely as a result on the gradual decrease in potential difference over time for the duration of the experiment. This can be seen from the gradual increase in CE with potential difference (Figure 6-17), whereas no visible trend was observed for CE as a function of the change in COD concentration (Figure 6-18). Regression analysis indicated R^2 values of 0.553 and 0.151 respectively which support this.

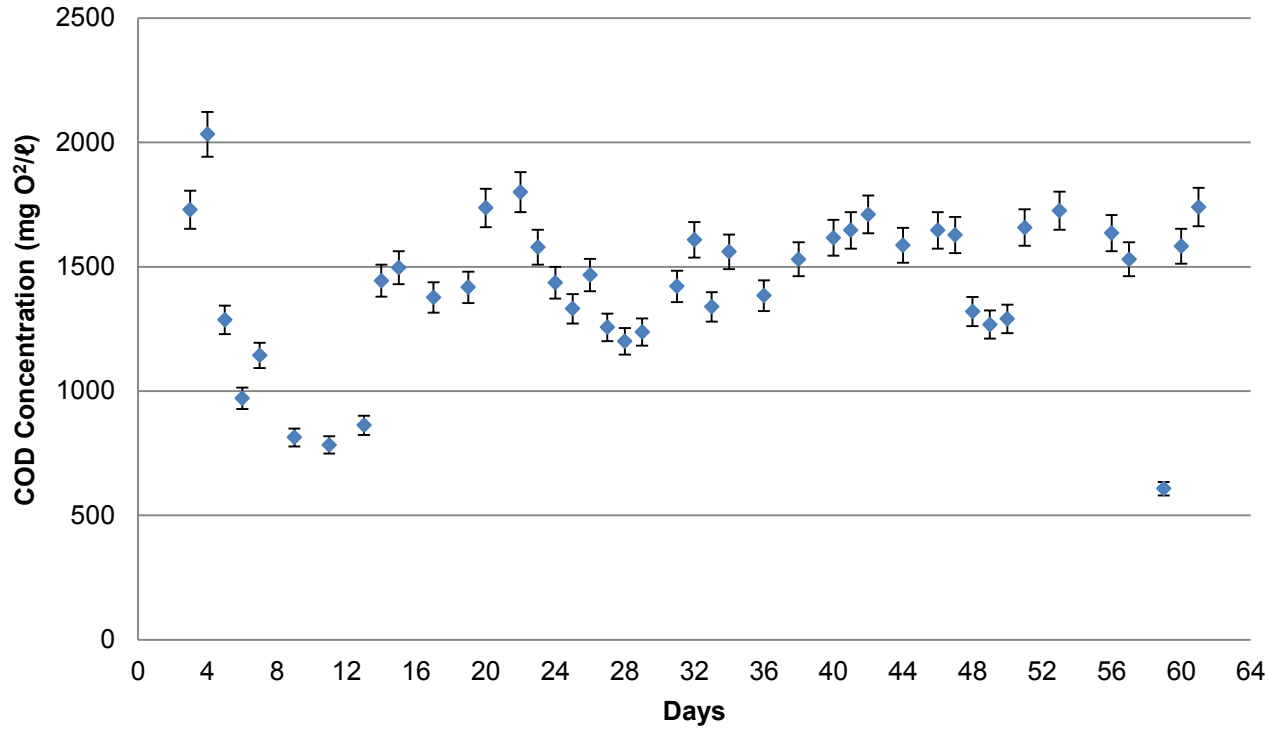

Figure 6-14: Effluent COD concentration as a function of time for the LFCR-MFC in parallel with a 10kΩ resistor and fed 10mM lactate

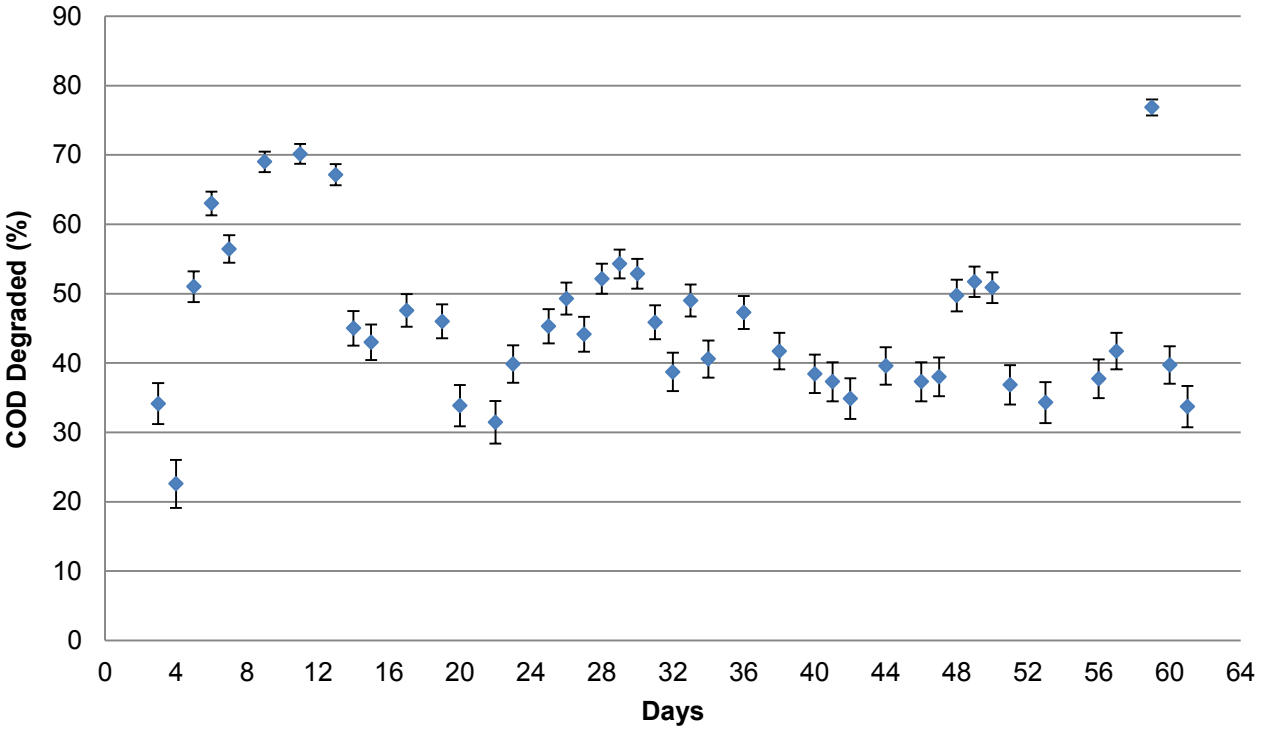

Figure 6-15: Percent of COD degraded as a function of time for the LFCR-MFC in parallel with a 10kΩ resistor and fed 10mM lactate

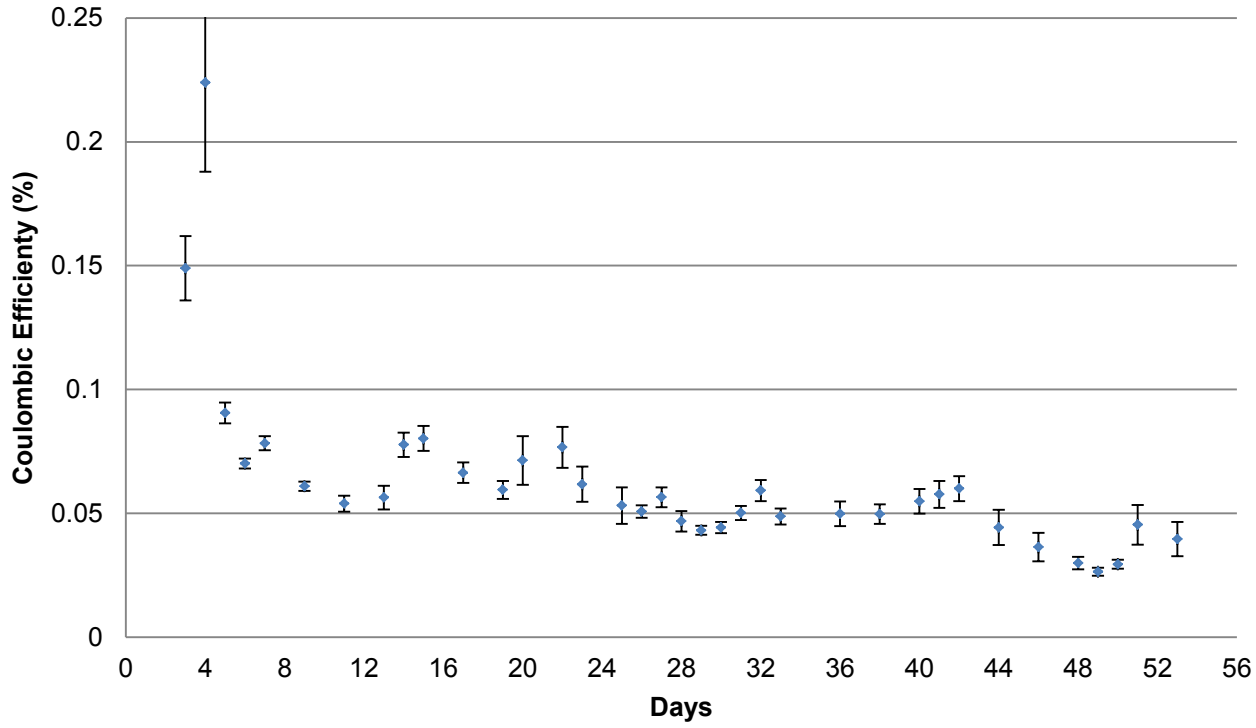

Figure 6-16: Coulombic efficiency as a function of time for the LFCR-MFC in parallel with a 10kΩ resistor and fed 10mM lactate

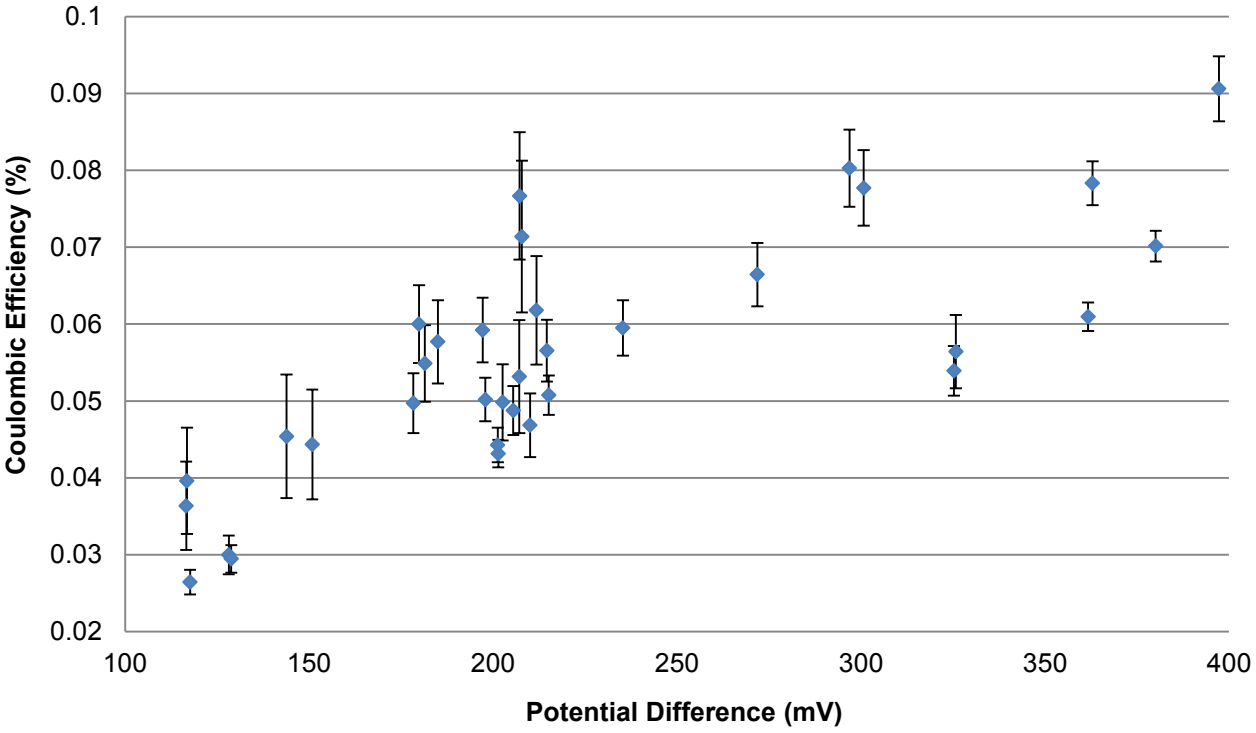

Figure 6-17: Potential difference as a function of coulombic efficiency for the LFCR-MFC in parallel with a 10kΩ resistor and fed 10mM lactate

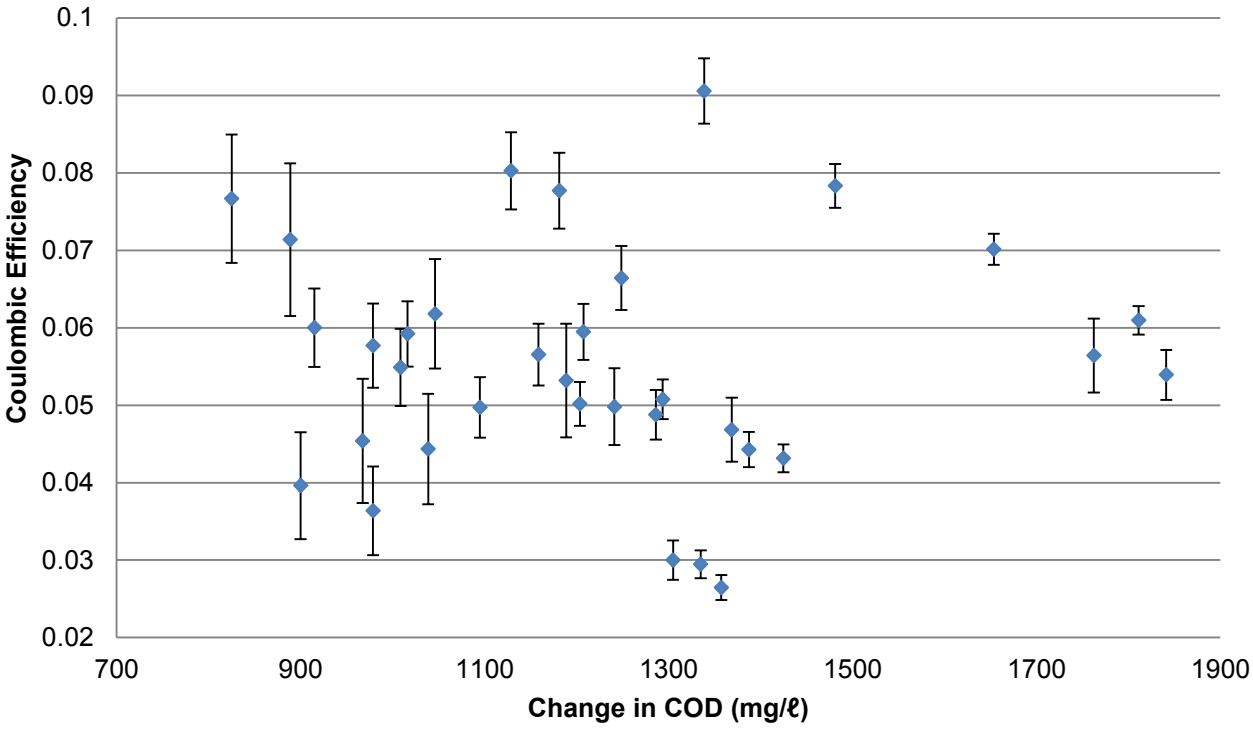

Figure 6-18: Change in COD concentration as a function of coulombic efficiency for the LFCR-MFC in parallel with a 10kΩ resistor and fed 10mM lactate

6.3.4 pH and Redox

The overall pH of the system decreased steadily from around pH 8.9 to around pH 7.5 over the first 19 days after inoculation, as can be seen from Figure 6-19. During this time the pH was fairly consistent across the reactor. From day 19 onwards it decreased more slowly, remaining between pH 7.5 and 7 until day 45, at which point the pH had decreased to between 6.4 and 7. In this lower pH range, the pH of the top layer was lower than the bottom layer. From day 45 until the end of the experiment the pH of the top left corner with the incoming feed was notably the lowest. The pH of the feed ranged between pH 5.5 and 6.5. After day 19 the variation in the pH of each sample point increased. At this point high pH inoculum was no longer added.

The magnitude of the redox potential of the reactor effluent decreased over the duration of the experiment from approximately between -430 mV and -410 mV to between -290 mV and -330 mV (wrt Ag/AgCl reference electrode) (Figure 6-20).

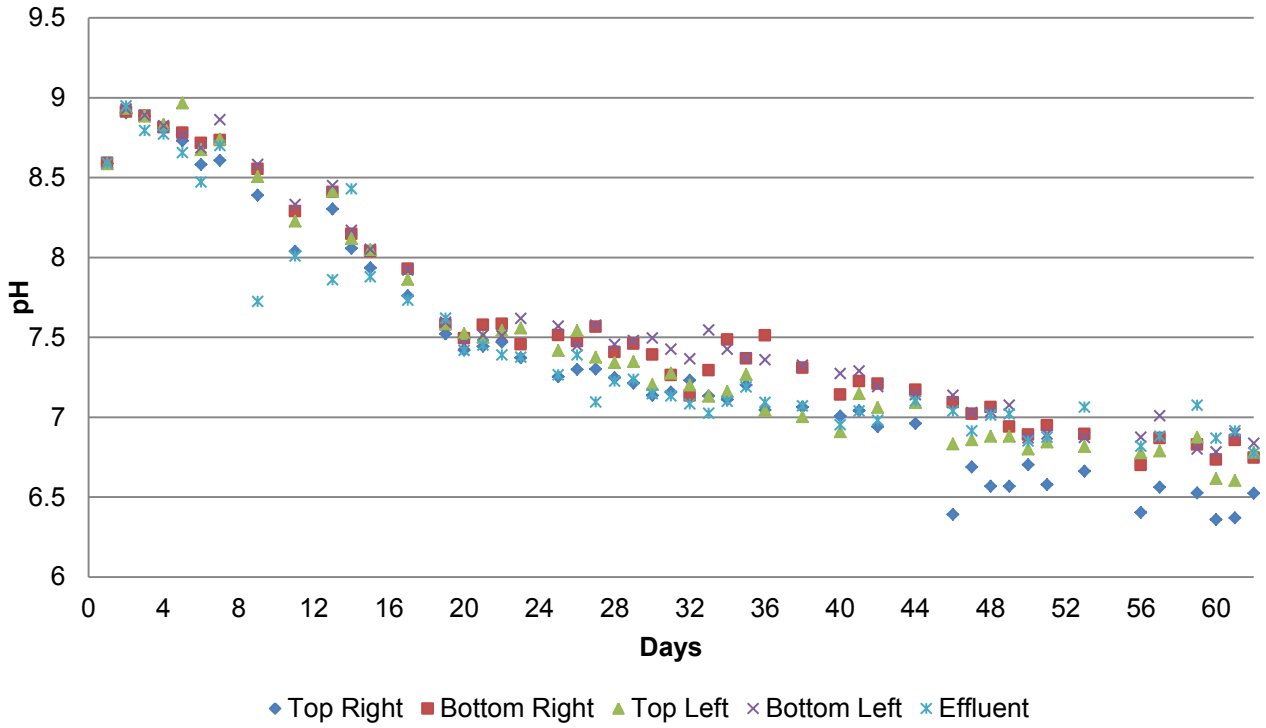

Figure 6-19: pH as a function of time for the LFCR-MFC in parallel with a 10 kΩ resistor and fed 10 mM lactate

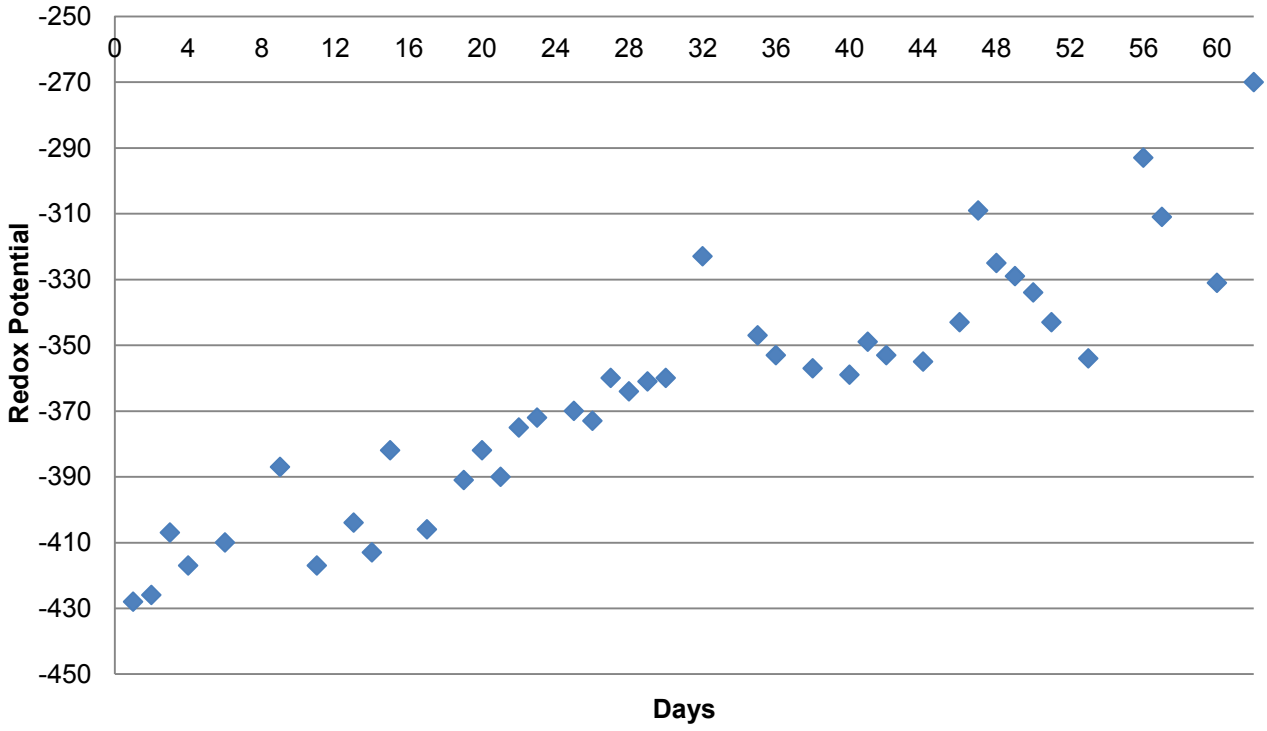

Figure 6-20: Redox potential (wrt Ag/AgCl reference electrode) as a function of time for the LFCR-MFC in parallel with a 10kΩ resistor and fed 10mM lactate

6.3.5 Cyclic Voltammetry

Cyclic voltammetry was conducted on fresh medium (Figure 6-21) and medium containing planktonic cells (Figure 6-22) over a range of -0.9 V to 0.9 V at a scan rate of 1mV/s. These results are discussed in detail in Section 5.3.5. CV was conducted on the LFCR-MFC (Figure 6-22) over a range of -0.7 V to 0.6 V at a scan rate of 1mV/s on day 53. The range was reduced as a result of no separation of current produced for the oxidative and reductive cycles above 0.5 V in normal medium and no strong peaks visible for the medium with planktonic cells.

In contrast to the planktonic cells suspended in medium, the CV conducted on the LFCR-MFC revealed a double peak between -0.51 and -0.38 V. The current produced was also significantly higher than that of the normal medium and planktonic cells in medium. There was no oxidative peak present and most of current produced on the oxidative cycle was thought to be capacitive current. The strong peaks produced confirmed faradaic current being produced in a reduction reaction mediated by microorganisms.

Upon zooming in on the CV of planktonic cells in medium, a small reduction peak was noted at approximately -0.75 V (Figure 6-22). In comparison to the reduction peaks produced by the LFCR-MFC, this was fairly insignificant. This suggested that the current produced in the CV of the LFCR-MFC was largely as a result of microorganisms in the biofilm. The SEM conducted on the electrodes of a single-chambered MFC (Figure 5-56) indicated that nanowires were present on some bacteria in the biofilm which is indicative of bacteria in the biofilm actively producing electrical current.

CV on the anode and cathode of the LFCR-MFC was not performed. CV performed on the anode and cathode of the single-chambered MFCs did not reveal any strong peaks or current. The LFCR-MFC likely had better colonisation of the anode as a result of it being carbon fibre and having a substantially larger area for bacterial adhesion. CV was also conducted after a longer period of time of cell operation. Electrodes in the single-chambered MFC became fouled with sulphur (Figure 5-53). This may be the cause of reduced electricity production with time and was likely to affect the mass transfer of substrate and charged particles to and from the electrode. It is likely that this affected CV performance on the individual electrodes. It is recommended that CV be conducted at various times throughout the experiment.

One of the electricity producing reactions is the oxidation of sulphide to sulphur at the anode either by chemical oxidation or mediated by sulphide oxidising bacteria (Sangcharoen *et al*., 2015). It is likely that in the case of the CV conducted on the colonised electrodes in fresh media, no sulphide was present and therefore no strong peaks were observed despite the biofilm actively contributing to electricity production.

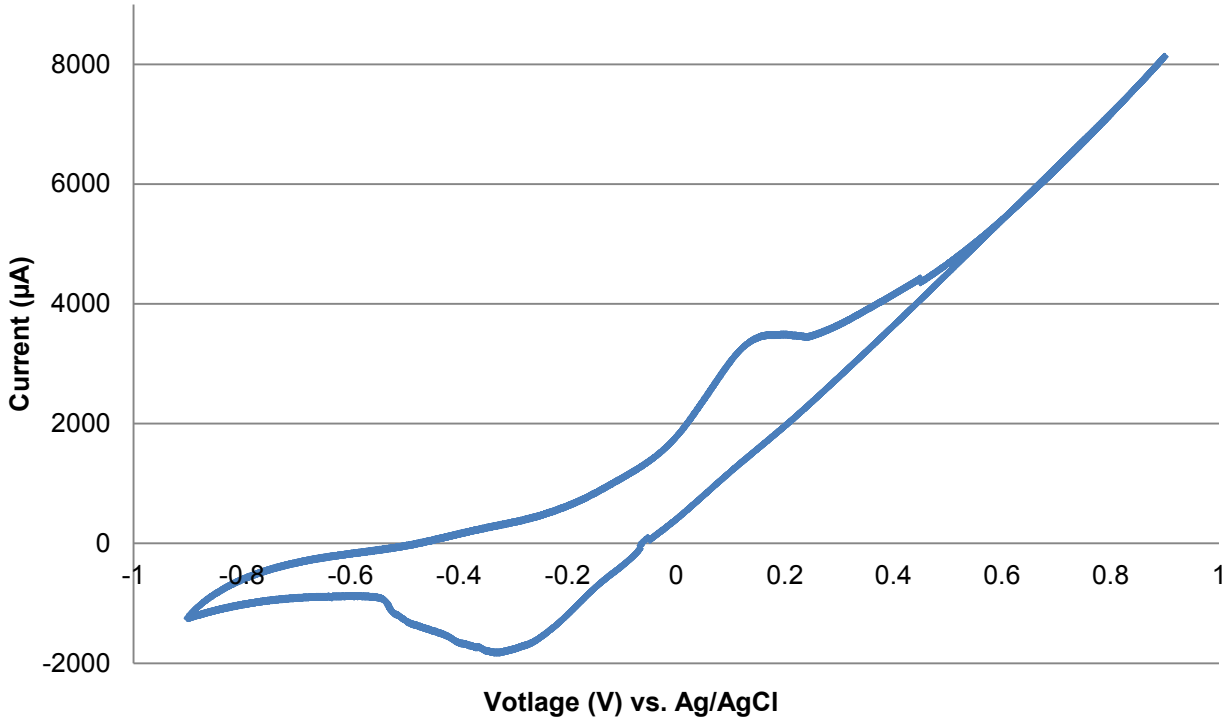

Figure 6-21: Cyclic voltammogram of abiotic fresh media at a scan rate of 1 mV/s

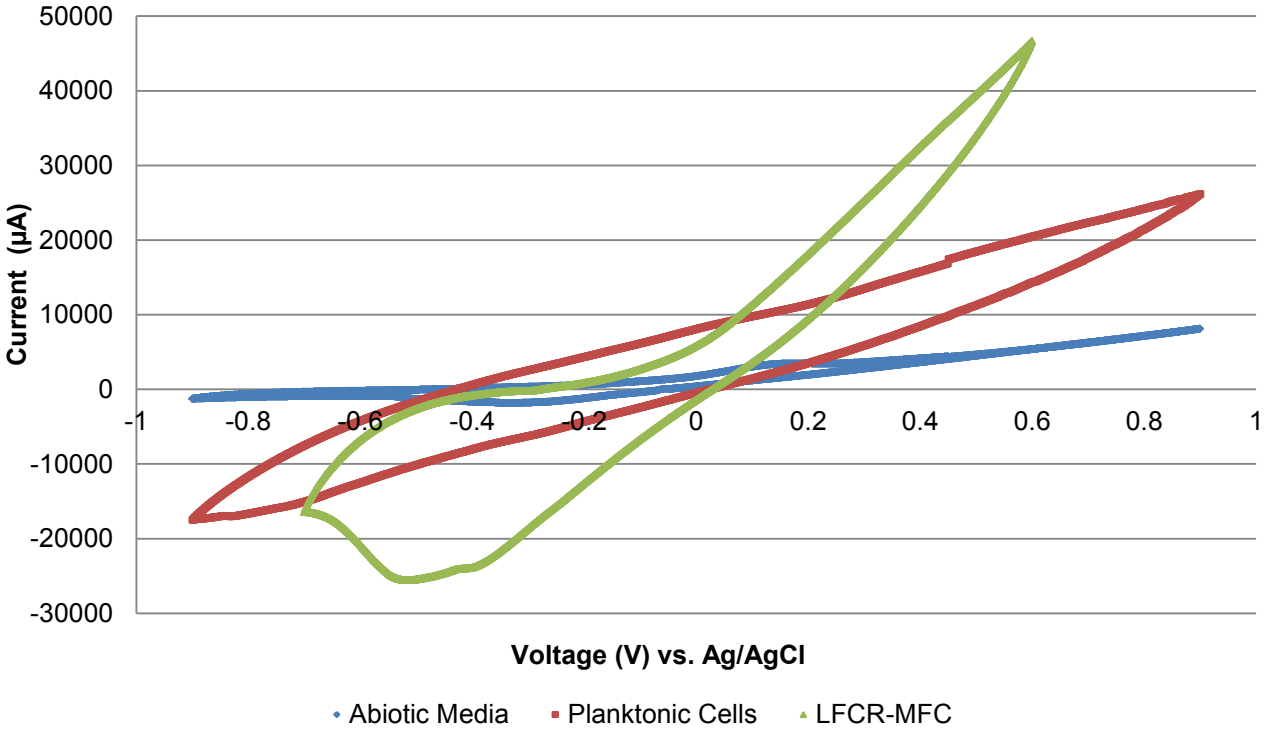

Figure 6-22: Cyclic voltammogram of various aspects of the LFCR-MFC at a scan rate of 1 mV/s

6.4 DISCUSSION

6.4.1 Electrical Performance

Although a slightly higher maximum power density was achieved by the single-chambered MFCs than by the LFCR-MFC (2.86 ± 0.009 mW/m^2 and 2.56 ± 0.005 mW/m^2 respectively), the LFCR-MFC achieved its maximum at a much lower resistance than that of the single-chambered MFCs (20600 Ω for single-chambered MFC and 980 ± 118 Ω for LFCR-MFC respectively). This indicates that the internal resistance of the flow through system was much lower than that of the smaller draw-and-fill MFC. The internal resistance achieved for the single-chambered MFC with the carbon fibre brush anode (7720 ± 253 Ω) is much closer to that achieved in the LFCR-MFC. The lower maximum power density (0.966 ± 0.002 mW/m^2) produced by the single-chambered MFC was thought to result from the time at which the polarisation curve was plotted. This is discussed in Section 5.4.2.

The difference in internal resistance may have resulted from several factors. The standard single-chambered MFC had two carbon felt electrodes 4 cm apart. This was expected to result in mass transfer limitation within the system as it was not mixed in any way and protons are required to diffuse the length of the reactor to partake in the reduction reaction at the cathode. In the LFCR-MFC, the flow of medium through the system aided mixing and the transfer of protons to the cathode. The anode brush was also in the centre of the reactor and some of the fibres were as close as 1 cm to the cathode. The shorter distance between the two electrodes would significantly aid mass transfer and lower internal resistance. The latter was also the case for the single-chambered MFC with the carbon fibre brush anode. The LFCR-MFC also had two cathode electrodes, resulting in a higher number of protons reaching a cathode and improving the reduction reaction.

The current produced by the LFCR-MFC was in the order of tenfold the magnitude of the current produced by the single-chambered MFC (Figure 5-4 and Figure 6-5). The carbon fibre anode in the LFCR-MFC had a considerably larger surface, allowing colonisation by a larger population of SRBs, therefore likely resulting in higher current generation.

Although the power produced by both systems was very small and requires substantial optimisation before effective use in electrical application, a major advantage of the flow through LFCR-MFC system is that the consistency of power generation compared with cyclic power generation in the single-chambered MFCs. The electricity produced by the continuous system could therefore more likely be used directly for an electrical application whereas the electricity produced by a cycling batch system would best be used to charge a battery for later use.

6.4.2 Stratification of Liquid Layers

The hydrodynamic study revealed the stratification of layers across the depth of the LFCR-MFC at all residence times investigated but especially at 0.163 ml/min (4 day residence time) which was the slowest flow rate tested and the flow rate used in this experiment. After seeding of the reactor was stopped on day 19, a difference in the sulphate concentration (Figure 6-6) sulphide concentration (Figure 6-7) and pH values (Figure 6-19) of the samples taken from the different sampling ports in the LFCR-MFC became more apparent and fairly regular. Here, the reactor was mixed solely by the incoming feed. The similarity in acetate concentrations in samples taken from the same level of the reactor, compared to that of samples taken on a different level (Figure 6-11) likely also indicates the presence of liquid layers in the reactor.

The collapse of the FSB on day 46 resulted in the decrease in potential difference over the MFC (Figure 6-4), simultaneous increase in concentration of sulphate throughout the reactor (Figure 6-6) and the increased lactate concentration in the upper levels of the reactor (Figure 6-10). The absence of the FSB will result in the increased diffusion of oxygen from the air into the bulk liquid (Mooruth, 2011). Although diffusion of oxygen occurred through the cathode electrodes on the sides of the

reactor, sulphur deposition and biofilm formation on the electrodes was assumed to have occurred when steady power production was established. This, coupled to the reduction reaction with oxygen, was assumed to limit oxygen transfer into the bulk liquid via the cathode electrodes. The majority of diffusion of oxygen is therefore assumed to have occurred at the air liquid interface and the concentration gradient was such that the dissolved oxygen concentration was highest at the air-liquid interface and decreased towards the base of the reactor. The presence of oxygen was likely to affect the metabolism of the anaerobic SRB and hinder their ability to degrade sulphate and lactate which would have resulted in the increased concentration of these two components, particularly in the upper level of the reactor where oxygen concentration was highest. Increased sulphate could also be as a result of the oxidation of sulphide back to sulphate instead of elemental sulphur as a result of the excess of oxygen.

The short circuiting of incoming feed along the top of the reactor was observed during the hydrodynamic study. This may have resulted from the reactor being short and almost square in shape. Minimal short circuiting was noted in the LFCR investigated by van Hille *et al*. (2015) which is almost twice the length of this LFCR-MFC. Short circuiting during the experiment was evident from the presence of lactate in some effluent samples.

The decrease in lactate concentration in the effluent, after the reactor was no longer seeded and a floating sulphur biofilm was allowed to fully develop, indicates that the biofilm may have reduced short circuiting of feed. The reappearance of lactate in the effluent and upper level of the reactor after day 48 (Figure 6-10) corresponded directly with the collapse of the FSB. In addition to short circuiting of the feed, the lactate concentration in the effluent was likely contributed to by the diffusion of unused lactate from the liquid level below the outlet which was normally prevented by the FSB and was present in larger quantities at the time as a result of increased oxygen availability.

6.4.3 Substrate Utilisation

As discussed in Section 2.8.2.5, electricity generation in a sulphate-fed MFC containing SRB and SOB is proposed to occur in one of two ways (Sangcharoen *et al*., 2015). The BSR by SRB either in the anodic biofilm or as planktonic cells, with concomitant oxidation of organic compounds produces sulphide. Sulphide is then either oxidised abiotically or by SOB to sulphur or polysulphide at the anode with concurrent electricity production. Organic compounds may also be removed by exoelectrogenic microorganisms (EEM) at the anode with concurrent electricity production.

The average concentration of sulphide within the reactor remained largely lower than that of the theoretical sulphide concentration (Figure 6-8) calculated from the sulphate reduction. This was to be expected as sulphide was oxidised for the formation of the FSB and in the electricity producing reaction at the anode. After the collapse of the biofilm on day 46 of the experiment, no visible decrease in measured sulphide concentration was noted (Figure 6-7). There was however a notable decrease in electricity production (Figure 6-4). It is possible that the sulphide used for the generation of electricity was used for the formation of new FSB.

The presence of propionate over the first 19 days of the experiment is likely as a result of the fermentation product being present in the effluent which was used to seed the reactor. Therefore fermentative bacteria are also present in the inocula.

SRB are capable of fermentative metabolism under sulphate limiting conditions. This is however unlikely as the sulphate concentration remained above 500 mg/ℓ in all areas of the reactor for the duration of the experiment. The presence of propionate in the reactor may therefore be mostly due to the presence of fermentative bacteria. The propionate concentration was used to determine the concentration of acetate as a result of the metabolism of SRBs opposed to fermentative bacteria. This acetate concentration was used to calculate the amount of sulphate reduced by partial oxidation and

therefore the concentration of sulphate which should be present in the reactor. This sulphate concentration as a function of time was similar to that of the measured concentration (Figure 6-6 and Figure 6-9) from day 30 onwards. This indicates that the SRB were mostly partial oxidisers, as expected with lactate as a carbon source

As can be seen from the graph of propionate concentration as a function of time for the LFCR-MFC (Figure 6-12), propionate decreased in concentration for the first 30 days for the experiment. Thereafter it increased for the remainder of the experiment to approximately the starting value (between 300-350 mg/ℓ). The gradual decrease in acetate concentration from day 32 onwards (Figure 6-11) could be due to its use by other contaminating bacteria such as MB or acetogens. By day 32 the additional VFAs and sulphate present in the feed had washed out and the concentration of components in the system was as a result of the degradation of the feed alone. As a result of the absence of additional substrate, MB and acetogens could have utilised acetate produced by the SRB.

Although the carbon microfiber brush anode was spread throughout the bulk liquid in the reactor, the majority of the fibre was concentrated in the bottom layer, especially around the bottom left end of the reactor. This, coupled with the oxygen gradient, was likely to result in the bulk of the anaerobic SRBs, being present in the lower level of the reactor. This is backed up by the concentrations of propionate in the samples taken from the bottom of reactor dropping more significantly (Figure 6-12) as well as the higher concentrations of sulphide (Figure 6-7).

The percent of COD degraded remained between 35-55% from day 19 until the end of the experiment. The coulombic efficiency remained below 0.1% for the duration of the experiment. This was of the same order of magnitude as the CE attained for many of the standard single-chambered MFCs (Figure 5-25 and Figure 5-28). The CE achieved for the single-chambered MFC with the carbon fibre brush anode (Figure 5-34) was higher (between 0.5 and 4%) although a similar degradation of COD was achieved. Both made use of a carbon fibre anode and had similar potential differences (100 mV-200 mV) when in parallel with a 10 kΩ resistor. It is likely that the continuous flow of feed through the LFCR-MFC aided the transfer of components in the system and therefore decreased internal resistance. However, sulphide was present in the effluent and could potentially have been oxidised at a longer residence time. Similarly, charged particles from the oxidation of substrate by EEM may also have been removed from the reactor before transfer from the anode to the cathode takes place. Therefore the electricity production and CE of the system may have decreased. Further, the LFCR has already been demonstrated as an effective wastewater treatment method. Organic substrate usage was also required to treat sulphate-rich wastewater and continued to do so with the integration of the MFC.

6.5 CONCLUSION

An integrated LFCR-MFC was demonstrated as capable of functioning as both a wastewater treatment reactor and a microbial fuel cell. The maximum power density produced by the LFCR-MFC was 2.56 ± 0.005 mW/m^2, corresponding to an internal resistance of 980 ± 118 Ω. The internal resistance was lower than that achieved by any single-chambered MFC, possibly as a result of improved mass transfer in the flow through system. The electrode and current collector set-up was similar to that used in the single-chambered MFCs and the same improvements to the cathode preparation and connection as suggested for the single-chambered MFC (Section 4.3.1) are recommended for improved current generation.

Cyclic voltammetry on the LFCR-MFC suggested that the bacteria in the biofilm on the electrodes play an important role in electricity generation. The oxidation of sulphide is an electricity producing reaction. The absence of faradaic current produced when CV was conducted on spent medium rich in sulphide indicated that bacteria in the biofilm contribute largely to electricity production as faradaic

current was produced for the CV of the LFCR-MFC. Further research is required to investigate the role of the bacteria in electricity generation and the species present in the system.

Fermentative bacteria were present in the system and competed with the SRB and SOB for substrate. The LFCR-MFC requires sulphide for both the formation of the FSB and in the production of electricity. In the LFCR-MFC, biological sulphate reduction, formation of elemental sulphur and the electricity production via the sulphide oxidation reaction are all expected to be hindered by competition of the fermenters for organic carbon.

7 CONCLUSIONS AND RECOMMENDATIONS

The overall aim of this study was to incorporate the elements of a MFC into a LFCR designed for combined biological sulphide reduction and sulphide oxidation to yield a sulphur product. The integration aimed to create a LFCR-MFC that functioned as a wastewater treatment reactor yielding a sulphur product and electricity through the MFC. A constructed single-chambered MFC was used to test the ability of the microbial community, selected for use in the linear flow channel reactor (LFCR), to produce electricity. It could therefore be concluded if the community was capable of electricity production (presented in Chapter 5). The performance of the mixed community from the LFCR in the single-chambered MFC provided a basis to which the integrated system could be compared and was used to determine whether an integrated system was likely to produce electricity (presented in Chapter 6).

The construction of the single-chambered MFC used for the testing of the microbial community from the LFCR was validated with a pure culture of *Shewanella oneidensis* MR-1 operating with a lactate feed as used by Wu *et al*. (2013b) (Chapter 4). The MFC produced a maximum power density of 13.7 ± 0.228 mW/m^2. This was 18.6% of that reported in literature. The reduced power density was attributed to shortcomings of the cathodes used in these experiments, including platinum loading, waterproofing and nature of the connections. It was hypothesised that improvements to the connection and construction of the cathode would improve performance. However, the single-chambered MFC was deemed to be adequately constructed and suitable for further testing with other microorganisms.

The microbial community, similar to that present in the LFCR, was found to be capable of electricity generation and produced a maximum power density of 2.86 ± 0.009 mW/m^2 of anode area in the single-chambered MFC with a carbon felt anode. The MFC demonstrated a high internal resistance of 20600 ± 571 Ω. This was reduced to 7720 ± 253 Ω by the changing of the felt anode to a carbon brush anode. The MFC with carbon brush anode resembling the retention matrix in the LFCR also demonstrated electricity generation. Owing to the electrogenic potential of this community, the integrated LFCR-MFC was considered likely to produce electricity and therefore an integrated LFCR-MFC was constructed.

The constructed integrated LFCR-MFC was demonstrated to function as both a wastewater treatment reactor and a microbial fuel cell. The maximum power density produced by the LFCR-MFC was 2.56 ± 0.005 mW/m^2, which corresponded to an internal resistance of 980 ± 118 Ω.

Fermentative bacteria were present in the inoculum for the LFCR and were found to compete with the SRB and SOB for substrate in both the single-chambered MFCs and the LFCR-MFC. The LFCR was designed for combined biological sulphide reduction and sulphide oxidation to yield an elemental sulphur product. Its primary function is to treat the wastewater. The LFCR-MFC requires sulphide for both the formation of the FSB and in the production of electricity. Under normal operating conditions for a LFCR competition between fermentative bacteria and SRBs may result in reduced sulphate reduction. In the case of the LFCR-MFC the electricity production via the sulphide oxidation reaction may also be hindered by competition. The competition with fermentative bacteria is thus an important challenge in the operation of the LFCR-MFC and requires careful selection of carbon source. The use of lactate as a carbon source is unrealistic in a real world application.

Recommendations are given to improve the cathode design used in the single chamber MFC and the LFCR-MFC and its connection to the external circuit for further research. This could significantly improve the electricity production by both the single-chambered MFCs and the LFCR-MFC. No optimisation studies were conducted in this research. Several system variables could be altered to

gain insight into the electricity generation in the system. It is recommended to study the effect of residence time. The production of sulphide through BSR is affected significantly by the residence time (van Hille *et al*., 2015). Electricity production through sulphide oxidation could therefore by altered by residence time. In addition, mixing time and mass transfer are altered by feed flow rate.

For long term operation of the LFCR-MFC, consideration should be given to the fouling of the platinum catalyst on the cathode electrode by sulphur deposition. The current design does not allow for changing of the electrode during operation. It is unclear to what extent electricity production was affected by fouling and mass transfer limitations. It is recommended to investigate this in future research. In addition, regular collapsing of the FSB is required for long term operation of the LFCR-MFC and it is unclear how electricity generation will be effected. The relationship between electricity generation from sulphide oxidation and formation and composition of the FSB could also be investigated. Furthermore, it has been suggested in some studies that sulphur may deposit on the carbon-fibre anode. In the LFCR-MFC, the carbon fibre brush forms both the matrix for retention of the SRB and the anode, hence interference between or inter-dependence of these activities should be considered.

The shape of the LFCR-MFC likely resulted in the short circuiting of feed across the surface of the bulk liquid. This could potentially be reduced by using the rectangular shaped reactor used by van Hille *et al*. (2015) or altering the position of the inlet to the reactor. It is proposed that for the scale up of the LFCR-MFC multiple cathode zones in a rectangular reactor of varied aspect ratio be explored.

REFERENCES

Aelterman, P., Rabaey, K., Pham, H. T., Boon, N. & Verstraete, W., 2006. Continuous Electricity Generation at High Voltages and Currents Using Stacked Microbial Fuel Cells. *Environmental Science and Technology,* 40(10), pp. 3388-3394.

APHA (American Public Health Association), 1975. *Standard methods for the examination of water and wastewater, 14th Edition,* New York: APHA.

Baskaran, V. & Nemati, M., 2006. Anaerobic reduction of sulfate in immobilised cell bioreactors, using a microbial culture originated from an oil reservoir. *Biochemical Engineering Journal,* Volume 31, pp. 148-159.

Bond, D. R. & Lovley, D. R., 2003. Electricity Production by Geobacter sulfurreducens Attached to Electrodes. *Applied and Environmental Microbiology,* 69(3), pp. 1548-1555.

Boshoff, G., Duncan, J. & Rose, P. D., 2004. Tannery effluent as a carbon source for biological sulphate reduction. *Water Research,* Volume 38, pp. 2651-2658.

Brandt, K. K., Vester, F., Jensen, A. N. & Ingvorsen, K., 2001. Sulfate Reduction Dynamics and Enumeration of Sulfate-Reducing Bacteria in Hypersaline Sediments of the Great Salt Lake (Utah, USA). *Microbial Ecology,* Volume 41, pp. 1-11.

Castro, H. F., Williams, N. H. & Ogram, A., 2000. Phylogeny of sulfate-reducing bacteria. *FEMS Microbiology Ecology,* Volume 31, pp. 1-9.

Cha, J., Choi, S., Yu, H., Kim, H. & Kim, C., 2010. Directly applicable microbial fuel cells in aeration tank for wastewater treatment. *Bioelectrochemistry,* Volume 78, pp. 72-79.

Chaundhuri, S. K. & Lovley, D. R., 2003. Electrcity generation by oxidation of glucose in mediatorless microbial fuel cells. *Nature Biotechnology,* 21(10), pp. 1229-1232.

Cheng, J., Zhu, X., Ni, J. & Borthwick, A., 2010. Palm oil mill effluent tratment using a two-stage microbial fuel cell system integrated with immobilized biological aerated filters. *Bioresource Technology,* Volume 101, pp. 2729-2734.

Cheng, S., Liu, H. & Logan, B. E., 2006a. Increased performance of single-chamber microbial fuel cellls using an improved cathode structure. *Electrochemsitry Communications,* Volume 8, pp. 489-494.

Cheng, S., Liu, H. & Logan, B. E., 2006b. Power Densities Using Different Cathode Catalysts (Pt and CoTMPP) and Polymer Binders (Nafion and PTFE) in Single Chamber Microbial Fuel Cells. *Environmental Science and Technology,* 40(1), pp. 364-369.

Cheng, S. & Logan, B. E., 2007. Ammonia treatment of carbon cloth anodes to enhance power generation of microbial fuel cells. *Electrochemistry Communications,* Volume 9, pp. 492-496.

Choi, Y., Kim, N., Kim, S. & Jung, S., 2003. Dynamic Behaviors of Redox Mediators within the Hydrophobic layers as an Important Factor for Effective Microbial Fuel Cell Operation. *Bulletin of the Korean Chemical Society,* 24(4), pp. 437-440.

Chou, T., Whiteley, C. G. & Lee, D., 2014. Anodic potential on dual-chambered microbial fuel cell with sulphate reducing bacteria biofilm. *Internation Journal of Hydrogen Energy ,* Volume 39, pp. 19225-19231.

Chou, T. Y., Whiteley, C. G., Lee, D. & Liao, Q., 2013. Control of dual-chambered microbial fuel cell by anodic potential: Implications with sulfate reducing bacteria. *International Journal of Hydrogen Energy,* Volume 38, pp. 15580-15589.

Clauwaert, P., van der Ha, D., Boon, N., Verbeken, K., Verhaege, M., Rabaey, K. & Verstraete, W., 2007. Open Air Biocathode Enables Effective Electricity Generation in Microbial Fuel Cells. *Environmental Science and Technology,* 41(21), pp. 7564-7569.

Cline, J. D., 1969. Spectrophotometric determination of hydrogen sulphide in natural waters. *Limnology and Oceanography,* Volume 14, pp. 454-458.

Cristiani, P., Carvalho, M. L., Guerrini, E., Daghio, M., Santoro, C. & Li, B., 2013. Cathodic and anodic biofilms in Single Chamber Microbial Fuel Cells. *Bioelectrochemistry,* Volume 92, pp. 6-13.

Dean, J. A., 1999. *Lange's Handbook of Chemistry.* 15th ed. New York: McGraw-Hill.

Dutta , P. K., Rabaey, K., Yuan, Z. & Keller, J., 2008. Spontaneous electrochemical removal of aqueous sulphide. *Water Research,* Volume 42, pp. 4965-4975.

Du, Z., Li, H. & Gu, T., 2007. A state of the art review on microbial fuel cells: A promising technology for wastewater treatment and bioenergy. *Biotechnology Advances,* Volume 25, pp. 464-482.

Gazea, B., Adam, K. & Kontopoulos , A., 1996. A review of passive systems for the treatment of acid mine drainage. *Mnerals Engineering,* 9(1), pp. 23-42.

Ghangrekar, M. M. & Shinde, V. B., 2007. Performance of membrane-less microbial fuel cell treating wastewater and effect of electrode distance and area on electricity production. *Bioresource Technology,* Volume 98, pp. 2879-2885.

Hammack, R. W., Edenborn, H. M. & Dvorak, D. H., 1994. Treatment of water from an open-pit copper mine using biogenic sulfide and limestone: A feasibility study. *Water Research,* 28(11), pp. 2321-2329.

Harnisch, F. & Freguia, S., 2012. A Basic Tutorial on Cyclic Voltammetry for the Investigation of Electroactive Microbial Biofilms. *Chemistry - An Asian Journal,* 7(3), pp. 466-475.

Hassan, S. H., Kim, Y. S. & Oh, S. E., 2012. Power generation from cellulose using mixed and pure cultures of cellulose-degrading bacteria in a microbial fuel cell. *Enzyme and Microbial Technology,* Volume 51, pp. 269-273.

Heidelberg, J. F., Paulsen, I. T., Nelson, K. E., Galdos, E. J. & Nelson, W. C., 2002. Genome sequence of dissimilatory metal ion-reducing bacterium Shewanella oneidensis. *Nature Biotechnology,* Volume 20, pp. 1118-1122.

Heimann, A. C., Friis, A. K. & Jakobsen, R., 2005. Effects of sulfate on anaerobic chloroethane degradation by an enriched culture under transient and steady-state hydrogen supply. *Water Research,* Volume 39, pp. 3579-3586.

Herrera, L. Hernandez, J., Bravo, L., Romo, L. & Vera, L., 1997. Biological Process for Sulfate and Metals Abatement from Mine Effluents. *Biological Process for Sulphate and Metals,* 12(2), pp. 101-107.

He, Z. & Angenent, L. T., 2006. Review: Application of Bacteria Biocathodes in Microbial Fuel Cells. *Electroanalysis,* Volume 18, pp. 2009-2015.

He, Z., Minteer, S. D. & Angenent, L. T., 2005. Electricity Generation from Artificial Wastewater Using and Upflow Microbial Fuel Cell. *Environmental Science and Technology,* 39(14), pp. 5262-5267.

Ieropoulos, I. A., Greenman, J., Melhuish, C. & Hart, J., 2005. Comparative study of three types of microbial fuel cell. *Enzyme and Microbial Technology,* Volume 37, pp. 238-245.

Jang, J. K. Pham, T. H., Chang, I. S., Kang, K. H., Moon, H., Cho, K. S. & Kim, B. H., 2004. Construction and operation of a novel mediator-less and membrane-less microbial fuel cell. *Process Biochemistry,* Volume 39, pp. 1007-1012.

Janssen, A. J., Ma, S. C., Lens, P. & Lettinga, G., 1997. Performance of a Sulfide-Oxidizing Expanded-Bed Reactor Supplied with Dissolved Oxygen. *Biotechnology and Bioengineering,* Volume 53, pp. 32-40.

Janssen, A. J., Meijer, S., Bontsema, J. & Lettinga, G., 1998. Application of the Redox Potential for Controlling a Sulfide Oxidizing Bioreactor. *Biotechnology and Bioengineering,* 60(2), pp. 147-155.

Jiang, J. K. & Li, B., 2009. Granular activated carbon single-chamber microbial fuel cell (GAC-SCMFCs): A design suitable for large-scale wastewater treatment processes. *Biochemical Engineering Journal,* Volume 47, pp. 31-37.

Johnson, D. B. & Hallberg, K. B., 2005. Acid mine drainage remediation options: a review. *Science of the Total Environment,* Volume 338, pp. 3-14.

Kaksonen, A. H., Riekkola-Vanhanen, M. L. & Puhakka, J. A., 2003. Optimization of metal sulphide precipitation in fluidized-bed treatment of acidic wastewater. *Water Research,* Volume 37, pp. 255-266.

Kim, B. H., Ikeda, T., Park, H. S., Kim, H. J., Hyum , M. S., Kano, K., Takagi, K. & Tatsumi, H., 1999. Electrochemical activity of an Fe(III)-reducing bacterium, Shewanella putrefaciens IR-1, in the presence of alternative elctron acceptors. *Biotechnology Techniques,* Volume 13, pp. 475-478.

Kim, H. J., Park, H. S., Hyum, M. S., Chang, I. S., Kim, M. & Kim, B. H., 2002. A mediator-less microbial fuel cell using a metal reducing bacterium, Shewanella putrefaciens. *Enzyme and Microbial Technology,* Volume 30, pp. 145-152..

Kokabian, B. & Gude, V. G., 2015. Role of membranes in bioelectrochemical systems. *Membrane Water Treatment,* 6(1).

Krishna, K. V., Sarkar, O. & Mohan, S. V., 2014. Bioelectrochemical treatment of paper and pulp wastewater in comparison with anaerobic process: Integrating chemical coagulation with simultaneous power production. *Bioresource Technology,* Volume 174, pp. 142-151.

Kuo, W. C. & Shu, T. Y., 2004. Biological pre-treatment of wastwater containing sulfate using anaerobic immobilized cells. *Journal of Hazardous Materials,* Volume 113, pp. 147-155.

Lanthier, M., Gregory, K. B. & Lovley, D. R., 2008. Growth with high planktonic biomass in Shewanella oneidensis fuel cells. *FEMS Microbiolgy Letters,* Volume 278, pp. 29-35.

Lee, D. J., Lee, C. Y. & Chang, J. S., 2012. Treatment and electricity harvesting from sulfate/sulfide-containing wastewaters using microbial fuel cell with enriched sulfate-reducing mixed culture. *Journal of Hazardous Materials,* Volume 243, pp. 67-72.

Lee, D. J., Liu, X. & Weng, H. L., 2014. Sulfate and organic carbon removal by microbial fuel cells with sulfate-reducing bacteria and sulphide-oxidisng bacteria. *Bioresource Technology,* Volume 156, pp. 14-19.

Lens, P. N., Visser, A., Janssen, A. J., Hulshoff Pol, L. W. & Lettinga, G., 1998. Biotechnological treatment of sulfate-rich wastewaters. *Critical Reviews in Environmental Science and Technology,* 28(1), pp. 41-88.

Liu, H., Cheng, S. & Logan, B. E., 2005a. Microbial Fuel Cells as a Function of Ionic Strength, Temperature and Reactor Configuration. *Environmental Science and Technology,* Volume 39, pp. 5488-5493.

Liu, H., Cheng, S. & Logan, B. E., 2005b. Production of Electricity from Acetate or Butyrate Using a Single-Chamber Microbial Fuel Cell. *Environmental Science and Technology,* 39(2), pp. 658-662.

Liu, H. & Logan, B. E., 2004. Electricity Generation Using an Air-Cathode Single Chamber Microbial Fuel Cell in the Presence and Absence of a Proton Exchange Membrane. *Environmental Science and Technology,* Volume 38, pp. 4040-4046.

Liu, X. W., Wang, Y. P., Huang, Y. X., Sun, X. F., Sheng, G. P., Zeng, R. J., Li, F., Dong, F., Wang, S. G., Tong, Z. H. & Yu, H. Q., 2011. Integration of a Microbial Fuel Cell With Activated Sludge Process for Energy-Saving Wastewater Treatment: Taking a Sequencing Batch Reactor as an Example. *Biotechnology and Bioengineering,* Volume 108, pp. 1260-1267.

Logan, B., Cheng, S., Watson, V. & Estadt, G., 2007. Graphite Fiber Brush ANodes for Increased Power Production in Air-Cathode Microbial Fuel Cells. *Environmental Science and Technology,* 41(9), pp. 3341-3346.

Logan, B. E., 2008. *Microbial Fuel Cells.* 1st ed. New Jersey: John Wiley & Sons Inc.

Logan, B. E., 2009. Exoelectrogenic bacteria that power microbial fuel cells. *Nature Reviews Microbiology,* Volume 7, pp. 375-381.

Logan, B. E., Hamelers, B., Rozendal, R., Schroder, U., Keller, J., Freguia, S., Aelterman, P., Verstraete, W. & Rabaey, K., 2006. Microbial Fuel Cells: Methodology and Technology. *Environmental Science and Technology,* 40(17), pp. 5181-5192.

Logan, B. E. & Regan, J. M., 2006. Electricity-producing bacterial communities in microbial fuel cells. *TRENDS in Microbiology,* 14(12), pp. 512-518.

Lovley, D. R. & Phillips, E. J., 1987. Competitive Mechanisms for Inhibition of Sulfate Reduction and Methane Production in the Zone of Ferric Iron Reduction in Sediments. *Applied and Environmental Microbiology,* 53(11), pp. 2636-2641.

Lovley, D. R., Phillips, E. J. & Lonergan, D. J., 1989. Hydrogen and Formate Oxidation Coupled to Dissimilatory Reduction of Iron or Manganese by Altermonas putrefaciens. *Applied and Environmental Microbiology,* 55(3), pp. 700-706.

Lowy, D. A., Tender, L. M., Zeikus, J. G., Park, D. H. & Lovley, D. R., 2006. Harvesting energy from the marine sediment-water interface II Kinetic activity of anode materials. *Biosensors and Bioelectronics,* Volume 21, pp. 2058-2063.

Menert, A., Paalme, V., Juhkam, J. & Vilu, R., 2004. Characterization of sulfate-reducing bacteria in yeast waste by microcalorimetry and PCR amplification. *Thermochimica Acta,* Volume 420, pp. 89-98.

Min, B. & Logan, B. E., 2004. Continuous Electricity Generation from Domestic Wastewater and Organic Substrate in a Flat Plate Microbial Fuel Cell. *Environmental Science and Technology,* 38(21), pp. 5809-5814.

Molwantwa, J. B. & Rose, P. D., 2013. Development of a Linear Flow Channel Reactor for the sulphur removal in acid mine wastewater treatment operations. *Water SA,* 39(5), pp. 649-653.

Mooruth, N., 2011. *Passive treatment of Acid Mine Drainage via a linear flow channel reactor utilising a floating sulphur biofilm.* Aachen, Germany, Internation Mine Water Association.

Moosa, S. & Harrison, S. T., 2006. Product inhibition by sulphide species on biological sulphate reduction for the treatment of acid mine drainage. *Hydrometallurgy,* Volume 83, pp. 214-222.

Myers, C. R. & Myers, J. M., 1992. Loacalization of Cytrochromes to the Outer Membrane of the Anaerobically Groqn Shewanella putrefaciens MR-1. *Journal of Bacteriology,* 174(11), pp. 3429-3438.

Nevin, K. P., Richter, H., Covalla, S. F., Johnson, J. P., Woodard, T. L., Orloff, A. L., Jia, H., Zhang, M. & Lovley, D. R., 2008. Power output and columbic efficiencies from biofilms of Geobacter sulfurreducens comparable to mixed community microbial fuel cells. *Environmental Microbiolgy,* 10(10), pp. 2505-2514.

Nielsen, P. H., 1987. Biofilm dynamics and kinetics during high rate sulfate reduction under anaerobic conditions. *Applied Environmental Microbiology,* 53(1), pp. 27-32.

O'Flaherty, V., Mahony, T., O'Kennedy, R. & Colleran, E., 1998. Effect of pH on growth kinetics and sulphide toxicity thresholds of a range of methanogenic, syntrophic and sulphate-reducing bacteria. *Process Biochemistry,* 33(5), pp. 555-569.

Omil, F., Lens, P., Hulshoff Pol, L. & Lettinga, G., 1996. Effect of Upward Velocity and SUlphide Concentration on Volatile Fatty Acid Degradation in a Sulphidogenic Granular Sludge Reactor. *Process Biochemistry,* 31(7), pp. 699-710.

Oude Elferink, S. J., Visser, A., Hulshoff Pol, L. W. & Stams, A. J., 1994. Sulfate reduction in methanogenic bioreactors. *FEMS Microbiology Reviews,* 15(2-3), pp. 119-136.

Oyekola, O. O., van Hille, R. P. & Harrions, S. T. L., 2009. Study of anaerobic lactate metabolism under biosulfidogenic conditions. *Water Research,* Volume 43, pp. 3345-3354.

Park, D. H. & Zeikus, J. G., 2000. Electricity Generation in Microbial Fuel Cells Using Neutral Red as an Electronophore. *Applied and Environmental Microbiology,* 66(4), pp. 1292-1297.

Park, D. H. & Zeikus, J. G., 2002. Impact of electrode composition on electricity generation in a single-compartment fuel cell using Shewanella putrefaciens. *Applied Microbiology and Biotechnology,* Volume 59, pp. 58-61.

Patidar, S. K. & Tare, V., 2005. Effect of molybdate on methanogenic and sulfiogenic activity of biomass. *Bioresource Technology,* Volume 96, pp. 1215-1222.

Pinchuk, G. E., Geydebrekht, O. V., Hill, E. A., Reed, J. L., Konopka, A. E., Beliaev, A. S &, Fredrickson, J. K., 2011. Puyruvate and Lactate Metabolism by Shewanella oneidensis MR-1 under Fermentation, Oxygen Limitation, and Fumerate Respiration Conditions. *Applied and Envrionmental Microbiology,* 77(23), pp. 8234-8240.

Pirbadian, S., Barchinger, S. E., Leung, K. M., Byun, H. S., Jangir, Y., Bouhenni, R. A., Reed, S. B., Romaine, M. F. & Saffarini, D. A., 2014. Shewanella oneidensis MR-1 nanowires are outer membrand and periplasmic extensions of the extracellular electron transport components. *PNAS,* 111(35), pp. 12883-12888.

Pokorna, D. & Zabranska, J., 2015. Sulfur-oxidizing bacteria in environmental technology. *Biotechnology Advances.*

Postgate, J., 1984. *The Sulfate-Reducing Bacteria.* 2nd ed. Cambridge: Cambridge University Press.

Purdy, K. J., Nedwell, D. B., Embley, T. M. & Takii, S., 1997. Use of 16s rRNA-targeted oligonucleotide probes to investigate the occurrence and selection of sulfate-reducing bacteria in response to nutrient addition to sediment slurry microcosms from a Japanese estuary. *FEMS Microbial Ecology,* Volume 24, pp. 221-234.

Rabaey, K., Boon, N., Siciliano, S. D., Verhaege, M. & Verstraete, W., 2004. Biofuel Cells Select for Microbial Consortia that Self-Mediate Electron Transfer. *Applied and Environmental Microbiology,* 70(9), pp. 5373-5382.

Rabaey, K., Clauwaert, P., Aelterman, P. & Verstraete, W., 2005. Tubular Microbial Fuel Cells for Efficient Electricity Generation. *Environmental Science and Technology,* Volume 39, pp. 8077-8082.

Rabaey, K, van de Sompel, K., Maignien, L., Boon, N. & Aelterman, P., 2006. Microbial Fuel Cells for Sulfide Removal. *Environmental Science and Technology,* 40(17), pp. 5218-5224.

Ravenschlag, K., Sahm , K., Knoblauch, C., Jorgensen, B. B. & Amann, R., 2000. Community Structure, Cellular rRNA Content and Activity of Sulfate-Reducing Bacteria in Marine Arctic Sediments. *Applied and Environmental Microbiology,* 66(8), pp. 3592-3602.

Ringeisen, B. R., Henderson, E., Wu, P. K., Pietron, J., Ray, R., Little, B., Biffinger, J. & Jones-Meehan, J M., 2006. High Power Density from a Miniature Microbial Fuel Cell Using Shewanella oneidensis DSP10. *Environmental Science and Technology,* Volume 40, pp. 2629-2634.

Ringø, E., Stenberg, E. & Strom, A. R., 1984. Amino Acid and Lactate Catabolism in Trimethylamine Oxide Respiration of Alteromonas putrefaciens NCMB 1735. *Applied and Environmental Microbiology,* 47(5), pp. 1084-1089.

Sangcharoen, A., Niyom, W. & Suwannaslip, B. B., 2015. A microbial fuel cell treating organic wastewater containing high sulfate under continuous operation: Performance and microbial community. *Process Biochemistry,* Volume 50, pp. 1648-1655.

Sevda, S., Dominguez-Benetton, X., Vanbroekhoven, K., De Wever, H., Sreekrishnan, T. E. & Pant, D., 2013. High strength wastewater treatment accompanied by power generation sing air cathode microbial fuel cell. *Applied Energy,* Volume 105, pp. 194-206.

Shen, Y. & Buick, R., 2004. The antiquity of microbial sulfate reduction. *Earth-Science Reviews,* Volume 64, pp. 243-272.

Sukkasem, C., Laehlah, S., Hniman, A., O'thong, S. & Boonsawang, P., 2011. Upflow bio-filter (UFBF): Biocatalyst microbial fuel cell (MFC) configuration and application to biodiesel wastewater treatment. *Bioresource Technology,* Volume 102, pp. 10363-10370.

Sun, M., Tong, Z. H., Sheng, G. P., Chen, Y. Z., Zhang, F., Mu, Z. X., Wang, H. L., Zeng, R. J., Liu, X. W., Yu, H. Q. & Ma, F., 2010. Microbial communities involved in electricity generation from sulfide oxidation in a microbial fuel cell. *Biosensors and Bioelectronics,* Volume 26, pp. 470-476.

Su, X., Tian, Y., Sun, Z., Lu, Y. & Li, Z., 2013. Performance of a combined system of microbial fuel cell and membrane bioreactor: Wastewater treatment, sludge reduction, energy recovery and membrane fouling. *Biosensors and Bioelectronics,* Volume 42, pp. 92-98.

Tang, Y. J., Meadows, A. L. & Keasling, J. D., 2007a. A Kinetic Model Describing Shewanella oneidensis MR-1 Growth, Substrate Consumption, and Product Secretion. *Biotechnology and Bioengineering,* 96(1), pp. 125-133.

Tang, Y. J., Meadows, A. L., Kirby, J. & Keasling, J. D., 2007b. Anaerobic Central Metabolic Pathways in Shewanella oneidensis MR-1 Reinterpreted in the Light of Isotopic Metabolite Labeling. *Journal of Bacteriology,* 189(3), pp. 894-901.

van Hille, R., Marais, T. & Harrison, S., 2015. *Biomass Retention and Recycling to Enhance Sulfate Reduction Kinetics.* Santiago, Chile, 10th ICARD & IMWA Annual Conference.

van Hille, R. P., van Vyk, N. & Mooruth, M. N., 2011. *Lessons in passive treatment: Towards efficient operation of a sulphate reduction-sulphide oxidation system.* Aachen, Germany, International Mine Water Association.

van Houten, R. T., van der Spoel, H., van Aelst, A. C., Hulshoff Pol, L. W. & Lettinga, G., 1995. Biological Sulfate Reduction Using Synthesis Gas as Energy and Carbon Source. *Biotechnology and Bioengineering,* Volume 50, pp. 135-144.

Visser, A., Hulshoff Pol, L. W. & Lettinga, G., 1996. Competition of methanogenic and sulfidogenic bacteria. *Water Science and Technology,* 33(3), pp. 99-110.

von Canstein, H., Ogawa, J., Shimizu, S. & Lloyd, J. R., 2008. Secretion of flavins by Shewanella species and their role in extracellular electron transfer. *Applied Environmental Microbiology,* 74(3), pp. 615-623.

Wang, H. & Pilon, L., 2012. Physical interpretation of cyclic voltammetry for measuring electric double layer capacitances. *Electrochimica Acta,* Volume 64, pp. 130-139.

Wang, Y., Liu, X., Li, W., Li, F., Wang, Y., Sheng, G., Zeng, R. J. & Yu, H., 2012. A microbial fuel cell-membrane bioreactor integrated system for cost effective wastewater treatment. *Applied Energy,* Volume 98, pp. 230-235.

Wang, Y., Zhang, H., Li, W., Liu, X., Sheng, G. & Yu, H., 2014. Improving electricity generation and substrate removal of a MFC-SBR system through optimization of COD loading distribution. *Biochemical Engineering Journal,* Volume 85, pp. 15-20.

Weng, H. L. & Lee, D. J., 2015. Performance of sulfate reducing bacteria-microbial fuel cells: reproducibility. *Journal of the Taiwan Institute of Chemical Engineers,* Volume 56, pp. 148-153.

Widdel, F., 1988. Microbiology and ecology of sulfate- and sulfur-reducing bacteria. In: J. B. Zehnder, ed. *Biology of anaerobic microorganisms.* New York: Wiley and Sons, pp. 469-526.

Winfield, J., Ieropoulos, I., Greenman, J. & Dennis, J., 2011. The overshoot phenomenon as a function of internal resistance in microbial fuel cells. *Bioelectrochemistry,* Volume 81, pp. 22-27.

Wu, C. et al., 2013a. Electron acceptor dependence of electron shuttle secretion and extracellular electron transfer by Shewanella oneidensis MR-1. *Bioresource Technology,* Volume 136, pp. 711-714.

Wu, D., Cheng, Y., Li, B., Li, W., Li, D. & Yu, H., 2013b. Ferric iron enhances electricity generation by Shewanella oneidensis MR-1 in MFCs. *Bioresource Technology,* Volume 135, pp. 630-634.

Wu, D., Xing, D., Mei, X., Liu, B., Guo, G. & Ren, N., 2013c. Electricity generation by Shewanella sp. HN-41 in microbial fuel cells. *International Journal of Hydrogen Energy,* Volume 38, pp. 15565-15573.

Xing, D., Zuo, Y., Cheng, S., Regan, J. M. & Logan, B. E., 2008. Electricity Generation by Rhodopseudomonas palustris DX-1. *Environmental Science and Technology,* 42(11), pp. 4146-4151.

You, S., Zhao, Q., Zhang, J., Jiang, J., Wan, C., Du, M. & Zhao, S., 2007. A graphite-granule membrane-less tubular air-cathode microbial fuel cell for power generation under continuously operational conditions. *Journal of Power Sources,* Volume 173, pp. 172-177.

Zhang, G., Wang, K., Zhao, Q., Jiao, Y. & Lee, D., 2012. Effect of cathode types on long-term performance and anode bacterial communities in microbial fuel cells. *Bioresource Technologies,* Volume 118, pp. 249-256.

Zhao, F., Rahunen, N., Varcoe, J. R., Chandra, A., Avignone-Rossa, C., Thumser, A. E. & Slade, R. C., 2008. Activated Carbon CLoth as Anode for Sulfate removal in Microbial Fuel Cell. *Environmental Science and Technology,* 42(13), pp. 4971-4976.

Zhao, F., Rahunen, N., Varcoe, J. R., Roberts, A. J., Avignone-Rossa, C., Thumser, A. E. & Slade, R. C., 2009. Factors affecting the performance of microbial fuel cells for sulfur pollutant removal. *Biosensors and Bioelectronics,* Volume 24, pp. 1931-1936.

Zhu, F., Wang, W., Zhang, X. & Tao, G., 2011. Electricity generation in a membrane-less microbial fuel cell with down-flow feeding onto the cathode. *Bioresource Technology,* Volume 102, pp. 7324-7328.

Appendix A

A.1 Determination of COD concentration

A.1.1 Shewanella oneidensis MR-1 Samples

Details of this method are given in Section 3 above

Standard Curve

Mean values: n=3; R^2 =0.9999

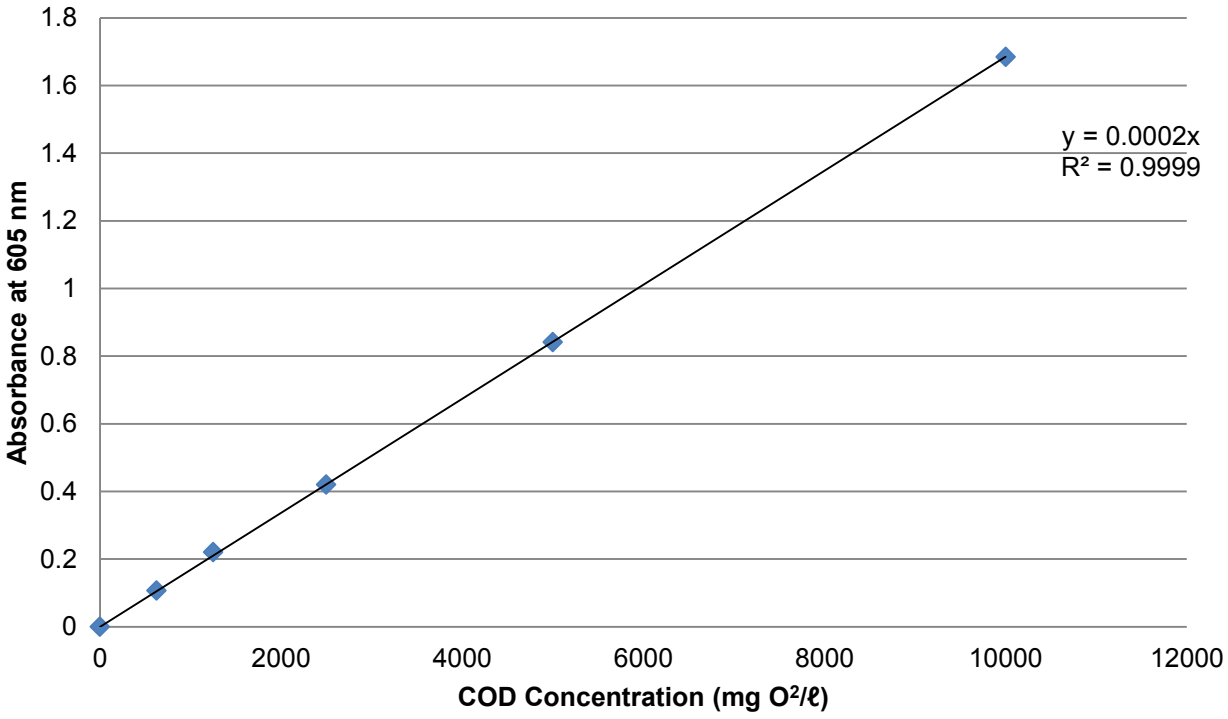

Figure A 1: High concentration (500-10000 mg/ℓ) COD standard curve

Reagents

3. COD reagent A (Merck 1.14679.0495)
4. COD reagent B (Merck 1.4680.0495)

A.1.2 Mixed Community of SRB and SOB Samples

Details of this method are given in Section 3 above

Standard Curve

Mean values: n=3; R2 =0.9976

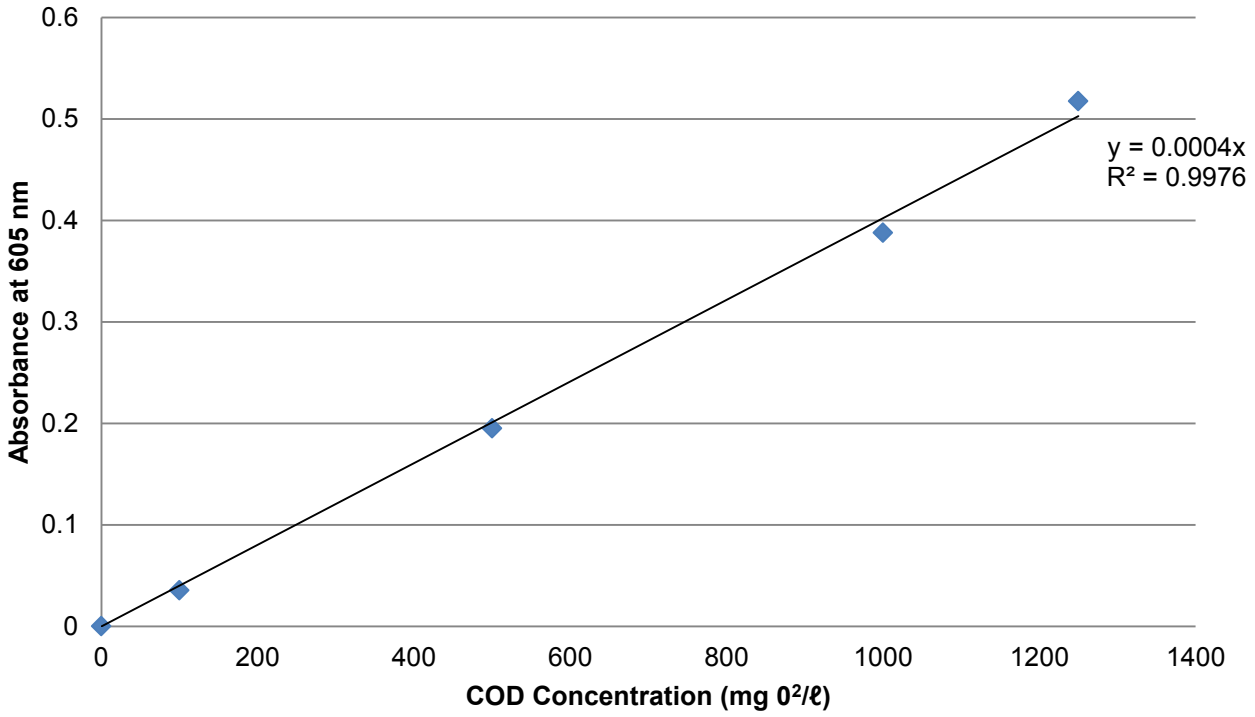

Figure A 2: Low concentration (100-1500 mg/ℓ) COD standard curve

Reagents

5. COD reagent A (Merck 1.14679.0065)
6. COD reagent B (Merck 1.4680.0495)

A.2 Determination of Volatile Fatty Acid Concentration

Details of the HPLC used to determine volatile fatty acid concentration are given in Section 3 above.

Standard Curve

A new standard curve was plotted for every run done using HPLC. This is an example of one curves plotted.

VFA	Lactate	Acetate	Propionate	Butyrate	Iso-butyrate	Valerate	Iso-valerate
R^2	0.9998	0.9997	0.9999	0.9999	0.9998	0.9999	0.9998
Gradient	1920.5	1431	1417.1	1704.3	1238	1379.8	1145.2

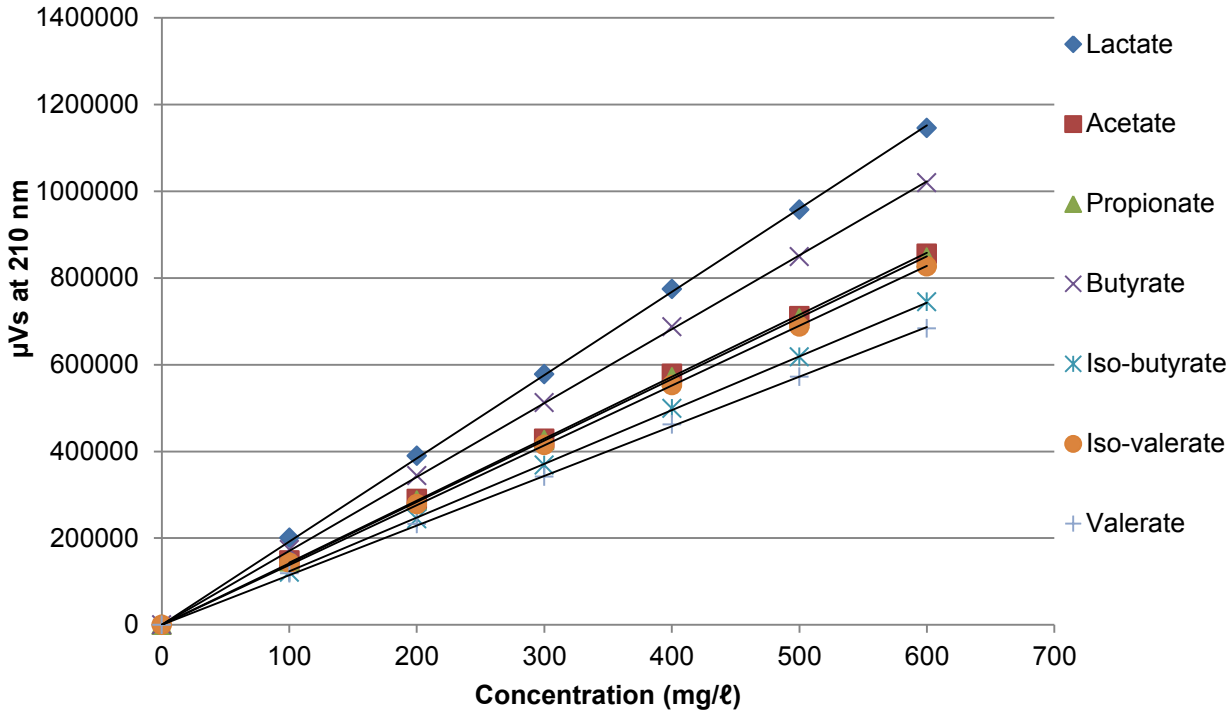

Figure A 3: Volatile fatty acid standard curve

Reagents:

A.3 Determination of Iron Concentration

Details of the assay method used to determine sulphate concentration are given in Section 3 above.

Standard Curve

Mean values: n=3, R^2=0.9999

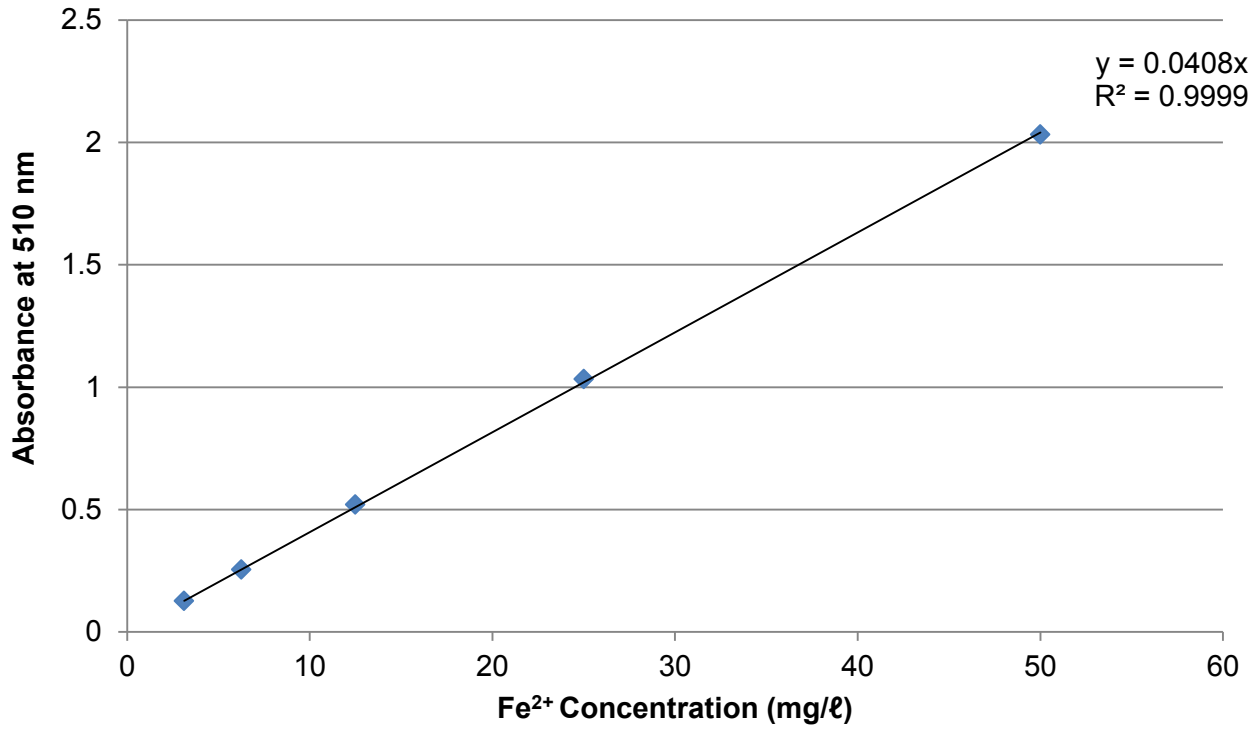

Figure A 4: Ferrous iron standard curve

Reagents:

7. Standard Ferrous iron solution (100 mg/ℓ Fe^{2+}): dissolved 497.629 mg of $FeSO_4.7H_2O$ in 20 mℓ of concentrated H_2SO_4 in 50 mℓ of deionised water. Dilute to 1000 mℓ with deionised water.
8. 1-10 phenanthroline indicator solution: 2127.708 mg of 1-10 phenanthroline (as $C_{12}H_8N_2.H_2O$) in about 100 mℓ of deionised water. Diluted to 1000 mℓ with deionised water giving a concentration of 1-10 phenanthroline in excess of the stoichiometric requirements.
9. Ammonium acetate buffer solution: 250 g of ammonium acetate ($NH_4C_2H_3O_2$) in 150 mℓ of deionised water. Add 700 mℓ of concentrated glacial acetic acid.

A.4 Determination of Sulphate Concentration

A.4.1 Using Ion Chromatography

Details of the IC method used to determine sulphate concentration are given in Section 3 above.

Standard Curve

A new standard curve was plotted for every run done using IC. This is an example of one curves plotted.

Mean values: R^2=0.9993

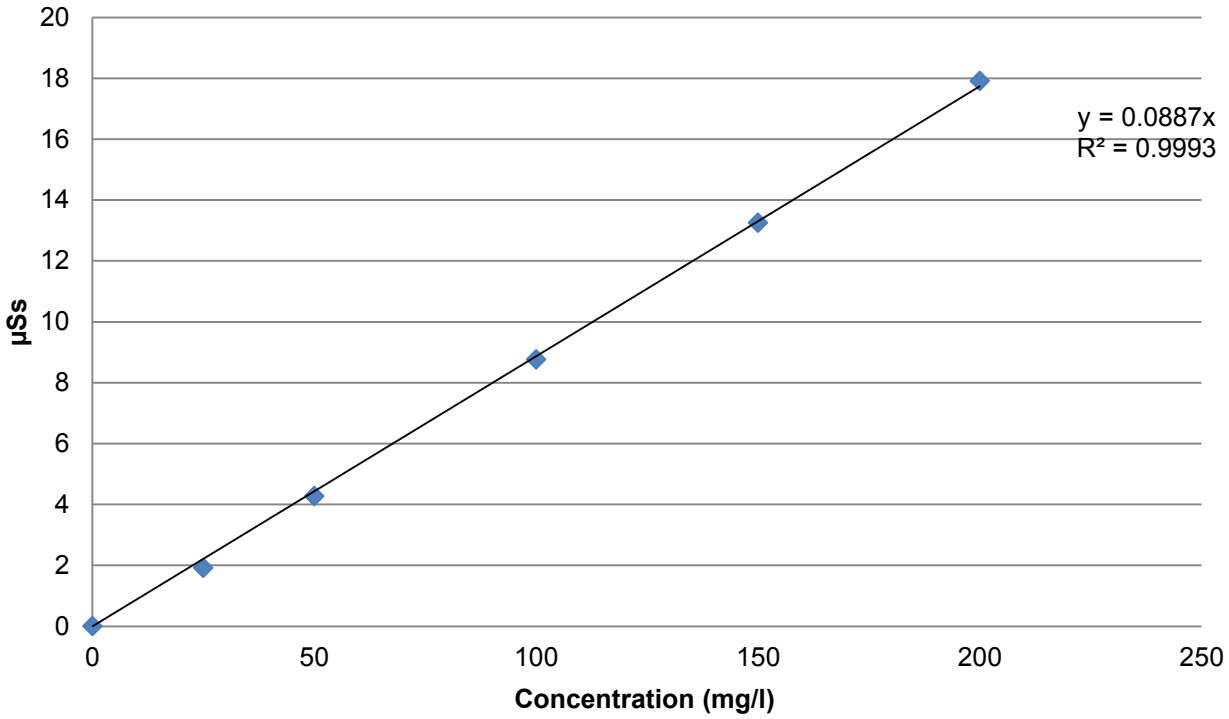

Figure A 5: Sulphate standard curve using ion chromatography

Reagents

10. Standard sulphate solution: 0.1479 g Na_2SO_4 in 1ℓ of deionised water to make 1g/ℓ solution

A.4.2 Using Barium Chloride Assay

Details of the assay method used to determine sulphate concentration are given in Section 3 above.

Standard Curve

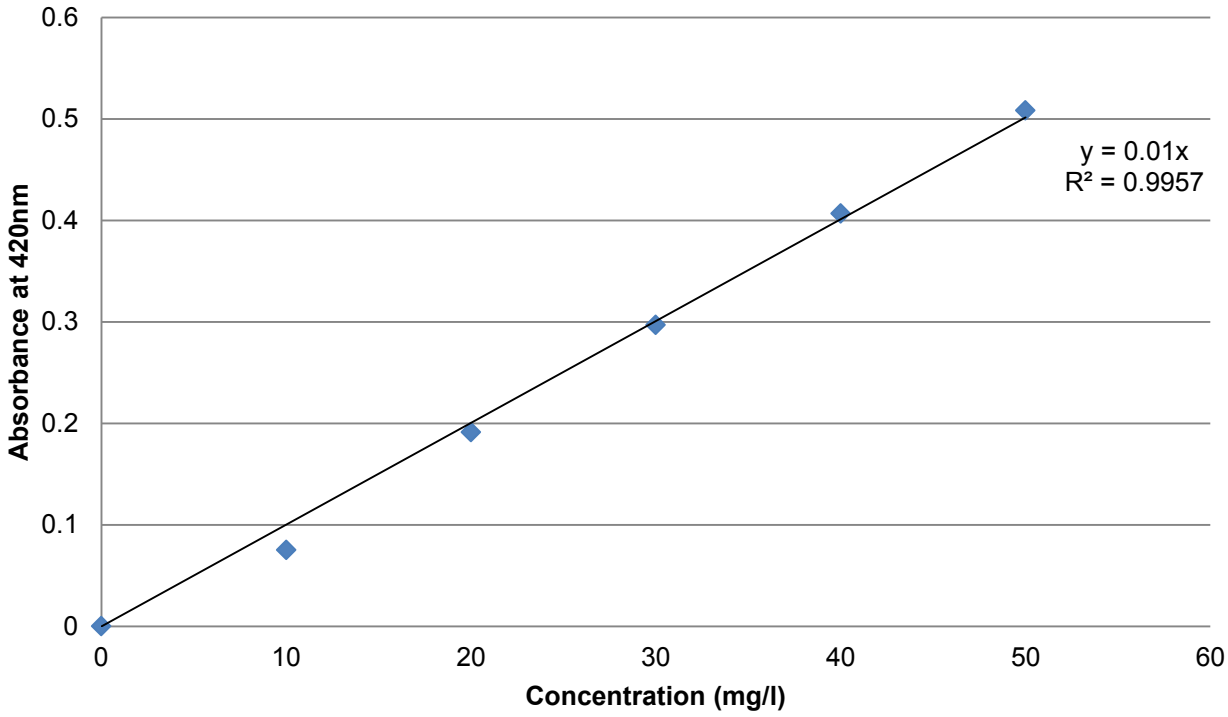

Figure A 6: Sulphate standard curve using a barium chloride assay

Reagents

11. Conditioning agent : 300 mℓ of deionised H_2O, 100 mℓ absolute ethanol, 50 mℓ glycerol, 30 mℓ 32% HCl and 75 g NaCl)
12. Barium chloride crystals : 20 to 30 mesh or finer
13. Standard sulphate solution: 0.1479 g Na_2SO_4 in 1ℓ of deionised water to make 1g/ℓ solution

A.5 Determination of Sulphide Concentration

Details of this method are given in Section 3 above.

Standard Curve

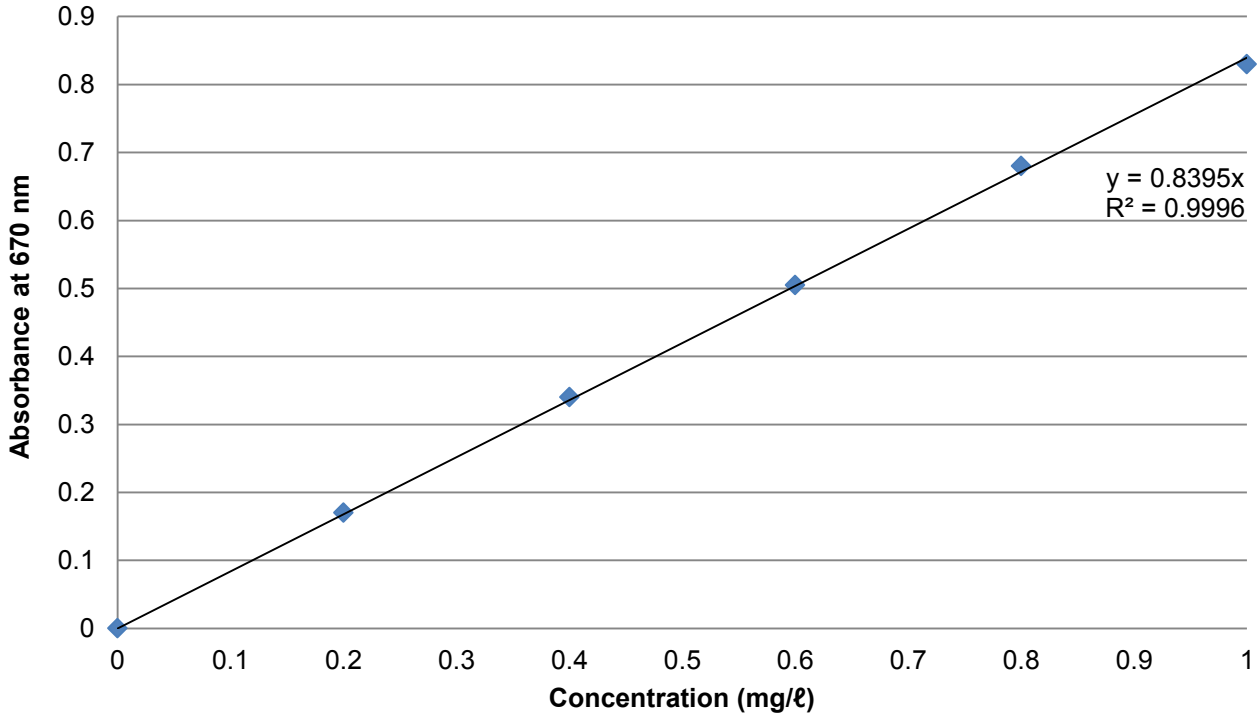

Figure A 7: Sulphide standard curve

Reagents

14. Zinc acetate solution: 10 g of zinc acetate dissolved in 1000 mℓ of deionised water
15. DMPD solution : 2 g of N,N-dimethyl-p-phenylenediamine dihydrochloride dissolved in 500 mℓ of 6 M HCl)
16. Ferric chloride solution: 8 g of ferric chloride dissolved in 6 M HCl
17. Standard sulphide solution: 750 mg of $Na_2S.9H_2O$ in 1000 mℓ of deionised water

Appendix B

B.1 Replication of Literature

B.1.1 Volatile Fatty Acids

Table A 1: Table of absorbance area at 210 nm obtained with HPLC and the corresponding lactate concentration for samples diluted 1:4

Days since inoculation	Lactate		Acetate	
	Area (μVs)	*Concentration (mg/ℓ)*	*Area (μVs)*	*Concentration (mg/ℓ)*
51	625026	1257	-	-
53	736539	1481	-	-
55	674289	1356	129056	322
57	943470	1897	-	-
59	788565	1586	-	-
61	804946	1619	-	-
63	801913	1613	-	-
65	783341	1575	-	-
67	629762	1266	-	-
69	734738	1478	-	-
71	798501	1606	-	-
73	604980	1217	59495	148
75	696521	1401	-	-
77	725391	1459	-	-
79	766883	1542	120907	302
81	519372	1044	102671	256
83	664914	1337	-	-
85	671275	1350	97455	243
87	544986	1096	-	-
89	632003	1271	70910	177

B.1.2 COD Concentration

Table A 2: Table of absorbance at 605 nm obtained and the corresponding COD concentration diluted 1:5

Days Since Inoculation	*Absorbance*				*Concentration (mg/ℓ)*
	1	**2**	**3**	**Average**	
47	0.619	0.606	0.606	0.610	15153
49	0.607	0.617	0.619	0.614	15253
51	0.485	0.487	0.491	0.488	12087
53	0.594	0.600	0.583	0.592	14703
55	0.577	0.575	0.619	0.590	14653

Days Since Inoculation	*Absorbance*				*Concentration (mg/ℓ)*
	1	**2**	**3**	**Average**	
57	0.606	0.605	0.599	0.603	14978
59	0.619	0.622	0.639	0.627	15562
61	0.606	0.603	0.614	0.608	15087
63	0.481	0.504	0.503	0.496	12295
65	0.524	0.490	0.508	0.507	12578
67	0.590	0.605	0.652	0.616	15287
69	0.601	0.573	0.604	0.593	14712
71	0.619	0.609	0.611	0.613	15220
73	0.624	0.577	0.624	0.608	15103
75	0.632	0.612	0.596	0.613	15228
77	0.425	0.410	0.414	0.416	10303
79	0.600	0.621	-	0.611	15158
81	0.613	0.631	0.602	0.615	15278
83	0.598	0.595	0.580	0.591	14670
85	0.614	0.618	0.615	0.616	15287
87	0.623	0.627	0.611	0.620	15403
89	0.623	0.618	0.640	0.627	15570

Table A 3: Results of t-test on lactate concentration and COD for MFC with a 10 kΩ and 100 kΩ resistor

	Lactate Concentration	**COD**
t-value	2.82	0.117
t-critical	2.10	2.36
p-critical	0.011	0.910

B.2 Effect of Lactate Concentration

B.2.1 Volatile Fatty Acids

Table A 4: Table of absorbance area at 210 nm obtained with HPLC and the corresponding lactate concentration for samples from MFCs fed 20 mM and 40 mM lactate feed and diluted 1:4

Days Since inoculation	20 mM Lactate		40 mM Lactate	
	Area (μVs)	*Concentration (mg/ℓ)*	*Area (μVs)*	*Concentration (mg/ℓ)*
17	-	-	1438232	3825
19	-	-	1487297	3956
21	-	-	-	-
23	-	-	1936542	3923
25	645672	1308	1877364	3803
27	606072	1228	1930033	3910
29	606814	1229	1971236	3994
31	638366	1293	1879422	3808
33	605046	1226	2080410	4215
35	482639	978	1629572	3301
37	655120	1327	1813597	3674
39	497338	1008	1594288	3230
41	617888	1252	1109997	2249
43	650421	1318	1479451	2997
45	675303.2	1368	1756393	3558
47	463560	939	1823436	3694
49	-	-	1688027	3420
51	381784.8	773	1895407	3840
53	509444	1032	2118178	4291
55	591428	1198	2128266	4312

B.2.2 COD Concentration

Table A 5: Table of absorbance at 605 nm obtained and the corresponding COD concentration for samples from MFCs fed 20 mM and 40 mM lactate feed diluted 1:5

	20 mM Lactate					40 mM Lactate				
Days Since Inoculation	*Absorbance*				*Concentration (mg/ℓ)*	*Absorbance*				*Concentration (mg/ℓ)*
	1	**2**	**3**	**Average**		**1**	**2**	**3**	**Average**	
17	-	-	-	-	-	-	-	-	-	-
19	-	-	-	-	-	-	-	-	-	-
21	-	-	-	-	-	-	-	-	-	-
23	-	-	-	-	-	0.668	0.710	0.668	0.682	16945
25	0.615	0.625	-	0.620	15395	0.607	0.636	0.614	0.619	15370
27	0.614	0.603	0.587	0.601	14928	0.678	0.676	0.680	0.678	16845
29	0.619	0.594	0.611	0.608	15095	0.653	0.688	0.659	0.667	16562
31	0.578	0.579	0.555	0.571	14162	0.676	0.669	0.666	0.670	16653
33	0.601	0.599	0.575	0.592	14687	0.422	0.417	0.417	0.419	10362
35	0.612	0.616	0.618	0.615	15278	0.656	0.666	0.666	0.663	16462
37	0.617	0.608	0.610	0.612	15187	0.673	0.672	0.666	0.670	16653
39	0.562	0.565	0.574	0.567	14070	0.646	0.676	0.673	0.665	16520
41	0.579	0.582	0.580	0.580	14403	0.621	0.616	0.667	0.635	15762
43	0.593	0.583	0.587	0.588	14587	0.658	0.674	0.652	0.661	16428
45	0.325	0.321	0.330	0.325	8028	-	-	-	-	-
47	0.608	0.610	0.608	0.609	15112	0.435	0.436	0.425	0.432	10695
49	0.608	0.639	0.605	0.617	15328	0.659	0.668	0.664	0.664	16487
51	0.100	0.109	0.091	0.100	2395	0.598	0.586	0.574	0.586	14545
53	0.586	0.587	0.581	0.585	14512	0.658	0.647	-	0.653	16208
55	0.463	0.469	0.470	0.467	11578	0.698	0.641	0.655	0.665	16512

B.3 Addition of Ferric Citrate

B.3.1 Volatile Fatty Acids

Table A 6: Table of absorbance area at 210 nm obtained with HPLC and the corresponding lactate concentration for samples from MFCs fed 20 mM lactate and 6 mM ferric citrate and diluted 1:4

Days since inoculation	Cell 1			Cell 1		
	Days	*Area (µVs)*	*Concentration (mg/ℓ)*	**Days**	*Area (µVs)*	*Concentration (mg/ℓ)*
61	2	115947	235	-	-	-
63	4	309634	627	-	-	-
65	6	691485	1401	-	-	-
67	8	658127	1334	2	306904	622
69	10	721795	1463	4	691668	1402
71	12	694361	1407	6	814007	1649
73	14	690446	1399	8	824537	1671
75	16	-	-	10	-	-
77	18	920721	1866	12	848487	1719
79	-	-	-	14	852310	1727
81	-	-	-	16	865703	1754
83	-	-	-	18	890186	1804

B.3.2 COD Concentration

Table A 7: Table of absorbance at 605 nm obtained and the corresponding COD concentration for samples from MFCs fed 20 mM lactate and 6 mM ferric citrate feed diluted 1:5

Days Since Inoculation	Cell 1						Cell 2					
	Days	*Absorbance*				*Concentration (mg/ℓ)*	Days	*Absorbance*				*Concentration (mg/ℓ)*
		1	2	3	Average			1	2	3	Average	
61	2	0.598	0.578	0.569	0.582	14437	-	-	-	-	-	-
63	4	0.519	0.524	0.500	0.514	12753	-	-	-	-	-	-
65	6	0.525	0.531	0.505	0.520	12903	-	-	-	-	-	-
67	8	0.654	0.645	-	0.650	16133	2	0.577	0.618	0.603	0.599	14878
69	10	0.603	0.649	0.622	0.625	15512	4	0.604	0.655	0.639	0.633	15712
71	12	0.644	0.648	0.643	0.645	16020	6	0.638	0.647	0.659	0.648	16095
73	14	0.649	0.644	0.656	0.650	16137	8	0.652	0.654	0.649	0.652	16187
75	16	0.680	0.660	0.648	0.663	16462	10	0.485	0.488	0.476	0.483	11970
77	18	0.673	0.636	0.680	0.663	16470	12	0.651	0.645	0.620	0.639	15862
79	-	-	-	-	-	-	14	0.635	0.665	0.638	0.646	16045
81	-	-	-	-	-	-	16	0.655	0.660	-	0.658	16333
83	-	-	-	-	-	-	18	0.628	0.607	0.597	0.611	15162

B.3.3 Iron Concentration

Table A 8: Table of absorbance at 510 nm obtained and the corresponding ferric iron concentration for samples from MFCs fed 20 mM lactate and 6 mM ferric citrate feed at various dilutions

Days Since Inoculation	Cell 1							Cell 2						
	Days	*Absorbance*				Dilution	*Concentration (mg/ℓ)*	Days	*Absorbance*				Dilution	*Concentration (mg/ℓ)*
		1	2	3	Average				1	2	3	Average		
61	2	0.175	0.171	0.169	0.099	2	4.86	-	-	-	-	-	-	-
63	4	0.034	0.023	0.024	0.033	10	8.07	-	-	-	-	-	-	-
65	6	0.040	0.046	0.031	0.067	6.67	10.9	-	-	-	-	-	-	-
67	8	0.090	0.103	0.090	0.057	1	1.38	2	0.124	0.228	0.258	0.135	1	3.31
69	10	0.015	0.019	0.022	0.029	2	1.41	4	0.064	0.068	0.070	0.054	2	2.64
71	12	0.034	0.040	0.043	0.037	2	1.82	6	0.035	0.033	-	0.073	2	3.59
73	14	0.035	0.037	0.034	0.021	2	1.04	8	0.088	0.087	0.124	0.058	2	2.84
75	16	0.009	0.008	0.005	0.047	2	2.29	10	0.016	0.017	0.017	0.029	2	1.43
77	18	0.089	0.083	0.087	0.066	1.67	2.67	12	0.040	0.039	0.046	0.035	1.67	1.44
79	20	0.033	0.031	0.070	0.045	1.43	1.56	14	0.032	0.028	0.027	0.027	2	1.30
81	-	-	-	-	-	-	-	16	0.023	0.024	0.025	0.024	1.67	0.992
83	-	-	-	-	-	-	-	18	0.025	0.026	0.023	0.023	1.25	0.703

Appendix C

C.1 Single-Chambered MFC with Carbon Felt Anode

C.1.1 Concentration of Sulphur Species

Table A 9: Table of area obtained with ion chromatography and the corresponding sulphate concentration for samples 4 MFCs and diluted 1:10

Days Since Inoculation	MFC 1		MFC 2		MFC 3		MFC 4	
	Area (µSs)	*Concentration (mg/ℓ)*	*Area (µSs)*	*Concentration (mg/ℓ)*	*Area (µSs)*	*Concentration (mg/ℓ)*	*Area (µSs)*	*Concentration (mg/ℓ)*
0	15.2	1741	15.2	1741	15.2	1741	-	-
1	18.0	2055	16.3	1866	17.5	1999	-	-
2	18.6	2122	20.0	2285	17.7	2020	23.13	2640
3	17.4	1990	18.8	2143	15.2	1732	17.65	2015
4	16.8	1919	14.3	1635	5.5	630	13.80	1575
5	15.7	1795	18.6	2122	10.3	1179	15.46	1765
6	15.6	1782	17.4	1987	15.5	1765	10.77	1230
7	15.7	1797	16.5	1887	15.4	1755	13.10	1495
8	5.77	659	15.1	1727	14.5	1651	12.92	1475
9	14.8	1686	15.9	1817	14.2	1620	11.65	1330
10	13.2	1502	14.1	1604	12.8	1462	-	-
11	14.0	1596	-	-	8.60	982	12.44	1420
12	12.2	1394	-	-	9.80	1119	-	-
13	11.9	1361	14.4	1641	9.17	1047	11.12	1269
14	11.4	1306	-	-	8.56	977	10.76	1228
15	11.6	1326	-	-	8.02	915	10.40	1187
16	11.2	1278	14.1	1610	8.08	923	9.81	1120
17	10.6	1212	-	-	-	-	9.59	1095

Days Since Inoculation	MFC 1		MFC 2		MFC 3		MFC 4	
	Area (µSs)	*Concentration (mg/ℓ)*	*Area (µSs)*	*Concentration (mg/ℓ)*	*Area (µSs)*	*Concentration (mg/ℓ)*	*Area (µSs)*	*Concentration (mg/ℓ)*
18	9.74	1112	-	-	7.13	814	9.69	1106
19	-	-	12.6	1438	-	-	9.42	1076
20	8.75	999	-	-	7.22	824	-	-
21	-	-	11.0	1258	-	-	10.08	1151
22	7.28	831			7.24	827	-	-
23	-	-	11.0	1254	-	-	11.85	1352
24	6.52	745	-	-	6.77	773	-	-
25	-	-	10.9	1243	-	-	13.49	1540
26	5.97	682	-	-	6.58	752	-	-
27	-	-	9.74	1112	-	-	-	-
28	15.6	1783	-	-	6.00	685	13.79	1574
30	5.97	681	-	-	-	-	12.45	1422
32	6.33	722	-	-	6.03	688	15.00	1712
33	-	-	5.98	683	-	-	-	-
34	-	-	-	-	5.93	677	12.44	1420
36	-	-	-	-	-	-	9.87	1127
38	-	-	-	-	3.87	442	9.93	1133
40	-	-	-	-	-	-	9.71	1109
42	-	-	-	-	-	-	9.62	1098
43	-	-	-	-	-	-	5.84	667
45	-	-	-	-	-	-	9.61	1097
47	-	-	-	-	-	-	8.70	993
49	-	-	-	-	-	-	7.89	900
51	-	-	-	-	-	-	7.24	827
53	-	-	-	-	-	-	7.49	855
55	-	-	-	-	-	-	6.40	730

Days Since Inoculation	MFC 1		MFC 2		MFC 3		MFC 4	
	Area (µSs)	*Concentration (mg/ℓ)*	*Area (µSs)*	*Concentration (mg/ℓ)*	*Area (µSs)*	*Concentration (mg/ℓ)*	*Area (µSs)*	*Concentration (mg/ℓ)*
57	-	-	-	-	-	-	6.49	740
59	-	-	-	-	-	-	6.06	692
61	-	-	-	-	-	-	6.18	706
63	-	-	-	-	-	-	7.02	802
65	-	-	-	-	-	-	6.07	693
67	-	-	-	-	-	-	5.34	610
69	-	-	-	-	-	-	6.04	689

Calculations

The rate of sulphate reduction over a given feeding cycle (r_n) in mg/ℓ/day was calculated by:

$$r_n = \frac{C_n - C_{n-1}}{n-1}$$ Equation 33

where C_n and C_{n-1} are the concentrations of sulphate in MFC at the end of day n the end of the previous feeding cycle respectively (mg/ℓ). The average sulphate reduction rate over a period of time was calculated by Equation 34.

$$r_s = \frac{\sum_{i=1}^{n} r_i}{n}$$ Equation 34

Table A 10: Results of t-test on the rates of sulphate reduction for MFC 1-3 from day 3 to day 10

MFC		MFC		
		1	2	3
1	t-value		-0.003	0.08
	t-critical		2.31	2.36
	P-value		0.998	0.938
2	t-value	-0.003		0.073
	t-critical	2.31		2.2
	P-value	0.998		0.943

C.1.2 Concentration of Volatile Fatty Acids

Table A 11: Table of absorbance area at 210 nm obtained with HPLC and the corresponding lactate concentration for samples from 4 MFCs and diluted 1:5

Days Since Inoculation	MFC 1		MFC 2		MFC 3		MFC 4	
	Area (μVs)	*Concentration (mg/ℓ)*	*Area (μVs)*	*Concentration (mg/ℓ)*	*Area (μVs)*	*Concentration (mg/ℓ)*	*Area (μVs)*	*Concentration (mg/ℓ)*
1	39762	140	47153	165	65986	232		
2	91278	320	118938	417	114800	403	444469	1187
3	102339	359	104766	368	94225	331	158585	424
4	33391	117	3104	10.9	3564	12.5	136500	365
5	0	0.00	2765	9.19	1135	3.77	134648	360
6	1189	3.95	3404	11.3	2535	8.43	80242	214
7	1221	4.06	2684	8.92	2257	7.50	50433	135
8	1694	5.63	3242	10.8	7071	23.5	40226	107
9	4229	14.06	5347	17.8	2269	7.54	3313	8.85
10	6496	21.60	4906	16.3	6761	22.5	-	-
11	-	-	-	-	520	4.31	8170	21.8
12	1051	8.71	-	-	1240	10.3	-	-
13	-	-	1641	13.6	688	5.70	0	0.00
14	1853	15.36	-	-	988	8.19	4373	14.5
15	-	-	-	-	722	5.98	7342	24.4
16	0	0.00	2931	7.78	0	0.00	0	0.00
17	-	-	-	-	0	0.00	3577	11.9
18	5135	13.63	-	-	0	0.00	0	0.00
19	-	-	0	0.00	-	-	4546	15.1
20	3732	9.90	18038	47.9	0	0.00	-	-
21	-	-	-	-	-	-	2092	6.96
22	1517	4.03	0	0.00	14562	38.52	-	-

Days Since Inoculation	MFC 1		MFC 2		MFC 3		MFC 4	
	Area (μVs)	*Concentration (mg/ℓ)*	*Area (μVs)*	*Concentration (mg/ℓ)*	*Area (μVs)*	*Concentration (mg/ℓ)*	*Area (μVs)*	*Concentration (mg/ℓ)*
23	-	-	-	-	-	-	0	0.00
24	966	2.56	0	0.00	0	0.00	-	-
25	-	-	-	-	-	-	2314	7.69
26	1306	3.47	2287	6.07	0	0.00	-	-
27	-	-	-	-	-	-	1864	6.20
28	999	2.65	699	1.85	0	0.00	20268	67.4
30	1561	4.14	0	0	0	0.00	13330	44.3
32	0	0	0	0	0	0.00	3574	11.9
34	-	-	-	-	1828	4.83	9250	30.8
36	-	-	-	-	9774	25.9	5552	18.5
38	-	-	-	-	-	-	0	0.00
40	-	-	-	-	-	-	24015	79.8
42	-	-	-	-	-	-	9791	32.6
43	-	-	-	-	-	-	11678	38.8
45	-	-	-	-	-	-	2368	19.6
47	-	-	-	-	-	-	789	6.54
49	-	-	-	-	-	-	0	0.00
51	-	-	-	-	-	-	0	0.00
53	-	-	-	-	-	-	0	0.00
55	-	-	-	-	-	-	0	0.00
57	-	-	-	-	-	-	0	0.00
59	-	-	-	-	-	-	0	0.00
61	-	-	-	-	-	-	0	0.00
63	-	-	-	-	-	-	0	0.00
65	-	-	-	-	-	-	0	0.00
67	-	-	-	-	-	-	0	0.00

Days Since Inoculation	MFC 1		MFC 2		MFC 3		MFC 4	
	Area (μVs)	*Concentration (mg/ℓ)*	*Area (μVs)*	*Concentration (mg/ℓ)*	*Area (μVs)*	*Concentration (mg/ℓ)*	*Area (μVs)*	*Concentration (mg/ℓ)*
69	-	-	-	-	-	-	0	0.00

Table A 12: Table of absorbance area at 210 nm obtained with HPLC and the corresponding acetate concentration for samples from 4 MFCs and diluted 1:5

Days Since Inoculation	MFC 1		MFC 2		MFC 3		MFC 4	
	Area (μVs)	*Concentration (mg/ℓ)*	*Area (μVs)*	*Concentration (mg/ℓ)*	*Area (μVs)*	*Concentration (mg/ℓ)*	*Area (μVs)*	*Concentration (mg/ℓ)*
1	138554	488	162116	571	161144	567	-	-
2	159705	562	165707	583	139681	492	345503	1226
3	12299	43.3	109238	385	12606	44.4	145548	516
4	4742	16.7	6617	23.3	6647	23.4	30273	107
5	6819	24.9	2933	10.7	1679	6.14	18668	66.2
6	5434	19.9	3387	12.4	2964	10.83	10157	36.0
7	7457	27.3	6209	22.7	1948	7.12	28811	102
8	12953	47.3	12266	44.8	4114	15.0	49255	175
9	10009	36.6	13081	47.8	2852	10.4	78102	277
10	81486	298	77437	283	8937	32.7	108106	383
11	-	-	-	-	18739	165	-	-
12	10111	89.1	-	-	15421	136	142820	484
13	-	-	8991	79.2	14551	128	-	-
14	8036	70.8	-	-	32668	288	161894	549
15	-	-	-	-	50248	443	149405	506
16	6017	20.8	6768	23.4	114417	404	156828	531
17	-	-	-	-	164379	581	145590	493
18	20635	71.4	-	-	205305	726	144738	490
19	-	-	26873	92.9	-	-	138440	469
20	59666	207	125573	434	221502	783	120961	410
21	-	-	-	-	-	-	-	-
22	67018	232	137224	474	264777	936	116541	395
23	-	-	-	-	-	-	-	-
24	88351	306	195821	677	263823	933	120855	410

Days Since Inoculation	MFC 1		MFC 2		MFC 3		MFC 4	
	Area (μVs)	*Concentration (mg/ℓ)*	*Area (μVs)*	*Concentration (mg/ℓ)*	*Area (μVs)*	*Concentration (mg/ℓ)*	*Area (μVs)*	*Concentration (mg/ℓ)*
25	-	-	-	-	-	-	-	-
26	136294	472	227040	785	147308	0.00	111145	377
27	-	-	-	-	-	-	-	-
28	170897	592	265419	917	284163	1004	89516	303
30	85534	296	291791	1008	282867	1000	84873	288
32	244116	845	329418	1138	313852	1109	157653	534
34	-	-	-	-	308396	1090	196024	664
36	-	-	-	-	311363	1101	103742	365
38	-	-	-	-	-	-	111644	393
40	-	-	-	-	-	-	263097	962
42	-	-	-	-	-	-	196369	718
43	-	-	-	-	-	-	248568	909
45	-	-	-	-	-	-	129551	1141
47	-	-	-	-	-	-	137087	1208
49	-	-	-	-	-	-	314865	1117
51	-	-	-	-	-	-	296665	1052
53	-	-	-	-	-	-	288465	1023
55	-	-	-	-	-	-	260800	925
57	-	-	-	-	-	-	289348	1026
59	-	-	-	-	-	-	298232	1058
61	-	-	-	-	-	-	238971	848
63	-	-	-	-	-	-	311604	1105
65	-	-	-	-	-	-	312405	1108
67	-	-	-	-	-	-	322784	1145
69	-	-	-	-	-	-	285869	1014

Table A 13: Table of absorbance area at 210 nm obtained with HPLC and the corresponding propionate concentration for samples from 4 MFCs and diluted 1:5

Days Since Inoculation	MFC 1		MFC 2		MFC 3		MFC 4	
	Area (μVs)	*Concentration (mg/ℓ)*	*Area (μVs)*	*Concentration (mg/ℓ)*	*Area (μVs)*	*Concentration (mg/ℓ)*	*Area (μVs)*	*Concentration (mg/ℓ)*
1	0	0	0	0	0	0	-	-
2	0	0	0	0	0	0	35626	132
3	0	0.0	0	0	0	0.0	8548	32
4	0	0.0	0	0.0	0	0.0	14046	52.1
5	5777	22.2	5985	23.0	5491	21.06	17685	65.7
6	6555	25.1	6291	24.1	5983	22.95	10970	41
7	6143	23.6	6212	23.8	6021	23.09	34283	127
8	5765	22.1	5815	22.3	5642	21.6	36652	136
9	5719	21.9	5994	23.0	5452	20.9	66278	246
10	6079	23	5939	23	5609	21.5	-	-
11	-	-	-	-	0	0	102523	381
12	1762	16.7	-	-	1833	17	-	-
13	-	-	1096	10.4	1514	14	115557	421
14	1843	17.5	-	-	1854	18	104979	383
15	-	-	-	-	1683	16	99689	363
16	160249	586.7	111576	408.7	175369	647	119250	435
17	-	-	-	-	198021	730	129410	472
18	181760	665.4	-	-	188309	695	166696	608
19	-	-	176820	647.6	-	-	127359	464
20	223341	818	150529	551	232518	858	-	-
21	-	-	-	-	-	-	111784	407
22	279250	1022	197511	723	247155	912	-	-
23	-	-	-	-	-	-	111276	406

Days Since Inoculation	MFC 1		MFC 2		MFC 3		MFC 4	
	Area (μVs)	*Concentration (mg/ℓ)*	*Area (μVs)*	*Concentration (mg/ℓ)*	*Area (μVs)*	*Concentration (mg/ℓ)*	*Area (μVs)*	*Concentration (mg/ℓ)*
24	299169	1095	265861	974	197422	728	-	-
25	-	-	-	-	-	-	123063	449
26	263406	964	289401	1060	105435	0.00	-	-
27	-	-	-	-	-	-	144001	525
28	207666	760	314808	1153	196290	724	91555	334
30	34195	125	305916	1120	177042	653	96495	352
32	28071	103	375855	1377	189617	699	39589	144
34	-	-	-	-	209768	774	19933	73
36	-	-	-	-	236733	873	0	0
38	-	-	-	-	-	-	0	0
40	-	-	-	-	-	-	5236	20
42	-	-	-	-	-	-	5627	22
43	-	-	-	-	-	-	0	0
45	-	-	-	-	-	-	26803	254
47	-	-	-	-	-	-	24964	236
49	-	-	-	-	-	-	37134	138
51	-	-	-	-	-	-	30492	113
53	-	-	-	-	-	-	31930	119
55	-	-	-	-	-	-	16605	62
57	-	-	-	-	-	-	22333	83
59	-	-	-	-	-	-	298232	1107
61	-	-	-	-	-	-	18879	70
63	-	-	-	-	-	-	16367	61
65	-	-	-	-	-	-	6609	25
67	-	-	-	-	-	-	22516	84

Days Since Inoculation	MFC 1		MFC 2		MFC 3		MFC 4	
	Area (μVs)	*Concentration (mg/ℓ)*	*Area (μVs)*	*Concentration (mg/ℓ)*	*Area (μVs)*	*Concentration (mg/ℓ)*	*Area (μVs)*	*Concentration (mg/ℓ)*
69	-	-	-	-	-	-	27110	101

C.1.3 Concentration of COD

Table A 14: Table of absorbance at 605 nm obtained and the corresponding COD concentration for 4 MFCs diluted to various concentrations

Days Since Inoculation	MFC 1			MFC 1			MFC 1			MFC 1		
	Abs	*Dilution*	*Concentration (mg/ℓ)*	*Abs*	*Dilution*	*Concentration (mg/ℓ)*	*Abs*	*Dilution*	*Concentration (mg/ℓ)*	*Abs*	*Dilution*	*Concentration (mg/ℓ)*
1	0.382	3	2865	0.338	3	2535	0.326	3	2445	-	-	-
2	0.414	3	3105	0.444	3	3330	0.372	3	2790	0.499	3	3743
3	0.194	3	1455	0.316	3	2370	0.152	3	1140	0.209	3	1568
4	0.104	3	780	0.071	3	533	0.065	3	488	0.115	3	863
5	0.045	3	338	0.050	3	375	0.053	3	398	0.195	3	1463
6	0.043	3	323	0.037	3	278	0.044	3	330	0.110	3	825
7	0.060	3	450	0.033	3	248	0.012	3	90.0	0.145	3	1088
8	0.050	3	375	0.054	3	405	0.023	3	173	0.183	3	1373
9	0.044	3	330	0.044	3	330	0.003	3	22.5	0.248	3	1860
10	0.095	3	713	0.077	3	578	0.029	3	218	-	-	-
11	-	-	-	-	-	-	-	-	-	0.213	3	1598
12	0.049	3	368	-	-	-	0.030	3	225	-	-	-
13	-	-	-	0.182	1	455	0.053	3	398	0.239	3	1793
14	0.249	1	622	-	-	-	0.234	1	584	-	-	-
15	-	-	-	-	-	-	0.358	1	896	0.254	3	1905
16	0.187	1	468	0.167	1	418	0.368	1	921	0.288	3	2160
17	-	-	-	-	-	-	-	-	-	-	-	-

Days Since Inoculation	MFC 1			MFC 1			MFC 1			MFC 1		
	Abs	*Dilution*	*Concentration (mg/ℓ)*	*Abs*	*Dilution*	*Concentration (mg/ℓ)*	*Abs*	*Dilution*	*Concentration (mg/ℓ)*	*Abs*	*Dilution*	*Concentration (mg/ℓ)*
18	0.268	1	669	-	-	-	0.571	1	1428	0.278	3	2085
19	-	-	-	0.233	1	582	-	-	-	-	-	-
20	0.342	1	855	0.306	1.5	1148	0.591	1	1478	-	-	-
21	-	-	-	-	-	-	-	-	-	0.230	3	1725
22	0.343	1	858	0.337	1.5	1264	0.417	1.5	1564	-	-	-
23	-	-	-	-	-	-	-	-	-	0.245	3	1838
24	0.252	1	631	0.324	1.5	1216	0.324	1.5	1216	-	-	-
25	-	-	-	-	-	-	-	-	-	0.250	3	1875
26	0.278	1.5	1043	0.394	1.5	1478	0.406	1.5	1521	-	-	-
27	-	-	-	-	-	-	-	-	-	-	-	-
28	0.321	1.52	1205	0.462	1.5	1733	0.445	1.5	1668	0.222	3	1665
30	0.368	1.52	1379	0.492	1.5	1844	0.495	1.5	1858	-	-	-
32	0.448	1.52	1681	0.558	1.5	2093	0.565	1.5	2118	0.106	4	1060
34	-	-	-	-	-	-	0.327	3	2453	0.180	3	1350
36	-	-	-	-	-	-	0.303	3	2269	0.217	3	1628
38	-	-	-	-	-	-	-	-	-	0.214	3	1605
40	-	-	-	-	-	-	-	-	-	0.265	3	1988
42	-	-	-	-	-	-	-	-	-	0.250	3	1875
43	-	-	-	-	-	-	-	-	-	0.248	3	1860
45	-	-	-	-	-	-	-	-	-	0.281	3	2108
47	-	-	-	-	-	-	-	-	-	0.779	1	1947
49	-	-	-	-	-	-	-	-	-	0.499	1.5	1870
51	-	-	-	-	-	-	-	-	-	0.533	1.5	1998
53	-	-	-	-	-	-	-	-	-	0.516	1.5	1935
55	-	-	-	-	-	-	-	-	-	0.496	1.5	1861
57	-	-	-	-	-	-	-	-	-	0.516	1.5	1935

Days Since Inoculation	MFC 1			MFC 1			MFC 1			MFC 1		
	Abs	*Dilution*	*Concentration (mg/ℓ)*	*Abs*	*Dilution*	*Concentration (mg/ℓ)*	*Abs*	*Dilution*	*Concentration (mg/ℓ)*	*Abs*	*Dilution*	*Concentration (mg/ℓ)*
59	-	-	-	-	-	-	-	-	-	0.490	1.5	1836
61	-	-	-	-	-	-	-	-	-	0.460	1.5	1725
63	-	-	-	-	-	-	-	-	-	0.479	1.5	1798
65	-	-	-	-	-	-	-	-	-	0.561	1.5	2105
67	-	-	-	-	-	-	-	-	-	0.309	3	2318
69	-	-	-	-	-	-	-	-	-	0.317	3	2374

C.1.4 Redox Potential and PH

Table A 15: Table of redox potential and pH for samples taken from 4 MFCs

Days Since Inoculation	MFC 1		MFC 2		MFC 3		MFC 4	
	Redox	*pH*	*Redox*	*pH*	*Redox*	*pH*	*Redox*	*pH*
0	-344	7.446	-344	7.446	-344	7.446	-	-
2	-300	7.979	-	8.173	-100	8.403	-	-
3	-273	8.393	-253	7.59	-336	8.132	-	-
4	-	8.372	-376	8.248	-351	8.287	-	-
5	-304	8.34	-420	8.116	-407	8.308	-	-
6	-383	8.173	-380	8.044	-292	8.175	-	-
7	-378	8.094	-399	7.915	-420	8.092	-	-
8	-374	8.034	-383	7.825	-320	8.147	-	-
9	-362	8.204	-340	8.05	-354	8.293	-	-
10	-350	7.835	-342	7.812	-340	8.126	-	-
11	-	-	-	-	-333	8.116	-	-
12	-358	8.023	-	-	-354	8.178	-	-
13	-	-	-250	8.023	-335	8.032	-	-
14	-275	8.245	-	-	-357	7.951	-286	6.837
15	-	-	-	-	-364	7.679	-292	6.977
16		8.287	-350	8.099	-341	7.715	-302	6.935
17	-	-	-	-	-333	7.27	-279	6.875
18	-227	8.024	-	-	-356	7.161	-284	6.938
19	-	-	-330	8.09	-	-	-273	7.074
20	-271	7.998	-328	7.456	-329	7.216	-	-
21	-	-	-	-	-	-	-244	7.143
23	-	-	-	-	-	-	-206	7.071
25	-	-	-	-	-	-	-259	7.051
27	-	-	-	-	-	-	-223	6.971
30	-	-	-	-	-	-	-250	7.162
32	-	-	-	-	-	-	-316	7.086
34	-	-	-	-	-	-	-326	7.248
36	-	-	-	-	-	-	-312	7.126
38	-	-	-	-	-	-	-214	7.38
40	-	-	-	-	-	-	-	7.386
42	-	-	-	-	-	-	-356	7.27
44	-	-	-	-	-	-	-331	7.405
46	-	-	-	-	-	-	-350	7.242
48	-	-	-	-	-	-	-344	7.266
50	-	-	-	-	-	-	-406	7.406
52	-	-	-	-	-	-	-351	7.084
54	-	-	-	-	-	-	319	7.213

C.2 Single-Chambered MFC with Carbon Brush Anode

C.2.1 Concentration of Sulphur Species

Table A 16: Table of absorbance at 420 nm obtained via turbidimetric assay and the corresponding sulphate concentration for a MFC with carbon brush anode and diluted 1:50

Days Since Inoculation	*Absorbance*	*Concentration (mg/ℓ)*
2	0.455	2275
5	0.437	2185
10	0.387	1935
15	0.263	1315
21	-	-
25	0.25	1250
30	0.223	1115
35	0.247	1235
40	0.371	1855
44	0.311	1555
49	0.299	1495
54	0.258	1290

Table A 17: Table of absorbance at 670 nm obtained via colorimetric assay and the corresponding sulphide concentration for a MFC with carbon brush anode and various dilutions

Days Since Inoculation	*Absorbance*				*Dilution*	*Concentration (mg/ℓ)*
	1	**2**	**3**	**Average**		
0	0.802	0.803	0.823	0.809	250	240.9
2	0	0	0	0.000	-	-
5	0.169	0.203	0.2	0.191	50	11.9
10	0.187	0.158	0.16	0.168	50	9.52
15	0.049	0.043	0.033	0.042	50	1.96
21	0	0	0	0.000	-	-
25	0.035	0.025	0.023	0.028	25	0.685
30	0.37	0.328	0.189	0.296	25	5.63
35	0.105	0.074	0.125	0.101	25	3.72
40	0.87	0.694	0.866	0.810	25	25.8
44	0.674	0.421	0.614	0.570	25	18.3
49	0.42	0.36	0.542	0.441	100	64.5
54	0.313	0.325	0.451	0.363	100	53.7

C.2.2 Concentration of Volatile Fatty Acids

Table A 18: Table of absorbance area at 210 nm obtained with HPLC and the corresponding lactate, acetate and propionate concentration for samples from a MFC with carbon fibre brush anode and diluted 1:5

Days Since Inoculation	Lactate		Acetate		Propionate	
	Area (μVs)	*Concentration (mg/ℓ)*	*Area (μVs)*	*Concentration (mg/ℓ)*	*Area (μVs)*	*Concentration (mg/ℓ)*
2	3774	9.76	381969	1325	87380	299
5	4840	12.5	169156	587	35424	121
10	0	0	135634	471	44450	152
15	0	0	130209	452	28497	97.7
21	1261	3.26	149067	517	29039	99.5
25	6467	16.7	168737	585	13429	46.0
30	0	0	208121	722	14085	48.3
35	0	0	130949	909	4584	15.7
40	0	0	335630	1164	55132	189
44	0	0	411527	1442	100983	357
49	0	0	494730	1733	160062	566
54	0	0	485377	1701	178185	630

C.2.3 Concentration of COD

Table A 19: Table of absorbance at 605 nm obtained and the corresponding COD concentration for samples from a MFC with carbon fibre brush anode and diluted to various concentrations

Days since inoculation	*Average*	*Dilution*	*Concentration (mg/ℓ)*
2	0.608	1.5	2280
5	0.503	1.5	1886.25
10	0.309	1.5	1158.75
15	0.334	1.5	1252.5
21	0.325	1.5	1218.75
25	0.312	1.5	1170
30	0.267	1.5	1001.25
35	0.106	1.5	397.5
40	0.706	1.5	2647.5
44	0.781	1.5	2928.75
49	0.503	3	3772.5
54	0.4	3	3000

C.2.4 Redox Potential and pH

Table A 20: Table of redox potential and pH for samples taken from a MFC with carbon fibre brush anode

Days Since Inoculation	*Redox*	*pH*
0	-427	8.238
2	-350	8.489
5	-394	8.044
10	-376	7.903
15	-	7.998
21	-360	7.651
25	-360	7.595
30	-357	7.278
35	-347	7.444
40	-365	7.098
44	-361	7.271
49	-360	6.972
54	-337	6.917

C.3 Single-Chambered MFC with Concentrated Feed

C.3.1 Concentration of Sulphur Species

Table A 21: Table of absorbance at 420 nm obtained via turbidimetric assay and the corresponding sulphate concentration for a connected and unconnected MFC fed concentrated media and diluted 1:100

Days Since Inoculation	Connected			Unconnected		
	Absorbance	*Dilution*	*Concentration (mg/ℓ)*	*Absorbance*	*Dilution*	*Concentration (mg/ℓ)*
1	0.336	100	3360	0.402	100	4020
2	0.345	100	3450	0.335	100	3350
3	0.477	100	4770	0.384	100	3840
4	0.331	100	3310	0.340	100	3400
6	0.408	100	4080	0.350	100	3500
8	0.298	100	2980	0.336	100	3360
10	0.294	100	2940	0.319	100	3190
12	0.256	100	2560	0.470	100	4700
14	0.251	100	2510	0.302	100	3020
17	-	-	-	0.324	100	3240
19	0.222	100	2220	0.264	100	2635
21	-	-	-	0.273	100	2730
23	-	-	-	0.293	100	2933
25	0.203	100	2027	-	-	-
28	-	-	-	0.319	100	3190
29	0.38	50	1900	-	-	-

Table A 22: Table of absorbance at 420 nm obtained via turbidimetric assay and the corresponding sulphate concentration for MFC 5and diluted 1:50

Days Since Inoculation	*Absorbance*	*Concentration (mg/ℓ)*
2	0.226	1130
3	0.351	1755
4	0.373	1865
6	0.386	1930
8	0.457	2285
10	0.407	2035
12	0.333	1665
15	0.468	2340
17	0.365	1825
19	0.336	1680
21	0.262	1310
25	0.233	1165
27	0.230	1150
29	0.222	1110
31	0.205	1025
33	0.440	2200
35	0.249	1245
37	0.249	1245
40	0.357	1785
43	0.437	2185
45	0.400	2000
47	0.413	2065
49	0.454	2270
51	0.447	2235
53	0.472	2360
55	0.461	2305

Table A 23: Table of absorbance at 670 nm obtained via colorimetric assay and the corresponding sulphide concentration for MFC 5 with various dilutions

Days Since Inoculation	*Absorbance*				*Dilution*	*Concentration (mg/ℓ)*
	1	**2**	**3**	**Average**		
0	0.802	0.803	0.823	0.809	250	241
2	0.000	0.000	0.000	0.000	-	0
4	0.000	0.000	0.000	0.000	-	0
6	0.000	0.000	0.000	0.000	-	0

Days Since Inoculation	*Absorbance*				*Dilution*	*Concentration (mg/ℓ)*
	1	**2**	**3**	**Average**		
8	0.184	0.193	0.200	0.192	25	5.72
10	0.018	0.030	0.016	0.021	25	0.635
12	0.060	0.103	0.174	0.112	25	3.34
17	0.167	0.136	0.094	0.132	25	2.80
19	0.916	0.739	0.713	0.789	25	21.2
21	0.121	0.112		0.117	50	0.00
23	0.000	0.000	0.000	0.000	0	0.00
25	0.026	0.021	0.016	0.021	50	0.95
27	0.185	0.148	0.143	0.159	25	4.26
29	0.175	0.177	0.122	0.158	50	7.26
31	0.047	0.040	0.016	0.034	50	0.952
33	0.156	0.160	0.158	0.158	25	4.70
35	0.228	0.132	0.227	0.196	25	6.76
37	0.202	0.189	0.203	0.198	25	6.04
39	0.234	0.231	0.222	0.229	25	6.61
41	0.624	0.707	0.546	0.626	25	16.3
43	0.291	0.195	0.284	0.257	25	8.45
45	0.375	0.364	0.335	0.358	25	9.97
47	0.411	0.445	0.355	0.404	25	10.6
49	0.256	0.246	0.311	0.271	25	9.26
51	0.294	0.276	0.271	0.280	25	8.07
53	0.216	0.294	0.301	0.270	25	8.96
55	0.238	0.270	0.192	0.233	25	5.71

Table A 24: Table of absorbance at 670 nm obtained via colorimetric assay and the corresponding sulphide concentration for a connected and unconnected MFC fed concentrated media

Days Since Inoculation	Connected						Unconnected					
	Absorbance				*Dilution*	*Concentration (mg/ℓ)*	*Absorbance*				*Dilution*	*Concentration (mg/ℓ)*
	1	**2**	**3**	**Average**			**1**	**2**	**3**	**Average**		
0	1.031	1.038	0.848	0.972	250	289	1.031	1.038	0.848	0.972	250	289
1	0.005	0.005	0.005	0.005	250	1.49	0.008	0.005	0.008	0.007	250	2.08
2	0	0	0	0.000	25	0	0	0	0	0.000	25	0.00
3	0	0	0	0.000	25	0	0	0	0	0.000	25	0.00
4	0.18	0.16	0.25	0.197	25	5.85	0.002	0.013	0.018	0.011	25	0.327
6	0.015	0.014	0.013	0.014	25	0.42	0.005	0.004	0.005	0.005	25	0.139
8	0.073	0.086	0.067	0.075	25	2.24	0.013	0.011	0.012	0.012	25	0.36
10	0.045	0.058	0.067	0.057	25	1.69	0	0	0	0.000	25	0.00
12	0.097	0.114	0.089	0.100	25	2.98	0.077	0.077	0.08	0.078	25	2.32
14	0.081	0.058	0.073	0.071	25	2.10	0.172	0.166	0.122	0.153	25	4.56
17	-	-	-	-	-	-	0.014	0.008	0.022	0.015	25	0.437
19	0.496	0.573	0.613	0.561	25	16.7	0.761	0.623	0.631	0.672	25	20.0
21	-	-	-	-	-	-	0.24	0.196	0.237	0.224	50	13.4
23	-	-	-	-	-	-	0.438	0.445	0.468	0.450	25	13.4
25	0.08	0.084	0.079	0.081	250	24.1	-	-	-	-	-	-
28	-	-	-	-	-	-	0	0	0	0	50	0
29	0.367	0.201	0.377	0.315	250	93.8	-	-	-	-	-	-

C.3.2 Concentration of Volatile Fatty Acids

Table A 25: Table of absorbance area at 210 nm obtained with HPLC and the corresponding lactate concentration for samples from a connected and unconnected MFC fed concentrated media and diluted 1:5

Days Since Inoculation	Connected		Unconnected	
	Area (μVs)	*Concentration (mg/ℓ)*	*Area (μVs)*	*Concentration (mg/ℓ)*
1	0	0	0	0
2	0	0	0	0
3	26949	69.7	311978	806
4	188151	486	0	0
6	0	0	0	0
8	0	0	0	0
10	0	0	0	0
12	0	0	0	0
14	0	0	0	0
17	-	-	0	0
19	0	0	0	0
21	-	-	0	0
23	-	-	0	0
25	0	0	-	-
28	-	-	-	-
29	-	-	-	-

Table A 26: Table of absorbance area at 210 nm obtained with HPLC and the corresponding acetate concentration for a connected and unconnected MFC fed concentrated media and diluted 1:5

Days Since Inoculation	Connected		Unconnected	
	Area (μVs)	*Concentration (mg/ℓ)*	*Area (μVs)*	*Concentration (mg/ℓ)*
1	302043	1058	312558	1095
2	119361	418	180133	631
3	29822	104	18689	65.5
4	76646	269	49828	175
6	144369	506	71271	250
8	219884	770	108984	382
10	335910	1177	119888	420
12	319760	1120	137577	482
14	411941	1439	266274	930
17	-	-	286327	1000
19	468473	1637	389697	1362
21	-	-	450126	1573
23	-	-	473684	1655

25	559119	1954	-	-
28	-	-	-	-
29	-	-	-	-

Table A 27: Table of absorbance area at 210 nm obtained with HPLC and the corresponding propionate concentration for a connected and unconnected MFC fed concentrated media and diluted 1:5

Days Since Inoculation	Connected		Unconnected	
	Area (μVs)	*Concentration (mg/ℓ)*	*Area (μVs)*	*Concentration (mg/ℓ)*
1	302043	1058	0	0
2	119361	418	0	0
3	29822	104	8691	30.7
4	76646	269	55163	195
6	144369	506	71160	252
8	219884	770	99714	353
10	335910	1177	47819	169
12	319760	1120	53184	188
14	411941	1439	90048	318
17	-	-	85072	301
19	468473	1637	49425	175
21	-	-	55901	198
23	-	-	68771	243
25	559119	1954	-	-
28	-	-	-	-
29	-	-	-	-

Table A 28: Table of absorbance area at 210 nm obtained with HPLC and the corresponding lactate, acetate and propionate concentration for samples from MFC 5 diluted 1:5

Day Since Inoculation	Lactate		Acetate		Propionate	
	Area (μVs)	*Concentration (mg/ℓ)*	*Area (μVs)*	*Concentration (mg/ℓ)*	*Area (μVs)*	*Concentration (mg/ℓ)*
2	0	0	57078	198	29616	101
3	0	0	31580	110	41709	143
4	0	0	22729	78.8	0	0.0
6	0	0	102743	356	21121	72.4
8	0	0	25294	87.7	11538	39.5
10	0	0	31118	108	7383	25.3
12	0	0	31772	110	7586	26.0
15	0	0	56802	197	9768	33.5
17	0	0	90042	312	17586	60.3
19	0	0	89992	312	5919	20.3

Day Since Inoculation	Lactate		Acetate		Propionate	
	Area (μVs)	*Concentration (mg/ℓ)*	*Area (μVs)*	*Concentration (mg/ℓ)*	*Area (μVs)*	*Concentration (mg/ℓ)*
21	2542	6.58	123697	429	14419	49.4
23	0	0	145223	504	15935	54.6
25	0	0	162436	564	13463	46.1
27	0	0	178958	621	15678	53.7
29	0	0	188052	652	18077	61.9
31	0	0	159929	555	17968	61.6
33	0	0	214725	745	25975	89.0
35	0	0	221537	769	35946	123
37	0	0	215943	749	42901	147
39	0	0	297822	1033	75750	260
41	0	0	358414	1243	73091	250
43	0	0	413888	1450	108400	383
45	0	0	433654	1519	126228	446
47	21184	54.8	466213	1634	152371	539
49	0	0	449252	1574	179017	633
51	0	0	435133	1525	200101	708
53	0	0	443229	1553	211522	748
55	0	0	351866	1233	181424	642

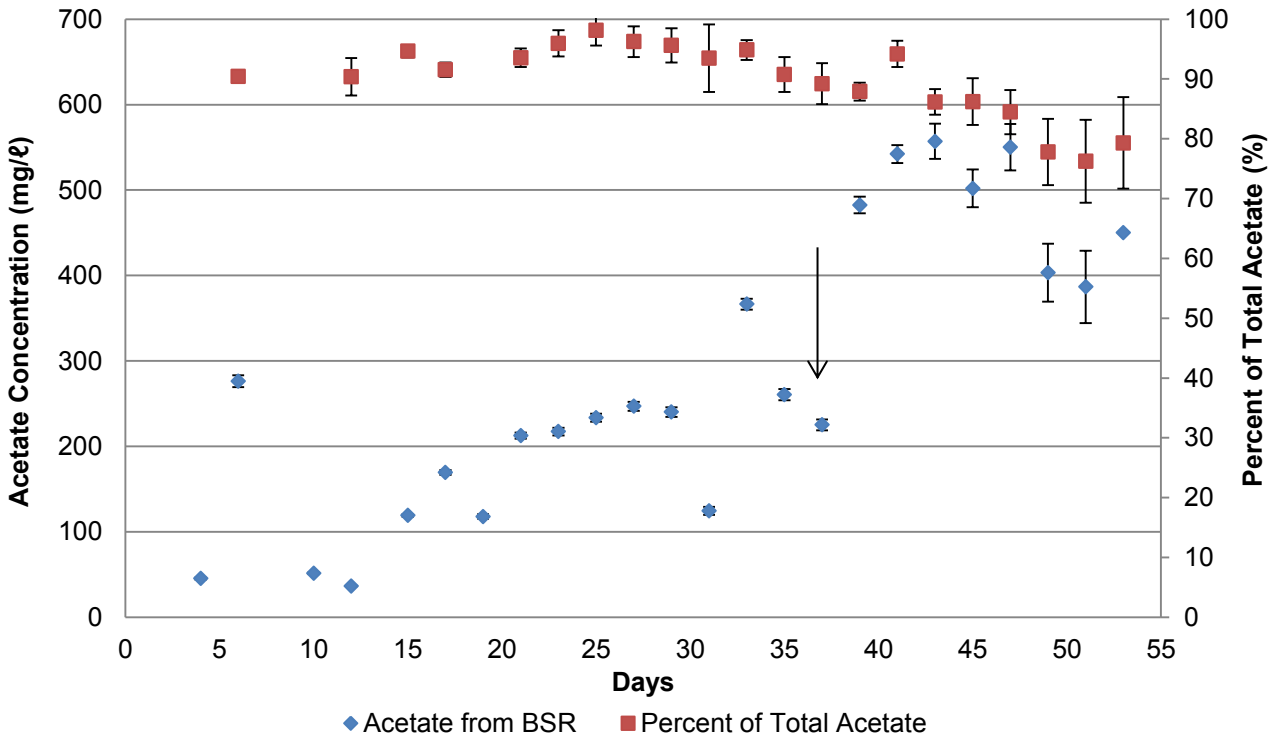

Figure A 8: Acetate concentration as a result of metabolism of SRBs and percent of total acetate as a function of time MFC 5 with standard and concentrated feed and change in feed marked by arrow

Calculations

The concentration of propionate (P_i) in mg/ℓ remaining in the fuel cell after each feeding cycle on a given day in the single-chambered MFCs was calculated by Equation 35.

$$P_i = \frac{P_{i-1} \times 0.018}{0.028}$$ Equation 35

where P_{i-1} is the concentration of propionate at the end of the previous feeding cycle (mg/ℓ) and 0.018 and 0.028 are the volumes (ℓ) of liquid which remains in the MFC and the reactor volume respectively. The concertation of acetate (A_i) remaining after a feeding cycle can also be calculated using Equation 35. The concentration of propionate (P) which was produced in a feeding cycle is calculated by Equation 34.

$$P = P_m - P_i$$ Equation 36

where P_m is the measured concentration of propionate in the system (mg/ℓ) at the end of a feed cycle determined by HPLC analysis.

All propionate was assumed to arise from the Equation 12:

$$3\ lactate \rightarrow\ acetate + 2\ propionate + CO_2 + H_2O\ \ (\Delta G_\circ = -169.7kJ)$$

The concentration of acetate (A_F) in mg/ℓ arising from the fermentative metabolism is calculated by Equation 37.

$$A_F = \frac{P \times M_A}{2M_P}$$ Equation 37

where M_P and M_A are the molar mass in g/mol of propionate and acetate respectively. The concentration of acetate arising from BSR (A_{BSR}) is given by Equation 38.

$$A_{BSR} = A_i - A_F$$ Equation 38

C.3.3 Concentration of COD

Table A 29: Table of absorbance at 605 nm obtained and the corresponding COD concentration for samples from a connected and unconnected MFC fed concentrated media and diluted to various concentrations

Days Since inoculation	Connected			Unconnected		
	Average	*Dilution*	*Concentration (mg/ℓ)*	*Average*	*Dilution*	*Concentration (mg/ℓ)*
1	0.505	1.5	1893.75	0.511	1.5	1916.25
2	0.22	1.5	825	0.357	1.5	1338.75
3	0.153	1.5	573.75	0.109	1.5	408.75
4	0.5	1.5	1875	0.485	1.5	1818.75
6	0.675	1.5	2531.25	0.323	1.5	1211.25
8	0.427	3	3202.5	0.323	1.5	1211.25
10	0.516	3	3870	0.373	1.5	1398.75
12	0.521	3	3907.5	0.482	1.5	1807.5
14	0.529	3	3967.5	0.226	3	1695
17	-	-	-	0.294	3	2205
19	0.612	3	4590	0.38	3	2850

21	-	-	-	0.412	3	3090
23	-	-	-	0.356	3	2670
25	0.684	3	5130	-	-	-
28	-	-	-	0.379	3	2842.5
29	-	-	-	-	-	-

Table A 30: Table of absorbance at 605 nm obtained and the corresponding COD concentration for samples from MFC 5 diluted to various concentrations

Days since inoculation	*Average*	*Dilution*	*Concentration (mg/ℓ)*
2	0.283	1.5	1061
3	0.213	1.5	799
4	0.155	1.5	581
6	0.188	1.5	705
8	0.110	1.5	413
10	0.136	1.5	510
12	0.130	1.5	488
15	0.141	1.5	529
17	0.265	1.5	994
19	0.170	1.5	638
21	0.251	1.5	941
25	0.215	1.5	806
27	0.265	1.5	994
29	0.247	1.5	926
31	0.243	1.5	911
33	0.416	1.5	1560
37	0.283	1.5	1061
40	0.609	1.5	2284
43	0.749	1.5	2809
45	0.725	1.5	2719
47	0.844	1.5	3165
49	0.525	3	3938
51	0.577	3	4328
53	0.557	3	4178
55	0.549	3	4118

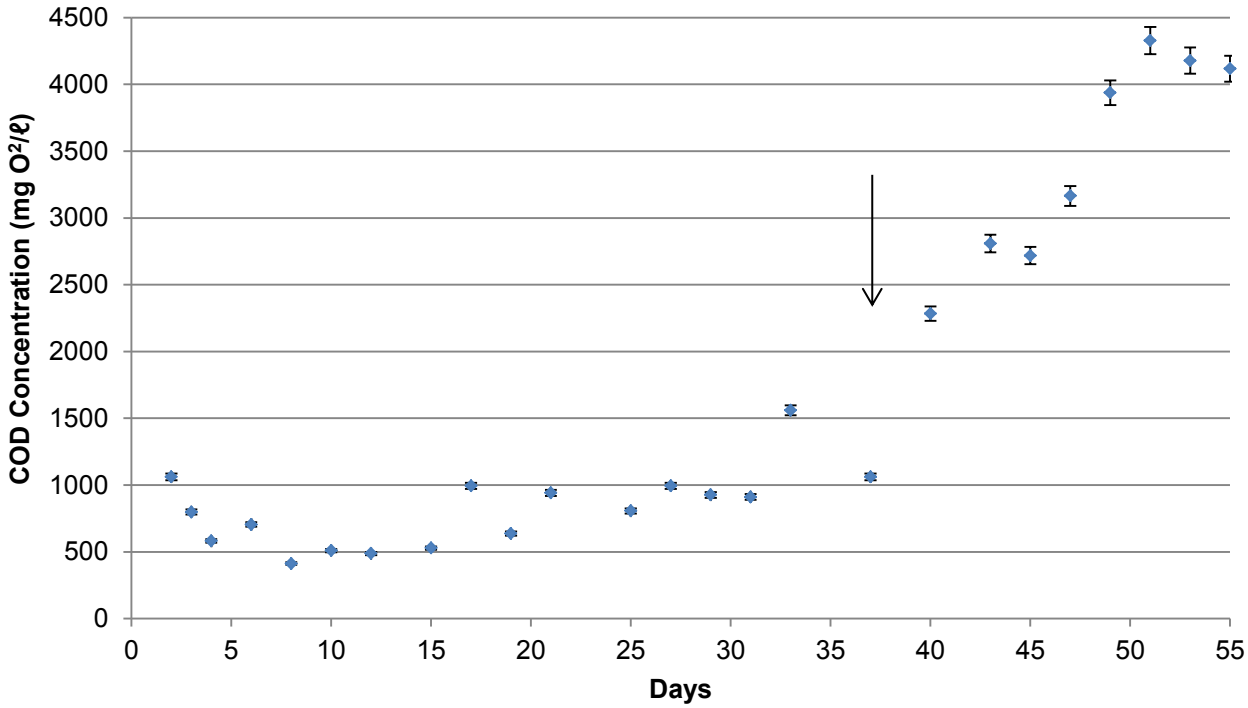

Figure A 9: Soluble COD concentration as a function of time for a MFC 5 with standard and concentrated feed and change in feed marked by arrow

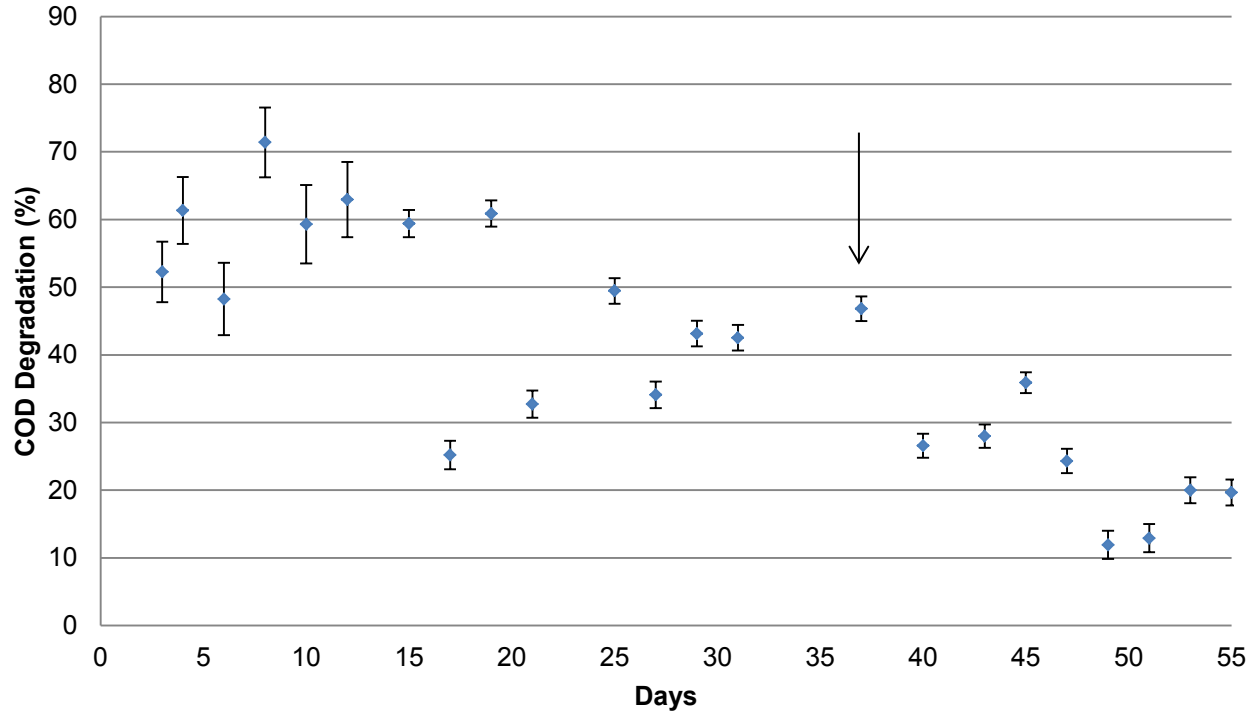

Figure A 10: Percent of soluble COD degraded as a function of time for a MFC 5 with standard and concentrated feed and change in feed marked by arrow

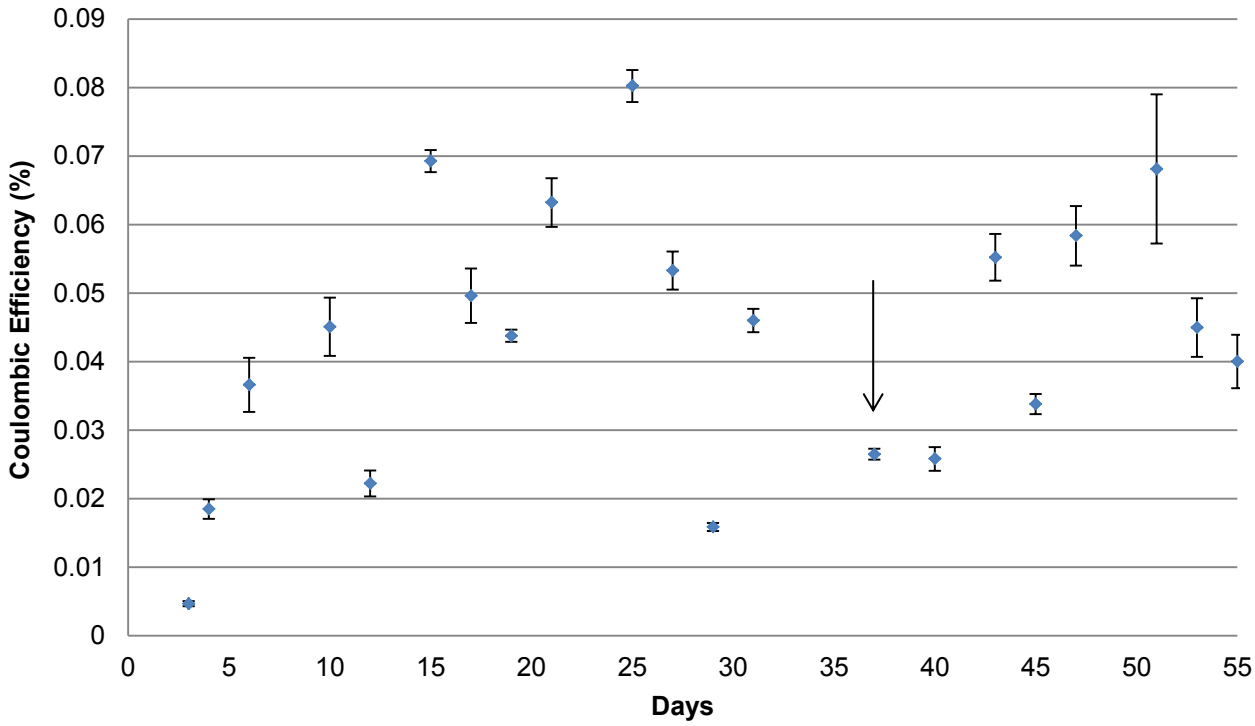

Figure A 11: Coulombic efficiency as a function of time for MFC 5 with standard and concentrated feed and change in feed marked by arrow

C.3.4 Redox Potential and pH

Table A 31: Table of redox potential and pH for samples taken from a connected and unconnected MFC fed concentrated media

Days Since Inoculation	Connected		Unconnected	
	Redox	*pH*	*Redox*	*pH*
0	-422	8.23	-422	8.223
1	-	8.755	-	8.837
2	-304	-	-	8.854
3	-384	8.187	-430	8.922
4	-373	7.474	-394	8.36
6	-353	7.451	-394	8.468
8	-337	7.34	-393	8.49
10	-332	7.09	-400	8.41
12	-331	6.93	-366	8.137
14	-294	6.926	-359	7.964
17	-	-	-365	8.132
19	-366	7.179	-395	7.881
21	-	-	-369	7.595

Days Since Inoculation	Connected		Unconnected	
	Redox	*pH*	*Redox*	*pH*
23	-	-	-352	7.63
25	-361	7.21	-	-
28	-	-	-379	8.074
29	-379	-	-	-

Table A 32: Table of redox potential and pH for samples taken from MFC 5

Days Since Inoculation	*Redox*	*pH*
0	-427	8.238
2	-311	8.428
4	-326	8.049
6	-380	8.349
8	-360	8.000
10	-351	8.030
12	-354	7.790
15	-384	7.900
17	-	8.308
19	-367	7.625
21	-363	7.494
23	-360	7.494
25	-	7.461
27	-356	7.560
29	-356	7.428
31	-355	7.656
33	-348	7.294
35	-351	7.295
37	-343	7.053
39	-354	7.055
41	-348	6.946
43	-337	7.170
45	-346	7.010
47	-350	6.957
49	-351	6.990
51	-335	7.020

Days Since Inoculation	*Redox*	*pH*
53	-331	6.990
55	-337	6.917

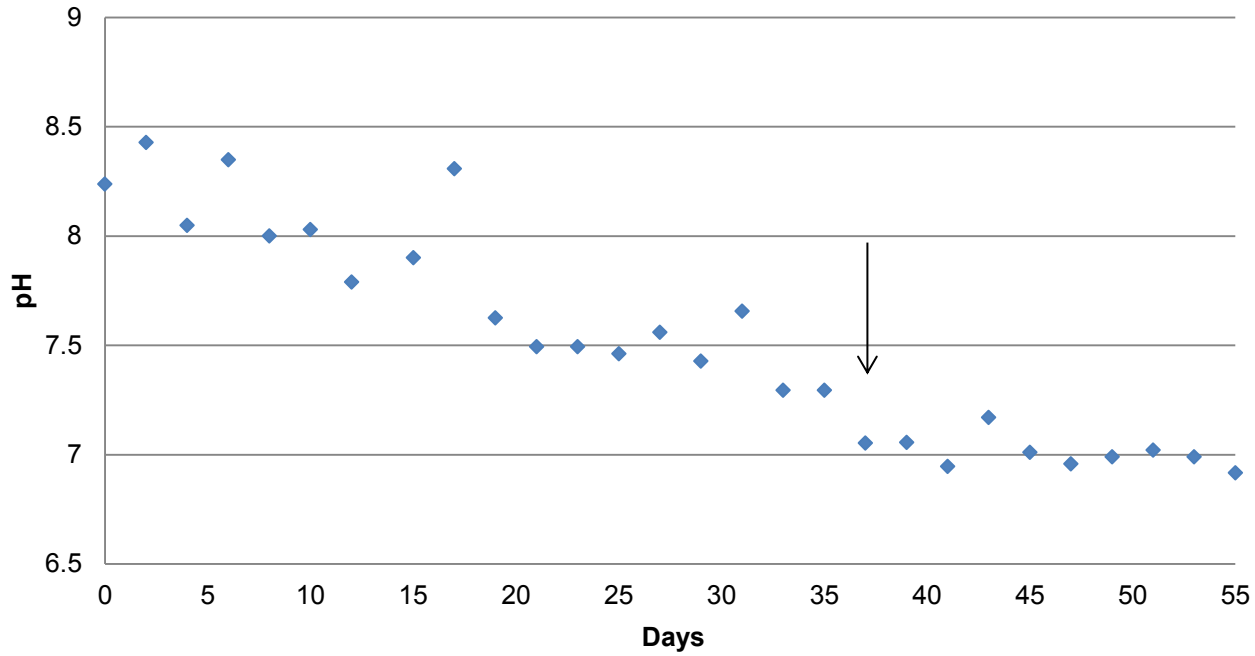

Figure A 12: pH as a function of time for MFC 5 with standard and concentrated feed and change in feed marked by arrow

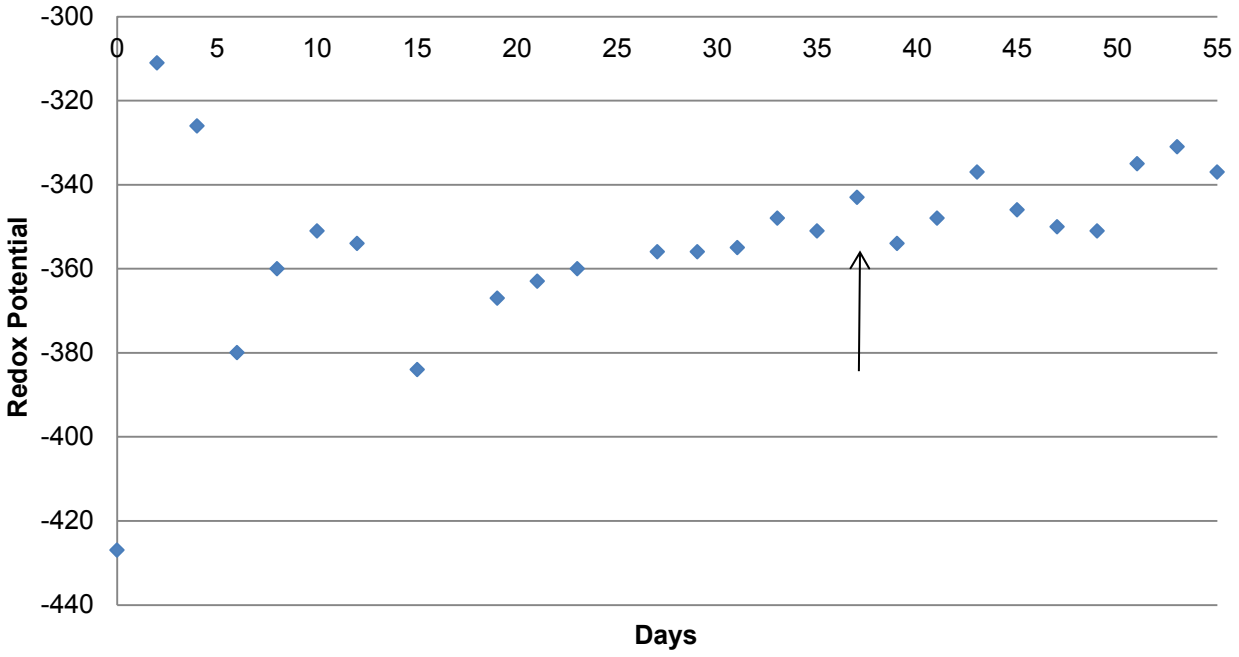

Figure A 13: Redox potential (wrt Ag/AgCl reference electrode) as a function of time for MFC 5 with standard and concentrated feed and change in feed marked by arrow

Appendix D

D.1 Concentration of Sulphur Species

Table A 33: Table of absorbance at 420 nm and the corresponding sulphate concentration for samples taken from various ports in the LFCR and diluted 1:50

Days Since Inoculation	Top Left		Bottom Left		Top Right		Bottom Right		Effluent	
	Abs	*Concentration (mg/ℓ)*	*Abs*	*Concentration (mg/ℓ)*	*Abs*	*Concentration (mg/ℓ)*	*Abs*	*Concentration (mg/ℓ)*	*Abs*	*Concentration (mg/ℓ)*
1	0.383	1915	0.378	1890	0.357	1785	0.364	1820	0.346	1730
2	0.321	1607	0.237	1185	0.321	1605	0.313	1565	0.342	1710
3	0.360	1800	0.387	1935	0.377	1885	0.389	1945	0.330	1650
4	0.373	1865	0.381	1905	0.394	1970	0.379	1895	0.324	1620
5	0.444	2220	0.401	2005	0.463	2315	0.395	1975	0.359	1795
6	0.345	1725	0.357	1785	0.331	1655	0.369	1845	0.141	705
7	0.299	1495	0.393	1965	0.347	1735	0.391	1955	0.313	1565
9	0.338	1690	0.342	1710	0.275	1375	0.257	1285	0.222	1110
11	0.358	1790	0.322	1610	0.367	1835	0.388	1940	0.249	1245
13	0.392	1958	0.356	1780	0.307	1535	0.378	1890	0.270	1348
14	0.370	1850	0.374	1870	0.307	1533	0.402	2008	0.317	1585
15	0.348	1738	0.348	1740	0.262	1310	0.418	2090	0.279	1395
17	0.279	1393	0.330	1650	0.295	1475	0.333	1663	0.344	1718
19	0.257	1283	0.383	1915	0.285	1425	0.334	1668	0.288	1438
20	0.290	1451	0.358	1790	0.329	1643	0.350	1750	0.260	1300
21	0.235	1173	0.352	1760	0.201	1005	0.315	1575	0.214	1068
22	0.212	1060	0.332	1660	0.311	1555	0.308	1540	-	-
23	0.257	1284	0.306	1530	0.303	1513	0.268	1338	0.229	1143
25	0.253	1266	0.306	1530	-	-	0.296	1478	0.206	1030
26	0.237	1185	0.293	1465	0.268	1340	0.309	1545	0.204	1018

Days Since Inoculation	Top Left		Bottom Left		Top Right		Bottom Right		Effluent	
	Abs	*Concentration (mg/ℓ)*	*Abs*	*Concentration (mg/ℓ)*	*Abs*	*Concentration (mg/ℓ)*	*Abs*	*Concentration (mg/ℓ)*	*Abs*	*Concentration (mg/ℓ)*
27	0.225	1125	0.223	1115	0.252	1258	0.236	1180	0.211	1055
28	0.208	1040	0.240	1200	0.125	625	0.287	1435	-	-
29	0.208	1042	0.248	1240	0.213	1065	0.294	1470	0.196	980
30	0.183	917	0.262	1310	0.118	590	0.369	1845	-	-
31	0.173	866	0.228	1140	0.181	905	0.145	725	0.172	858
32	0.166	831	0.192	960	0.203	1015	0.245	1223	0.193	965
33	0.155	773	0.153	765	0.180	900	0.225	1123	0.171	853
34	0.171	855	0.216	1080	0.163	815	0.217	1085	0.178	890
35	0.148	740	0.168	840	0.177	885	0.246	1230	0.190	950
36	0.099	495	0.184	920	0.122	610	0.169	845	0.187	935
38	0.185	925	0.160	800	0.152	760	0.185	925	0.189	945
40	0.161	805	0.154	770	0.175	875	0.161	805	0.175	875
41	0.102	510	0.139	695	0.143	715	0.190	950	0.175	875
42	0.153	765	0.133	665	0.140	700	0.122	610	0.114	570
44	0.137	685	0.122	610	0.147	735	0.128	640	0.159	795
46	0.138	690	0.097	485	0.134	670	0.087	435	0.110	550
48	0.126	630	0.112	560	0.131	655	0.098	490	0.127	635
49	0.115	575	0.108	540	0.097	485	0.098	490	0.103	515
50	0.093	465	0.089	445	0.115	575	0.114	570	0.133	665
51	0.133	665	0.081	405	0.146	730	0.100	500	0.134	670
53	0.145	725	0.118	590	0.117	585	0.106	530	0.145	725
56	0.149	745	0.154	770	0.151	755	0.174	870	0.156	780
57	0.142	710	0.167	835	0.155	775	0.157	785	0.176	880
59	0.148	740	0.135	675	0.158	790	0.139	695	0.176	880
60	0.152	760	0.113	565	0.162	810	0.135	675	0.184	920
61	0.163	815	0.124	620	0.165	825	0.124	620	0.186	930

Days Since Inoculation	Top Left		Bottom Left		Top Right		Bottom Right		Effluent	
	Abs	*Concentration (mg/ℓ)*	*Abs*	*Concentration (mg/ℓ)*	*Abs*	*Concentration (mg/ℓ)*	*Abs*	*Concentration (mg/ℓ)*	*Abs*	*Concentration (mg/ℓ)*
62	0.140	700	0.125	625	0.159	795	0.143	715	0.160	800

Table A 34: Table of absorbance at 670 nm and the corresponding sulphide concentration for samples taken from various ports in the LFCR and diluted 1:250

Days Since Inoculation	Top Left		Bottom Left		Top Right		Bottom Right		Effluent	
	Abs	*Concentration (mg/ℓ)*	*Abs*	*Concentration (mg/ℓ)*	*Abs*	*Concentration (mg/ℓ)*	*Abs*	*Concentration (mg/ℓ)*	*Abs*	*Concentration (mg/ℓ)*
1	0.841	250	1.210	360	0.910	270.8	0.930	276.8	0.000	0.0
2	0.152	45.2	0.169	50.3	0.142	42.3	0.151	44.9	0.128	38.1
3	0.397	118.2	0.420	125	0.408	121	0.376	112	0.113	33.6
4	0.180	53.6	0.254	75.6	0.227	67.6	0.243	72.3	0.021	6.3
5	0.360	107	0.494	147	0.288	85.7	0.489	146	0.167	49.7
6	0.103	30.7	0.132	39.3	0.096	28.6	0.116	34.5	0.015	4.5
7	0.340	101	0.408	121	0.308	91.7	0.265	78.9	0.124	36.9
9	0.264	78.6	0.508	151	0.384	114	0.299	89.0	0.042	12.5
11	0.251	74.7	0.249	74.1	0.299	89.0	0.407	121	0.044	13.1
13	0.184	54.8	0.317	94.3	0.196	58.3	0.204	60.7	0.038	11.3
14	0.220	65.5	0.116	34.5	0.214	63.7	0.249	74.1	0.050	14.9
15	0.190	56.5	0.127	37.8	0.124	36.9	0.154	45.8	0.054	16.1
17	0.316	94.0	0.289	86.0	0.330	98.2	0.250	74.4	0.120	35.7
19	0.362	108	0.316	94.0	0.136	40.5	0.449	134	0.078	23.2
20	0.242	72.0	0.229	68.2	0.163	48.5	0.226	67.3	0.086	25.6
21	0.200	59.5	0.231	68.8	0.221	65.8	0.250	74.4	0.088	26.2
22	0.163	48.5	0.156	46.4	0.134	39.9	0.134	39.9	0.052	15.5

Days Since Inoculation	Top Left		Bottom Left		Top Right		Bottom Right		Effluent	
	Abs	*Concentration (mg/ℓ)*	*Abs*	*Concentration (mg/ℓ)*	*Abs*	*Concentration (mg/ℓ)*	*Abs*	*Concentration (mg/ℓ)*	*Abs*	*Concentration (mg/ℓ)*
23	0.227	67.6	0.314	93.5	0.239	71.1	0.347	103	0.064	19.0
25	0.162	48.2	0.190	56.5	0.108	32.1	0.112	33.3	0.040	11.9
26	0.117	34.8	0.199	59.2	0.056	16.7	0.181	53.9	0.061	18.2
27	0.224	66.7	0.330	98.2	0.129	38.4	0.231	68.8	0.081	24.1
28	0.300	89.3	0.421	125	0.205	61.0	0.369	110	0.090	26.8
29	0.218	64.9	0.333	99.1	0.134	39.9	0.279	83.0	0.059	17.6
30	0.335	99.7	0.506	151	0.236	70.2	0.413	123	0.091	27.1
31	0.326	97.0	0.564	168	0.249	74.1	0.437	130	0.110	32.7
32	0.267	79.5	0.361	107	0.133	39.6	0.266	79.2	0.072	21.4
33	0.291	86.6	0.466	139	0.168	50.0	0.312	92.9	0.070	20.8
34	0.213	63.4	0.262	78.0	0.113	33.6	0.226	67.3	0.071	21.1
35	0.067	19.9	0.197	58.6	0.112	33.3	0.113	33.6	0.059	17.6
36	0.161	47.9	0.305	90.8	0.133	39.6	0.255	75.9	0.082	24.4
38	0.144	42.9	0.319	94.9	0.156	46.4	0.208	61.9	0.090	26.8
40	0.182	54.2	0.253	75.3	0.071	21.1	0.130	38.7	0.053	15.8
41	0.129	38.4	0.292	86.9	0.116	34.5	0.257	76.5	0.080	23.8
42	0.139	41.4	0.291	86.6	0.097	28.9	0.223	66.4	0.085	25.3
44	0.127	37.8	0.187	55.7	0.085	25.3	0.211	62.8	0.065	19.3
46	0.117	34.8	0.208	61.9	0.099	29.5	0.162	48.2	0.079	23.5
47	0.122	36.3	0.259	77.1	0.094	28.0	0.136	40.5	0.050	14.9
48	0.065	19.3	0.245	72.9	0.126	37.5	0.224	66.7	0.076	22.6
49	0.142	42.3	0.287	85.4	0.124	36.9	0.329	97.9	0.088	26.2
50	0.140	41.7	0.201	59.8	0.118	35.1	0.129	38.4	0.070	20.8
51	0.115	34.2	0.223	66.4	0.103	30.7	0.250	74.4	0.072	21.4
53	0.214	63.7	0.287	85.4	0.247	73.5	0.265	78.9	0.110	32.7
56	0.138	41.1	0.143	42.6	0.072	21.4	0.114	33.9	0.055	16.4

Days Since Inoculation	Top Left		Bottom Left		Top Right		Bottom Right		Effluent	
	Abs	*Concentration (mg/ℓ)*	*Abs*	*Concentration (mg/ℓ)*	*Abs*	*Concentration (mg/ℓ)*	*Abs*	*Concentration (mg/ℓ)*	*Abs*	*Concentration (mg/ℓ)*
57	0.149	44.3	0.258	76.8	0.126	37.5	0.235	69.9	0.077	22.9
59	0.121	36.0	0.304	90.5	0.072	21.4	0.315	93.8	0.030	8.9
60	0.107	31.8	0.296	88.1	0.096	28.6	0.314	93.5	0.029	8.6
61	0.042	12.5	0.108	32.1	0.038	11.3	0.063	18.8	0.015	4.5
62	0.145	43.2	0.315	93.8	0.116	34.5	0.211	62.8	0.057	17.0

D.2 Concentration of Volatile Fatty Acids

Table A 35: Table of absorbance area at 210 nm obtained by HPLC and the corresponding lactate concentration for samples taken from various ports in the LFCR and diluted 1:4

Days Since Inoculation	Top Left		Bottom Left		Top Right		Bottom Right		Effluent	
	Area (μVs)	*Concentration (mg/ℓ)*	*Area (μVs)*	*Concentration (mg/ℓ)*	*Area (μVs)*	*Concentration (mg/ℓ)*	*Area (μVs)*	*Concentration (mg/ℓ)*	*Area (μVs)*	*Concentration (mg/ℓ)*
1	44161	115	56128	146	50434	131	49444	128	48248	125
3	30397	79.0	33195	86.2	40992	106	39104	102	101523	264
4	37067	96.3	18162	47.2	24272	63.1	22141	57.5	47697	124
5	6053	15.7	0	0.00	7286	18.9	0	0.00	16604	43.1
6	0	0.00	0	0.00	0	0.00	0	0.00	19905	51.7
7	0	0.00	0	0.00	0	0.00	0	0.00	0	0.00
9	0	0.00	0	0.00	0	0.00	0	0.00	145183	377
11	4466	11.60	0	0.00	0	0.00	0	0.00	0	0.00
13	0	0.00	0	0.00	6986	18.0	1997	5.15	0	0.00
14	0	0.00	0	0.00	0	0.00	0	0.00	0	0.00
15	2543	6.56	0	0.00	0	0.00	0	0.00	24679	63.6

Days Since Inoculation	Top Left		Bottom Left		Top Right		Bottom Right		Effluent	
	Area (µVs)	*Concentration (mg/ℓ)*	*Area (µVs)*	*Concentration (mg/ℓ)*	*Area (µVs)*	*Concentration (mg/ℓ)*	*Area (µVs)*	*Concentration (mg/ℓ)*	*Area (µVs)*	*Concentration (mg/ℓ)*
17	2428	6.26	4920	12.7	17377	44.8	1921	4.96	2870	7.40
19	4369	11.3	1711	4.41	4200	10.8	1426	3.68	11237	29.0
20	6195	16.0	2961	7.64	0	13.6	2767	7.14	28219	72.8
21	0	0.00	0	0.00	0	0.00	0	0.00	6545	16.9
23	0	0.00	0	0.00	0	0.00	0	0.00	0	0.00
25	0	0.00	0	0.00	0	0.00	0	0.00	0	0.00
26	0	0.00	0	0.00	0	0.00	0	0.00	0	0.00
27	0	0.00	0	0.00	0	0.00	0	0.00	8834	22.67
28	0	0.00	0	0.00	0	0.00	0	0.00	4932	12.66
29	14439	37.6	0	0.00	0	0.00	0	0.00	35472	92.35
31	0	0.00	0	0.00	0	0.00	0	0.00	0	0.00
32	0	0.00	0	0.00	0	0.00	0	0.00	0	0.00
33	0	0.00	0	0.00	0	0.00	0	0.00	0	0.00
35	0	0.00	0	0.00	0	0.00	0	0.00	0	0.00
36	0	0.00	0	0.00	0	0.00	0	0.00	0	0.00
38	0	0.00	0	0.00	0	0.00	0	0.00	0	0.00
40	0	0.00	0	0.00	0	0.00	0	0.00	0	0.00
42	0	0.00	0	0.00	0	0.00	0	0.00	0	0.00
44	0	0.00	0	0.00	0	0.00	0	0.00	0	0.00
46	0	0.00	0	0.00	0	0.00	0	0.00	0	0.00
48	174283	454	37326	97.2	28524	74.3	5886	15.3	0	0.00
50	46372	121	0	0.00	53969	141	33945	88.4	40091	104
51	13	0.03	0	0.00	57700	150	0	0.00	15572	40.5
53	0	0.00	0	0.00	5347	13.9	4038	10.5	43647	114
56	19990	52.0	0	0.00	0	0.00	0	0.00	0	0.00
57	13149	34.2	0	0.00	0	0.00	0	0.00	0	0.00

Days Since Inoculation	Top Left		Bottom Left		Top Right		Bottom Right		Effluent	
	Area (μVs)	*Concentration (mg/ℓ)*	*Area (μVs)*	*Concentration (mg/ℓ)*	*Area (μVs)*	*Concentration (mg/ℓ)*	*Area (μVs)*	*Concentration (mg/ℓ)*	*Area (μVs)*	*Concentration (mg/ℓ)*
59	64828	169	0	0.00	0	0.00	0	0.00	0	0.00

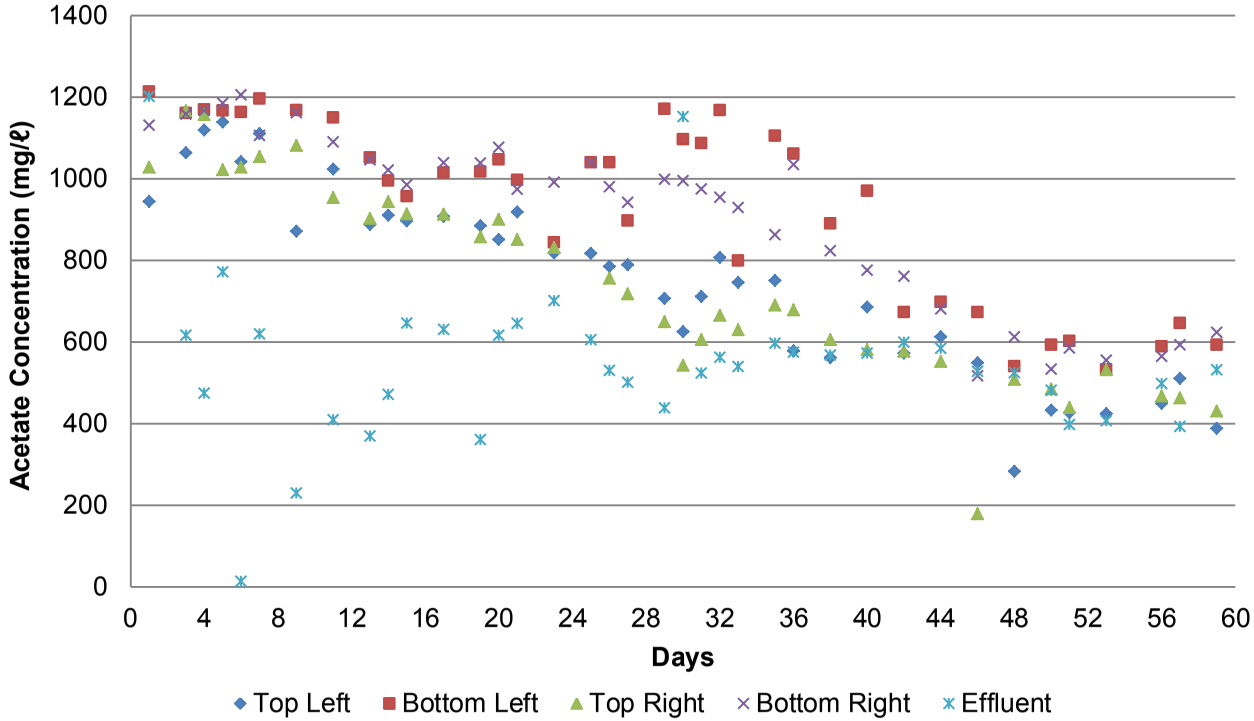

Figure A 14: Acetate concentration as a result of BSR as a function of time for the LFCR-MFC in parallel with a 10 kΩ resistor and fed 10 mM lactate

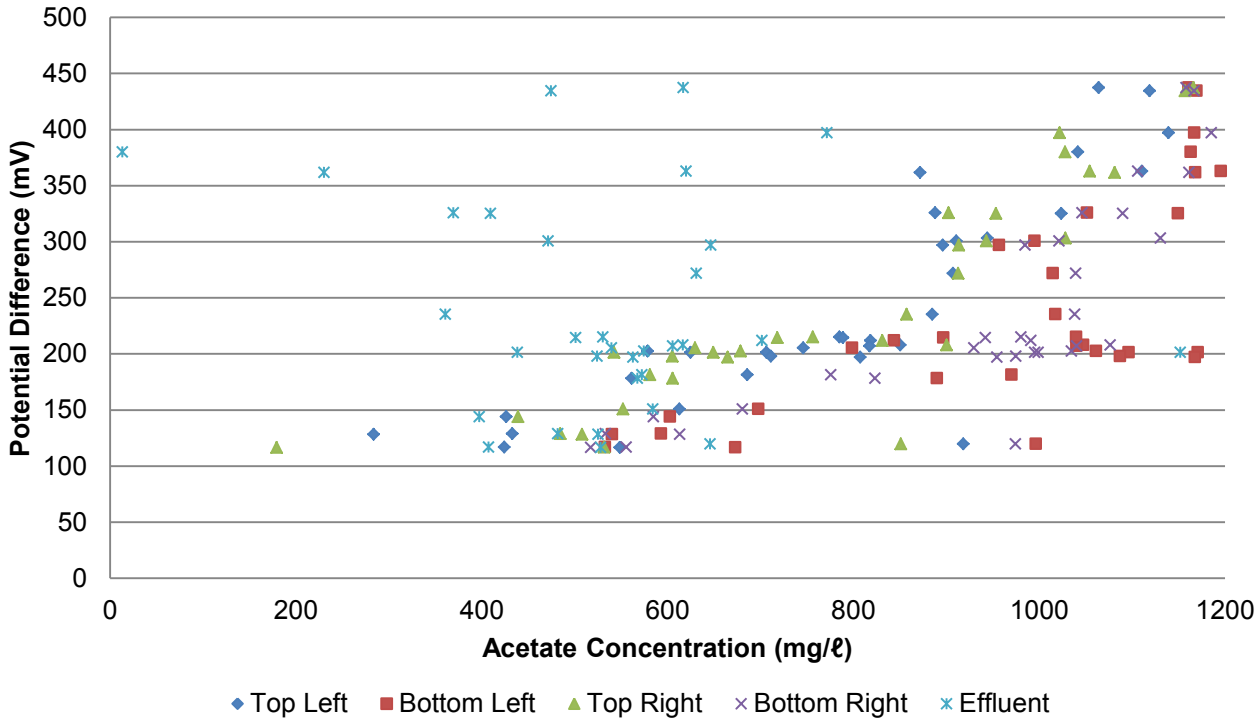

Figure A 15: Potential difference as a function of acetate concentration from BSR for the LFCR-MFC in parallel with a 10 kΩ resistor and fed 10 mM lactate

Calculations

The concentration of propionate at any time in the LFCR-MFC was used to calculate the acetate concentration arising from fermentation by Equation 37. The concentration of acetate arising from BSR (A_{BSR}) was calculated by Equation 38. Equation 4 for partial oxidation by SRB was used to calculate the concentration of sulphate expected (S_E).

$$2\ lactate + SO_4^{2-} \rightarrow\ 2\ acetate + 2HCO_3^- + HS^- + H^+\ \ (\Delta G_\circ = -160.1\ kJ)$$

$$S_E = \frac{A_{BSR} \times M_A}{2M_S}$$ Equation 39

where M_A and M_S are the molar masses (g/mol) of acetate and sulphate respectively.

Table A 36: Table of absorbance area at 210 nm obtained by HPLC and the corresponding acetate concentration for samples taken from various ports in the LFCR and diluted 1:4

Days Since Inoculation	Top Left		Bottom Left		Top Right		Bottom Right		Effluent	
	Area (μVs)	*Concentration (mg/ℓ)*	*Area (μVs)*	*Concentration (mg/ℓ)*	*Area (μVs)*	*Concentration (mg/ℓ)*	*Area (μVs)*	*Concentration (mg/ℓ)*	*Area (μVs)*	*Concentration (mg/ℓ)*
1	302321	1057	386290	1350	329407	1151	358934	1255	356852	1247
3	338848	1184	367095	1283	368939	1290	367542	1285	190585	666
4	351626	1229	367063	1283	366553	1281	368894	1289	164533	575
5	362068	1266	369658	1292	327227	1144	373289	1305	232168	811
6	332053	1161	371316	1298	329536	1152	381928	1335	19905	70
7	347271	1214	378575	1323	335676	1173	352483	1232	192207	672
9	277156	969	370848	1296	344786	1205	370062	1293	82378	288
11	321396	1123	362968	1269	300637	1051	346647	1212	130317	455
13	285737	986	337221	1164	289954	1001	333708	1152	120093	415
14	296340	1023	322177	1112	305905	1056	328844	1135	155073	535
15	288711	997	309517	1068	294047	1015	317937	1097	203765	703
17	291105	1005	326529	1127	290074	1001	330796	1142	192855	666
19	280898	970	323455	1116	273794	945	331443	1144	119122	411
20	271778	938	333050	1150	286371	988	341972	1180	193332	667
21	293638	1014	317497	1096	271302	936	310419	1071	188474	651
23	259574	896	268996	928	264157	912	315161	1088	219480	758
25	263294	908	329181	1135	-	-	330114	1139	192128	663
26	253303	874	328534	1133	244465	843	311380	1074	175848	607
27	254248	877	281089	970	230909	797	299914	1035	165103	570
28	228329	788	352489	1216	214439	740	311522	1075	162357	560
29	202916	709	325732	1138	174226	609	305762	1068	352293	1231
31	225469	778	324395	1119	195918	676	301123	1039	177377	612
32	253520	875	347155	1198	215018	742	295231	1018	190630	658
33	236226	815	236291	815	205625	709	289237	998	186558	644

Days Since Inoculation	Top Left		Bottom Left		Top Right		Bottom Right		Effluent	
	Area (µVs)	*Concentration (mg/ℓ)*	*Area (µVs)*	*Concentration (mg/ℓ)*	*Area (µVs)*	*Concentration (mg/ℓ)*	*Area (µVs)*	*Concentration (mg/ℓ)*	*Area (µVs)*	*Concentration (mg/ℓ)*
35	236025	825	316230	1105	224115	783	267751	936	194626	680
36	191797	672	310502	1088	218336	765	312008	1093	191260	670
38	190580	657	266027	918	202727	699	259155	894	197138	680
40	227581	795	290218	1014	198487	694	246553	861	197644	691
42	195428	683	218774	764	198372	693	241846	845	204845	716
44	209686	733	227871	796	192271	672	223221	780	202656	708
46	192493	673	218774	764	86763	303	178055	622	183542	641
48	121157	423	184554	645	177723	621	204142	713	184367	644
50	164920	576	204192	713	175197	612	186729	652	171896	601
51	160562	561	211455	739	167668	586	202381	707	149955	524
53	169901	594	189273	661	190765	667	197520	690	150113	525
56	175276	612	210106	734	170368	595	202499	708	172987	604
57	183850	642	218240	763	165703	579	200996	702	148388	518
59	156865	548	206664	722	161850	566	214271	749	152276	532

Table A 37: Table of absorbance area at 210 nm obtained by HPLC and the corresponding propionate concentration for samples taken from various ports in the LFCR and diluted 1:4

Days Since Inoculation	Top Left		Bottom Left		Top Right		Bottom Right		Effluent	
	Area (μVs)	*Concentration (mg/ℓ)*	*Area (μVs)*	*Concentration (mg/ℓ)*	*Area (μVs)*	*Concentration (mg/ℓ)*	*Area (μVs)*	*Concentration (mg/ℓ)*	*Area (μVs)*	*Concentration (mg/ℓ)*
1	78807	278	95888	338	86312	305	86824	306	91427	323
3	84409	298	85551	302	86550	306	88697	313	31910	113
4	77139	272	79404	280	87024	307	85931	303	34550	122
5	88593	313	87561	309	85300	301	83635	295	70546	249
6	83295	294	94186	332	86836	307	90474	319	27867	98.4
7	72365	255	89247	315	83382	294	88120	311	39562	140
9	67966	240	89809	317	86736	306	92549	327	36305	128
11	69761	246	83454	295	68137	241	85314	301	40532	143
13	70438	243	80562	278	70652	243	75974	262	33174	114
14	80373	277	83947	289	80838	279	81722	282	32446	112
15	71963	248	79968	276	72804	251	80836	278	45793	158
17	70100	242	80537	277	63372	218	73516	253	40734	140
19	60666	209	70952	244	63042	217	75926	262	25014	86
20	62784	216	73319	253	63232	218	74521	257	36193	125
21	68251	235	71250	245	61333	211	69685	240	36586	126
23	55758	192	60628	209	57808	199	69371	239	3355	11.6
25	64291	224	67505	236	-	-	69632	243	39711	139
26	62815	219	66171	231	61677	215	66393	232	40447	141
27	62550	218	51378	179	55593	194	65402	228	54039	189
28	57410	200	31839	111	64067	224	53672	187	48499	169
29	58827	208	29066	103	46361	164	51135	181	85195	301
31	47181	165	22523	78.6	49975	174	45284	158	55836	195
32	47497	166	21099	73.7	54410	190	45341	158	62075	217
33	48845	171	11407	39.8	56556	197	48103	168	67217	235

Days Since Inoculation	Top Left		Bottom Left		Top Right		Bottom Right		Effluent	
	Area (µVs)	*Concentration (mg/ℓ)*	*Area (µVs)*	*Concentration (mg/ℓ)*	*Area (µVs)*	*Concentration (mg/ℓ)*	*Area (µVs)*	*Concentration (mg/ℓ)*	*Area (µVs)*	*Concentration (mg/ℓ)*
35	51705	183	-	-	64990	230	50612	179	72765	257
36	65460	232	18703	66.1	60410	214	40901	145	58216	206
38	67961	237	19450	67.9	66525	232	50118	175	67723	236
40	76536	271	30440	108	78631	278	60090	213	78632	278
42	77159	273	64022	226	80777	286	58895	208	82760	293
44	83939	297	68820	243	83820	296	69442	246	81656	289
46	86678	307	64022	226	86763	307	73433	260	86804	307
48	97809	346	73026	258	79131	280	70236	248	79322	281
50	100398	355	84257	298	89330	316	83576	296	83378	295
51	94206	333	95232	337	102781	363	85553	303	83263	294
53	118660	420	90026	318	94387	334	94095	333	88465	313
56	113884	403	101557	359	89595	317	100011	354	82022	290
57	92095	326	81393	288	81240	287	76580	271	74391	263
59	111723	395	90430	320	94271	333	87509	309	87801	311

D.3 Concentration of COD

Table A 38: Table of absorbance at 605 nm obtained and the corresponding COD concentration for effluent samples taken from the LFCR and diluted to various concentrations

Days since inoculation	*Absorbance*	*Dilution*	*Concentration (mg/ℓ)*
1	-	-	-
2	-	-	-
3	0.461	1.5	1729
4	0.542	1.5	2033
5	0.343	1.5	1286
6	0.259	1.5	971
7	0.305	1.5	1144
9	0.217	1.5	814
11	0.209	1.5	784
13	0.23	1.5	863
14	0.385	1.5	1444
15	0.399	1.5	1496
17	0.367	1.5	1376
19	0.378	1.5	1418
20	0.463	1.5	1736
21	-	-	-
22	0.48	1.5	1800
23	0.421	1.5	1579
24	0.383	1.5	1436
25	0.355	1.5	1331
26	0.391	1.5	1466
27	0.335	1.5	1256
28	0.32	1.5	1200
29	0.33	1.5	1238
31	0.379	1.5	1421
32	0.429	1.5	1609
33	0.357	1.5	1339
34	0.416	1.5	1560
36	0.369	1.5	1384
38	0.408	1.5	1530
40	0.431	1.5	1616
41	0.439	1.5	1646
42	0.456	1.5	1710
44	0.423	1.5	1586
46	0.439	1.5	1646
47	0.217	3	1628
48	0.176	3	1320
49	0.169	3	1268
50	0.172	3	1290
51	0.221	3	1658
53	0.23	3	1725

Days since inoculation	*Absorbance*	*Dilution*	*Concentration (mg/ℓ)*
56	0.218	3	1635
57	0.204	3	1530
59	0.081	3	608
60	0.211	3	1583
61	0.232	3	1740
62	-	-	-

D.4 Redox and pH

Table A 39: Table of redox potential and pH for samples taken from various ports in the LFCR

	pH					Redox Potential
Days Since Inoculation	Top Left	Bottom Left	Top Right	Bottom Right	Effluent	Effluent
1	8.587	8.592	8.585	8.592	8.589	-428
2	8.904	8.912	8.932	8.928	8.949	-426
3	8.886	8.887	8.885	8.890	8.794	-407
4	8.805	8.814	8.833	8.825	8.773	-417
5	8.730	8.780	8.967	8.765	8.657	-475
6	8.581	8.717	8.674	8.687	8.472	-410
7	8.608	8.735	8.740	8.862	8.701	-
9	8.390	8.553	8.505	8.581	7.724	-387
11	8.040	8.289	8.228	8.331	8.009	-417
13	8.303	8.409	8.414	8.449	7.860	-404
14	8.057	8.147	8.118	8.169	8.429	-413
15	7.934	8.038	8.049	8.051	7.878	-382
17	7.760	7.929	7.863	7.920	7.733	-406
19	7.522	7.580	7.584	7.594	7.620	-391
20	7.420	7.493	7.523	7.456	7.417	-382
21	7.443	7.577	7.499	7.513	7.451	-390
22	7.469	7.583	7.542	7.510	7.389	-375
23	7.372	7.455	7.557	7.617	7.375	-372
25	7.253	7.514	7.417	7.570	7.265	-370
26	7.299	7.476	7.542	7.447	7.390	-373
27	7.302	7.565	7.375	7.575	7.095	-360
28	7.248	7.408	7.342	7.456	7.226	-364
29	7.213	7.460	7.348	7.480	7.237	-361
30	7.137	7.392	7.202	7.496	7.146	-360
31	7.157	7.264	7.276	7.425	7.133	-271
32	7.232	7.135	7.200	7.365	7.083	-323
33	7.132	7.293	7.131	7.545	7.024	-270
34	7.111	7.485	7.160	7.426	7.098	-257
35	7.200	7.368	7.267	7.372	7.189	-347
36	7.044	7.512	7.042	7.359	7.093	-353

38	7.062	7.310	7.003	7.325	7.070	-357
40	7.006	7.140	6.908	7.273	6.952	-359
41	7.040	7.225	7.147	7.289	7.038	-349
42	6.940	7.210	7.060	7.190	6.980	-353
44	6.960	7.170	7.090	7.140	7.100	-355
46	6.391	7.093	6.833	7.136	7.038	-343
47	6.688	7.020	6.858	7.028	6.914	-309
48	6.568	7.063	6.880	7.035	7.012	-325
49	6.568	6.941	6.880	7.075	7.021	-329
50	6.702	6.890	6.800	6.870	6.850	-334
51	6.578	6.948	6.845	6.895	6.875	-343
53	6.662	6.895	6.816	6.872	7.063	-354
56	6.404	6.699	6.776	6.875	6.819	-293
57	6.561	6.869	6.788	7.008	6.880	-311
59	6.525	6.829	6.874	6.801	7.075	-215
60	6.359	6.735	6.615	6.783	6.869	-331
61	6.370	6.857	6.603	6.897	6.915	-234
62	6.524	6.746	6.780	6.837	6.777	-270

ETHICS FORM

EBE Faculty: Assessment of Ethics in Research Projects

Any person planning to undertake research in the Faculty of Engineering and the Built Environment at the University of Cape Town is required to complete this form before collecting or analysing data. When completed it should be submitted to the supervisor (where applicable) and from there to the Head of Department. If any of the questions below have been answered YES, and the applicant is NOT a fourth year student, the Head should forward this form for approval by the Faculty EIR committee: submit to Ms Zakiya Chikte (Zakiya.chikte@uct.ac.za); New EBE Building, Ph 021 650 5739).

Please note – It is important to keep a signed copy of this form as students must include a copy of the completed form with the dissertation/thesis when it is submitted for examination.

Name of Principal Researcher/Student: Jennifer Cooke-Simunovic **Department:** Chemical Engineering

If a Student: **Degree:** MSc Engineering **Supervisor:** Prof Sue Harrison

If a Research Contract indicate source of funding/sponsorship:

Research Project Title: Integrating Microbial Fuel Cells (MFCs) into the Treatment Systems for Industrial Wastewater

Overview of ethics issues in your research project:

Question 1: Is there a possibility that your research could cause harm to a third party (i.e. a person not involved in your project)?	YES	(NO)
Question 2: Is your research making use of human subjects as sources of data? If your answer is YES, please complete Addendum 2	YES	(NO)
Question 3: Does your research involve the participation of or provision of services to communities? If your answer is YES, please complete Addendum 3.	YES	(NO)
Question 4: If your research is sponsored, is there any potential for conflicts of interest? If your answer is YES, please complete Addendum 4.	YES	(NO)

If you have answered YES to any of the above questions, please append a copy of your research proposal, as well as any interview schedules or questionnaires (Addendum 1) and please complete further addenda as appropriate.

I hereby undertake to carry out my research in such a way that

- there is no apparent legal objection to the nature or the method of research; and
- the research will not compromise staff or students or the other responsibilities of the University;
- the stated objective will be achieved, and the findings will have a high degree of validity;
- limitations and alternative interpretations will be considered;
- the findings could be subject to peer review and publicly available; and
- I will comply with the conventions of copyright and avoid any practice that would constitute plagiarism.

Signed by:

	Full name and signature	Date
Principal Researcher/Student:		31/03/2016

This application is approved by:

Supervisor (if applicable):		31/03/2016
HOD (or delegated nominee): Final authority for all assessments with NO to all questions and for all undergraduate research.		31-3-2016
Chair: Faculty EIR Committee For applicants other than undergraduate students who have answered YES to any of the above questions.		

ADDENDUM 1:
Please append a copy of the research proposal here, as well as any interview schedules or questionnaires:

ADDENDUM 2: To be completed if you answered YES to Question 2:

It is assumed that you have read the UCT Code for Research involving Human Subjects (available at http://web.uct.ac.za/depts/educate/download/uctcodeforresearchinvolvinghumansubjects.pdf) in order to be able to answer the questions in this addendum.

2.1 Does the research discriminate against participation by individuals, or differentiate between participants, on the grounds of gender, race or ethnic group, age range, religion, income, handicap, illness or any similar classification?	YES	NO
2.2 Does the research require the participation of socially or physically vulnerable people (children, aged, disabled, etc) or legally restricted groups?	YES	NO
2.3 Will you not be able to secure the informed consent of all participants in the research? (In the case of children, will you not be able to obtain the consent of their guardians or parents?)	YES	NO
2.4 Will any confidential data be collected or will identifiable records of individuals be kept?	YES	NO
2.5 In reporting on this research is there any possibility that you will not be able to keep the identities of the individuals involved anonymous?	YES	NO
2.6 Are there any foreseeable risks of physical, psychological or social harm to participants that might occur in the course of the research?	YES	NO
2.7 Does the research include making payments or giving gifts to any participants?	YES	NO

If you have answered YES to any of these questions, please describe how you plan to address these issues (append to form):

ADDENDUM 3: To be completed if you answered YES to Question 3:

3.1 Is the community expected to make decisions for, during or based on the research?	YES	NO
3.2 At the end of the research will any economic or social process be terminated or left unsupported, or equipment or facilities used in the research be recovered from the participants or community?	YES	NO
3.3 Will any service be provided at a level below the generally accepted standards?	YES	NO

If you have answered YES to any of these questions, please describe how you plan to address these issues (append to form)

ADDENDUM 4: To be completed if you answered YES to Question 4

4.1 Is there any existing or potential conflict of interest between a research sponsor, academic supervisor, other researchers or participants?	YES	NO
4.2 Will information that reveals the identity of participants be supplied to a research sponsor, other than with the permission of the individuals?	YES	NO
4.3 Does the proposed research potentially conflict with the research of any other individual or group within the University?	YES	NO

If you have answered YES to any of these questions, please describe how you plan to address these issues(append to form)